Regulation of Induced Nitric Oxide Synthase in Vascular Smooth Muscle Cells by Glucocorticoids

Mahdi Alsugoor

Completed under the supervision of
Professor. Anwar Baydoun and Dr. Shori Thakur

Submitted to the University of Hertfordshire in partial fulfilment of the requirements of the degree of Doctor of Philosophy

School of Life and Medical Sciences
University of Hertfordshire
February 2017

Declaration

I, Mahdi Alsugoor, hereby declare that I prepared this doctoral thesis, titled *Regulation of Induced Nitric Oxide Synthase in Vascular Smooth Muscle Cells by Glucocorticoids*, for the degree of doctor of philosophy. The work presented within it is my own and produced by me from my original research. I declare that all of the information provided in this document adheres to the academic rules and ethical conduct of the University of Hertfordshire. The contributions of my supervisors and others to the research and to this thesis are in keeping with normal supervisory practice.

I certify that this work has not been previously submitted to any university or institution for the award of any other degree or for a diploma in my name. To the best of my knowledge, this work contains no previously published material or any work written by another person other than where cited in the text. I also certify that no part of this work will be used in any future submission in my name for any other degree or diploma to any university or institution without the approval of the University of Hertfordshire.

Acknowledgments

I would like to express my deepest appreciation to my principal supervisor, Professor Anwar Baydoun. It was a true privilege to work with his research group, and I would like to thank him for encouraging my research, discussing its ideas, and helping me to develop this thesis. Professor Baydoun has had significant influence on my knowledge and research practice, and without his precious advice and critical viewpoints, this work would not have been possible.

I would also like to thank Dr. Shori Thakur for her continuous support and feedback. She always provided valuable advice during meetings as well as in seminars.

I would additionally like to thank my colleague, Ashish Patidar, for his crucial support upon my joining the research group. He was supportive and shared his extensive experience with me, which was incredibly helpful. I would also like to especially thank another colleague, Yousif Shumsdeen, for his assistance in cell culture and for sharing his knowledge.

I also wish to express my gratitude to my colleagues in the laboratory, namely Hema Pramod, Nasima Chowdary, Nimer Alsabeelah, Gagan Maan, and Adem Nasraddin, for their encouragement and camaraderie.

Special thanks also go to my parents, Hussain Alsugoor and Hamdah Alsenan, as well as to my wife, Rahmah Alyami, and my daughters, Mayar and Leena, who consistently and unconditionally supported me during my work.

Lastly, I would like to thank the Saudi Arabian government for providing me with the financial assistance to undertake and complete this research project.

Abstract

The upregulation of the inducible nitric oxide synthase (iNOS) and nitric oxide (NO) production have been implicated in inflammatory pathologies. Although research has revealed that glucocorticoids (GCs) such as dexamethasone and hydrocortisone inhibit iNOS expression and NO production, it remains unclear how these compounds attenuate iNOS expression and function. In response, this thesis has compared the effects of nonselective GCs (i.e., dexamethasone and hydrocortisone) with a selective GC namely, fluticasone propionate (fluticasone) to identify the precise GC actions that regulate the iNOS pathway. Additional investigations were performed to distinguish the GC and non-GC actions using receptor antagonists. Since the effects of GCs on upstream signalling pathways remain vague, further studies were conducted to investigate whether fluticasone regulates the p38 mitogen-activated protein kinases or protein kinase B (Akt) pathways, both of which have been reported to be critical for the induction of iNOS. All experiments were conducted using primary cultures of rat aortic smooth muscle cells (RASMCs). The cells were activated with bacterial LPS (100 μg/mL) and interferon-gamma (IFN-γ, 100 U/mL) to induce iNOS and NO. Nitrite levels in cellular supernatants were quantified by the Griess assay, and expressions of iNOS, phospho-p38 (P-p38), and phospho-Akt (P-Akt) were investigated by western blotting.

Dexamethasone (0.1–10.0 μM) inhibited iNOS expression and NO production in a concentration dependent manner that was significant at higher concentrations (0.3–10.0 μM). Hydrocortisone (0.01–10.0 μM) also inhibited iNOS expression and NO production in a concentration dependent manner which was significant at the higher concentrations (0.1–10.0 μM). By contrast, fluticasone (0.1 nM–3.0 μM) inhibited NO production and iNOS expression only partially (~50%), and the effects were significant at 1 nM–3 μM. RU-486 (10 μM), a GC receptor (GCR) blocker, was able to reverse the inhibitions caused by

dexamethasone, hydrocortisone, and fluticasone, though eplerenone (0.1–10.0 μM), the mineralocortocoid receptor blocker, had no effect. Fluticasone also inhibited the phosphorylation of p38 and Akt in activated RASMCs. The inhibitions were reversed upon incubation with RU-486 (10 μM) for 1 h prior to the addition of fluticasone. The partial inhibition of iNOS and NO by fluticasone suggests that the actions of dexamethasone and hydrocortisone were not restricted solely to GCR and that other receptors or pathways, if not both, might regulate iNOS and NO in RASMCs. In conclusion, the nonselective GCs (i.e., dexamethasone and hydrocortisone) showed a full inhibition of iNOS expression and function, whereas fluticasone only partially inhibited both processes. The inhibitions were reversed by RU-486, but not eplerenone, which strongly suggests a GC-mediated response to all three compounds investigated. Regarding fluticasone, mechanistic studies revealed that the GC can regulate key signalling pathways associated with the induction of iNOS. More specifically, fluticasone reduced the phosphorylation of p38 and Akt, thereby suggesting that its actions can be mediated by suppressing these kinase pathways, which are widely reported to critically regulate iNOS expression and function.

Keywords: Glucocorticoids, Dexamethasone, Fluticasone propionate, Nitric oxide, Inducible nitric oxide, P38, Akt

Table of Contents

List of Figures

List of Tables

List of Abbreviations,

ACE	Angiotensin-converting enzyme
Akt	Protein kinase B
AP-1	Activator protein 1
APS	Ammonium persulfate
APS	Ammonium persulfate
BCA	Bicinchoninic acid
BSA	Bovine serum albumin
CD14	Lipopolysaccharide-binding protein and cluster of differentiation 14
cGMP	3,5-cyclic guanosine monophosphate
CM	Complete medium
CYC A	Cyclophilin A
DMEM	Dulbecco's modified Eagle's medium
EDRF	Endothelial-derived relaxing factor
EIF2α	Eukaryotic initiation factor 2-α
eNOS	Endothelial nitric oxide synthase
Fluticasone	Fluticasone propionate
GC	Glucocorticoid
GCR	Glucocorticoid receptor
GCR-α	Glucocorticoid receptor alpha
GRE	Glucocorticoid-responsive element
HKG	Housekeeping gene
IFN-γ	Interferon gamma
IL-1	Interleukin-1
IL-1β	Interleukin-1-beta

IL-6	Interleukin-6
iNOS	Induced nitric oxide synthase
JAK	Janus kinase signalling pathway
LBP	Lipopolysaccharide-binding protein
LPS	Lipopolysaccharide
MKP-1	Mitogen-activated protein kinase phosphatase 1
MR	Mineralocorticoid receptor
MTT	3-(4,5-dimethylthiazol-2yl)-2,5-diphenyltetrazolium bromide assay
NF-κB	Nuclear transcription factor kappa B
NO	Nitric oxide
PAF	Platelet-activating factor
PBS	Phosphate-buffered saline
PKR	Double-stranded RNA-dependent protein kinase
RA	Rheumatoid arthritis
RASMC	Rat aortic smooth muscle cell
RPL13A	ribosomal protein L13A
SDS	Sodium dodecyl sulphate
STAT	Signal transduction and transcription protein
TEMED	Tetramethylethylenediamine
TLR	Toll-like receptor
TNF	Tumour necrosis factor
TNF-α	Tumour necrosis factor-alpha

1. Introduction

1.1. Inflammation

Inflammation derives from the Latin *inflammare*, meaning 'to burn'. In the 1st century CE, Aulus Cornelius Celsus first described signs of inflammation as heat, pain, redness, and swelling (Tracy, 2006). Although this description matches the classical description of acute inflammation today, inflammation is currently classified as either acute or chronic, as well as either local or systemic.

Inflammation is a complicated, nonspecific defensive biological response initiated in the body to eliminate or repair damaged tissue or to counteract harmful agents (Rankin, 2004). The initial response to acute inflammation is a change in small blood vessels where arterioles contract, followed by dilation and, in time, the accumulation of fluid. Lewis (1942) described those responses in what has been dubbed the 'triple response of Lewis', in which physiological changes in inflammation are accompanied by increased vascular permeability and cellular responses (Lewis, 1942). In normal conditions, vessels are permeable to the extent that water and small solutes may pass through them, and increased vessel permeability allows more water and proteins to pass through the vessels' walls. Since those proteins contain immunoglobulins and other components, they eliminate pathogens at the site of inflammation. Via that same process, endothelial cells contract as a result of the release of certain chemicals such as histamines. Leukocytes are also attracted to the site of inflammation through a process termed *chemotaxis*.

Numerous chemotactic molecules exist. All of the mediators that facilitate inflammation in terms of vasodilation, vascular permeability, leukocyte migration, and chemotaxis are known as *inflammatory mediators*. Molecules that attract neutrophils to the site of inflammation include cytokines such as interleukin-1 (IL-1) and tumour necrosis factor (TNF), as well as

prostaglandin E2 and leukotriene B4 (Kunkel et al., 1988; Laskin & Pendino, 1995; McMahon et al., 2006).

The first step of an inflammation cascade is the recognition of the pathogen or injury through specific receptors including toll-like receptors (TLRs) (Roach et al., 2005), which often lead to the activation of the nuclear transcription factor kappa B (NF-κB) (Kawai & Akira, 2007). After activation, NF-κB translocates to the nucleus where it regulates the transcription of targeted genes. This transcriptional regulation triggers the expression of proinflammatory cytokines such as interleukin-1-beta (IL-1β), interlukin-6 (IL-6), and tumor necrosis factor-alpha (TNF-α) (Tak & Firestein, 2001). Some key inflammatory signalling systems are discussed in the sections that follow.

1.2. Kinin system

Kinins constitute a family of vasoactive peptides, of which bradykinin is the most recognised. Bradykinin has a low molecular weight and is rapidly metabolised by numerous enzymes, including the angiotensin-converting enzyme (ACE). As such, it plays several biological roles in smooth muscle contractility regulation, vasodilation, increasing vascular permeability (Yarovaya & Neshkova, 2015), as well as in hypertension and the release of inflammatory mediators (Maurer et al., 2011) as shown in Figure 1. Researchers have scrutinised the physiological role of bradykinin in the body by either blocking receptors (e.g., endothelial B1 and B2) or inhibiting ACE (Han et al., 2002; Madeddu et al., 1999; Regoli & Barabe, 1980).

Kinins act through specific receptors including the B2 receptors which are expressed constitutively in various cell types such as endothelial cells. The activation of these receptors results in activation of Phospholipase C downstream, leading to formation of diacylglycerol and inositol 1, 4, 5-trisphosphate (IP3). Consequently, cytoplasmic concentration of calcium

increases. This results in various effects including generation of endothelial NO (Kuhr et al., 2010) . B2 receptor activation also causes the activation of phospholipase A2, which catalyses arachidonic acid production. The B1 receptor is mainly induced under abnormal conditions such as inflammation, and its activation induces NO. Many studies have shown that B1 expression is implicated in various inflammatory diseases such as septic shock, asthma, and arthritis (Campos et al., 2006). Consequently, researchers have developed B1 receptor antagonists as potential anti-inflammatory drugs (Calixto et al., 2004).

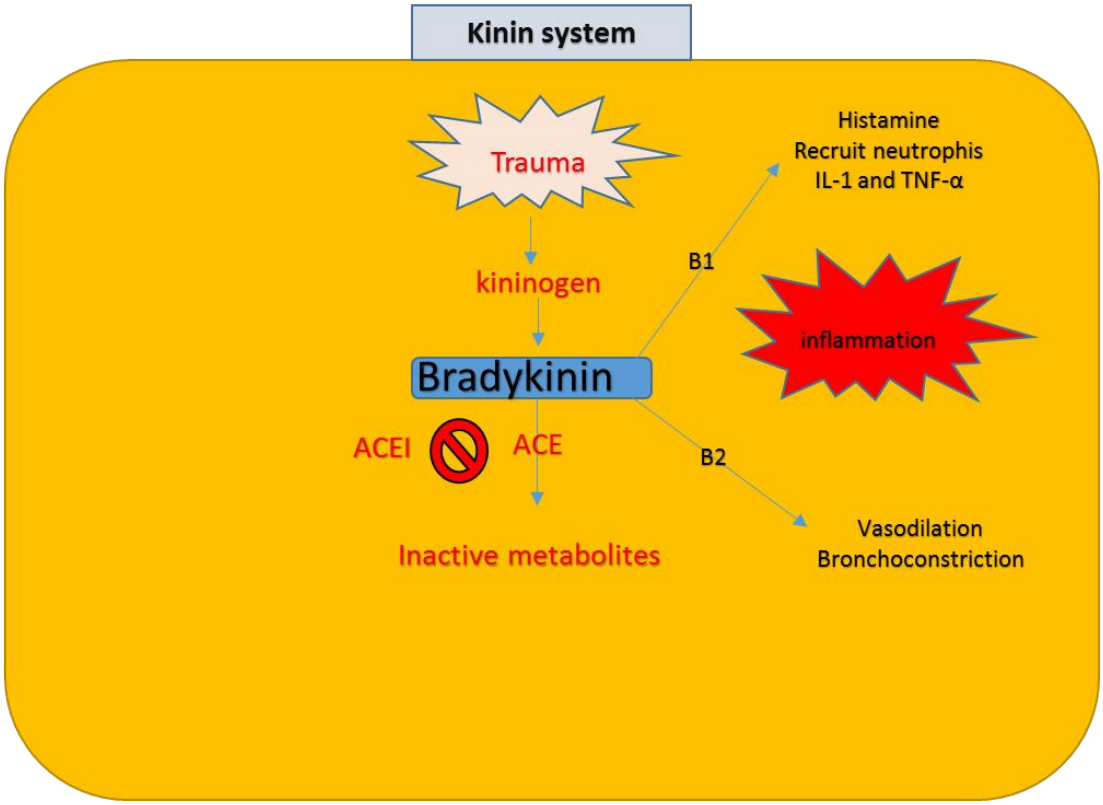

Figure 1. Kinin mechanisms of action

1.3. Histamine

Histamine is a nitrogenous compound that mediates various physiological and pathological conditions—among them, sleepiness, wakefulness, and hormonal secretion (Parmentier et al.,

2002). Histamine is also involved in gastric secretions, as well as implicated in various pathological conditions such as allergic and inflammatory reactions (Leurs et al., 1995). Therefore considered to be an important inflammatory mediator, it is produced from basophils, enterochromaffin-like cells, and mast cells. It acts on different receptors, including H1, H2, H3, H4, and H_{1c}, which vary in their location of expression, second messengers, and binding characteristics (MacGlashan, 2003). As a consequence of the involvement of histamines in allergies and inflammation, various histamine blockers have been developed, and thousands of studies have been conducted on the topic (Thurmond et al., 2008; Tiligada et al., 2009).

1.4. Eicosanoids

Eicosanoids are signaling molecules that play a major role in both physiological and pathological conditions. They involve various families such as prostaglandins and leukotrienes (Funk, 2001) generated in nearly all cells and are synthesised from arachidonic acid by cyclooxygenase (COX) isozymes and 5-lipoxygenase pathways following exposure of cells to stimuli or trauma (Figure 2). COX-1 is responsible for the biosynthesis of the constitutive basal homeostatic prostaglandins, whereas COX-2 is mainly responsible for the synthesis of pathophysiological prostaglandins, which mediate inflammations.

COX-1 is widely and constitutively expressed in most of the tissues of the body and required for homeostatic function such as regulation of vascular tone and for gastric cytoprotection (Franco et al., 1999). COX-2 is generally induced as a response to various inflammatory mediators and also expressed in most cell types (Crofford, 1997). COX-2, like COX-1 can also be found in normal healthy cell. A significant amount of cyclooxygenase 2 (COX2) is constitutively expressed in platelets which was more than the amount of COX1 (Hu et al., 2017). In addition, they can both up-regulated under

pathophysiological conditions (Zidar et al., 2009). As a consequence of the fact that COX-2 is also produced in normal healthy cell, its inhibition could potentially impair its homeostatic function resulting in cardiovascular side effects (Grosser et al.,2006; Marnett, 2009).

Leukotrienes are produced by inflammatory cells, including macrophages and mast cells, and exert chemotactic and vasoconstrictor effects (Dubois et al., 1998; Funk, 2001).

1.5. Platelet-Activating Factor (PAF)

The platelet-activating factor (PAF) ranks among mediators of inflammation derived from phospholipids by phospholipase A2 (Figure 2). In vivo studies have indicated that PAF is among the most important mediators of atherosclerotic lesions, as supported by the fact that using the PAF inhibitor, WEB 2086, has significantly reduced fatty streak formation (Subbanagounder et al., 1999). Extensive research has confirmed the proinflammatory actions of PAF, including increases in vascular permeability, leukocyte recruitment, and leukocyte activation (McManus & Pinckard, 2000).

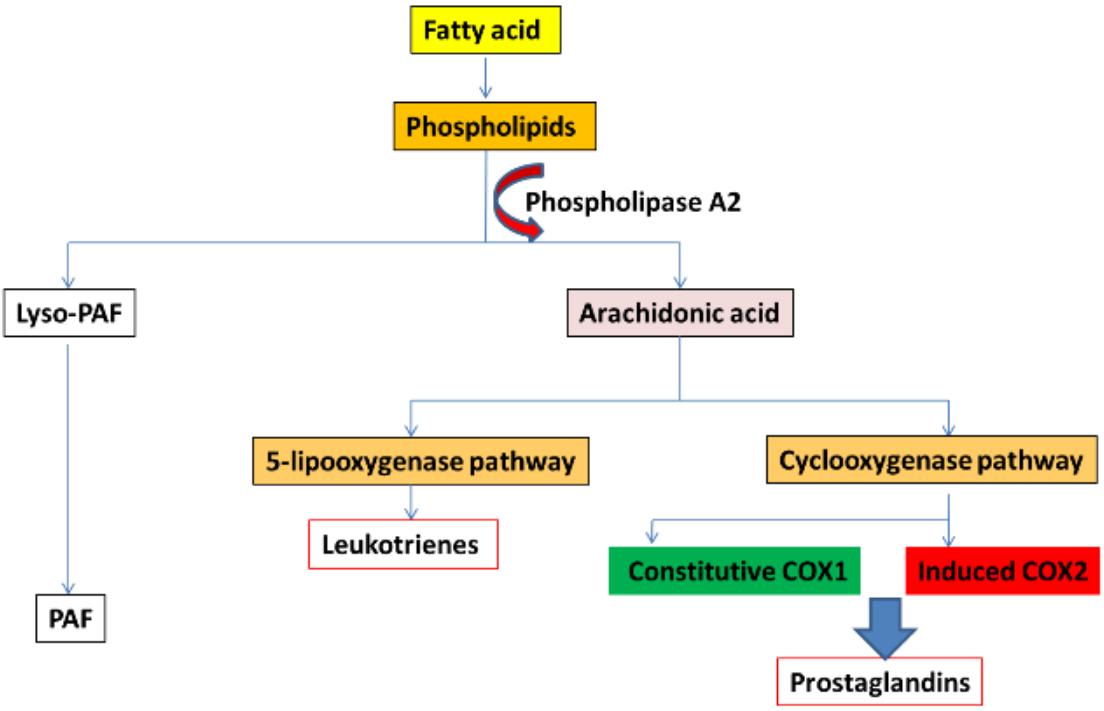

Figure 2. Formation of inflammatory mediators from phospholipids

1.6. History and Production of NO

Ranked among the most important inflammatory mediators, NO is produced in large amounts under certain pathological conditions via induced NO synthases (iNOS). Since its discovery, NO has been the focus of a great deal of research, including the present thesis.

NO is a diatomic free radical consisting of nitrogen and oxygen. As a major signalling molecule, NO plays many roles in both physiological and pathophysiological systems, and its simple chemical structure is responsible for various and even contradictory biological activities (Evans, 1995; Komers & Anderson, 2003; Scicinski et al., 2015; Wink et al., 1998). For instance, it has been reported to exert an antiapoptotic effect on different cell types, including endothelial ones (Ceneviva et al., 1998; Tzeng et al., 1997) and hepatocytes (Wang et al., 2002), but induces a proapoptotic effect in macrophages (Messmer & Brüne, 1996; Messmer et al., 1995). At the same time, different concentrations of NO exert different responses. For example, in MCF7 and endothelial cells, low concentrations of NO prompt the phosphorylation of extracellular signal-regulated kinases, whereas NO prompts the

phosphorylation of protein kinase B (Akt) at higher concentrations (Pervin et al., 2007; Prueitt et al., 2007; Thomas et al., 2004).

As a dichotomous signalling mediator, NO was first discovered as an endothelial-derived relaxing factor (EDRF) that induces the relaxation of blood vessels in the presence of an intact endothelium due to the addition of acetylcholine (Furchgott & Zawadzki, 1980). Seven years later, it was suggested that NO was itself the relaxing factor (Ignarro et al., 1987). With that proposal, scientists observed that NO's effects on vascular smooth muscle closely mimic the effects of EDRF. At that time, not only did Ignarro et al. (1987) propose that the EDRF was NO, but Robert F. Furchgott also independently suggested the same (Moncada & Higgs, 2006). The journal Science named NO 'The Molecule of the Year' in 1992 (Cech et al., 1992), and in 1998, the discovery of NO merited the Nobel Prize for Physiology and Medicine, to Robert F. Furchgott, Louis J. Ignarro, and Ferid Murad (Moncada & Higgs, 2006; SoRelle, 1998).

1.7. Major Regulatory Roles of NO

Produced naturally in small amounts by neuronal NO synthase and endothelial NO synthase (eNOS), NO plays important roles in normal physiological functions, including the maintenance of vascular tone (Knowles & Moncada, 1994), the inhibition of smooth muscle cell proliferation (Cooke & Dzau, 1997; Sarkar & Webb, 1998), the inhibition of platelet aggregation and maintenance of coronary perfusion (Drexler & Hornig, 1999; Kojda & Kottenberg, 1999; Radomski et al., 1996), the maintenance of ventilation and mucus secretion in the lungs (Hart, 1999; Singh & Evans, 1997), and the modulation of endocrine secretion (Kadekaro, 2004). NO is also a neurotransmitter and plays a role as a neuroprotector (Jaffrey & Snyder, 1995). By extension, platelet-derived NO suppresses

platelet activation and intravascular thrombosis (Gkaliagkousi et al., 2007), and NO interacts with superoxide to form peroxynitrite, which has a bactericidal activity (Brunelli et al., 1995). Studies have additionally shown that NO has an anticancer effect (Bian & Murad, 2014)

Perhaps the most vital role of NO is in its regulation of vascular tone. As shown in Figure 3, NO maintains smooth muscle relaxation; once produced, it activates guanylate cyclase, which in turn increases the production of 3,5-cyclic guanosine monophosphate (cGMP). cGMP catalyses a sequence of events that result in the activation of cGMP kinases and, in turn, the activation of potassium channels and inhibition of calcium channels. Such actions decrease the concentration of intracellular calcium, which results in smooth muscle relaxation (Jin & Loscalzo, 2010).

NO is also critical in inhibiting platelet activation and aggregation. NO exerts its antiplatelet function via its ability to activate cGMP, after which it diffuses into platelets and bind to soluble guanylyl cyclase, which once activated increases cGMP and decreases intracellular Ca^{2+} flux (Moro et al., 1996; Rao et al., 1990). This decrease in Ca^{2+} flux may inhibit the formation of the active conformation of glycoprotein IIb/IIIa and decrease fibrinogen binding to platelets (Mendelsohn et al., 1990; Michelson et al., 1996). cGMP can also indirectly increase intracellular cyclic adenosine monophosphate (cAMP). This occurs by the ability of cGMP to inhibit cAMP breakdown (Maurice & Haslam, 1990). This was suggested to occur through crosstalk between cGMP and cAMP where they compete for the catalytic phosphdiestrease sites. The increase of cGMP level causes it to compete with cAMP for interaction with these sites and cause cAMP degradation decrease, thus increasing its level (Francis et al., 2010).Thus the increase of the cGMP level along with cGMP acts synergistically to inhibit platelet aggregation (Bowen et al., 1989; Stamler et al., 1989).. In

all, the reduction of NO precipitates platelet activation and the development of thrombosis (Loscalzo, 2001). Figure 3 highlights some of NO's regulatory functions.

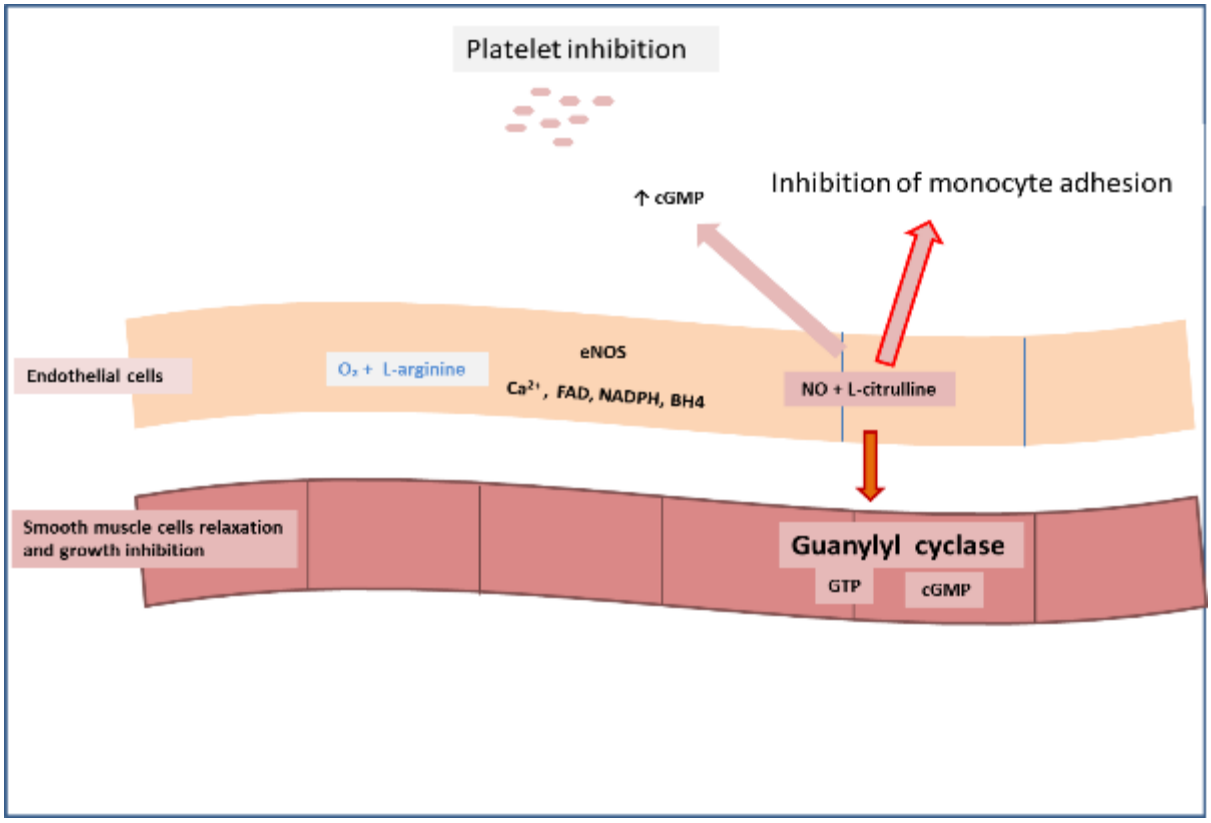

Figure 3. Some regulatory roles of NO

iNOS, which produces NO in large amounts, is expressed in cellular inflammatory conditions in response to inflammatory mediators. For instance, iNOS is expressed and produced NO in high amount in septic shock (King et al., 1999), asthma (Al-Ali & Howarth, 1998), and RA (Farrell et al., 1992; Grabowski et al., 1996; Hilliquin et al., 1997). The expression of this enzyme results from the induction or exposure to certain cytokines or microbial products termed *proinflammatory mediators*. iNOS remains highly stable in terms of both messenger RNA (mRNA) and protein levels and generates large amounts of NO, which may be detrimental to cells, tissues, and hosts. Indeed, the expression of iNOS in biological systems has been linked to inflammatory and autoimmune diseases (Geller & Billiar, 1998;

MacMicking et al., 1997; Vodovotz et al., 1993). It is therefore vital to regulate iNOS expression in order to restrict its deleterious actions, as well as to continue to examine its complexity and functions, particularly concerning various inflammatory diseases.

1.8. NO and Diseases

Due to its important involvement in inflammation, iNOS and its roles in various types of acute and chronic inflammation have attracted the attention of researchers, as described in the follow sections.

1.8.1 NO and septic shock

Sepsis, which is categorised as acute inflammation, is among the most common reasons that patients are admitted to intensive care units all over the world. It is defined as the systemic response to infection, in which the blood is invaded and contaminated with bacteria (Bone, 1994). Almost 50% of sepsis patients develop septic shock, which has a mortality rate of 40–60% (Rackow & Astiz, 1991; Thiemermann, 1997; Titheradge, 1999). Despite advances in medical care, septicaemia continues to rank among the most expensive conditions in US hospitals, where the total cost of its treatment in 2011 was USD $20.3 billion, or 5.2% of total US healthcare costs (Torio & Andrews, 2013).

Clinically, septic shock is characterised by systemic hypotension and reflected in vitro by vascular smooth muscle cell hyporeactivity to adrenergic mimetics (Bone, 1994; Epstein & Parrillo, 1993). As research suggests, once an infection occurs, circulating concentrations of catecholamines, glucagon, and cortisol rise, thereby leading to tachycardia and peripheral vasoconstriction (Rackow & Astiz, 1991). Those elements are followed by progressive vasodilation, which leads to severe hypotension and cardiac failure. Consequently, a lack of tissue perfusion occurs, which leads to organs failure (Thiemermann, 1997).

The main mediator of the high morbidity and mortality of septic shock is the Gram-negative bacterial membrane component bacterial lipopolysaccharide (LPS). The presence of LPS, as an exogenous bacterial component, triggers the release of endogenous cytokines such as TNF-α, IL-1β, interferon gamma (IFN-γ), and IL-6. The release of proinflammatory cytokines leads to iNOS expression and, in turn, NO production, which in excess can cause severe hypotension. By using iNOS inhibitors, however, blood pressure may be restored and endotoxin-induced hypotension reversed in various septic shock models (King et al., 1999; Matejovic et al., 2004; Nin et al., 2004; Unno et al., 1997). Altogether, such findings demonstrate the crucial role of iNOS-generated NO in septic shock.

As mentioned earlier, the increase in NO level during septic shock contributes to the hypotension associated with this condition and may result in poor organ perfusion and the consequent organ failure. As a result, there has been considerable interest in developing and investigating iNOS inhibitor in controlling and treating septic shock amongst other inflammatory diseases associated with NO overproduction. One of the NOS inhibitors investigated is NG-monomethyl-L-arginine (L-NMMA), a competitive L-arginine analogue which inhibit NOS and thus NO synthesis (Evans et al., 1994).

Inhibiting NO under the condition above was shown to result in increased blood pressure and systemic vascular resistance (Avontuur et al., 1998). However, the use of this NOS inhibitor was shown to be associated with mortality of septic patients. The main limitation is the fact that it has been found the NOS inhibitor caused a fall in cardiac output which would exaggerate organ failure (Petros et al., 1994). In addition, septic shock is associated with an increase in inflammatory mediators. This could be reduced by anti-inflammatory medication but this could result in a hypo-inflammatory phase. This phase would reduce the patient's immunity leading to secondary infection. Thus, a balance between hyper and hypo-inflammation is requires (Tsirigotis et al., 2016).

1.8.2 NO and asthma

Ranking among the most common inflammatory diseases, asthma affects roughly 300 million patients worldwide (Bousquet et al., 2010). Characterised by a recurrent reversible bronchospasm, asthma occurs with the recruitment and activation of mast cells, macrophages, neutrophils, eosinophils, and T lymphocytes, as well as the increased production of Th2 cytokines such as interleukin-4 (IL-4), IL-5, IL-9, and IL-13 and CD4+ lymphocytes (Redington, 2006). In effect, such activation precipitates airway inflammation and cellular infiltration.

NO is among the most important mediators of asthma pathogenesis. Gustafsson et al. (1991) reported that the exhaled breath of rabbits, guinea pigs, and humans generally contains NO, whose physiological production appears to play a bronchoprotecive role (de Gouw et al., 1999). At the same time, other reports have revealed increased NO in the exhaled breath of asthmatic patients (Al-Ali & Howarth, 1998; Hamid et al., 1993), as well as that selective iNOS inhibitors appear to reduce NO levels (Hansel et al., 2003). In addition, recent research showed increased iNOS expression in central airway tissue in asthmatic patient but alveolar compartment showed no change in iNOS mRNA (Tufvesson et al., 2017). By extension, the overproduction of NO is thought to play a role in tissue injury, which contributes to airway dysfunction in asthma (Redington, 2006). However, several studies have indicated reduced NO without any significant effects on early or late asthmatic responses to allergens (Hesslinger et al., 2009), which suggests that the overproduction of NO might not be critical in asthma.

1.8.3 NO and rheumatoid arthritis (RA)

Rheumatoid arthritis (RA) is a common chronic autoimmune inflammatory disease that affects approximately 1% of the world's population (Gabriel, 2001). Clinically characterised by joint pain, stiffness, and swelling, RA and its pathogenesis derive from the critical involvement of T cells, B cells, and cytokines (Smolen et al., 2007; Smolen & Steiner, 2003). In RA, T cells differentiate into T helper cells 17, which results in the production of the potent cytokine IL-17 that plays a pathological role in promoting synovitis in RA as highlighted in Figure 4. B cells contribute to RA antigen presentation and the production of antibodies and cytokines (Smolen et al., 2007). RA is also associated with NO production from iNOS (Farrell et al., 1992; Grabowski et al., 1996; Hilliquin et al., 1997), and studies using animal models have suggested that NO plays a pathological role in RA, whose severity dropped with the administration of iNOS inhibitors (Ialenti et al., 1993; McCartney–Francis et al., 1993; Nishida et al., 2000; Stefanovic–Racic et al., 1994).

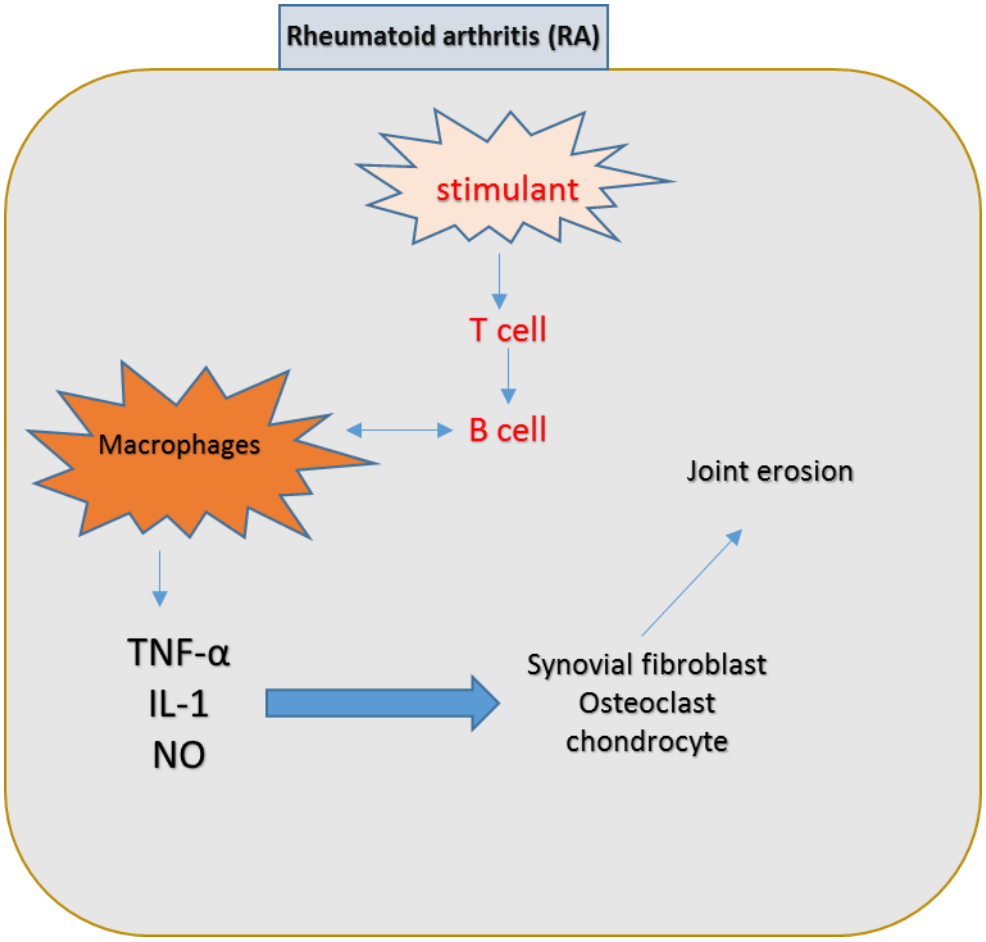

Figure 4. Rheumatoid arthritis pathogenesis

1.8.4 NO and osteoporosis

Stemming from the Greek for 'porous bones' (Parvez, 2004), *osteoporosis* is defined as a progressive systemic bone disorder distinguished by bone loss and the deterioration of bone tissues, both of which increase the risk of bone fracture. The World Health Organization ranks osteoporosis among the most serious global diseases, given its worldwide patient population of approximately 200 million (Goel et al., 2014; Reginster & Burlet, 2006).

In osteoporosis, the accumulation of inflammatory mediators in synovial fluid and imbalance of bone formation and bone resorption result from oestrogen depletion, which correlates highly with the condition. As in other inflammatory diseases, iNOS expression plays a

pathological role in osteoporosis (Khosla et al., 2011), yet can be inhibited, along with NO production, as part of the anti-inflammatory effect of oestrogen (Cuzzocrea et al., 2003). NO is also associated with reduced bone density in osteoporosis (Armour et al., 1999), and interestingly, L-arginine, an NO substrate, has been shown to increase bone mineral density (Goel et al., 2014).

1.8.5 NO and atherosclerosis

Atherosclerosis is a complex disease characterised by an accumulation of lipids, macrophages, and smooth muscle cells in the intima of large and medium-sized epicardial coronary arteries. Atherosclerosis is however not only limited to coronary arteries but also affects carotid, renal and peripheral arteries. Such accumulation leads to the obstruction of blood vessels, myocardial infarction, and peripheral vascular diseases (Lamon & Hajjar, 2008; Sanchez & Veith, 1998). The impairment of endothelial integrity and thus its function plays a critical role in the pathogenesis of atherosclerosis. Among its many functions, endothelium acts as a barrier between circulation and the arterial wall and produces endothelial NO, which plays many physiological roles, as mentioned earlier (Anderson, 2004).

Although smooth muscle cells express iNOS and thus NO in atherosclerosis, the role of iNOS in the disease remains controversial insofar as it is either deleterious or anti-inflammatory. In a mouse carotid artery ligation model and cardiac transplant model, the deletion of an iNOS gene had a deleterious effect, whereas other models have indicated an opposite effect (Tsutsui et al., 2014). In addition, it has been found that early atherosclerosis development in female apolipoprotein E-deficient mice is associated with iNOS expression mediating the generation of reactive oxygen species (Delgado-Roche et al., 2016).

1.9 Rat aortic Smooth muscle cells

The aorta is the largest artery in the body, which originates from the left ventricle of the heart curving down to the abdomen. In general, arteries and veins consist of three main layers

- Tunica adventitia: This is the outermost layer, which is composed of connective tissue, elastic fibres, and collagen. These fibres provide stability and prevent the blood vessels from being overstretched during blood flow.
- Tunica media: This is the middle layer, composed of elastic tissues and smooth muscles. It is located between the tunica intima on the inside and the tunica adventitia on the outside.
- Tunica intima: This is the innermost layer and consists of endothelial cells and connective tissue.

In our model, we use the smooth muscle cell to induce expression of iNOS and NO as these cells have been shown to be key site of expression of iNOS within the vasculature in septicemia (Knowles et al., 1990). Moreover, these cells have been widely used to investigate the regulation iNOS within the vasculature and well characterized in our laboratory (Baydoun et al., 1999).

1.10 Synthesis of NO

To produce NO and L-citrulline, NO synthases induce the oxidation of L-arginine in a process that occurs in the presence of cofactors such as oxygen and nicotinamide adenine dinucleotide phosphate. First, the NOS enzyme hydroxylates the nitrogen of L-arginine to produce N-hydroxy-L-arginine, which is oxidised to further produce NO and L-citrulline. Tetrahydrobiopterin is also required as a cofactor (Forstermann & Sessa, 2012), as shown in Figure 5A. However, the reduction in BH4 lead to NOS uncoupling which in turn results in increased superoxide production by the uncoupled enzyme. Superoxide react with NO

leading to the formation of peroxynitrite as well as a reduction of NO as shown in Figure 5B (Kuzkaya et al., 2003).

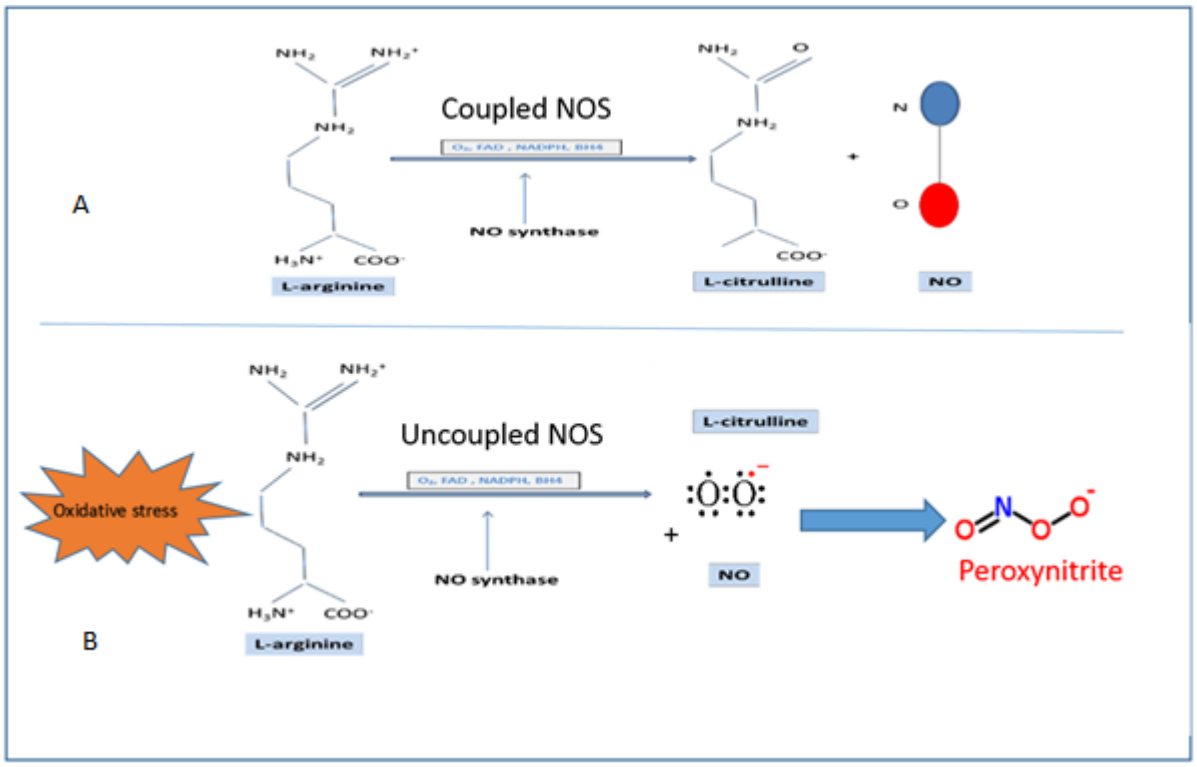

Figure 5. The L-arginine–nitric oxide pathway; NADPH: Nicotinamide adenine dinucleotide phosphate, BH4: Tetrahydropterin (Figure A). Peroxynitrite formation in response to oxidative stress (Figure B)

NO synthesis can be regulated by a family of monomeric cationic amino acid transporters (CATs) that deliver the substrate L-arginine into cells. In smooth muscle cells, the CATs protein family has three members: CAT-1, CAT-2A, and CAT-2B (Baydoun et al., 1999). CAT-1 is ubiquitously expressed in many cell systems, although not in the liver (Baydoun et al., 1999). By contrast, CAT-2A and CAT-3 are constitutively expressed in a few cell systems, including those of the liver and brain (MacLeod & Kakuda, 1996). Various external stimuli, including mitogens, LPS, IL-1β, insulin, TNF, and angiotensin II, can alter the expression of CATs.

1.11 iNOS and NO Induction

The expression of iNOS has been routinely induced in cells, largely through the use of proinflammatory mediators such as:

- LPS, a molecule in the membrane of Gram-negative bacteria that can work as an endotoxin, effectively induce inflammation and immune response in cells, and induce many mediators involved in septic shock (Raetz & Whitfield, 2002); and
- IFN-γ, a cytokine produced after viral or bacterial infection, though its activity is not fully understood (Doherty et al., 1992).

Having a synergistic effect in inducing inflammation (Weisz et al., 1994), LPS and IFN-γ have been widely used to mimic inflammatory effects in vitro.

1.11.1 LPS

LPS is a significantly important part of the cell membrane of Gram-negative bacteria. It forms an immunostimulatory element in bacteria, and in the case of abnormal or extreme signalling, is responsible for the induction of inflammation and sepsis. This component is responsible for many conditions such as the severe hypotension in septic shock as well as the production of pro-inflammatory cytokines and proteins. Examples of these cytokines include tumour necrosis factor-α (TNF-α) and interferon-β (IFN-β) as well as pro-inflammatory proteins such as iNOS. More specifically, the stimulation of Toll-like receptor 4 (TLR4) through LPS leads to the release of key proinflammatory cytokines, which are essential to trigger strong immune responses (Lu et al., 2008).

1.11.2 LPS-binding protein (LBP) and cluster of differentiation 14 (CD14)

LPS begins the signalling pathway by binding to the LPS-binding protein (LBP) (Schumann et al., 1990), produced in the liver and released into the bloodstream, in either its free or

intact form (i.e., bacteria) to produce the LPS–LBP complex. The role of LBP is to deliver LPS to cluster of differentiation 14 (CD14), which also forms a complex, and in turn transfer LPS to its multipart receptor, which consists of TLR4 and myeloid differentiation (MD) protein (MD-2) (Tobias et al., 1995). As a soluble protein that interacts directly and binds to LPS, LBP aids the union of LPS and CD14. As research has shown, CD14 is a glycosylphosphatidylinositol-anchored protein that can promote the transport of LPS to the TLR4–MD-2 receptor complex, as well as aid LPS recognition. Two forms of CD14 have been identified (Lu et al., 2008): a soluble form found in plasma, which aids the transfer of LPS signals in cells without membrane-bound CD14 such as endothelial and epithelial cells, and a membrane-bound form found in many types of cells, including monocytes, macrophages, and granulocytes. As such, LPS can directly bind to those cells (Ferrero & Goyert, 1988; Sugiyama & Wright, 2001; Wright et al., 1990).

Although earlier findings suggested that CD14 was an LPS receptor (Wright et al., 1990), more recent research has clarified that the actual receptor is TLR4. Subsequent work has demonstrated that CD14 binds with LPS, guides it toward MD-2 and TLR4, and is vital for TLR pathways (Muroi & Tanamoto, 2002). Despite the demonstrated importance of CD14 in LPS signalling, however, studies with knockout mouse have established CD14's independent effects on LPS (Haziot et al., 1996; Haziot et al., 1998).

1.11.3 MD-2

An essential glycoprotein, MD-2 acts as an adaptor protein that facilitates LPS's activation of TLR4, as made clear by studies in which mutant forms of MD-2 or MD-2 knockout mice did not respond to LPS, whereas wild types responded in full (Nagai et al., 2002; Schromm et al., 2001). It has been reported that MD-2 is also a soluble protein that can noncovalently associate with TLR4, as well as interact directly with LPS and produce a complex in the

absence of TLR4 (Gioannini et al., 2004; Nagai et al., 2002; Shimazu et al., 1999). Despite a lack of evidence that TLR4 can directly bind to LPS, TLR4 can increase LPS's capacity to bind with MD-2. Moreover, the novel drug E5531, developed as an LPS inhibitor to treat endotoxic shock, has been shown to directly inhibit the MD-2–TLR4 complex (Akashi et al., 2003), thereby suggesting that the drug inhibits MD-2, yet does not interfere with CD14.

1.11.4 TLR4

TLRs are expressed by innate immune system cells activated by structural motifs that are characteristically expressed by bacteria, viruses, and fungi known as *pathogen-associated molecular patterns* (Akira et al., 2006; Janeway & Medzhitov, 2002). Once TLR4 was identified as the first TLR and dubbed the human Toll (Medzhitov et al., 1997), evidence that TLR4 was an LPS receptor emerged in studies with mice with a single point mutation in the Toll-IL-1 receptor (TIR) domain of TLR4 (Poltorak et al., 1998). Other research has added that LPS analogues such as tetra-acyldisaccharide precursor of lipid A and penta-acyl lipid A antagonise LPS in humans and act as agonists in mice (Triantafilou et al., 2004).

1.11.5 Adaptor proteins

The TLR4 signalling pathway that mediates LPS's activation of TLR4 requires adaptor proteins, with which TLR4 associates via interactions with TIR domains after binding with LPS and undergoing oligomerisation. Many adaptors have been identified, including myeloid differentiation factor 88 (MyD88), the MyD88 adaptor-like protein, the TIR-containing adapter molecule (TICAM), and the TICAM-related adaptor molecule. Depending on the different roles of those adaptor proteins, TLR4 signalling may be divided into MyD88 dependent or independent (i.e., TICAM-dependent) pathway (Lu et al., 2008).

1.11.6 MD primary response protein 88-dependent pathway

MD primary response protein 88 contains TIR and death domains (DD), the latter of which can attract different substances. Following treatment with LPS, MyD88 triggers IL-1 receptor-associated kinase-4, which dissociates and activates TNF receptor-associated factor 6, whose recruitment leads to series of consequences, including the activation of the MAP3 kinase pathway and of the IKKα/β/γ complex. As a result, the phosphorylation and degradation of IκB occurs, which leads to the activation and translocation of NF-κB (Zhang & Ghosh, 2000).

1.11.7 NF-κB activation

NF-κB is a complex protein that, as a transcription factor, plays an important role in autoimmune and inflammatory diseases (Ghosh et al., 1998). NF-κB consists of several protein subunits, including p65, p50, p52, RelB, and c-Rel. Under normal conditions, NF-κB accumulates in the cytosol in its inactive form noncovalently bound to IκB, which inhibits NF-κB. Once IκB is phosphorylated, it becomes degraded and releases NF-κB, which translocates to the nucleus to enhance gene expression, including of iNOS, TNF, and COX-2 (Ghosh et al., 1998).

1.11.8 Interferon- γ and signal transducer and activator of transcription alpha (STAT1) pathway

Signal transducer and activator of transcription (STAT) alpha (STAT1) is a transcription factor consisting of an SH2 domain that is essential for DNA binding and dimerisation. The C-terminal domain contains two phosphorylation sites, S727 and Y701. STAT1 phosphorylation at S727 is important for activating the transcription of target genes (Decker & Kovarik, 2000).

Although STAT1 activation is critical, it alone cannot activate gene transcription, but instead requires a series of processes. First, IFN-γ binds to IFN-γ receptor 1, which in turn induces JAK2's autophosphorylation leading to JAK1's transphosphorylation. Once activated, JAK1 phosphorylate tyrosine residues of IFN receptor 1 (Schroder et al., 2004) form two adjacent docking sites for STAT1. STAT1's phosphorylation subsequently occurs at Y701, which triggers the dissociation of STAT1 from the receptor (Greenlund et al., 1994; Heim et al., 1995). STAT1:STAT1:IFN regulatory factor (IRF)-9 and STAT1:STAT2:IRF-9 (i.e., IFN-stimulated gene factor 3, or ISGF3) complexes are produced, although to a lesser extent, by IFN signalling (Paludan, 1998; Schroder et al., 2004). STAT1 is transported to the nucleus and either initiates or suppresses the transcription of IFN- γ regulated genes by binding to promoter IFN-γ activation site (GAS) elements. In fact, IFN-γ regulated transcription factors that initiate the transcription of genes take aid from STAT1:STAT1:IRF-9 heterodimers, ISGF3, and IRF-1, which bind to IFN-stimulated response element (ISRE) promoter regions in target genes (Paludan, 1998). STAT1:STAT1:IFN regulatory factor (IRF)-1 can also promote the transcription of STAT1 through an unusual ISRE site (IRF-E/GAS/IRF-E) (Schroder et al., 2004). IFN-γ can additionally augment the induction of iNOS via LPS by stabilising iNOS mRNA once induced by LPS (Weisz et al., 1994).

Apart from actions at the nuclear level, LPS and IFN-γ may also act upstream, activating key signalling kinase pathways to initiate iNOS induction.

1.11.9 P38 mitogen-activated protein kinase (MAPK)

Expressed in most cells, p38 mitogen-activated protein kinase (MAPK) plays a significant role in stimulating immune response (Cuenda & Rousseau, 2007). P38 MAPK belongs to a class of MAPKs that respond to many factors, including cytokines, heat shock, and osmotic shock, and that are critical in various cellular activities, including differentiation, apoptosis, and autophagy (Sui et al., 2014). Of relevance to this thesis, p38 MAPK is also involved in

the induction of proinflammatory mediators such as cytokines, COX-2, and iNOS (Schindler et al., 2007). Several reports have additionally demonstrated that p38 regulates iNOS expression (Baydoun et al., 1999). Additionally, p38 may affect iNOS expression at the post-transcriptional level by stabilising iNOS mRNA (Fechir et al., 2005). The signalling pathway that activates p38 and other related signalling molecules is summarised in Figure 6.

Convincing evidence that p38 regulates iNOS expression has been generated using potent inhibitors of the kinase, including 4-(4-fluorophenyl)-2-(4-methylsulfinylphenyl)-5-(4-pyridyl) 1H-imidazole (SB203580), or with the overexpression of a dominant negative p38 MAPKα protein. In both cases, iNOS mRNA and protein expression were suppressed, which strongly suggests the critical role of p38 in inducing iNOS (Baydoun et al., 1999; Fechir et al., 2005).

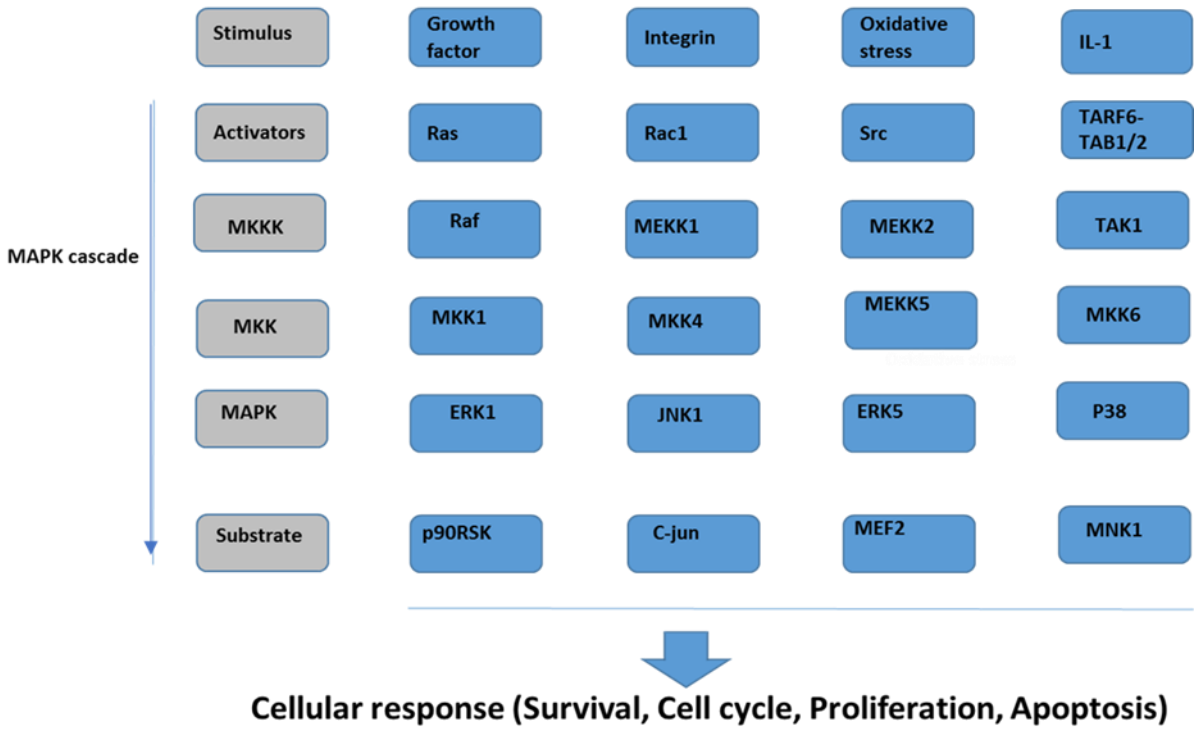

Figure 6. Cell signalling pathway: MAPKinase activated system activate various components as shown in this figure which lead to activation of different cascades leading to its cellular response involving growth factor, integrin signalling, oxidative stress and interlukin-1.

1.11.10 Akt

Also known as protein kinase B, Akt is critical as an antiapoptotic protein that regulates cell survival (Hausenloy & Yellon, 2009) and plays an important role in inflammation and TLR activation (Troutman et al., 2012). In that regard, LPS has been shown to induce iNOS in rat aortic smooth muscle cells (RASMCs) by activating Akt, which in turn activates NF-κB. The use of LY294002, a pharmacological inhibitor of Akt, significantly reduced the phosphorylation of Akt and inhibited the activation of NF-κB by decreasing the phosphorylation of IκB (Hattori et al., 2003).

1.11.11 Double-stranded RNA-dependent protein kinase (PKR)

Double-stranded RNA-dependent protein kinase (PKR) is activated by IFN and double-stranded RNA. Not only has PKR been reported to regulate NF-κB activation in embryo fibroblasts following stimulation with IFN-γ (Kumar et al., 1997), but it could also be involved in p38 activation in embryonic fibroblasts following activation with LPS (Goh et al., 2000). PKR also phosphorylates eukaryotic initiation factor 2-α (EIF2α), which in turn inhibits protein synthesis (Dabo & Meurs, 2012). More important however is the fact that PKR regulates the expression of iNOS in murine RAW 264.7 macrophages, which suggests that PKR plays a role in the inducing of iNOS (Maggi et al., 2000).

1.11.12 Regulation of iNOS expression by eukaryotic translation initiation factors

Among the several eukaryotic translation factors that might regulate iNOS expression at the translational level, the heterotrimer EIF2α consists of an alpha, beta, and gamma subunits. Alpha subunit is required to initiate the translation stage of protein synthesis, in which the ribosome builds proteins according to the information encoded in mRNA.

EIF2α mediates the binding of transfer RNA to the ribosome in a GTP-dependent manner (Kimball, 1999). Once initiation is completed, EIF2α is released from the ribosome and is

bound to GDP as an inactive binary complex. To participate in a round of translation initiation, the GDP is exchanged for GTP (Kimball, 1999). EIF2α is therefore a translation initiation factor involved in the first regulated step of translation. This factor is generally reversibly phosphorylated by kinases, including PKR, heme-regulated inhibitor protein kinase, unfolded protein response kinase, and general control nonderepressible-2 kinase (Wek et al., 2006). All of those kinases are typically activated in physiological responses to stress, including heat shock, viral infection, oxidative stress, and amino acid starvation. Once EIF2α is phosphorylated, it becomes inactive and suppresses the translation of certain mRNAs (Harding et al., 2000).

At least one study has claimed that EIF2α plays a key role in regulating iNOS expression in astrocytes (Lee et al., 2003), despite research with macrophages showing that the translational reduction of iNOS by L-arginine depletion is not associated with the increased phosphorylation of EIF2α (König et al., 2009). More importantly, little is known about the regulation of EIF2α by GCs and is it not clear whether upstream signalling pathways reported to regulate iNOS expression do in fact feed through EIF2α and this needs to be investigated.

In addition to the previous mentioned signalling pathways, other pathways could also be involved in the process of inflammation and these are summarised in Table 1.

Table 1. Signalling pathways in response to various inflammatory mediators

Mediator	Signalling	Reference(s)
IFN-γ	JAK/STAT1	(Teng et al., 2002)
IL-1β	PKC-ERK1/2	(Ginnan et al., 2006)
IL-1β /TNF-α	p42 / p44 MAPK	(Doi et al., 2000)
LPS+IFN-γ	c-Jun N-terminal kinase	(Chan & Riches, 2001)
LPS	Akt	(Hattori et al., 2003)
LPS+IFN-γ	P38	(Baydoun et al., 1999)

1.12 Glucocorticoids (GCs)

Among the most widely prescribed medications worldwide (Oakley & Cidlowski, 2013), natural glucocorticoids (GCs) and synthetic derivatives exert their biological effects mainly through binding to GC receptor alpha (GCR-α). Another form of GCR in which GCR-β is not activated by GC–ligand binding has been proposed in cases of asthma, as have the roles of those receptors (Sousa et al., 2000).

Expressed in nearly all tissues, GCR-α belongs to the steroid receptor superfamily. Once receptors are occupied with high affinity, the activation or repression of targeted transcription factors occurs. GCRs differ from other steroid receptors due to being located predominantly in the cytoplasm in the absence of GCs, which, once bound, the GCRs translocate to the nucleus. Interestingly, some reports have found that GCRs reside in the nucleus in the absence of GCs (Webster et al., 1994). As GCs are lipophilic, they passively diffuse through

the plasma membrane. However, at least one study has suggested that active uptake is required (Rao et al., 1977).

The classical genomic activation of GCs leads to either the transactivation or transrepression of transcription factors, both of which effects are responsible for both the desired anti-inflammatory effect and unwanted side effects. GCs, however, have many effects that have inspired extensive research.

1.12.1 Genomic action

GCs influence the transcription factors of many genes by activating GCRs. Such regulation can be categorised as either protein–DNA or protein–protein binding interactions.

1.12.2 Gene activation and repression by direct DNA binding

Once GCs bind to their receptors in the cytoplasm, they relocate to the nucleus (Vandevyver et al., 2012).The ligand–receptor complex binds to the GC responsive element (GRE), thereby transactivating various genes, including tyrosine aminotransferase and phosphoenolpyruvate carboxykinase (Newton, 2000), which are involved in liver gluconeogenesis. This attribute explains the metabolic side effects of GCs. By contrast, the ligand–receptor complex could bind to the DNA's negative GRE, which leads to the repression of genes such as prolactin and serotonin (Newton & Holden, 2007; Revollo & Cidlowski, 2009). Whereas genes known to be repressed by this mechanism are few, those repressed by GCs via protein–protein interactions are numerous.

1.12.3 Gene activation and repression by protein–protein interaction

Gene activity can either be activated or repressed by ligand–receptor binding, although to the protein and not to the DNA. STATs demonstrate that phenomenon, as in the Janus kinase signalling pathway (JAK), an important signalling pathway that, when activated, in turn

activates STATs that translocate to the nucleus (Revollo & Cidlowski, 2009), where they interact with response elements on the DNA. Reportedly, STAT5 interacts with GR-α without directly binding to DNA, which transactivates various genes such as liver insulin-like growth factor 1 (Revollo & Cidlowski, 2009).

Most gene repression caused by GR-α occurs through protein–protein interactions (i.e., transrepression) NF-κB and activator protein 1 (AP-1) are examples of transcription factors that mediate such interactions. NF-κB is a critical transcription factor that plays an important role in inflammation. GR-α can bind to the p65 subunit and inhibit the activation of NF-κB in several ways, including by sequestering NF-κB given GCR-α's ability to interact with p65 and thereby prevent it from binding to the DNA. GCR-α can also interact with DNA-bound NF-κB, thus inhibiting the recruitment of transcriptional process (McKay & Cidlowski, 1998).

AP-1 is another transcription factor that mediates gene expression in response to various physiological and pathological stimuli, including growth factors, cytokines, stress, and infections (Hess et al., 2004). Similar to NF-κB, GCR-α interacts with AP-1 to suppress its activation (Schüle et al., 1990)

Along with transcription factors, intracellular proteins transduce extracellular signals, including the SMAD signalling pathway. Together with other critical transcription factors such as NF-AT and IRF, such proteins can be inhibited by GCR-α (Almawi & Melemedjian, 2002; O'Neill, 2006; Song et al., 1999), which play important roles in inflammation.

1.12.4 Relation of GCRs with MAPKs

Along with the direct actions mentioned above, GCR-α also exerts secondary actions via components that alter signalling molecules. Studies have demonstrated, for example, that

GCR-α induces the expression of MAPK phosphatases 1 (MKP-1), which in turn dephosphorylates and inactivates c-Jun N-terminal kinase and p38 (Abraham et al., 2006), which are critical in cellular signalling, including the regulation of iNOS expression, as mentioned earlier. In addition, in human A549 bronchial epithelial cells, dexamethasone increased the expression of MKP-1 which led to dephosphorylation of p38 and thus reduced cytokines (Keränen et al., 2017).

The negative role of MKP-1 in inflammation has also been supported by studies with MKP-1 knockout mice, the models of which showed a far more severe response to inflammatory mediators and produced significantly greater inflammatory cytokines than the wild type (Wang et al., 2007). At the same time, in an experimental animal ischemic model, dexamethasone showed a cardioprotective action via the expression of MKP-1 and inactivation of p38 (Abraham et al., 2006). It has also been demonstrated in mast cells that dexamethasone interferes with transcription factors such as AP-1 and NF-κB by dephosphorylating ERK1/2 by inducing the expression and reducing the degradation of MKP-1 (Kassel et al., 2001).

1.12.5 Nongenomic action of GCs

GCs are known to exert their effects largely via genomic actions. However, some evidence supports a nongenomic action involving direct interaction with MAPKs (Ayroldi et al., 2012). Such nongenomic action differs from genomic actions given their rapid onset, which can last minutes or even seconds, whereas genomic actions take hours.

The rapid nongenomic effect of steroids was described roughly 80 years ago in reports suggesting that steroids cause rapid effects, including the induction of anaesthesia within minutes. Another example of a nongenomic action is the effect of dexamethasone on the

regulation of eNOS via the PI3k–Akt pathway (Hafezi–Moghadam et al., 2002). In these studies, dexamethasone stimulated PI3k and Akt which led to eNOS activation.

1.12.6 GCs and iNOS

Studies have demonstrated that GCs can inhibit iNOS in vascular smooth muscle cells, vascular endothelial cells, macrophages, hepatocytes, and epithelial cells, among others (Di Rosa et al., 1990; Geller et al., 1993; Kanno et al., 1993; Radomski et al., 1990; Salzman et al., 1996). Various mechanisms have been suggested to explain how GCs inhibit iNOS, and most findings have demonstrated that the inhibitory effects are regulated at the transcriptional or post-transcriptional levels. At the transcriptional level, GCs may act through NF-κB, reducing its nuclear translocation to the nucleus, or by binding to DNA. Such effects might stem from the ability of GCs to elevate the level of inhibitory IκB (Katsuyama et al., 1999; Kleinert et al., 1996; Salzman et al., 1996) and thus result in NF-κB's sequestration in the cytoplasm in a complex with IκB, which will inhibit iNOS gene transcription. Such action may however be cell-type specific, however, since in mesangial cells and mouse macrophages, dexamethasone reduced iNOS via reduction of iNOS mRNA and iNOS protein stability (Kunz et al., 1996; Walker et al., 2001). In addition, it has been found that dexamethasone can reverse the increase of iNOS expression and mRNA induced by LPS in mice lung (Al-Harbi et al., 2016).

On the other hand, there are contradictory reports in the same cell type. For example, in RASMCs dexamethasone reduced iNOS by suppressing NF-κB (Matsumura et al., 2001), whereas onother report suggested that dexamethasone enhanced iNOS mRNA but suppressed iNOS protein expression, thereby suggesting an action at the post-transcriptional level (Thakur & Baydoun, 2012). This could be explained by the difference in methodology which will be discussed in the discussion chapter.

1.13 Aims and Objectives of the Research

Currently, the regulation of iNOS expression by GCs, especially dexamethasone, though documented well, remains largely unclear in terms of the underlying mechanisms that mediate the reported effects. Indeed, some results have suggested that dexamethasone exerts its effect on iNOS transcriptionally, whereas other studies have suggested a post-transcriptional action. At the same time, dexamethasone is not a selective GC that acts exclusively on the GCR, but acts also upon other receptors, including mineralocorticoids, progesterone, oestrogen, and androgen receptors (Bigsby, 1993; Inder et al., 2010; Lan et al., 1982; Yang et al., 2001). Such nonexclusivity complicates concluding that dexamethasone blocks iNOS expression simply with a blockade of GCR. In response, studies were conducted for this thesis to compare the actions of dexamethasone to those of hydrocortisone, another nonselective GC that also acts on mineralocorticoids, androgen, and progesterone receptors (Born et al., 1987; Karalis et al., 1996; Sonneveld et al., 2005), and those of fluticasone, a selective GC agonist (Austin et al., 2002). The mechanisms by which fluticasone might exert its effect on iNOS expression and function were also investigated in detail, looking at its ability to regulate p38 MAPKs or Akt pathways, both of which have been deemed critical for inducing iNOS (Baydoun et al., 1999; Hattori et al., 2003).

2. Materials and Methods

2.1 Cell Culture of RASMCs

Smooth muscle cells were isolated from male Wistar rat aorta and maintained in complete medium (CM) comprising Dulbecco's modified Eagle's medium (DMEM), 10% foetal bovine serum, 100 U/mL of penicillin, and 100 µg/mL of streptomycin. RASMCs were placed in a sterile cell culture hood, and the fat and connective tissues were removed (Figure 7). The aorta was cut longitudinally and the lumen scraped to remove the endothelial layer before it was cut into 2-mm pieces, four to six of which were distributed in a T25 flask. Four mL of CM was added to the bottom of each flask, which was stood upright to keep the pieces of aorta attached to the wall of the flask and prevent them from floating. Each flask was transferred to the cell culture incubator and kept upright for 3 h (Figure 8) before being placed horizontally to ensure that the medium covered the tissue segments without dislodging them. Throughout incubation for 1 week, cells grew from the segments onto the surface of the flask.

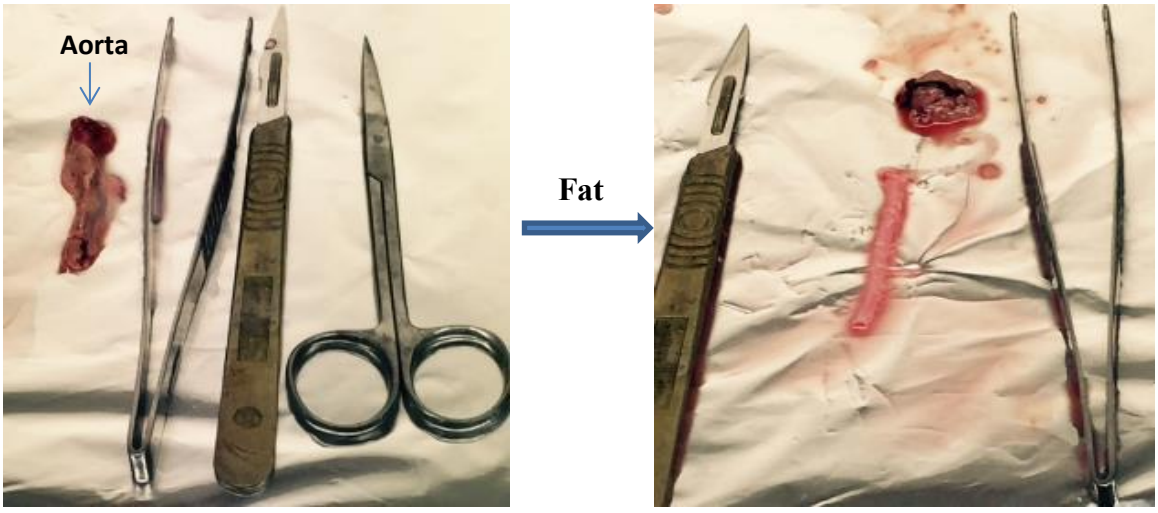

Figure 7. Preparation of rat aorta in CM for explants

Figure 8. Aortic explants attached to tissue culture flask. Each explant was placed with its luminal surface downward for attachment to the flask, which was kept upright for 3 h to allow the firm attachment of the tissue. Four mL of CM was placed in each flask.

2.2 Trypsinization

Confluent monolayers of cells were routinely trypsinized for either passage or plating for experimentation. In that process, the CM was removed, and the cells were washed three times with 1× phosphate-buffered saline (PBS) and covered with 2 mL of 1% trypsin for approximately 5 s. Excess trypsin was aspired to leave approximately 0.5 mL. The flask was tapped to detach the cells from the wall's surface, and the cells were suspended with CM as necessary for either the flasks or plates. After each trypsinization, the passage number increased by 1.

2.3 Cell Counting

Cell counting is an essential procedure to determine the amount of cells that survive after trypsinization. Following trypsinization, cells diluted in CM were centrifuged, and both the CM and trypsin were removed. The pallet was suspended in 5 mL of CM and mixed. Next, 20 µL of the cell suspension was mixed in an Eppendorf tube with 20 µL of 0.4% trypan blue. A cover glass was centred on the counting chambers of a haemocytometer, which were filled with 20 µL of cell suspension to be counted. Under an OLYMPUS^{TM} electronic microscope, the viable cells appeared translucent, whereas the dead ones were stained blue due to the penetration of trypan blue into the cytoplasm. Surviving cells were counted on the four large outer squares (Figure 9) and the average number calculated per Equation 1. To calculate viable cells in each 1 mL, the average of the cells, which represents 0.1 mm^3, was multiplied by 10,000.

Total cells / mL = Total cells counted × Dilution factor × 10,000 / Number of chambers (1)

Depending on the number of cells per 1 mL, the required cell density to be plated could be calculated.

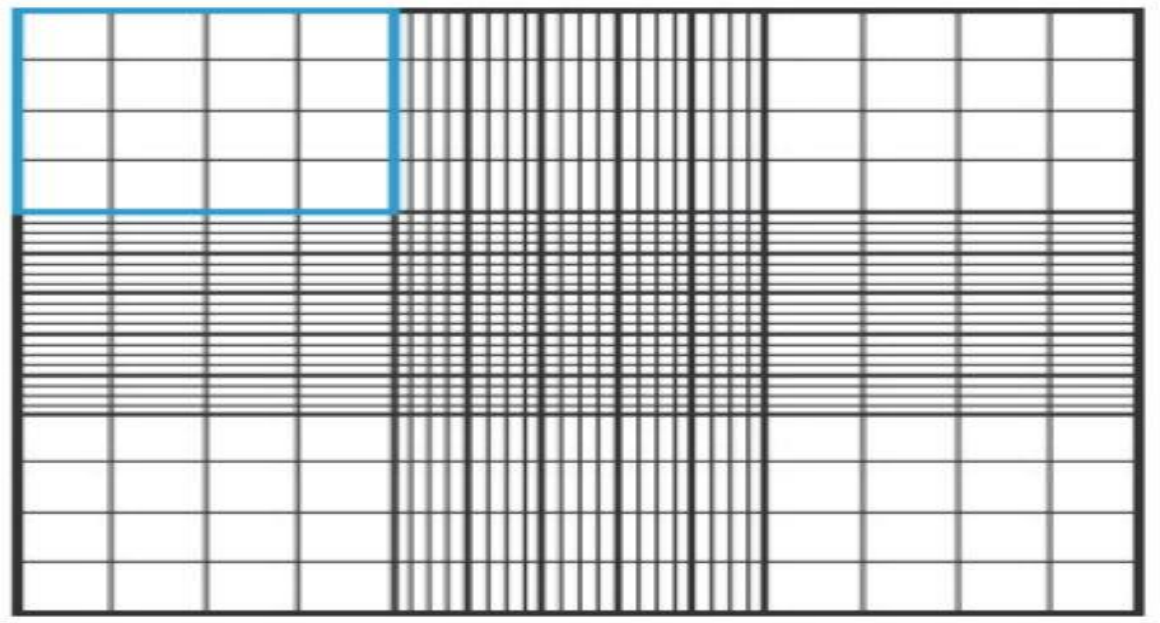

Figure 9. Haemocytometer used for cell counting

2.4 MTT Assay

A 3-(4,5-dimethylthiazol-2yl)-2,5-diphenyltetrazolium bromide (MTT) assay was used to measure the enzymatic activity of the cells to indicate cell viability and the toxicity induced after adding different concentrations of drugs. The calometric assay was based on the reduction of yellow tetrazolium salt 3-(4, 5-dimethylthiazol-2-yl)-2, 5-diphenyltetrazolium bromide to dark blue, water-insoluble formazan crystals by mitochondrial enzyme succinate dehydrogenase, which occurs in living cells (Figure 10).

A 5-mg/mL MTT was prepared by dissolving 0.05 g of MTT in 10 mL of PBS, which was diluted to 1:10 in CM to yield a working stock solution of 0.5 mg/mL.

To determine whether the various drugs used in the experiments caused any cytotoxicity, CM was removed at the end of drug treatment and replaced with 200 µL of 0.5 mg/mL MTT solution. Next, each plate was incubated for 4 h at 37 °C. The MTT solution was subsequently removed, and the purple formazan crystals formed from the metabolism of MTT (Figure 10) were dissolved in 200 µL of isopropanol by placing the plate on a shaker for 15 min. Absorbance was read at 540 nm on a Multiskan II plate reader.

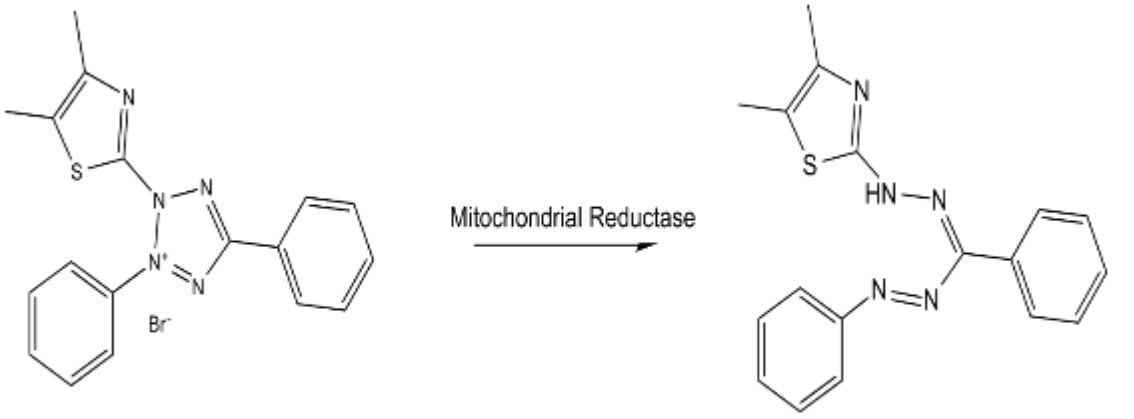

Figure 10. Reduction reaction of MTT to formazan by mitochondrial reductase enzymes

2.5 Activation of Cells with LPS and IFN-γ

Confluent monolayers of cells were treated with LPS (100 µg/mL) and IFN-γ (100 U/mL) for 24 h, after which the CM was collected to analyse nitrite production using Griess assay. Cells were lysed for protein quantification and for western blotting.

2.6 Griess Assay

Griess assay is a spectrophotometric assay to determine nitrite ($NO2^-$) levels. The principle of Griess assay is that unstable NO breaks down to stable measurable nitrite and nitrate. The assay is a diazotisation reaction established by Griess by which nitrite reacts with 0.2% N-1-naphthylethylenediamine dihydrochloride (Griess reagent I) to form a diazonium salt that, in turn, reacts with 2% sulphanilamide (Griess reagent II) in 5% phosphoric acid to produce a pink diazo compound.

After 24 h activation with LPS (100 µg/mL) and IFN-γ (100 U/mL), 100 µL of the CM was removed from each well in triplicate and added to the inner wells of a 96-well plate. Sodium nitrite standards (1–10 nmol/well) were prepared in CM, and 100 µL of Griess reagent (i.e., 2% sulphanilamide amine and 0.2% napthylethylenediamine, plus 10% phosphoric acid) was added to each well. Plates were incubated on a shaker at room temperature for 15 min. Absorbance readings were taken at 540 nm, and the amount of nitrite was calculated using the standard curve (Figure 11).

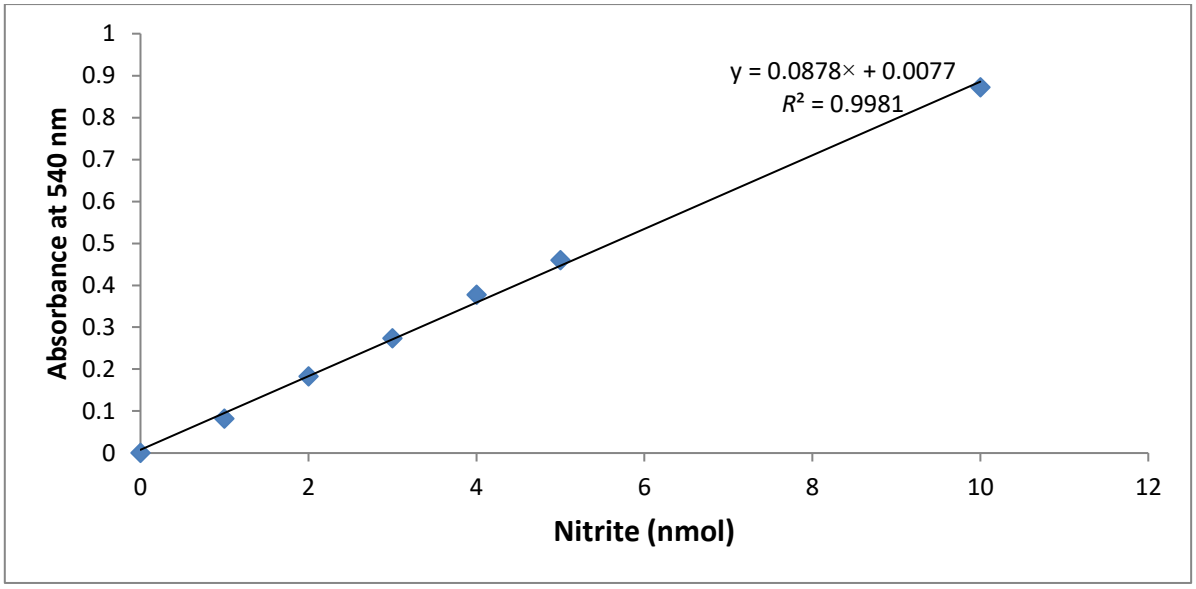

Figure 11. Nitrite standard curve

2.7 Cell Lysis and Protein Quantification

After Griess assay, cells in 24 well plates were washed with 500 µL of 1× PBS. Each well was lysed with hot lysis buffer (2 mM Tris-HCl, pH 7.4 and 1% sodium dodecyl sulphate [SDS]). Cells were scratched, collected in Eppendorf tubes, heated for 5 min at 95 °C, and sonicated for 30 s three times. Tubes were centrifuged for 25 min at 13,226 xg. The supernatant was stored at -20 °C. This procedure was amended for the detection of phospho-proteins by adding a phosphatase inhibitor cocktail (1:100 dilution) to avoid the degradation of phospho-protein.

2.8 Quantification of Total Cell Protein Using Bicinchoninic Acid (BCA)

Quantification assay relied on reducing Cu^{+2} to Cu^{+1} by protein in an alkaline medium with a highly sensitive, selective colourimetric detection of the chelation of Cu^{+1} by BCA reagent, which forms a purple product measured at 620 nm. To determine total cell protein, a protein standard curve was constructed by dissolving 0.01 g of bovine serum albumin (BSA) in 1 mL of distilled water to generate a 10 mg/mL stock solution that was further diluted to produce various concentrations of BSA standards (Table 2).

Table 2. Preparation of standards from a 10 mg/mL BSA stock solution

BSA from stock 0.01 g/mL (µL)	Double-distilled water (µL)	Final concentration (µg/µL)
0.0	1,000.0	0.0
20.0	980.0	0.2
40.0	960.0	0.4
60.0	940.0	0.6
100.0	900.0	1.0
200.0	800.0	2.0

Five µL of each working solution was added in triplicate to the outer wells in 96-well plates together with 5 µL of lysis buffer (1×). Five µL of protein sample was added in triplicate to the inner wells, together with 5 µL of distilled water. The BCA reagent was prepared by adding 9.8 mL of reagent A to 0.2 mL of reagent B, after which 100 µL of the final mix was added to each well. Plates were incubated on a shaker for 45 min and absorbance read at 620 nm. The protein concentration was calculated from the standard curve generated (Figure 12).

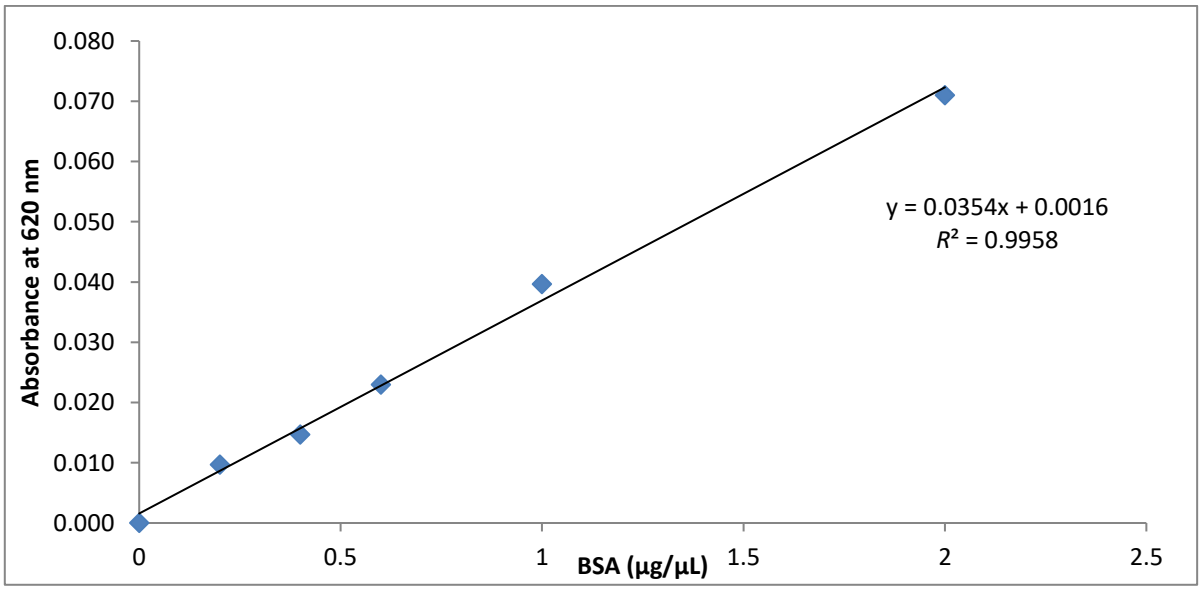

Figure 12. Protein standard curve

2.9 Western Blotting

Western blotting is a semiquantitative method widely used to detect specific proteins in a sample. The procedure involves the preparation of cell lysate samples, protein separation using gel electrophoresis, protein transfer from the gel to a membrane, and the detection of the protein using specific antibodies. Immunoblotting is used to detect protein bands and compare their molecular weight to known sizes of the protein ladder.

2.9.1 Sample and gel preparation

A calculated volume of the sample to load 10 µg of protein per lane was determined and mixed with 1/4 volume of 5× sample buffer, which contained 250 mM of Tris-HCl (pH 6.8) 10% SDS, 30% glycerol, 5% β-mercaptoethanol, and 0.02% bromophenol blue. A Bio-Rad Mini-PROTEAN II system was used for gel electrophoresis and a resolving gel prepared (Table 3). The amounts of reagents used were based on the volume of 10 or 20 mL of gels made.

Table 3. Composition of resolving gels

Resolving gel	10 mL (2 gels)	20 mL (4 gels)
Distilled water	4.64 mL	9.28 mL
30% acrylamide	2.66 mL	5.32 mL
1.5 M Tris-HCl (pH 8.8 at 4 °C)	2.50 mL	5.00 mL
10% SDS stock solution at room temperature	100.00 µL	200.00 µL
10% ammonium persulphate (APS)	100.00 µL	200.00 µL
TEMED (catalytic agent)	6.00 µL	12.00 µL

Ammonium persulfate (APS) and tetramethylethylenediamine (TEMED) were added, and the mixture was immediately poured between the glass plates to form the gels. A small amount of isobutanol was added to the top of the resolving gel to remove air bubbles and isolate the gel from oxygen, which could prevent polymerisation. After the gel set, the isobutanol was removed using filter paper to absorb the solution. The stacking gel was prepared (Table 4) and poured over the resolving gel.

Table 4. Composition of stacking gels

Stacking gel	4 mL (two gels)	10 mL (four gels)
Distilled water	2.44 mL	6.1 mL
30% acrylamide–bisacrylamide mixture	0.52 mL	1.3 mL
0.5M Tris-HCl (pH 6.8 at 4 ºC)	1.00 mL	2.5 mL
10% SDS stock solution at room temperature	40.00 µL	100.0 µL
10% ammonium persulphate (starting agent)	20.00 µL	50.0 µL
TEMED (catalytic agent)	4.00 µL	10.0 µL

To create loading wells for samples, a comb was placed inside the stacking gel and kept in place until the stacking gel set. The gel was placed in the electrophoresis tank and filled with 1% tank buffer (0.025 M Tris, 0.192 M glycine, and 0.1% SDS).

Samples were boiled at 95 °C for 3–5 min before 10 µg of protein was loaded into each well. Ten µL of molecular weight ladder was loaded into the first well. Electrophoresis was initiated by running the gels at 20 mA/gel until the samples ran through the stacking phase and then to 25 mA/gel until the dye front reached the bottom of the gel. The voltage was set at a constant 220 V throughout the process.

2.9.2 Protein transference from gel to polyvinylidene difluoride membrane

Prior to the transfer of proteins, polyvinylidene difluoride membranes were cut, rinsed with 75% methanol for 30 s, and washed with distilled water for a couple of minutes to make the membrane hydrophilic. The gel was placed on the membrane, with three filter papers both above and beneath it. That gel sandwich was assembled on the transfer apparatus and saturated with 1× transfer buffer consisting of 48 mM Tris base (pH 7.5), 39 mM glycine, 0.0375% SDS, and 20% methanol. The transfer apparatus was set to run at a voltage of 25 V for 20–25 min.

2.9.3 Membrane blocking

Blocking buffer was prepared by adding 10 mL of 10× washing buffer (10 mM Tris-base and 100 mM sodium chloride [pH 7.5]), 100 µL of tween 20, 5 g of 5% fat-free milk, and 90 mL of double-distilled water. The fat-free milk was replaced with 5% BSA for the detection of phospho-proteins. The membranes were placed into a plastic box with the blocking buffers and left on the shaker for 1 h.

2.9.4 Incubation with the primary antibody

Five mL of blocking buffer was placed in bijoux, and the relevant primary antibodies were added at the required dilution (Table 5), along with β-actin antibody 1 µL/5,000 µL of blocking buffer. The membranes were placed in a plastic bag together with the antibodies, taped to a shaker, and incubated overnight at 4 °C.

Table 5. Antibodies used

Primary antibody	Dilution	Molecular weight (KDa)	Secondary antibody	Dilution
iNOS	1:2,500	130	Antimouse	1:5,000
P-p38 MAPK	1:1,000	60	Antirabbit	1:2,000
P-Akt	1:1,000	43	Antirabbit	1:2,000
P-PKR	1:1,000	67	Antirabbit	1:2,000
P-EIF2α	1:1,000	38	Antirabbit	1:2,000

2.9.5 Incubation with secondary antibodies

Two L of 1× washing buffer was prepared from a 10× stock (100 mM NaCl, 10 mM Tris [pH 7.4]), and 2 mL of tween 20 was added. The membranes were washed for 10 min with washing buffer three times. Secondary antibodies were prepared (Table 5), and antibiotin 1 µL/1,000 µL blocking buffer was added and incubated for 1 h with the membranes, as

described previously. The membranes were washed for 10 min with washing buffer five times.

2.9.6 Developing the film

The enhanced chemiluminescence solution used to detect the bands was prepared as follows:

- Solution A: 5 mL of 100 mM Tris (pH 8.5), 25 µL/gel of 90 mM p-coumaric acid, and 50 µL/ gel of 250 mM luminol
- Solution B: 5 mL of 100 mM Tris (pH 8.5) and 3 µL of 30% H_2O_2

Solutions A and B were mixed, poured on the membrane in a sandwich box, and incubated for 5 min. The membrane was subsequently placed on a cling film, after which a film strip was cut to size and placed on top of the membrane, and both were transferred into a developing cassette. The film was exposed for 1 min before being developed until the bands appeared. The film was washed with water and placed until transparent. Each film was washed again and left to dry.

2.10. Materials

All materials used in this thesis are presented in the appendix.

2.11. Statistical analysis

Statistical analysis was conducted using Graph Pad Prism 5.0 software. Data are expressed as M ± *SEM*, as indicated for at least three experiments. Data were analysed using one-way analysis of variance (ANOVA), followed by Dunnett's post hoc test.

3. Cell Culture Techniques and Cell Activation Model

3.1. Introduction

Cell culture is an important technique to analyse the biological properties of a targeted cell. Many factors bear critical influence on the quality and success of cell cultures, including the facilities and equipment, the selection of appropriate media and growth conditions for the targeted cell type, propagation, and maintenance of cells for optimal growth.

Good aseptic cell culture techniques produce reliable cultures and, in turn, reliable results. A starting point of the research in this thesis was therefore to develop techniques for isolating smooth muscle cells from explants and culturing them in a healthy state over several passages. Various biochemical protocols were also developed, including the characterisation of isolated smooth muscle cells for α-actin, the induction of nitrite production by Griess assay, the determination of cytotoxicity by MTT assay, and the detection of changes in protein expression by western blotting.

3.2 Materials and Methods

3.2.1 Characterisation of RASMCs

Smooth muscle cells are identified and characterised by the presence of α-smooth muscle actin, which distinguishes them from morphologically similar cells such as fibroblasts (Skalli *et al.*, 1986; Hofmann & Goger, 1976). To ensure that cells routinely isolated were smooth muscle cells, cultures were frequently stained for α-actin. For that assay, cells at passages 3–6 were seeded at low density in CM in Lab-Tek wells and allowed to grow to roughly 50% within 2–3 d. The medium was removed, and the cells were washed twice with 1× PBS prior to fixing with ice-cold 100% methanol for 20 min. The fixed monolayers were blocked for 30 min with 5% BSA dissolved in 1× PBS and incubated for 1 h with an anti-SM22 alpha antibody diluted to 1:200 in 5% BSA in PBS. The cells were washed four times with BPS every 5 min prior to incubation with a 1:500 dilution of the secondary antibody goat and antirabbit IgG secondary antibody (Alexa Fluor® 488) at a dilution of 1:1,000 in 5% BSA.

The cells were mounted with a drop of 100% glycerol and covered with a cover slip before visualisation with a Nikon Confocal Microscope TE-2000 U at a magnification of 100×.

3.2.2 Different seeding densities for nitrite measurement

RASMCs were isolated and cultured in CM, as described in section 2.1. Cells were plated in 24-well plates at different seeding densities ranging from 10,000 to 600,000 cells per well, allowed to grow for 3 d, and activated with 100 µg/mL of LPS and 100 U/mL of IFN-γ for 24 h. The CM was collected for nitrite measurement by Griess assay following the method described in section 2.6. Then, 75,000 cells per well were cultured, as determined from studies described in section 3.2.2.1. They were allowed to grow to confluence over 3 d, after which they were activated with 100 µg/mL of LPS and 100 U/mL of IFN-γ for 24 h. The CM was collected for nitrite measurement by Griess assay following the method described in section 2.6. The expression of iNOS was determined by western blotting following the method described in section 2.9.

3.3 Results

3.3.1 Culture of smooth muscle cells from rat aortic explants

As stated in section 2.1, SMCs were cultured from rat aorta using explants stripped of adipose tissue and endothelium. As Figure 13 shows, the incubation of explants in CM resulted in the migration of SMCs from the aortic tissue onto the plastic, which was evident from Day 7 from the migration and proliferation of cells over time. The cells showed a polygonal, epithelioid shape, but were not tightly packed, thereby exhibiting the characteristic spindle shape of SMCs (Figure 13; also see Figure 14A). The cultures were routinely trypsinized and subcultured to expand the cell number and ensure that sufficient cells were

derived for use in experiments. In culture, the cells proliferated in a uniform monolayer to reach full confluency in 3–4 d (Figure 14B).

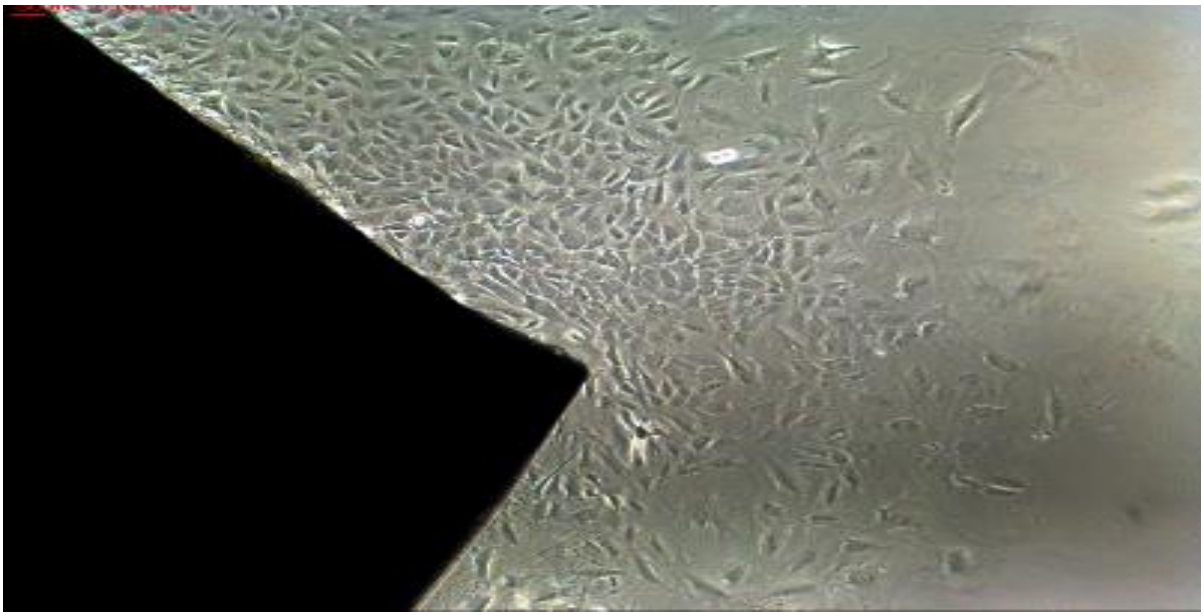

Figure 13. Migration of RASMCs from explants in culture. Rat aorta were stripped of the fat surrounding the outer wall and of the endothelium in the luminal surface. Each aorta was cut into 2-mm pieces, which were plated in T25 flasks, and left to grow for 2–3 weeks, with the media replaced every 3 d. The migration and growth of cells were monitored via observation under an OLYMPUS™ electronic microscope at a magnification of 40×. The image in Figure 13 was taken during week 2.

3.3.2 Growth and morphology of RASMCs in culture

Cells at passages 3–6 were used in 24-well plates in all experiments. For the experiments reported in this section, cells were seeded at 75,000 cells per well and allowed to grow to confluency, while under daily observation with an OLYMPUS™ electronic microscope. Figure 14A illustrates the cells in the subconfluent stage of growth 24 h after plating, whereas Figure 14B shows the cells in the confluent stage of growth 3–4 d after being plated. As previously described, the cells exhibited a polygonal, epithelioid shape with the characteristic spindle shape of SMCs, particularly when the cultures appeared as single cells (Figure 14A).

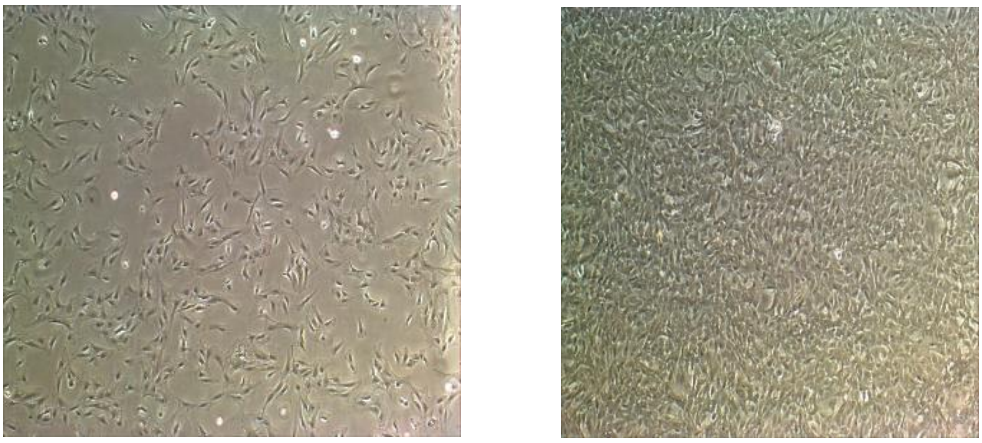

(A) (B)

Figure 14. Growth and morphology of RASMCs in culture. RASMCs at passage 3 were seeded at a density of 75,000 cells/mL and cultured to confluency for 3–4 d in a 24-well plate. The growth medium in the flask was replenished every 2 d. The initial growth and confluent stages were confirmed through the observation of cells under an OLYMPUS™ electronic microscope at a magnification of 40×. Figure 14A is a photograph taken after 24 h of plating cells, whereas Figure 14B was taken 3 d after the cells were subcultured and had reached confluency.

3.3.3 Effects of seeding density on NO production in RASMCs

This study involved investigating the effect of cell seeding density on the ability of RASMCs to induce NO when stimulated with LPS and IFN-γ. Cells were seeded at densities ranging from 10,000 –600,000 cells per well in a 24-well plate before being activated with LPS (100 μg/mL) and IFN-γ (100 U/mL) for 24 h. Results shown in Figure 15 clearly demonstrate that cell seeding density does indeed affect responses to LPS and IFN-γ. As Figure 15 demonstrates, hardly any nitrite was detectable above basal when cells were plated at 10,000 per well. The marginal increase at 50,000 cells per well became even more pronounced at 100,000 cells per well and further increased marginally up to 600,000 cells per well. Higher seeding densities, however, caused cells to reach full confluency far more quickly than desired. To prevent that effect in additional studies, a seeding density of 75,000 cells per well

was selected, at which cell monolayers were well maintained and nitrite production was significantly above basal levels.

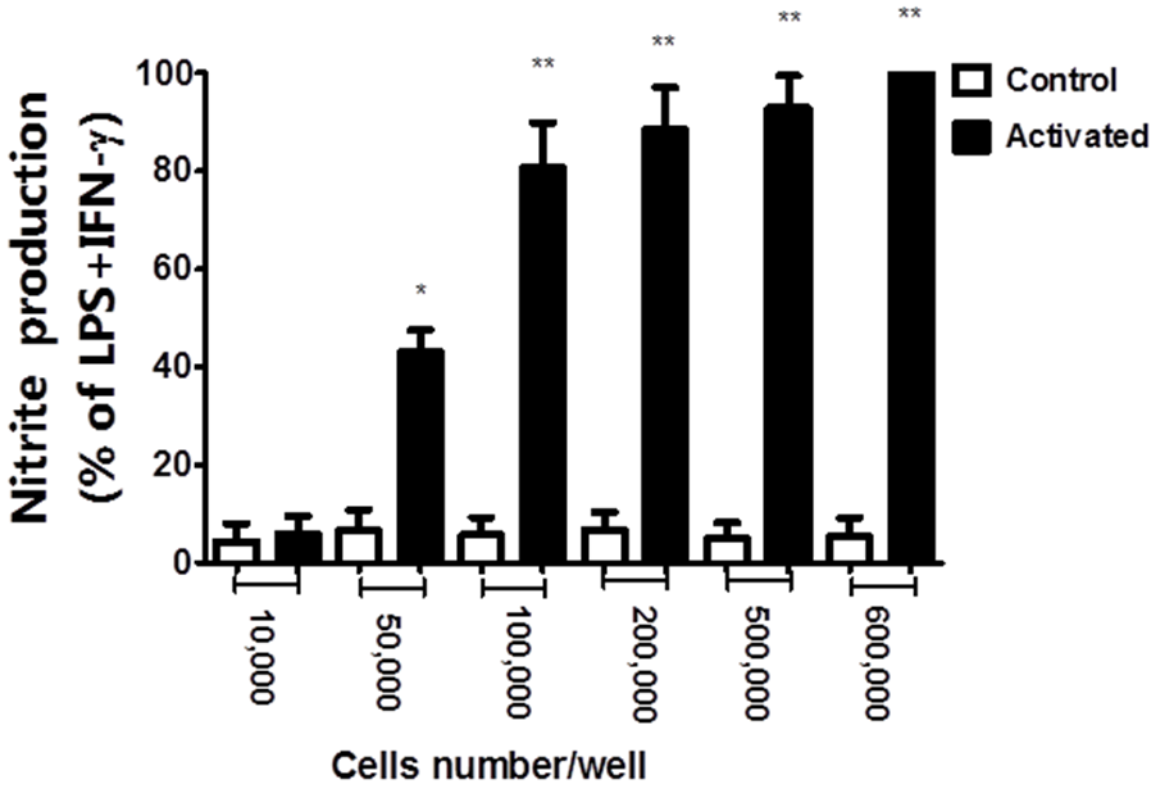

Figure 15. Effect of cell seeding density on nitrite production in RASMCs. Different densities of RASMCs were plated in 24-well plates for 3 d, after which they were activated with 100 µg/mL of LPS and 100 U/mL of IFN-γ for 24 h. The culture medium was analysed by Griess assay to determine total nitrite levels following the method described in section 2.6. Data are expressed as a percentage of nitrite production, with the response to LPS (100 µg/mL) plus IFN-γ (100 U/mL) at the higher seeding density of 600,000 cells taken as 100%. Data show the M ± SEM of at least three independent experiments. Statistical differences were determined by one-way ANOVA, followed by Dunnett's multiple comparisons test of the normalised data; * denotes $p < .05$ and ** $p < .01$, both compared to t control.

3.3.4 Characterisation of RASMCs by staining for α-actin

To further characterise cells isolated from the aorta, cultures were stained for α-actin. Figure 16 shows that nonconfluent monolayers of cells displayed spindle morphology that, more

importantly, fluoresced green under ultraviolet light when probed with an anti-α-antibody, which confirms that the cells isolated were smooth muscle cells.

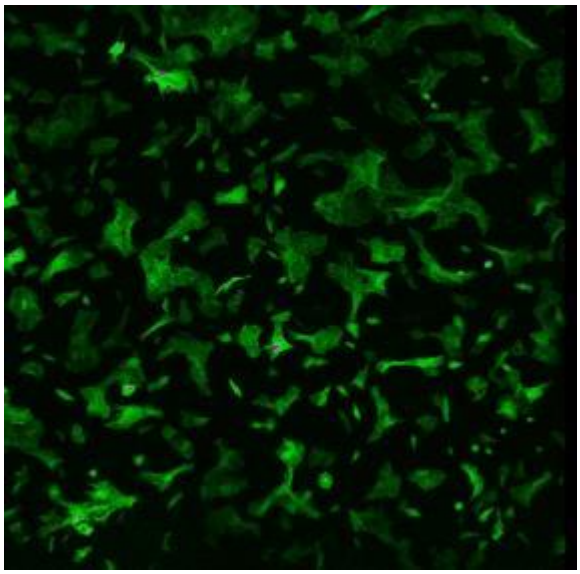

Figure 16. Morphology and α-actin staining of RASMCs. Smooth muscle cells at passage 4 cultured in Lab-Tek wells were stained for α-actin using a selective anti-α-actin antibody as described in section 3.2.1. Taken under a Nikon confocal microscope, the photograph represents at least three experiments performed at different passages and times

3.3.5 Induction of iNOS and NO production by LPS and IFN-γ in cells seeded at 75,000 cells per well

In additional experiments, cells were plated at a density of 75,000 cells per well in a 24-well plate and allowed to reach confluency before being activated with 100 µg/mL of LPS and 100 U/mL of IFN-γ for 24 h. Nitrite production was measured by Griess assay and iNOS expression was determined using western blotting following methods described in sections 2.6 and 2.9, respectively. Control nonactivated cells, activated with IFN-γ or with LPS alone produced little or no nitrite (Figure 17) or iNOS expression (Figure 18), in contrast to a marked detection of nitrite and iNOS when LPS was used in combination with IFN-γ.

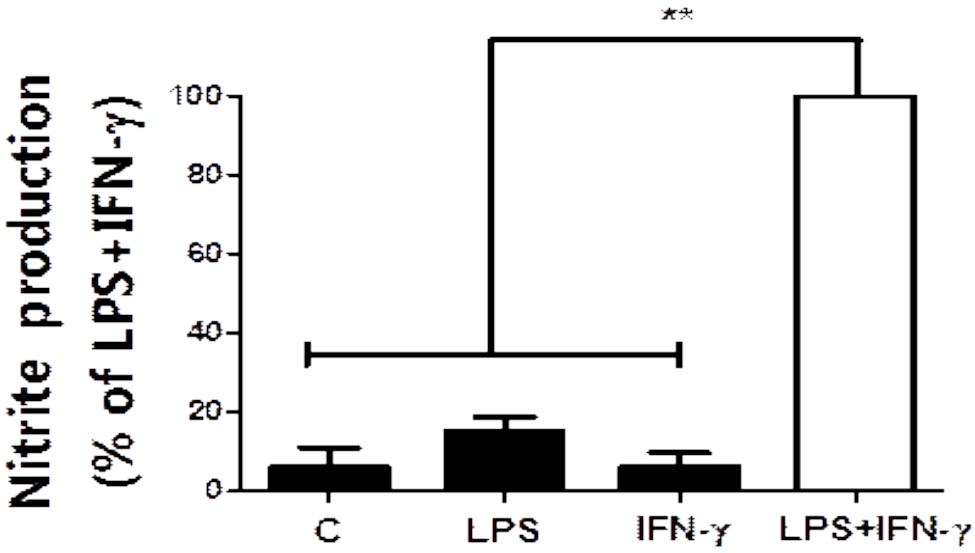

Figure 17. Induction of NO by LPS and IFN-γ in RASMCs. Confluent monolayers of RASMCs in 24-well plates were activated with 100 μg/mL of LPS or 100 U/mL of IFN-γ or both for 24 h. The culture medium was analysed by Griess assay to determine total nitrite levels following the method described in section 2.6. Data are expressed as a percentage of nitrite production, with the response to LPS (100 μg/mL) plus IFN-γ (100 U/mL) taken as 100%. Data show the M ± SEM of at least three independent experiments. Statistical differences were determined by one-way ANOVA, followed by Dunnett's multiple comparisons test of the normalised data; ** denotes $p < .01$ compared to the activated control.

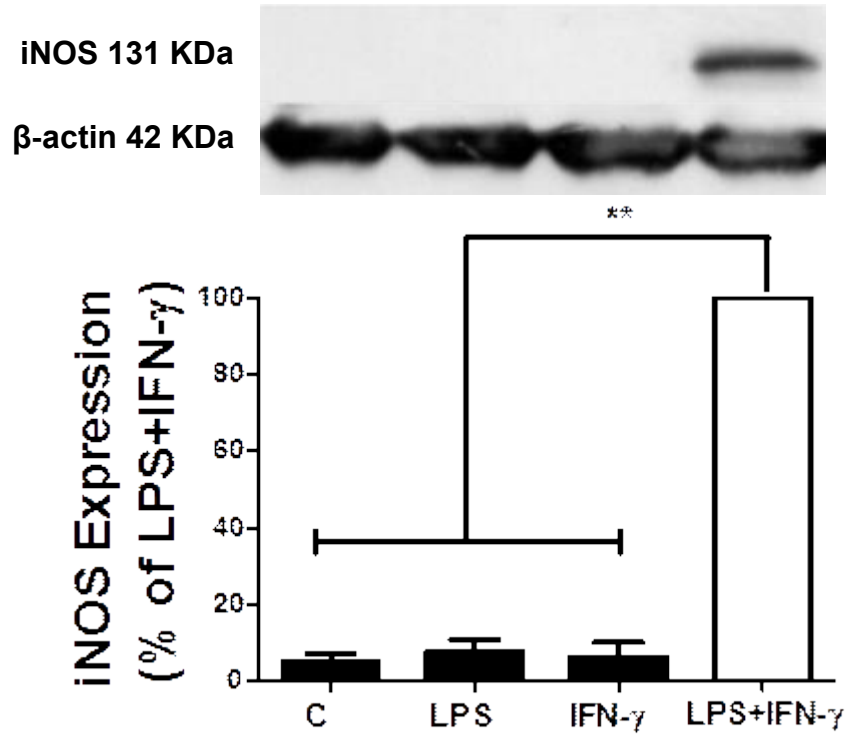

Figure 18. Induction of iNOS expression by LPS and IFN-γ in RASMCs. Confluent monolayers of RASMCs in 24-well plates were activated with 100 μg/mL of LPS or 100 U/mL of IFN-γ or both for 24 h. The expression of iNOS was determined by western blotting following the method described in section 2.9. The blot is representative of at least three independent experiments, and the bar graph depicts densitometric data expressed as a percentage of iNOS expression, with the response to LPS (100 μg/mL) plus IFN-γ (100 U/mL) taken as 100%. Data represent the M ± SEM of at least three independent experiments. Statistical differences were determined by one-way ANOVA, followed by Dunnett's multiple comparisons test for normalised data; ** denotes $p < .01$ compared to the activated control.

3.4 Discussion

The experiments described in this chapter were performed to establish the cell culture model needed to conduct the research of this thesis. The key aims were to develop good aseptic cell culture techniques, as well as to establish a model for the consistent, sustained induction of iNOS. The latter is critical as the bulk of the studies are focused on establishing how the induction of iNOS and thus NO may be regulated by GCs, distinguishing between different molecules within this class of compounds. The importance of this regulation derives from the fact that iNOS is widely expressed under inflammatory conditions and that the NO that iNOS produces could play a critical role in mediating some deleterious effects associated with inflammation. Although GCs are routinely used in inflammatory disease states, their precise mechanism of action, which potentially includes regulating iNOS expression, remains to be fully established.

All of the studies described in this thesis were performed in smooth muscle cells characterised well in terms of iNOS expression in vascular inflammation. Smooth muscle cells were isolated from rat aortas using explants, which constitute a well-established method of generating viable cultures of cells that respond readily to inflammatory mediators in order to express iNOS. In culture, the isolated cells grew as a monolayer and were characterised by their polygonal, epithelioid shape, with single cells that showed characteristic spindle-shaped morphology, as confirmed with photographs of routine cultures that showed the cells' characteristic morphology.

Other than morphology, the smooth muscle cells were also characterised in terms of α-actin. It is essential to rely not only on morphology, since smooth muscle cells can be indistinguishable from fibroblasts based on morphology alone (Hofmann & Goger, 1976). Ultimately, the incubation of isolated cultures with an anti-α-actin antibody stained positively for α-actin, thereby confirming smooth muscle cells. More importantly, the entire monolayer stained positive, which suggests little or no contamination of cultures with other cell types.

Good aseptic cell culture techniques were also developed to ensure that cells could be maintained in continuous culture without being contaminated with microorganisms such as bacteria, fungus, and yeast. Each cell isolate was successfully cultured over several passages without infection or loss of morphology.

To study the induction of iNOS, the first step was to determine which cell seeding density range would yield detectable, reproducible levels of NO. Without that consideration, inconsistent high seeding density would make cells overly confluent too quickly before being fully established. Otherwise, too few cells could fail to respond adequately to inflammatory mediators. Accordingly, the experiments involved examining various seeding densities to determine the number of cells that would allow full establishment without becoming overly confluent, as well as respond effectively to LPS and IFN-γ in order to express iNOS and NO production. To that end, seeding densities used ranged from 10,000 to 600,000 cells per well. Ultimately, the lowest plating density was inadequate because nitrite production was barely above basal levels. At higher densities, by contrast, nitrite was detectable, but cells became overly confluent too early, which caused cell loss and inconsistent results. A plating density of 75,000 cells per well was thus chosen as the ideal seeding density, for it achieved 100% confluency within 3–4 d and showed a consistent induction of nitrite production and iNOS protein expression.

Other studies with different cell types have also recognised the importance of cell density on cellular function and integrity. For example, high seeding density has been shown to enhance the differentiation of osteoprogenitor marrow stromal cells, yet also diminish proliferation. Low seeding density, by contrast, diminishes both elements and can cause poor intercellular communication, whereas high seeding density might produce an unfavourable microenvironment (Goldstein, 2001).

Still other studies have found that cell seeding density can affect the expression of some genes. For example, in cultured granulosa cells, the ratio of oestrogenic to progestagenic enzyme was altered according to variation in cell density (Portela et al., 2010). In RASMCs, low cell density and repeated cell passage caused a loss of protein kinase G1, which led to the proliferation of vascular smooth muscle cells (Lin et al., 2004). Since such results confirm seeding density's effects on normal intercellular function and communication, the plating of a suitable cell number is critical in obtaining consistently reliable results.

Since cell density affects the targeted duration of confluency, it is essential to choose a seeding density that allows sufficient time for cells to be established but not fail to grow to confluency. Accordingly, the seeding density selected for the experiments in this thesis was 75,000 cells per well, which allowed confluency within 3–4 d. By contrast, reaching confluency too early (1–2 d) or too late (>5 d) would have an undesirable impact on cells. Since studies have shown that trypsinization suppresses bradykinin receptors, if cells are not allowed sufficient time to re-establish after treatment with trypsin, then they might fail to respond to bradykinin (Sung et al., 1989). Rapid excess confluency can also arrest growth due to contact inhibition and, in turn, cell senescence and death. However, too few cells might take longer to establish and grow to confluency, which could prompt cell ageing and senescence and thereby alter the biological function of affected cells. As a result, 75,000 cells per well were chosen because a lower seeding density resulted in inadequate NO production. In contrast, higher seeding densities caused the cells to reach confluence early and this may affect their response to treatment.

A multitude of stimuli have been used to induce the expression of iNOS and thus NO production in various types of cells. They include LPS (Liu et al., 2010), and granulocyte–macrophage colony-stimulating factor (Cruz et al., 2001). In addition, cytokines such as IFN-γ, TNF-α, IL-1-β, and IL-6 have also demonstrated the capability to induce NO production by

inducing iNOS expression (Kleinert et al., 2003). The stimuli used are often determined by the cell type being investigated, and routinely, smooth muscle cells are activated with LPS and a cytokine. In the laboratory used for the experiments in this thesis, the cytokine of choice was IFN-γ, which is reported to stabilise iNOS mRNA and potentiate the effects of LPS (Weisz et al., 1994). Accordingly, experiments involved gauging responses to LPS alone, IFN-γ alone, and a combination of the two. Controls were incubated with CM only.

The results obtained confirmed previous reports that no significant amounts of NO or iNOS expression can be detected with either LPS or IFN-γ alone. However, their combination can generate a profound induction of iNOS and thus NO production, as consistent with previous results concerning RASMCs (Baydoun et al., 1999). The combination of LPS and IFN-γ is required not only for RASMCs, but for several other types of cells as well, including C6 astroglioma cells and astrocytes (Bonafini et al., 2015; Nicoletti et al., 1998).

IFN-γ can stabilise iNOS mRNA, as explained earlier, as well as decrease the anti-inflammatory interleukin 10 (Schroder et al., 2004), which has been found to inhibit LPS-induced iNOS (Molina–Holgado et al., 2001). It is thus likely that inhibiting IL-10 can also enhance iNOS expression. The effect of IFN-γ is mediated by glycogen synthase kinase-3 (Lin et al., 2008), although whether IFN-γ acts via that mechanism in inducing iNOS in smooth muscle cells remains unclear.

In sum, cell culture techniques have been developed and optimised for culturing smooth muscle cells from rat aortic explants. Generated cells were successfully used to establish the model for inducing iNOS and NO production using the combination of LPS and IFN-γ, which provided a basis for the detailed studies of the induction of iNOS by GCs, as described in the following chapters.

4. Effect of GCs on iNOS Expression and Function

4.1 Introduction

Produced naturally by the adrenal cortex, although also able to be synthesised and manufactured, GCs are steroid hormones commonly described as double-edged swords given their therapeutic benefits as well as undesirable effects. One endogenous GC is cortisol, or hydrocortisone, whereas dexamethasone, one of the most widely studied compounds in the group, is a synthetic GC (Coutinho & Chapman, 2011) that facilitates anti-inflammatory and immunosuppressant effects and helps to relieve inflammation (e.g., swelling, heat, redness, and pain).

Given their potent anti-inflammatory action, GCs have been used extensively in inflammatory diseases such as asthma, RA, inflammatory skin disorder, and inflammatory bowel disease. All of those diseases have been associated with the induction of iNOS, which makes it likely that GCs' therapeutic benefits involve the regulation of iNOS expression and function. This is however not conclusive in every instance but interest in the ability of GCs to regulate iNOS has been significant.

GCs have been shown to inhibit iNOS expression and function in many different cell types, including hepatocytes (Geller et al., 1993), RASMCs (Wileman et al., 1995), murine macrophage cell line (Baydoun et al., 1993; Walker et al., 1997), embryonal cortical neurons (Golde et al., 2003), and mesangial cells (Kunz et al., 1996). Inhibitions have been shown not only with dexamethasone, but also with hydrocortisone (Suzuki et al., 1994).

The underlying mechanisms that mediate the action of dexamethasone appear to differ by cell type. Although it reduces iNOS transcriptionally by inhibiting NF-κB in RASMCs (Matsumura et al., 2001), rat hepatocytes (De Vera et al., 1997), human A549/8 cells (Kleinert et al., 1996), and RAW 264.7 cells (Jeon et al., 1998), the expression of iNOS in C6 glioma cells was inhibited by dexamethasone at the post-transcriptional level, given that the GC reduced iNOS protein expression significantly but showed negligible effects on its mRNA (Shinoda et al., 2003). Dexamethasone has also been reported to destabilise iNOS

mRNA in macrophages (Korhonen et al., 2002; Söderberg et al., 2007). This observation contradicts those made in our laboratory which revealed that dexamethasone enhanced iNOS mRNA expression but block expression of the protein (Thakur & Baydoun, 2012). Such inconsistent reports underscore that dexamethasone's mechanism of action remains unclear and requires further investigation. Whether other GCs such as hydrocortisone and fluticasone act on any of the above mentioned targets also remains to be established. Perhaps more important, however, is determining whether the transcriptional and post-transcriptional effects already described reflect a true GC action. Such research matters because, as already highlighted, both dexamethasone and hydrocortisone are not selective GCs and act on steroid receptors (Bigsby, 1993; Born et al., 1987; Inder et al., 2010; Karaliset al., 1996; Lan et al., 1982; Sonneveld et al., 2005; Yang et al., 2001). Establishing whether the regulation of iNOS induction occurs via a GC action has therefore been a primary objective of this thesis, starting by comparing the effects of dexamethasone and hydrocortisone, as nonselective GCs, with those of fluticasone, a known selective GC, on the regulation of iNOS expression and function. The studies in this chapter have also been developed to explore potential cellular mechanisms that might mediate the effects of GCs. The data of those studies appear in subsequent chapters.

4.2 Material and Methods

4.2.1 Experimental conditions

4.2.1.1 Time dependent induction of iNOS and NO production in activated RASMCs

To determine the optimal time point for iNOS expression, time course studies were performed by assessing nitrite production over a 24-h period. In the experiments, confluent monolayers of RASMCs were treated with LPS (100 μg/mL) and IFN-γ (100 U/mL) at different time points ranging between 1–24 h. The culture medium was analysed by Griess

assay, following the method described in section 2.6, while the expression of iNOS was determined through western blotting, following the method described in section 2.9.

4.2.1.2 Effect of dexamethasone on NO production and iNOS expression

Confluent monolayers of cells were preincubated with dexamethasone at a concentration of 0.1–10.0 µM; hydrocortisone (0.01–10.00 µM) or fluticasone (1 nM–3 µM) for 30 min prior to activation with LPS (100 µg/mL) and IFN-γ (100 U/mL) for 24 h. NO production and iNOS expression were determined by Griess assay and western blotting, respectively, following methods described in sections 2.6 and 2.9, also respectively. MTT assay, as described in section 2.4, was also performed to determine whether any of the observed effects with dexamethasone were associated with cytotoxicity.

4.3 Results

4.3.1 Effects of GCs on the viability of RASMCs

Experiments were conducted to determine whether different concentrations of the GCs studied exerted a cytotoxic effect. Control cells were considered 100% viable and compared to the different concentrations of dexamethasone (Figure 19), hydrocortisone (Figure 20), and fluticasone (Figure 21), with and without the activation of cells. Although a decrease in MTT metabolism was observed, it was marginal and not statistically significant in any concentration used. The full concentration range of each compound was thus used in subsequent experiments.

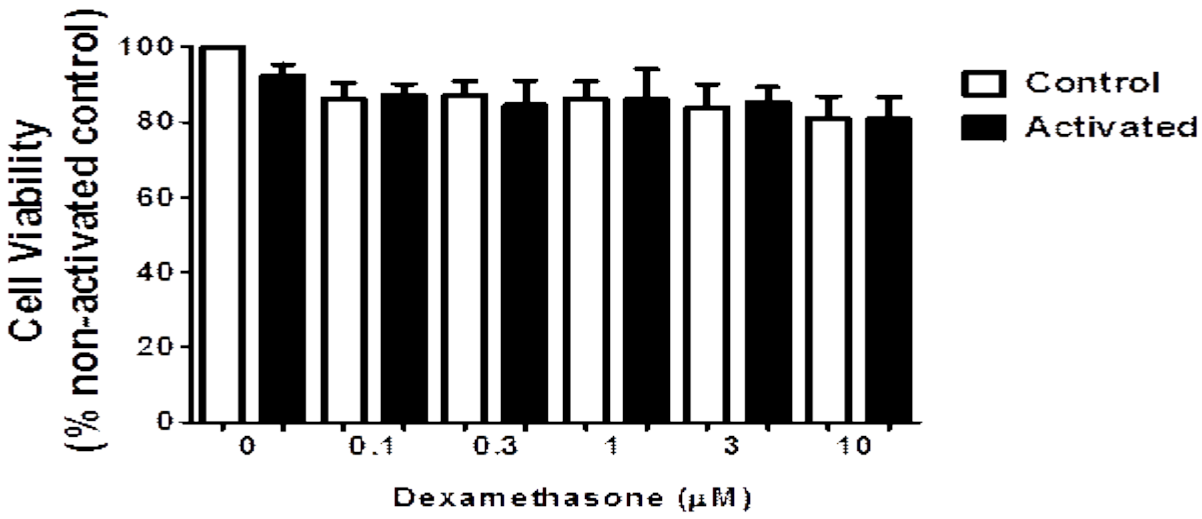

Figure 19. Effect of different concentrations of dexamethasone on the viability of RASMCs. Confluent monolayers of RASMCs in a 96-well plate were pretreated with either CM or with different concentrations of dexamethasone (0.1–10.0 μM) for 30 min prior to activation with both LPS (100 μg/mL) and IFN-γ (100 U/mL) for 24 h. The metabolism of MTT was determined colourimetrically following the method described in section 2.4. The white bars represent controls, and the black ones represent activated cells. Data are presented as the percentage of viable cells compared to controls and represent the M ± SEM of at least three individual experiments. Statistical differences were determined by one-way ANOVA, followed by Dunnett's multiple comparisons test of the normalised data; $p > .05$ confirmed that there was no significant difference compared to the nonactivated control.

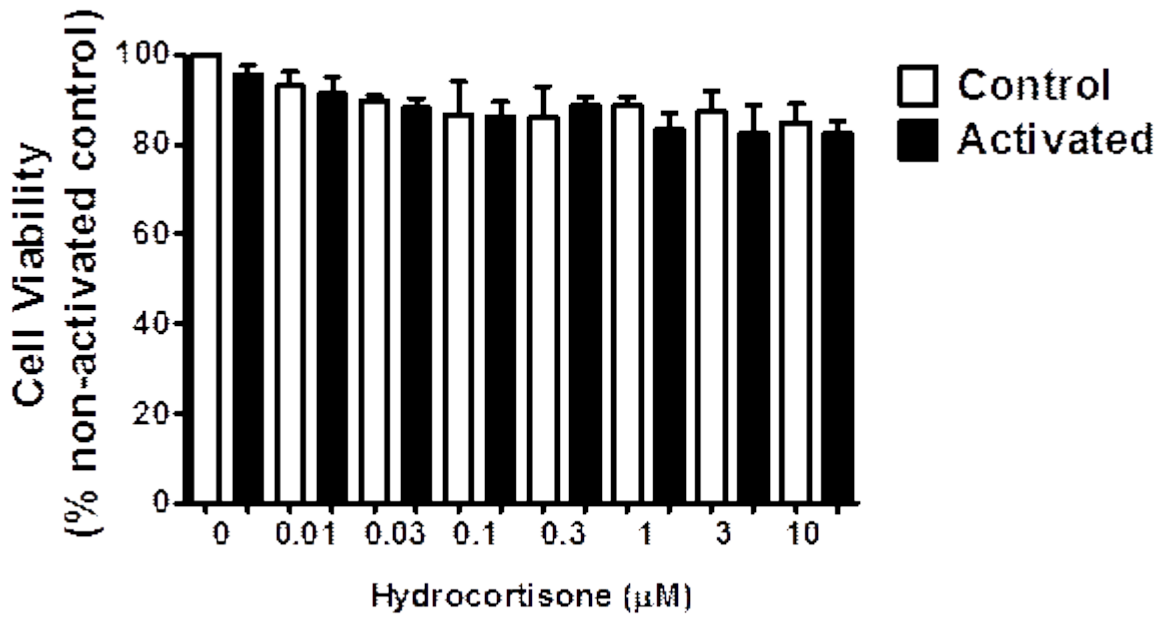

Figure 20. Effect of different concentrations of hydrocortisone on the viability of RASMCs. Confluent monolayers of RASMCs in a 96-well plate were pretreated with either CM or with different concentrations of hydrocortisone (0.01–10.0 μM) for 30 min prior to activation with both LPS (100 μg/mL) and IFN-γ (100 U/mL) for 24 h. The metabolism of MTT was determined colourimetrically following the method described in section 2.4. The white bars represent controls, and the black ones represent activated cells. Data are presented as the percentage of viable cell compared to the controls and represent the M ± SEM of at least three individual experiments. Statistical differences were determined by one-way ANOVA, followed by Dunnett's multiple comparisons test of the normalised data; $p > .05$ confirmed that there was no significant difference compared to the nonactivated control.

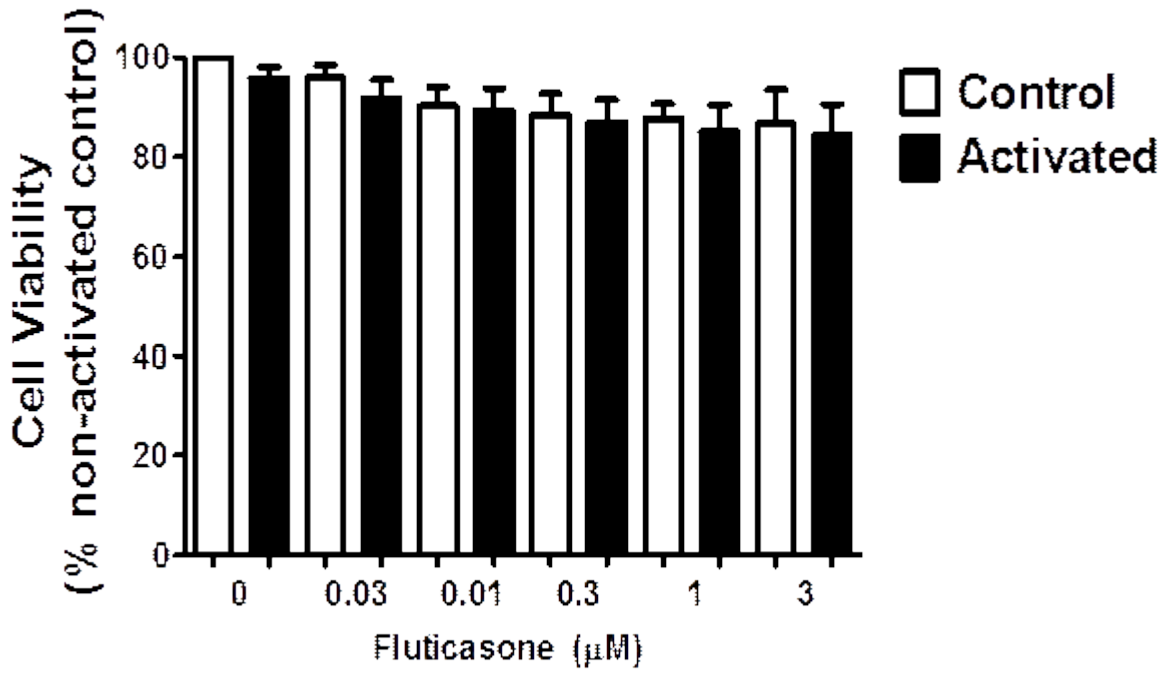

Figure 21. Effect of different concentrations of fluticasone on the viability of RASMCs. Confluent monolayers of RASMCs in 96-well plate were pretreated with either CM alone or with different concentrations of fluticasone (0.03–3.00 μM) alone for 30 min prior to activation with both LPS (100 μg/mL) and IFN-γ (100 U/mL) for 24 h. Metabolism of MTT was determined colourimetrically following the method described in section 2.4. The white bars represent controls, and the black ones represent activated cells. Data are presented as the percentage of viable cells compared to the controls and represent the M ± SEM of at least three individual experiments. Statistical differences were determined by one-way ANOVA, followed by Dunnett's multiple comparisons test of the normalised data; $p > .05$ confirmed that there was no significant difference compared to the nonactivated control.

4.3.2 Time dependent induction of iNOS and NO production in activated RASMCs

To identify the optimal time point for iNOS expression and NO production, candidate time points of activation with LPS and IFN-γ during a 24-h period were examined. Nitrite was clearly detected after 12 h of activation and increased in a time dependent manner past 24 h postactivation (Figure 22). A similar trend was found with iNOS expression, which emerged at 12 h and increased steadily during the remainder of the 24-h period (Figure 23).

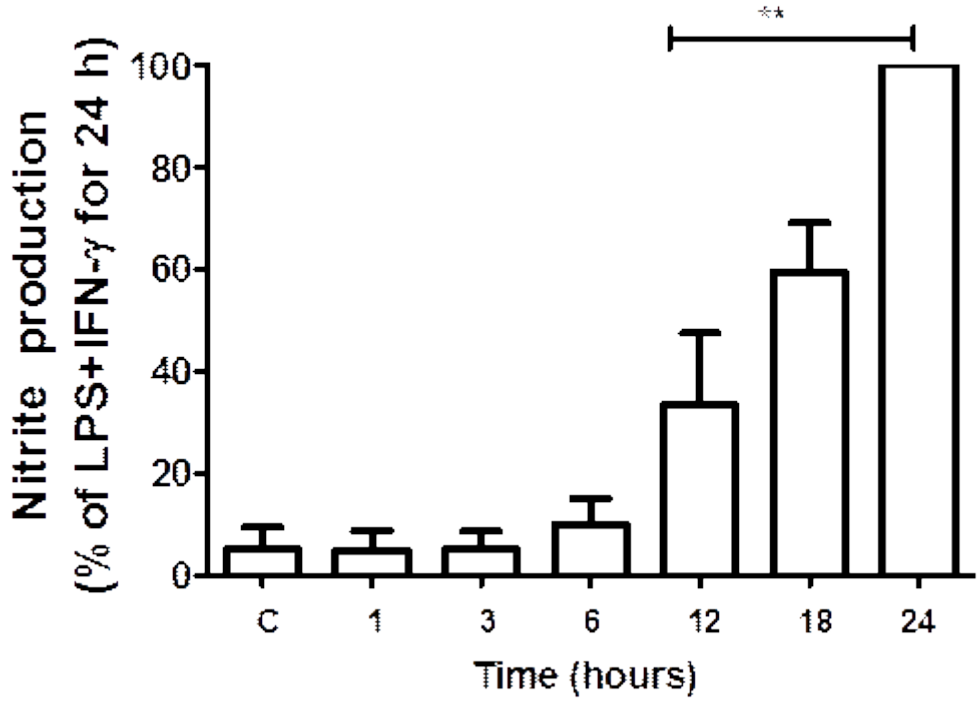

Figure 22. Time dependent increase in nitrite production in activated RASMCs. Confluent monolayers of RASMCs in a 24-well plates were activated with a combination of LPS (100 μg/mL) and IFN-γ 100 U/mL at different time points. The culture medium was analysed by Griess assay to determine total nitrite levels following the method described in section 2.6. Data are expressed as the percentage of nitrite production, with the response to LPS (100 μg/mL) plus IFN-γ (100 U/mL) for 24 h taken as 100%. Data are the M ± SEM of at least three independent experiments. Statistical differences were determined by one-way ANOVA, followed by Dunnett's multiple comparisons test of the normalised data; ** denotes $p < .01$ compared to the control.

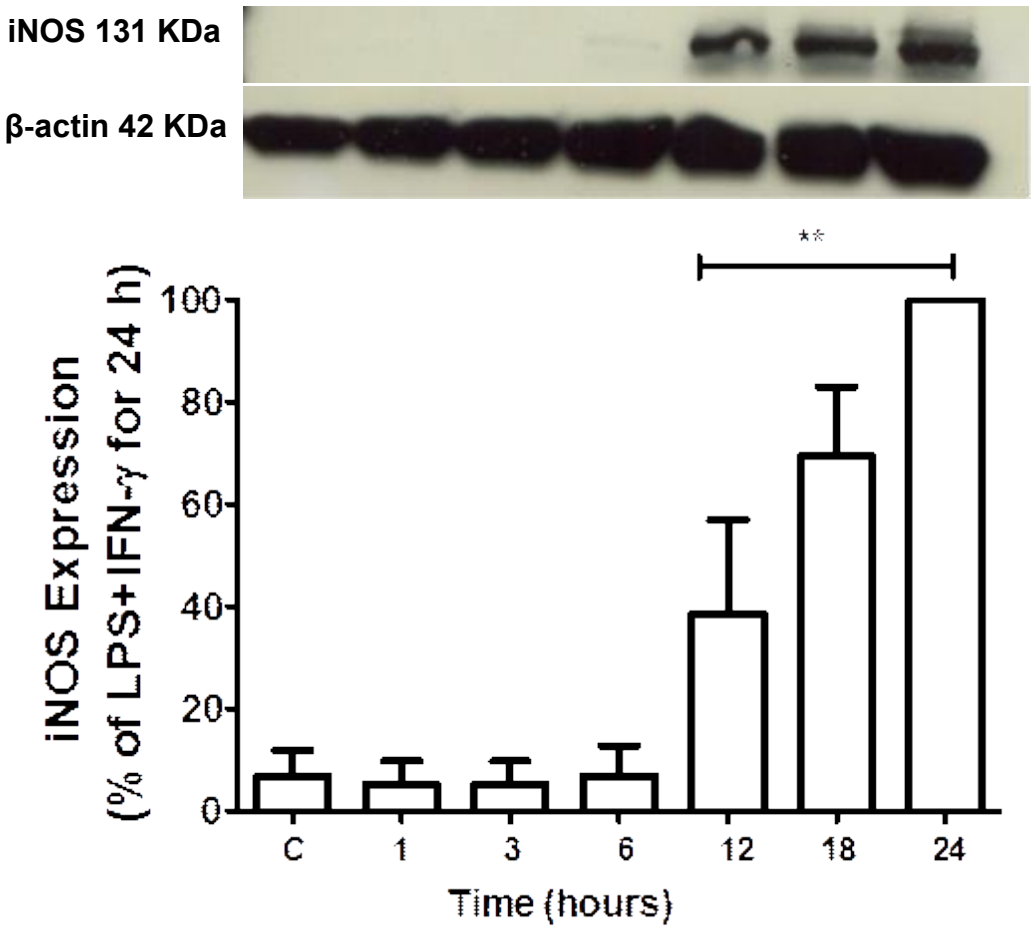

Figure 23.Time dependent increase in iNOS expression in activated RASMCs. Confluent monolayers of RASMCs in 24-well plates were activated with a combination of LPS (100 μg/mL) and IFN-γ (100 U/mL) at different time points. The expression of iNOS was determined by western blotting following the method described in section 2.9. The blot is representative of at least three independent experiments, and the bar graph depicts densitometric data expressed as a percentage of iNOS expression, with the response to LPS (100 μg/mL) plus IFN-γ (100 U/mL) for 24 h taken as 100%. Data represent the M ± SEM of at least three independent experiments. Statistical differences were determined by one-way ANOVA, followed by Dunnett's multiple comparisons test for normalised data; ** denotes $p < .01$ compared to the control.

4.3.3 Effects of dexamethasone on NO production

To confirm that dexamethasone can regulate induced nitrite production, cells were pretreated with the compound (0.1–10.0 µM) 30 min prior to activation with 100 µg/mL of LPS and 100 U/mL of IFN-γ for 24 h. An increased concentration of dexamethasone decreased nitrite production in a concentration dependent manner. The nitrite level was decreased from 17.3 ± 2 to 1.4 ± 1.1 nmol/ml at 10 µM dexamethasone. The decrease in NO production was statistically significant at concentrations of ≥0.3 µM compared to levels detected with LPS or IFN-γ alone.

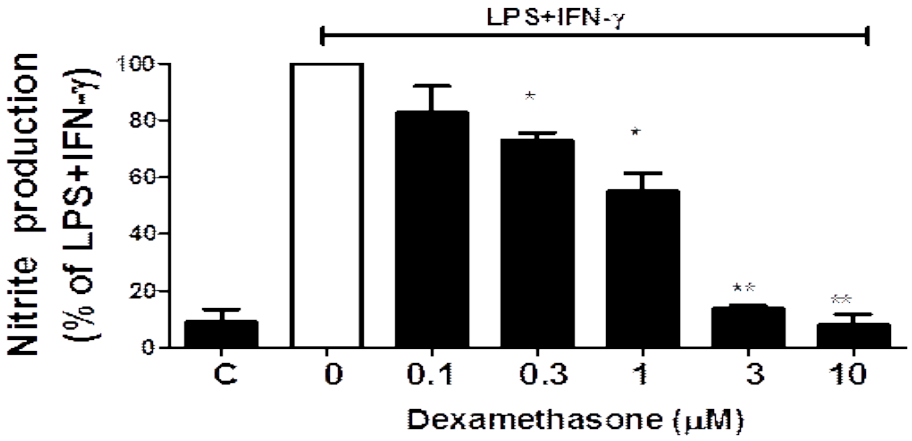

Figure 24. Effect of different concentrations of dexamethasone on nitrite production. Confluent monolayers of RASMCs in 24-well plates were pretreated with concentrations of dexamethasone for 30 min before activation with 100 µg/mL of LPS and 100 U/mL of IFN-γ for 24 h. The culture medium was analysed by Griess assay to determine total nitrite levels following the method described in section 2.6. Data are expressed as a percentage of nitrite production, with the response to LPS (100 µg/mL) plus IFN-γ (100 U/mL) taken as 100%. Data are the M ± SEM of at least three independent experiments. Statistical differences were determined by one-way ANOVA, followed by Dunnett's multiple comparisons test of the normalised data; * denotes $p < .05$ and **$p < .01$, both compared to the activated control.

4.3.4 Effects of dexamethasone on iNOS expression

To confirm that dexamethasone regulated iNOS expression, cell lysates were generated after removing the culture medium for Griess assay and subjected to western blotting. As Figure 25 shows, no iNOS was induced under control conditions, though it did induce after treatment with LPS and IFN-γ. Moreover, the induction was blocked by dexamethasone in a concentration dependent manner, which was significant at 1–10 μM.

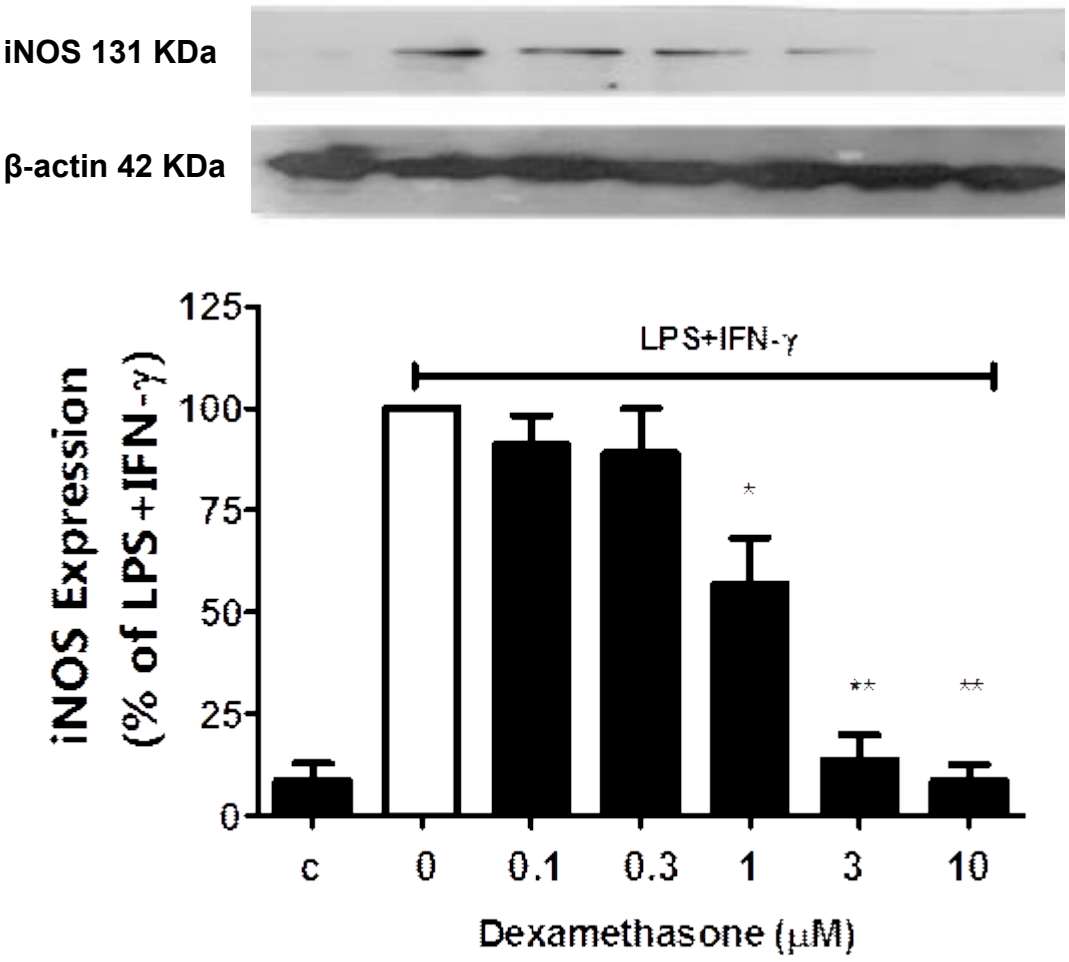

Figure 25. Effect of dexamethasone on iNOS expression. Confluent monolayers of RASMCs in 24-well plates were pretreated with concentrations of dexamethasone for 30 min before activation with 100 μg/mL of LPS and 100 U/mL of IFN-γ for 24 h. The expression of iNOS was determined by western blotting following the method described in section 2.9. The blot is representative of at least three independent experiments, and the bar graph depicts the densitometric data expressed as a percentage of iNOS expression, with the response to LPS (100 μg/mL) plus IFN-γ (100 U/mL) taken as 100%. Data represent the M ± SEM of at least three independent experiments. Statistical differences were determined by one-way ANOVA, followed by Dunnett's multiple comparisons test of the normalised data; * denotes $p < .05$ and **$p < .01$, both compared to the activated control.

4.3.5 Effects of hydrocortisone on NO production

To investigate whether hydrocortisone could regulate induced nitrite production, cells were pretreated with the compound (0.01–10.00 µM) 30 min prior to activation with 100 µg/mL of LPS and 100 U/mL of IFN-γ for 24 h. NO production was also inhibited in a concentration dependent manner, which was statistically significant at 0.01–10.00 µM hydrocortisone compared to levels detected with LPS or IFN-γ alone (Figure 26). The higher concentration of hydrocortisone decreased nitrite level from 18.9 ± 3.8 to 1.8 ± 1.4 nmol/ml. Hydrocortisone appeared more potent than dexamethasone at the lower concentration range (0.1–0.3 µM).

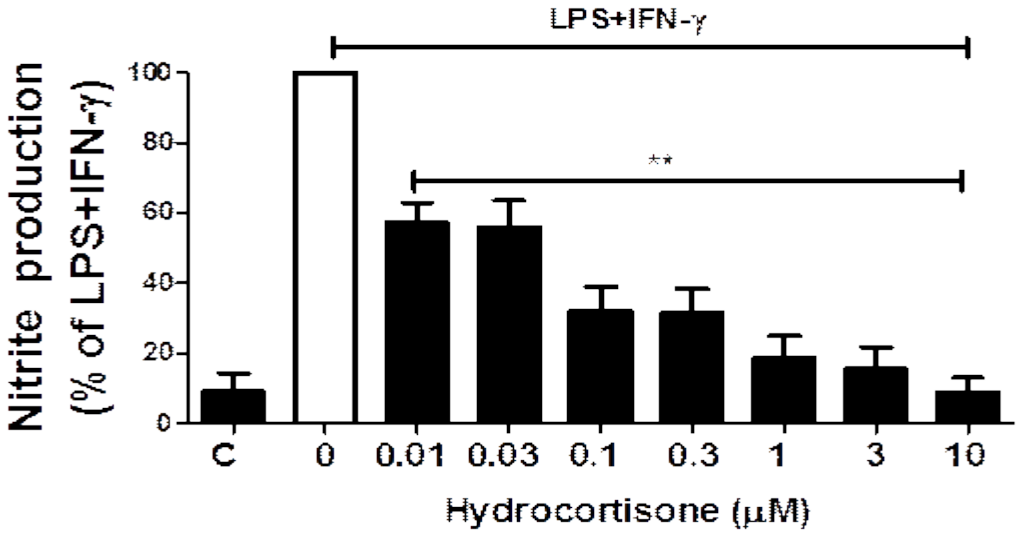

Figure 26. Effect of different concentrations of hydrocortisone on nitrite production. Confluent monolayers of RASMCs in 24-well plates were pretreated with concentrations of hydrocortisone for 30 min before activation with 100 µg/mL of LPS and 100 U/mL of IFN-γ for 24 h. The culture medium was analysed by Griess assay to determine the total nitrite levels following the method described in section 2.6. Data are expressed as a percentage of nitrite production, with the response to LPS (100 µg/mL) plus IFN-γ (100 U/mL) taken as 100%. Statistical differences were determined by one-way ANOVA, followed by Dunnett's multiple comparisons test of normalised data; ** denotes $p < .01$ compared to the activated control.

4.3.6 Effects of hydrocortisone on iNOS expression

To confirm whether hydrocortisone regulated NO production by suppressing iNOS expression, cell lysates were generated after removing the culture medium for Griess assay and analysed by western blotting. As Figure 27 shows, no iNOS was induced under control conditions, but it did induce following treatment with LPS and IFN-γ. Moreover, the induction was blocked by hydrocortisone, which appeared to completely abolish the expression of iNOS protein at 10 μM. The reduction was significant at concentrations of 0.1–10.0 μM.

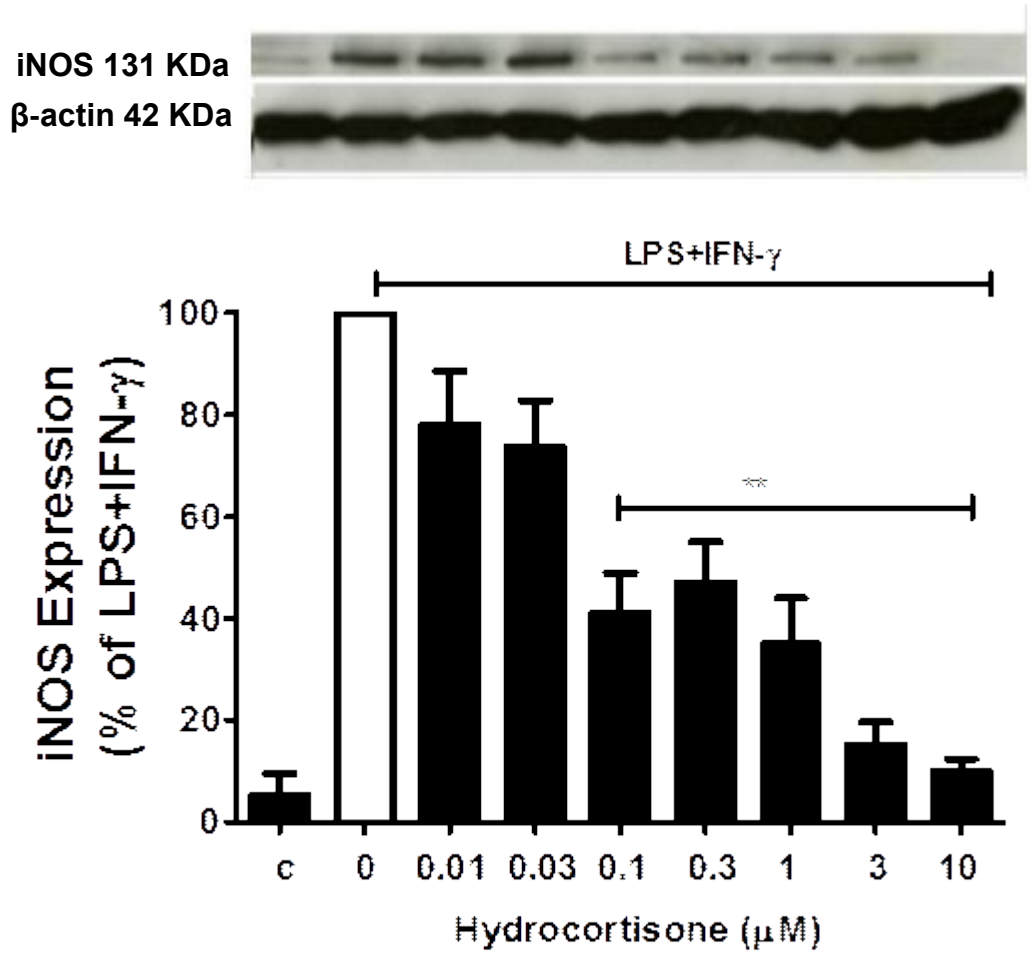

Figure 27. Effect of hydrocortisone on iNOS expression. Confluent monolayers of RASMCs in 24-well plates were pretreated with concentrations of hydrocortisone for 30 min before the activation with 100 μg/mL of LPS and 100 U/mL of IFN-γ for 24 h. The expression of iNOS was determined by western blotting following the method described in section 2.9. The blot is representative of at least three independent experiments, and the bar graph depicts densitometric data expressed as a percentage of iNOS expression, with the response to LPS (100 μg/mL) plus IFN-γ (100 U/mL) taken as 100%. Data represent the M ± SEM of at least three independent experiments. Statistical differences were determined by one-way ANOVA, followed by Dunnett's multiple comparisons test of the normalised data; ** denotes $p < .01$ compared to the activated control.

4.3.7 Effects of fluticasone on NO production

To investigate whether fluticasone could regulate induced nitrite production, cells were pretreated with the compound (0.03–3.00 µM) for 30 min prior to activation with 100 µg/mL of LPS and 100 U/mL of IFN-γ for 24 h. Each concentration of fluticasone used decreased nitrite production in a way seemingly independent of concentration, given that the extent of inhibition was similar in each case. The decrease in NO production was nevertheless statistically significant at all concentrations (0.03–3.00 µM), as Figure 28 shows. Moreover, the inhibitions with fluticasone were only partial, in contrast to the near-maximal inhibitions caused by dexamethasone and hydrocortisone.

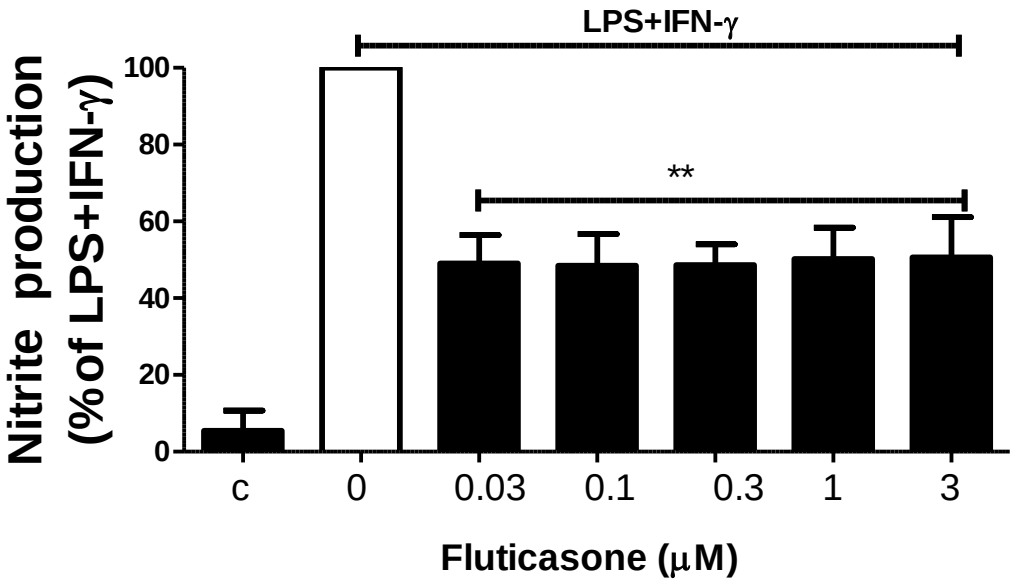

Figure 28. Effect of different concentrations of fluticasone on nitrite production. Confluent monolayers of RASMCs in 24-well plates were pretreated with concentrations of fluticasone for 30 min before activation with 100 µg/mL of LPS and 100 U/mL of IFN-γ for 24 h. The culture medium was analysed by Griess assay to determine total nitrite levels following the method described in section 2.6. Data are expressed as a percentage of nitrite production, with the response to LPS (100 µg/mL) plus IFN-γ (100 U/mL) taken as 100%. Data represent the M ± SEM of at least three independent experiments. Statistical differences were determined by one-way ANOVA, followed by Dunnett's multiple comparisons test of the normalised data; ** denotes $p < .01$ compared to the activated control.

4.3.8 Effects of lower concentrations of fluticasone on NO production

Since all concentrations of fluticasone exerted a similar effect on NO production, it was worthwhile to investigate lower concentrations (0.1–30.0 nM). As in previous studies, cells were incubated with each concentration for 30 min prior to activation with 100 µg/mL of LPS and 100 U/mL of IFN-γ for a 24 h. The experiments demonstrated that fluticasone decreased nitrite production in a concentration dependent manner, with the maximum effect achieved at 1 nM (Figure 29). The higher concentration of fluticasone decreased nitrite level from 21.7 ± 3.4 to 9.8 ± 2.3 nmol/ml

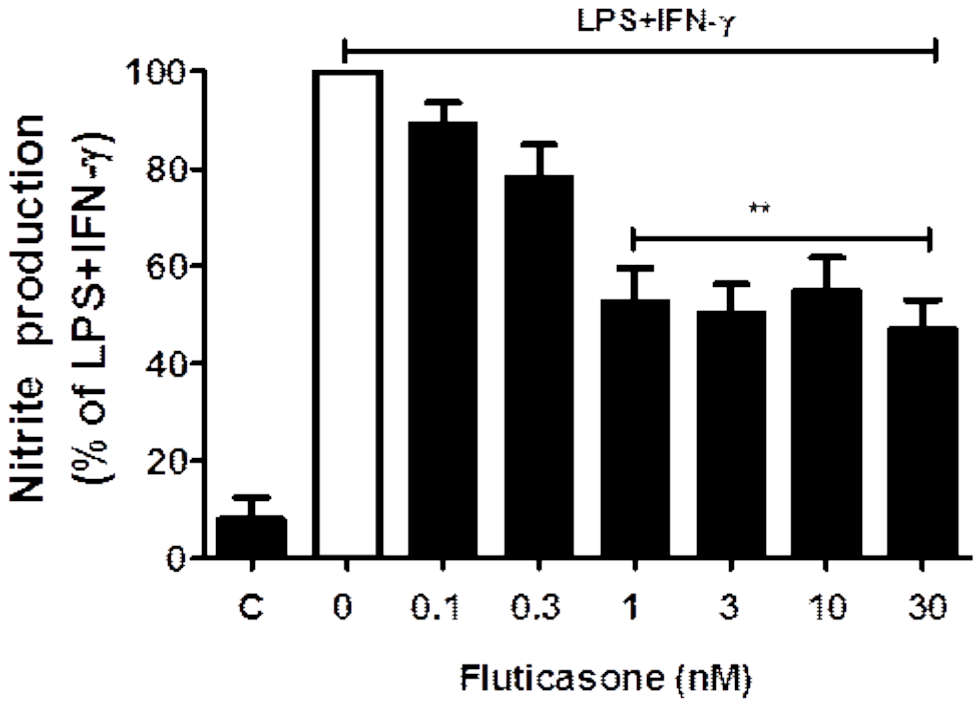

Figure 29. Effect of lesser concentrations of fluticasone on nitrite production. Confluent monolayers of RASMCs in 24-well plates were pretreated with concentrations of fluticasone for 30 min before activation with 100 µg/mL of LPS and 100 U/mL of IFN-γ for 24 h. The culture medium was analysed by Griess assay to determine total nitrite levels following the method described in section 2.6. Data are expressed as a percentage of nitrite production, with the response to LPS (100 µg/mL) plus IFN-γ (100 U/mL) taken as 100%. Data are the M ± SEM of at least three independent experiments. Statistical differences were determined by

one-way ANOVA, followed by Dunnett's multiple comparisons test of the normalised data; ** denotes $p < .05$ compared to the activated control.

4.3.9 Effects of fluticasone on iNOS expression

Consistent with previous observations, Figure 30 shows that there was no iNOS under control conditions. The enzyme was significantly induced following treatment with LPS and IFN-γ. Moreover, induction was reduced only partially, as consistent with nitrite's trend, and was significant at 1–30 nM.

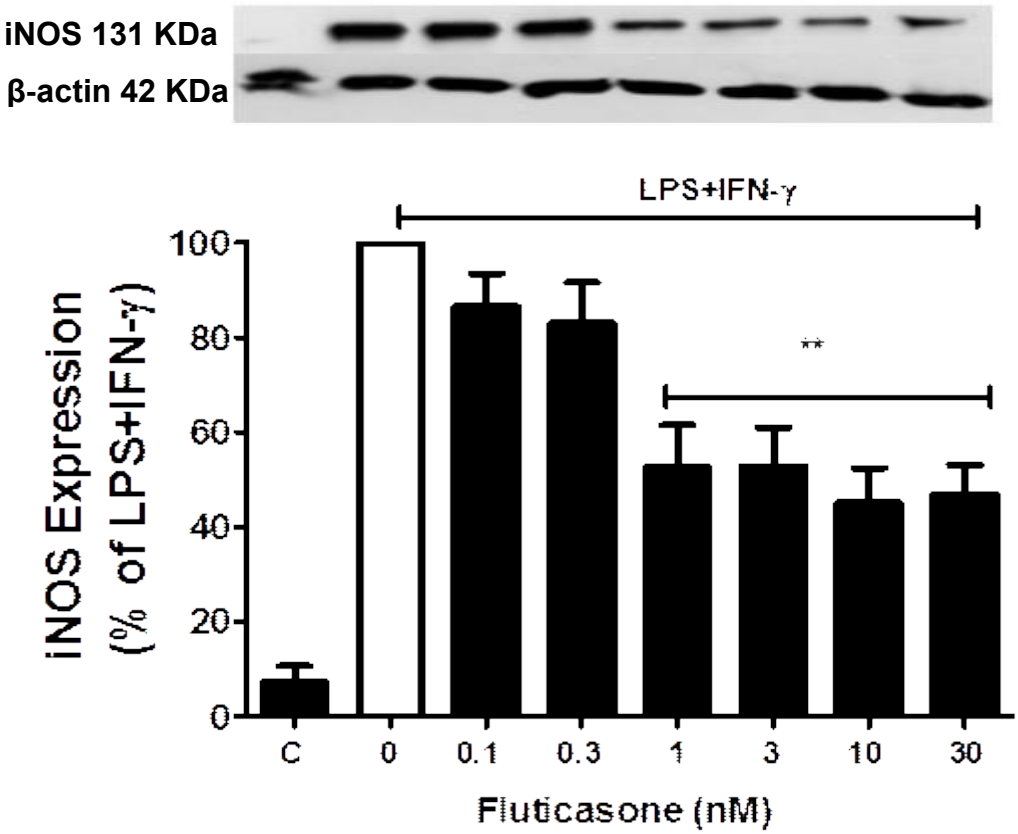

Figure 30. Effect of fluticasone on iNOS expression induced by LPS and IFN-γ in RASMCs. Confluent monolayers of RASMCs in 24-well plates were pretreated with concentrations of fluticasone 30 min before activation with 100 µg/mL of LPS and 100 U/mL of IFN-γ for 24 h. The expression of iNOS was determined by western blotting following the method described in section 2.9. The blot is representative of at least three independent experiments, and the bar graph depicts densitometric data expressed as a percentage of iNOS expression, with the response to LPS (100 µg/mL) plus IFN-γ (100 U/mL) taken as 100%. Statistical

differences were determined by one-way ANOVA, followed by Dunnett's multiple comparisons test of the normalised data; ** denotes $p < .05$ compared to the activated control.

4.4 Discussion

The aim of this chapter was to investigate the effect of different GCs on iNOS expression and NO production in order to determine whether they affect those processes in the same manner and potentially through a common mechanism. The studies were pursued because, despite the wide use of dexamethasone as the standard experimental GC for regulating inflammation, its effects on iNOS expression and function have not always been clearly ascribed to a pure GC action. Accordingly, experiments were performed to examine the actions of three compounds, including dexamethasone, as well as hydrocortisone and fluticasone, the last of which was deemed a selective GC that works primarily on GCR.

Before the experiments, the potential cytotoxic effects of the different concentrations of GCs, both with and without LPS and IFN-γ, were excluded according to the results of MTT assay, which revealed that none of the drugs caused any statistically significant change in the metabolism of MTT, meaning that they were tolerated well in RASMCs and caused little or no cytotoxicity even at the high concentrations tested. The decreases in MTT metabolism observed were no more than 15 % of the maximum and were not statistically significant when compared to controls. The standard error of the mean was within 10% of the mean showing consistency in the effect with less variability. moreover, this did not show any concentration dependency and because of this the N value was maintained at a minimum of three independent experiments per condition. The time dependent effects of LPS and IFN-γ on NO production and iNOS expression were also investigated to confirm the time points at which the processes peaked. Findings showed that both increased in a time dependent manner and that changes in NO production mirrored those observed in iNOS expression. In both

instances, levels increased for over 24 h, which confirmed the findings of previous studies with RASMCs (Hattori et al., 1999), L6 rat skeletal myoblast cells stimulated with IL-1β–IFN-γ or IL-1β–IFN-γ–TNF-α (Adams et al., 2002), frog urinary bladder epithelial cells activated with LPS (Nikolaeva et al., 2012), and J774 macrophages activated with LPS (Baydoun et al., 1993).

After establishing the effects of LPS and IFN-γ on iNOS and NO production, experiments were performed to confirm the actions of GCs on both processes. Different concentrations of each GC were investigated, and each was found to inhibit both NO production and iNOS expression. More importantly, interesting trends emerged among the three compounds, in that dexamethasone at 0.1–10.0 μM and hydrocortisone at 0.01–10.00 μM both inhibited NO and iNOS expression in a concentration dependent manner, virtually abolishing both at 3–10 μM. By contrast, the inhibitions caused by fluticasone were only partial. In fact, increasing its concentration to 3 μM showed no further decrease in NO production. Such observations reveal that the selective GC was only partially effective in suppressing the induction of iNOS and NO production, which suggests that dexamethasone and hydrocortisone could exert their effects not only via the classic GCR pathway but potentially also independently of the latter.

Results generated with dexamethasone are consistent with previous findings showing that it decreases nitrite production and iNOS expression in different types of cells, including mesangial cells (Kunz et al., 1996), human lung epithelial cells (Robbins et al., 1994), hepatocytes (Geller et al., 1994), cultured rat cardiocytes (Tsujino et al., 1994), human joint-derived cells such as chondrocytes, synovial fibroblasts, and osteoblasts (Grabowski et al., 1996), human airway epithelial cells (Kao et al., 2001), cultured rat astrocytes (Lavista et al., 1999), J774 macrophages (Korhonen et al., 2002), C6 glioma cells (Shinoda et al., 2003), neonate rat brain cells (Wang et al., 2005), chromaffin cells (Pérez–Rodríguez et al., 2009), and RASMCs (Thakur & Baydoun, 2012; Wileman et al., 1995).

Research focusing on mechanisms by which dexamethasone inhibits iNOS expression and NO production has tended to claim that the mechanisms are either transciptional or post-transcptional. At the transcriptional level, dexamethasone is reportedly able to inhibit NF-κB, possibly by reducing the nuclear translocation or DNA binding of NF-κB, if not both (Katsuyama et al., 1999; Kleinert et al., 1996; Salzman et al., 1996). By contrast, the post-transcriptional effect of GCs (i.e., dexamethasone) has been suggested in C6 glioma cells (Shinoda et al., 2003), with a proposed post-transcriptional mechanism of action on iNOS expression by which dexamethasone destabilises iNOS mRNA in machrophages (Korhonen et al., 2002; Söderberg et al., 2007). Other findings suggest that the post-transcriptional mechanism operates via dexamethasone's ability to enhance the process of iNOS protein degradation, at least in mouse machrophages and rat mesangial cells (Kunz et al., 1996; Walker et al., 2001).

Numerous studies with RASMCs have investigated the potential mechanisms by which dexamethasone regulates iNOS expression and functions, including the inhibition of iNOS expression and its function by suppressing NF-κB induced by IL-1β (Katsuyama et al., 1999) or by LPS together with IFN-γ (Matsumura et al., 2001). By constrast, other research has suggested that dexamethasone does not affect iNOS expression at the transcriptional level but most likely does at the post-transcriptional level, given its suppression of iNOS protein but not mRNA expression (Thakur & Baydoun, 2012).

The most important GC for humans, hydrocortisone is essential for sustaining life by regulating and supporting various vital cardiovascular, metabolic, immunologic, and homeostatic functions. It is also used both in replacement therapy for GC deficiency and as an immune system suppressant. Hydrocortisone is moreover widely used in septic shock (Sprung et al., 2008) and, along with binding to GC receptors, performs mineralocorticoid activity that distinguishes it from other synthetic GCs (Druce et al., 2008). It has additionally

been found to inhibit iNOS expression and functions in many cell types, including LPS-activated rat microglial cells (Lieb et al., 2003), LPS-activated murine macrophages and bovine chondrocytes (Patel et al., 1999), and IL-1-activated human chondrocytes (Palmer et al., 1993), as well as IL-1β-induced NO production in RASMCs (Suzuki et al., 1994). Consistent with those results, data from this thesis have shown that hydrocortisone can inhibit iNOS expression and function. However, it remains unclear whether that effect is mediated purely thorugh its GC or mineralocorticoid action or both.

Studies have also indicated that, apart from dexamethasone and hydrocortisone, the selective GC fluticasone might regulate iNOS and reduce bronchial NO flux in asthmatic patients (Lehtimaki et al., 2001). Such findings suggest that iNOS expression might be regulated via a GC action, which the studies in this thesis have confirmed. Data clearly show that fluticasone exerts direct action on the induction of iNOS and thus NO production, by suppressing both processes in RASMCs treated with LPS and IFN-γ. Notably, fluticasone caused only partial inhibitions even at the highest concentrations, in contrast to the actions of dexamethasone and hydrocortisone, which caused complete reductions.

Several factors could account for the differences in responses. Dexamethasone is a nonselective GC with mineralocorticoid activity that shows roughly 30% affinity for mineralocorticoid receptors (MR), as Lan et al. (1982) have revealed. Moreover, dexamethasone may act on other receptors, including those for progesterone, oestrogen (Bigsby, 1993; Yang et al., 2001), and androgen (Inder et al., 2010). All these receptors have a potential role in inflammation and on NO production (Cronauer et al., 2007; Juliet et al., 2004; Karpuzoglu & Ahmed, 2006; Lei et al., 2014). It is therefore possible that they may also regulate NO production, but this remains to be established especially by implicating an action of dexamethasone through these protein targets to regulate NO synthesis.

Hydrocortisone, like dexamethasone, is not a selective glucocorticoid and additionally exerts effect on minerlaocortcoid (Born et al., 1987), as well as androgen (Sonneveld et al., 2005) and progesterone receptors (Karalis et al., 1996). By contrast, fluticasone is a highly selective and potent GC agonist with a negligible or nonexistent effect on the steroid nuclear receptor family. It has no effect on oestrogen receptors, and it is a weak antagonist of MRs and androgen and progesterone receptors (Austin et al., 2002). Such characteristics could explain the differences between the compounds in regulating iNOS expression and NO synthesis. More importantly, data from the present research suggest that both processes can be only partially regulated via the GC signalling pathway and that complete inhibition with dexamethasone and hydrocortisone might be due to additional non-GC actions. The EC50 of dexamethasone, hydrocortisone and fluticasone are 2nM, 25nM and 0.1nM respectively (Adcock et al., 1999; Johnson, 1995). However, in our project, higher concentrations showed effect on iNOS expression and NO production. The reason behind that is the difference in the system where EC50 measured in ideal system in test tube. However, the cell system is much more complex and not as tightly controlled as in a test tube. Thus, the effective concentration in the two different conditions is expected to vary.

5. Potential Involvement of GCRs and MRs on iNOS Expression and Function in RASMCs

5.1 Introduction

Dexamethasone, hydrocortisone, and fluticasone inhibited iNOS expression and function, as reported in the previous chapter. The selective GC fluticasone caused partial inhibition, whereas dexamethasone and hydrocortisone virtually abolished iNOS expression and function. Such findings suggest that the induction of iNOS might be only partially regulated through the GC pathway and that the significant inhibitions caused by dexamethasone and hydrocortisone could be due to their other non-GC actions, presumably involving mineralocorticoids. Additional experiments were therefore conducted to examine the effects of RU-486 (i.e., a GCR antagonist) and eplerenone (i.e., an MR antagonist) on the inhibition of iNOS expression and NO production caused by GCs.

5.2 Methods

5.2.1 Effect of GCR and MR antagonism on NO production and iNOS expression

Confluent monolayers of RASMCs in 24-well plates were pretreated for 1 h with RU-486 at 10.0 µM or eplerenone at 0.1–10.0, followed by the addition of dexamethasone (3 µM and 10 µM), hydrocortisone (3 µM and 10 µM), or fluticasone (1 and 3 nM) 30 min prior to activation with 100 µg/mL of LPS and 100 U/mL of IFN-γ for an additional 24 h. In parallel experiments, dexamethasone, hydrocortisone, and fluticasone were omitted, and the cells were treated only with RU-486 at 10 µM for 1 h before activation with 100 µg/mL of LPS and 100 U/mL of IFN-γ for 24 h. The culture medium was analysed by Griess assay to determine total nitrite levels following the method described in section 2.6. The expression of iNOS was determined by western blotting, and changes in cell viability were examined by the MTT following the methods described in sections 2.9 and 2.4, respectively.

5.3 Results

5.3.1 Effects of RU-486 on the viability of RASMCs in the presence of GCs

This experiment was conducted to determine whether different concentrations of RU-486 exerted a cytotoxic effect in the presence of GCs in either control or activated cells. In pilot studies, RU-486 alone did not show much cytotoxicity. The metabolism of MTT by control cells was taken as 100% viability and compared to responses seen with different concentrations of RU-486 (0.1–10.0 µM) in the presence of dexamethasone (10 µM; Figure31), hydrocortisone (10 µM; Figure 32), or fluticasone (3 nM; Figure 33) in activated and nonactivated cells. Despite decreases in the metabolism of MTT, the effects were marginal and not statistically significant. As such, the combination of RU-486 with any of the three GCs meant no cytotoxicity for the cells, and consequently, additional experiments were performed using the full concentration range investigated above.

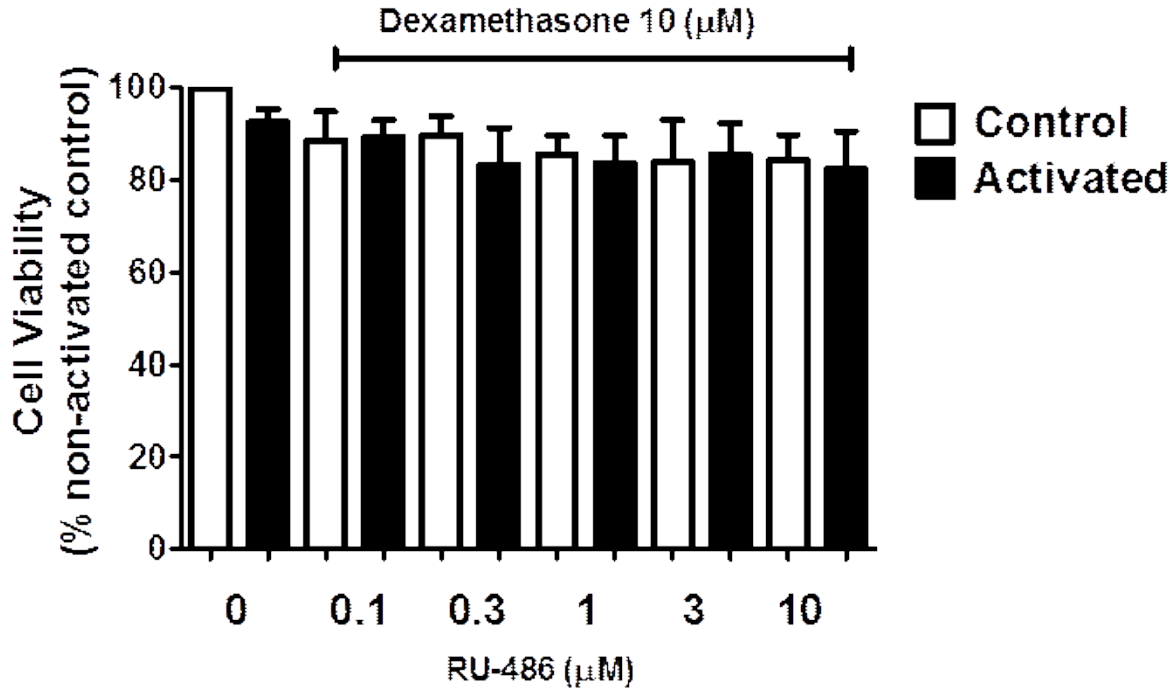

Figure 31. Effect of different concentrations of RU-486 on the viability of RASMCs in the presence of dexamethasone. Confluent monolayers of RASMCs in 96-well plates were pretreated with different concentrations of RU-486 (0.1–10.0 µM) 1 h prior to the addition of

10 μM dexamethasone for 30 min before activation with LPS (100 μg/mL) and IFN-γ (100 U/mL) for 24 h. Metabolism of MTT was determined colourimetrically following the method described in section 2.4. The white bars represent controls, and the black ones represent activated cells. Data are presented as the percentage of viable cells compared to the controls and represent the M ± SEM of at least three individual experiments. Statistical differences were determined by one-way ANOVA, followed by Dunnett's multiple comparisons test of the normalised data; $p > .05$ confirmed that there was no significant difference compared to the nonactivated control.

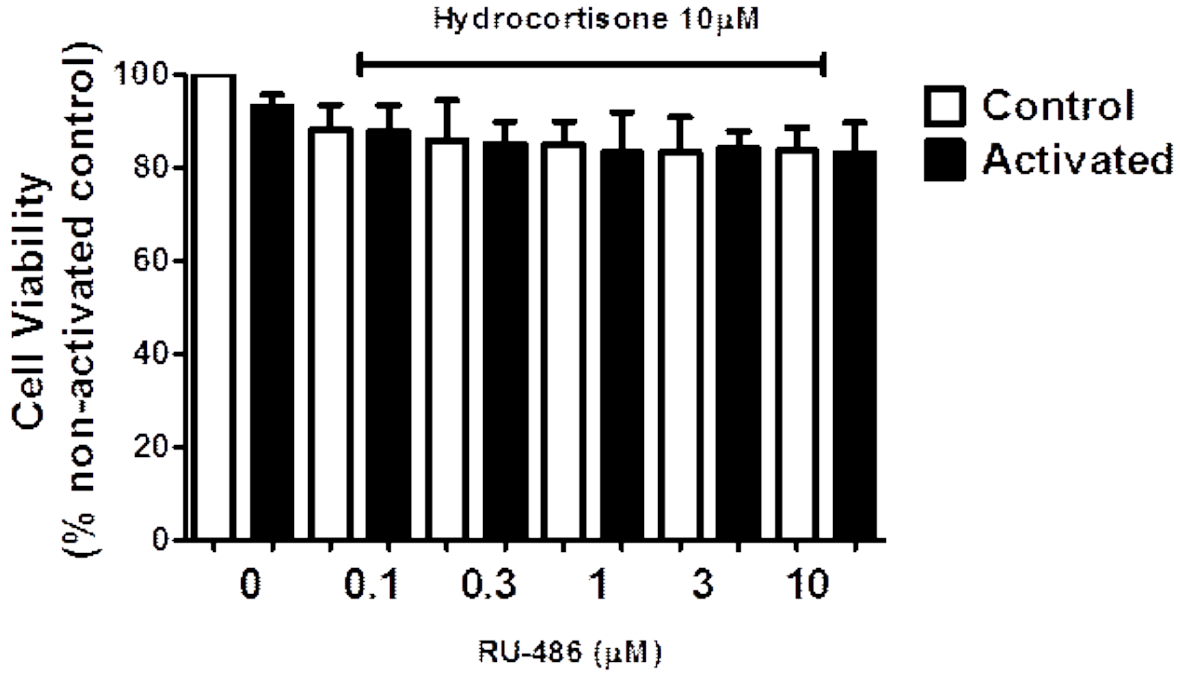

Figure 32. Effect of different concentrations of RU-486 on the viability of RASMCs in the presence of hydrocortisone. Confluent monolayers of RASMCs in 96-well plates were pretreated with different concentrations of RU-486 (0.1–10.0 μM) 1 h prior to the addition of 10 μM of hydrocortisone for 30 min before activation with LPS (100 μg/mL) and IFN-γ (100 U/mL) for 24 h. The metabolism of MTT was determined colourimetrically following the method described in section 2.4. The white bars represent controls, and the black ones represent activated cells. Data are presented as the percentage of viable cells compared to the controls and represent the M ± SEM of at least three individual experiments. Statistical differences were determined by one-way ANOVA, followed by Dunnett's multiple

comparisons test of the normalised data; $p > .05$ confirmed that there was no significant difference compared to the nonactivated control.

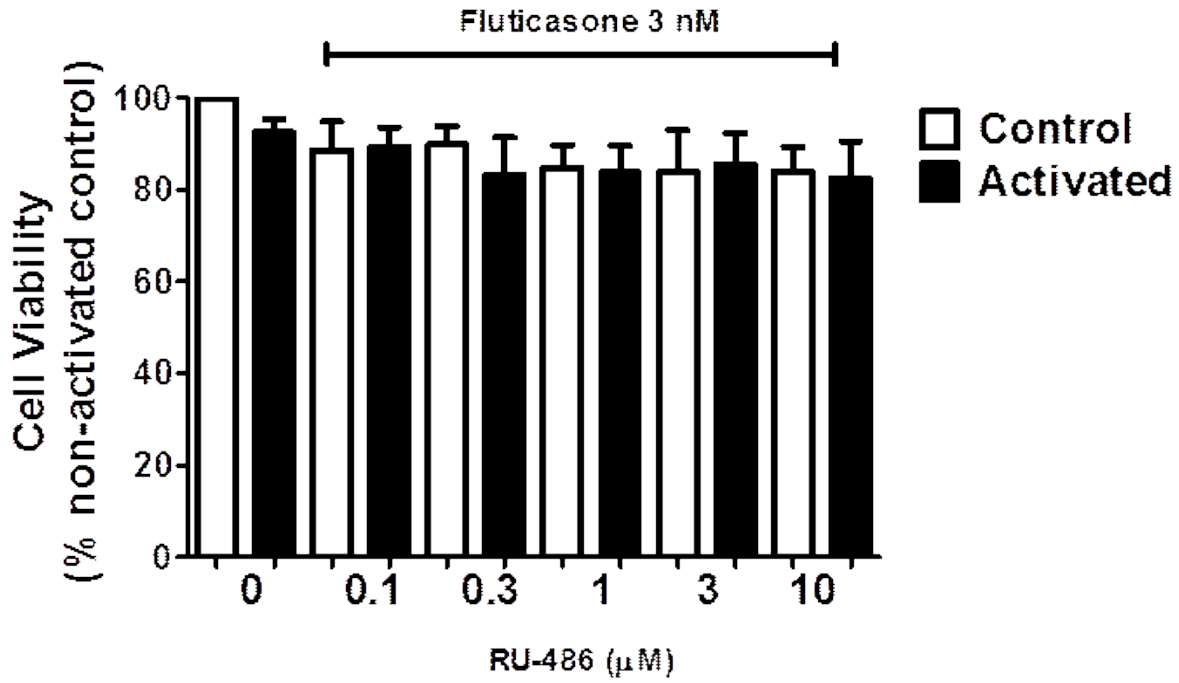

Figure 33. Effect of different concentrations of RU-486 on the viability of RASMCs in the presence of fluticasone. Confluent monolayers of RASMCs in 96-well plates were pretreated with different concentrations of RU-486 (0.1–10.0 μM) 1 h prior to the addition of 3 nM fluticasone for 30 min before activation with LPS (100 μg/mL) and IFN-γ (100 U/mL) for 24 h. The metabolism of MTT was determined colourimetrically following the method described in section 2.4. The white bars represent controls, and the black ones represent activated cells. Data are presented as the percentage of viable cells in comparison to the controls and represent the M ± SEM of at least three individual experiments. Statistical differences were determined by one-way ANOVA, followed by Dunnett's multiple comparisons test of the normalised data; $p > .05$ confirmed that there was no significant difference compared to the nonactivated control.

5.3.2 Effects of MR blocker eplerenone on the viability of RASMCs in the presence of GCs

This experiment was conducted to determine whether different concentrations of eplerenone exert a cytotoxic effect in the presence of GCs in either control or activated cells. As in

previous studies, the metabolism of MTT by control cells was taken as 100% viability and compared to responses of the different concentrations of eplerenone (0.1–10.0 μM) in the presence of dexamethasone (10 μM; Figure 34), hydrocortisone (10 μM; Figure 35), or fluticasone (3 nM; Figure 36) in activated and nonactivated cells. Despite decreases in the metabolism of MTT, the effects were only marginal and not statistically significant. The combination of eplerenone with any of the three GCs thus did not mean any cytotoxicity for the cells, and consequently, additional experiments were performed using the full concentration range investigated above.

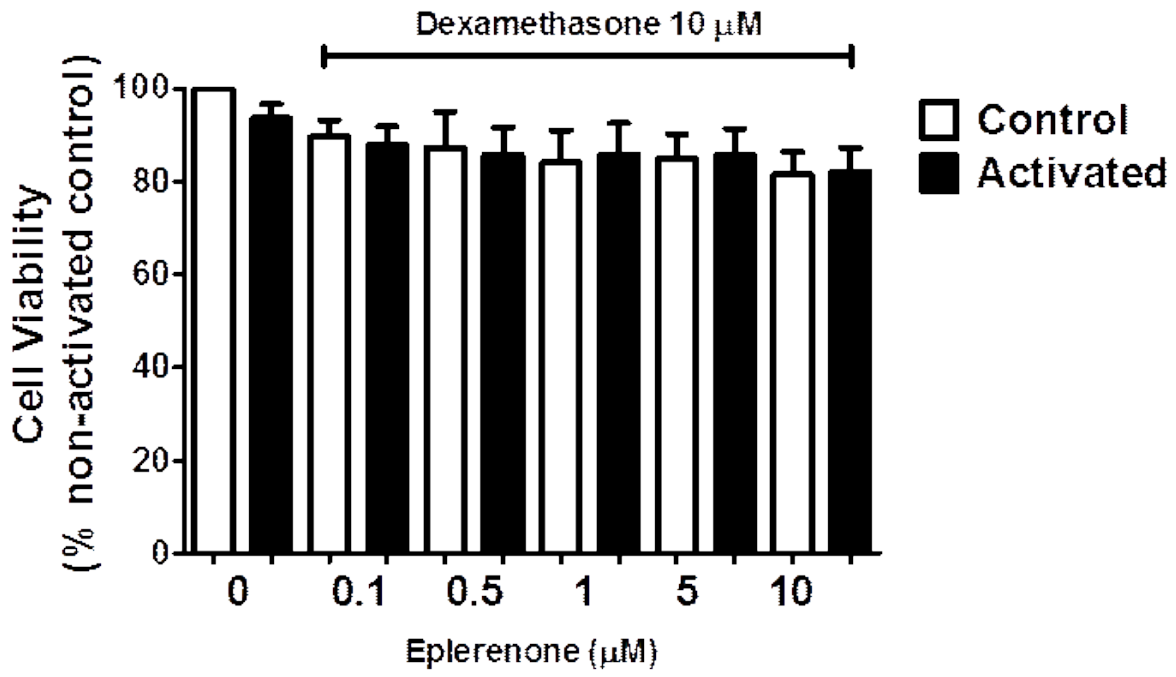

Figure 34. Effect of different concentrations of eplerenone on the viability of RASMCs in the presence of dexamethasone. Confluent monolayers of RASMCs in 96-well plates were pretreated with different concentrations of eplerenone (0.1–10.0 μM) 1 h prior to the addition of 10 μM dexamethasone for 30 min before activation with LPS (100 μg/mL) and IFN-γ (100 U/mL) for 24 h. The metabolism of MTT was determined colourimetrically following the method described in section 2.4. The white bars represent controls, and the black ones represent activated cells. Data are presented as the percentage of viable cells compared to the controls and represent the M ± SEM of at least three individual experiments. Statistical

differences were determined by one-way ANOVA, followed by Dunnett's multiple comparisons test of normalised data; $p > .05$ confirmed that there was no significant difference compared to the nonactivated control.

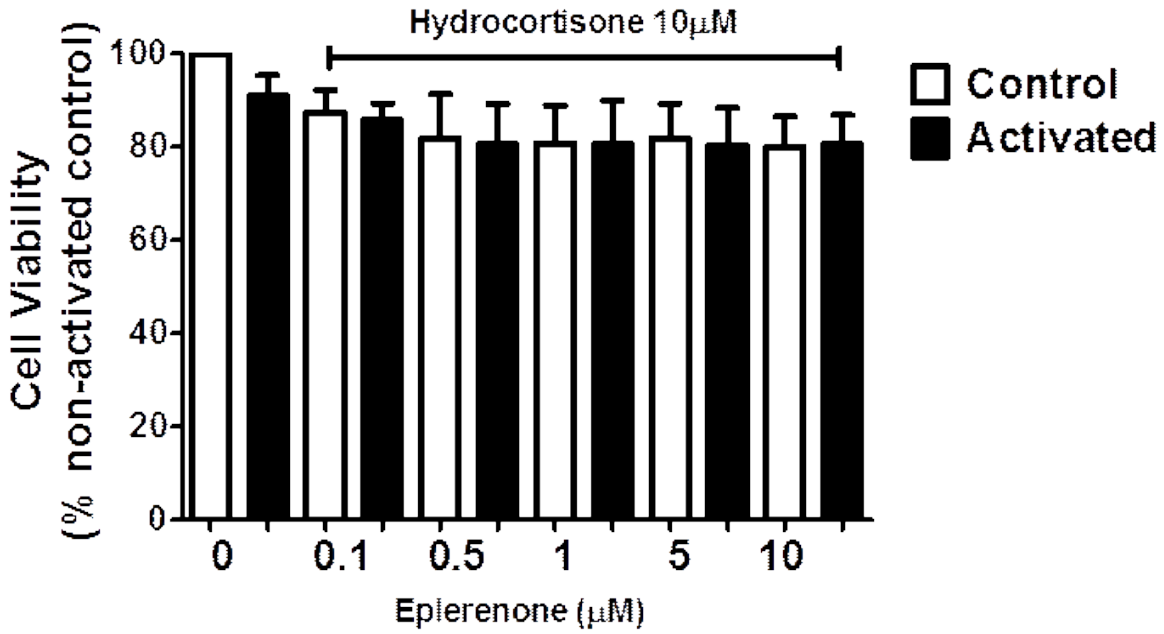

Figure 35. Effect of different concentrations of eplerenone on the viability of RASMCs in the presence of hydrocortisone. Confluent monolayers of RASMCs in 96-well plates were pretreated with different concentrations of eplerenone (0.1–10.0 μM) 1 h prior to the addition of 10 μM hydrocortisone for 30 min before activation with LPS (100 μg/mL) and IFN-γ (100 U/mL) for 24 h. The metabolism of MTT was determined colourimetrically following the method described in section 2.4. The white bars represent controls, and the black ones represent activated cells. Data are presented as the percentage of viable cells compared to the controls and represent the M ± SEM of at least three individual experiments. Statistical differences were determined by one-way ANOVA, followed by Dunnett's multiple comparisons test of the normalised data; $p > .05$ confirmed that there was no significant difference compared to the nonactivated control.

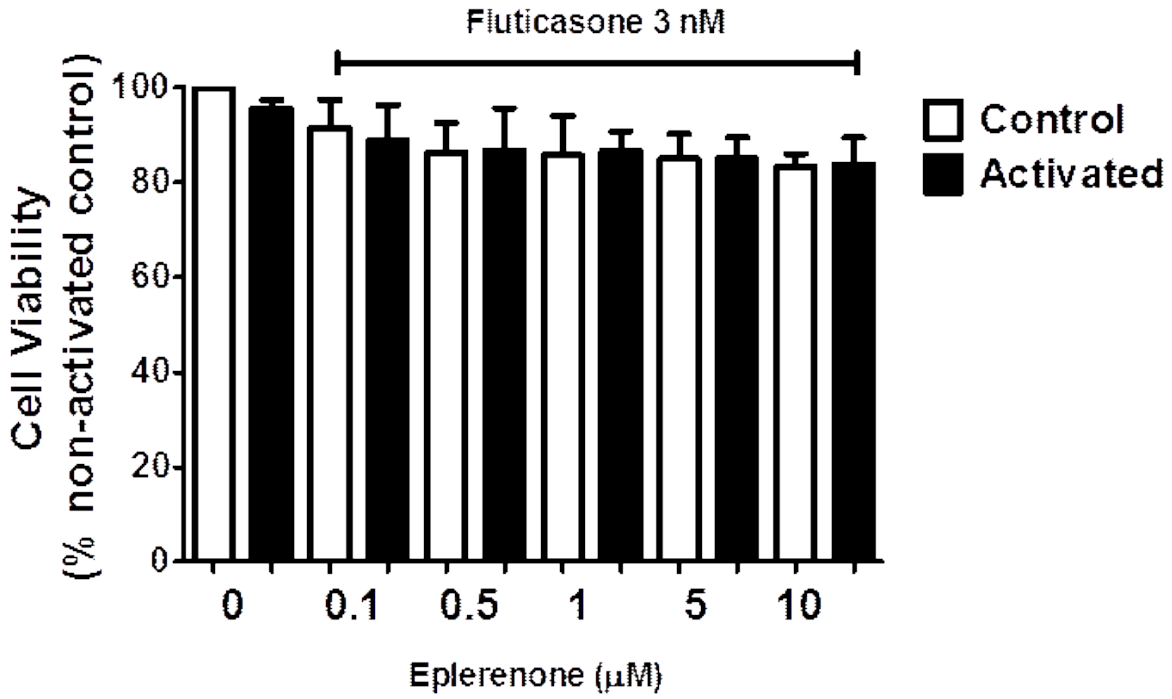

Figure 36. Effect of different concentrations of eplerenone on the viability of RASMCs in the presence of fluticasone. Confluent monolayers of RASMCs in 96-well plates were pretreated with different concentrations of eplerenone (0.1–10.0 μM) 1 h prior to the addition of 3 nM of fluticasone for 30 min before activation with LPS (100 μg/mL) and IFN-γ (100 U/mL) for 24 h. The metabolism of MTT was determined colourimetrically according to the method described in section 2.4. The white bars represent controls, and the black ones represent activated cells. Data are presented as the percentage of viable cells compared to the controls and represent the M ± SEM of at least three individual experiments. Statistical differences were determined by one-way ANOVA, followed by Dunnett's multiple comparisons test of the normalised data; $p > .05$ confirmed that there was no significant difference compared to the nonactivated control.

5.3.3 Effect of different concentrations of RU-486 on the inhibition of NO production by dexamethasone

Cells were activated with LPS (100 μg/mL) and IFN-γ (100 U/mL) in the presence and absence of dexamethasone (10 μM) and its receptor antagonist RU-486 (0.1–10 μM). Not only did dexamethasone significantly inhibit NO production, as consistent with earlier results, but 3–10 μM of RU-486 moreover reversed inhibition in a concentration dependent

manner and restored nitrite production back to the activated control level (Figure 37). Accordingly, 10 μM of RU-486 will be used to compare GCs.

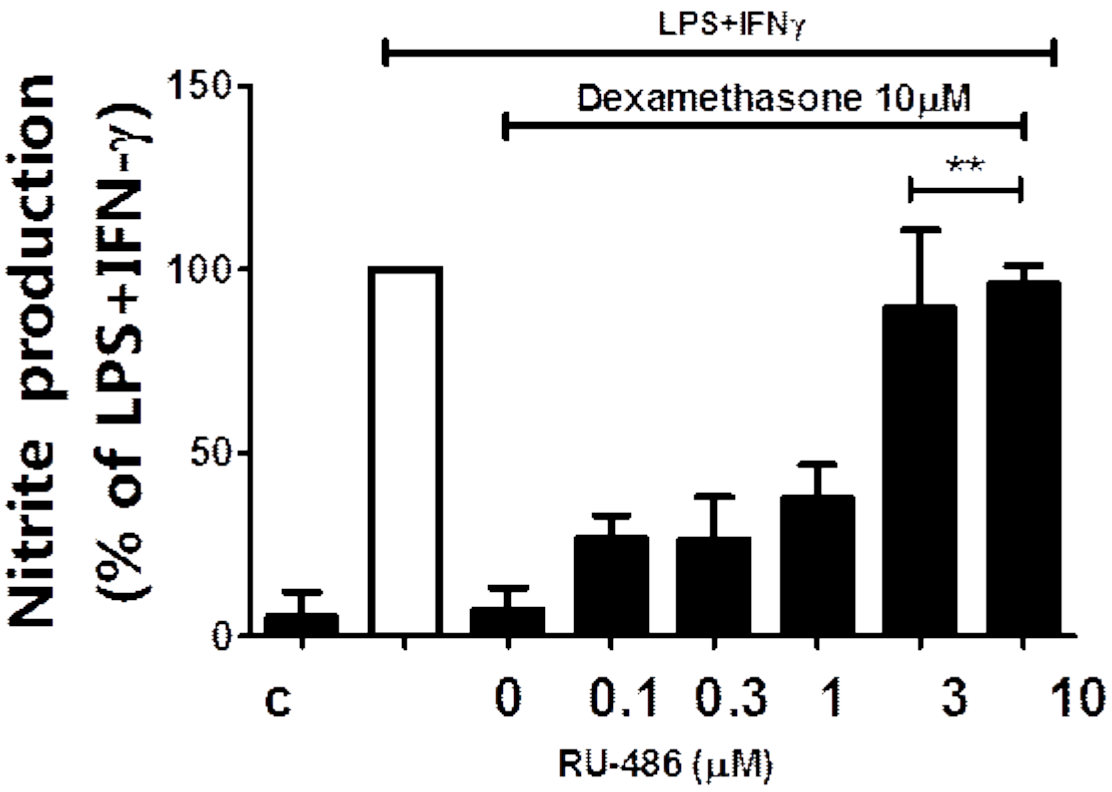

Figure 37. Effect of different concentrations of RU-486 on the inhibition of NO production by dexamethasone. Confluent monolayers of RASMCs in 24-well plates were pretreated for 1 h with 0.1–10.0 μM of RU-486, followed by the addition of 10 mM dexamethasone for 30 min before activation with 100 μg/mL of LPS and 100 U/mL of IFN-γ for 24 h. The culture medium was analysed by Griess assay to determine total nitrite levels following the method described in section 2.6. Data are expressed as a percentage of nitrite production with the response to LPS (100 μg/mL) plus IFN-γ (100 U/mL) taken as 100%. Data are the M ± SEM of at least three independent experiments. Statistical differences were determined by one-way ANOVA, followed by Dunnett's multiple comparisons test of the normalised data; ** denotes $p < .01$ compared to the activated treated with dexamethasone.

5.3.4 Effect of RU-486 on NO production

To investigate whether RU-486 alone had any effect on NO production, experiments were performed to investigate its effects against LPS and IFN-γ-activated cells. Results showed that RU-486 had no effect on either basal or induced NO production. Thus, the responses seen above must reflect antagonism of the actions of dexamethasone.

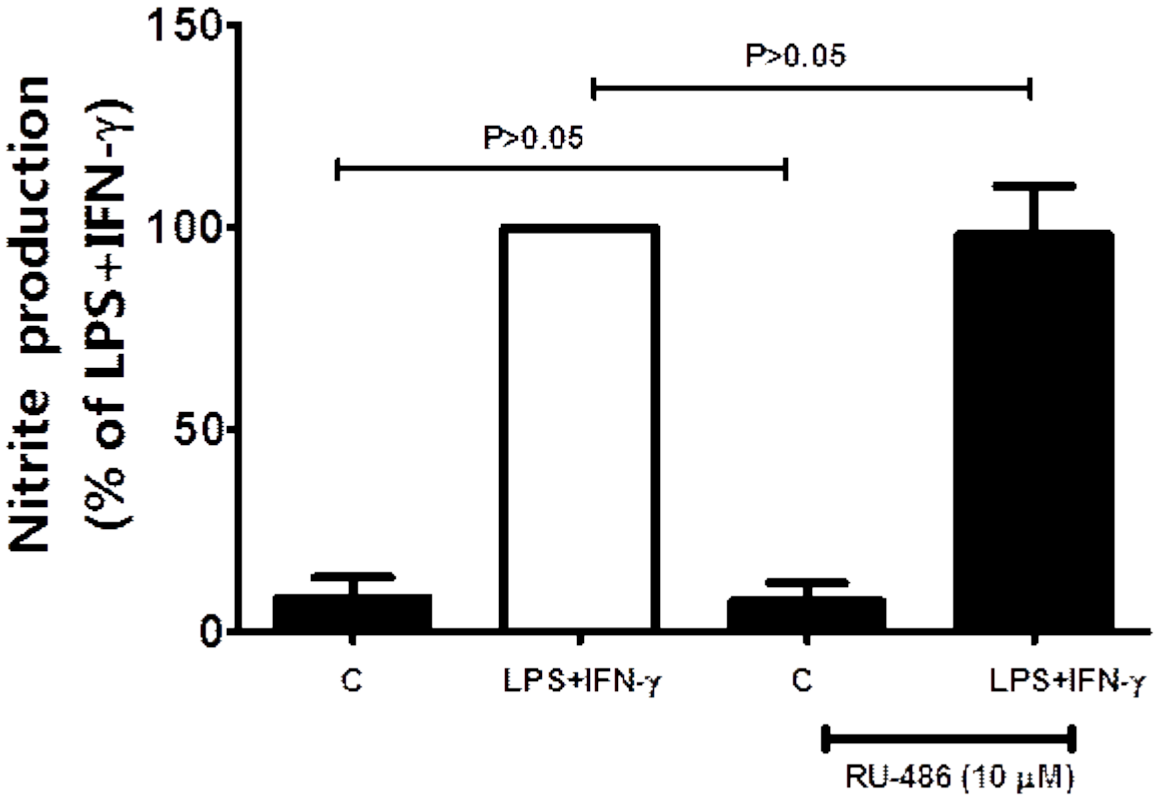

Figure 38. Effect of RU-486 on NO production. Confluent monolayers of RASMCs in 24-well plates were pretreated for 1 h with RU-486 at 10 μM prior to activation with 100 μg/mL of LPS and 100 U/mL of IFN-γ for a further 24 h. The culture medium was analysed by Griess assay to determine total nitrite levels following the method described in section 2.6. Data are expressed as a percentage of nitrite production, with the response to LPS (100 μg/mL) plus IFN-γ (100 U/mL) taken as 100%. Data are the M ± SEM of at least three independent experiments. Statistical differences were determined by one-way ANOVA, followed by Dunnett's multiple comparisons test of the normalised data; $p > .05$ confirmed that there was no significant difference.

5.3.5 Effect of RU-486 on iNOS expression

To investigate whether RU-486 had any effect on iNOS expression, changes in iNOS expression were examined in cells treated with RU-486 in the absence and presence of LPS and IFN-γ. As with NO production, RU-486 did not alter basal or induced iNOS expression (Figure 39), as consistent with the lack of effect seen on NO synthesis as well.

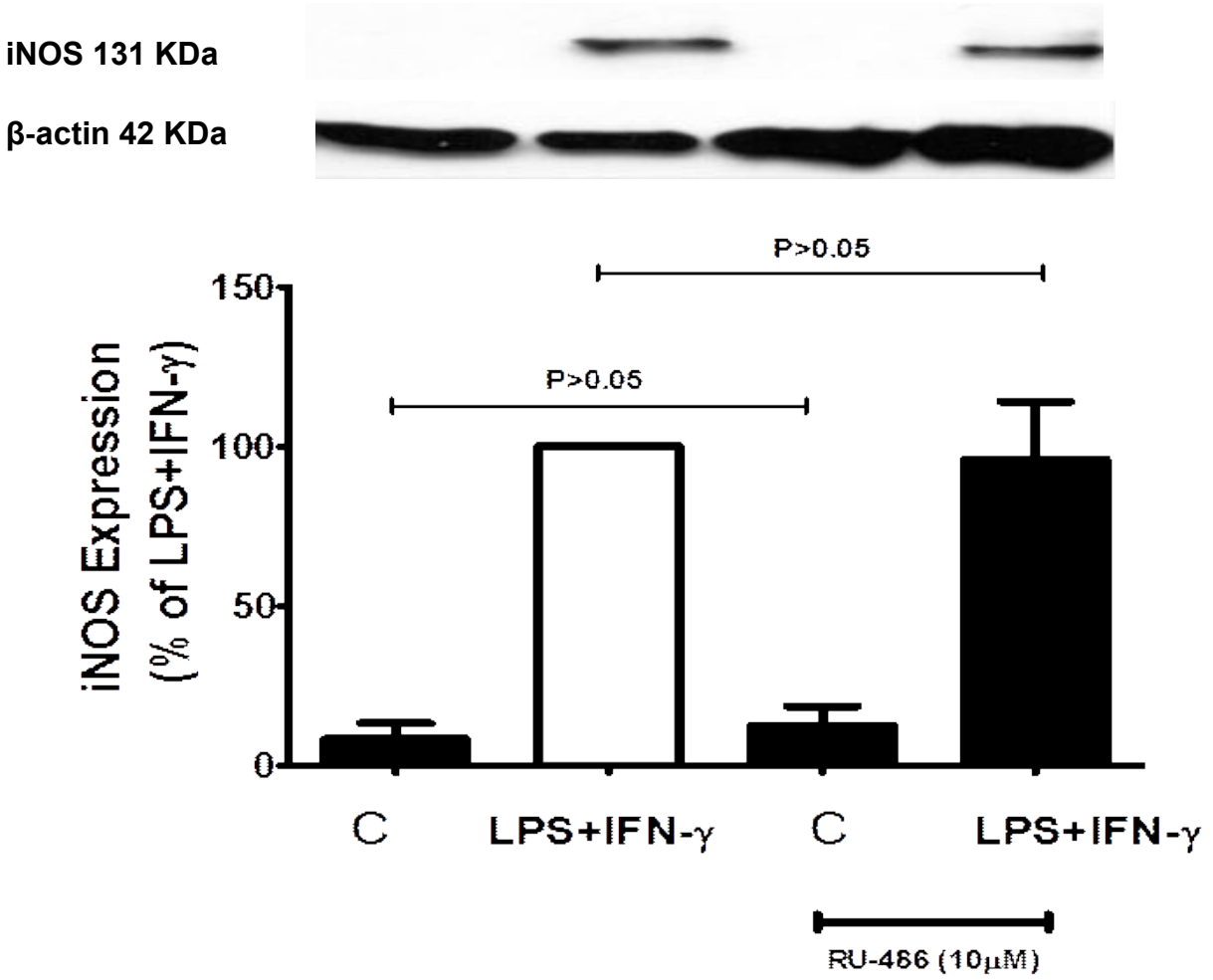

Figure 39. Effect of RU-486 on iNOS expression. Confluent monolayers of RASMCs in 24-well plates were pretreated for 1 h with RU-486 at 10 μM prior to activation with 100 μg/mL of LPS and 100 U/mL of IFN-γ for 24 h. The expression of iNOS was determined by western blotting following the method described in section 2.9. The blot is representative of at least three independent experiments, and the bar graph depicts densitometric data expressed as a percentage of iNOS expression, with the response to LPS (100 μg/mL) plus IFN-γ (100 U/mL) taken as 100%. Data represent the M ± SEM of at least three independent experiments. Statistical differences were determined by one-way ANOVA, followed by Dunnett's multiple comparisons test of the normalised data; $p > .05$ confirmed that there was no significant difference.

5.3.6 Effect of RU-486 on the inhibition of NO production caused by dexamethasone

To determine whether the effects of dexamethasone on the inhibition of NO production involved interaction with the GCR, experiments were performed using RU-486 in which cells were pretreated with 10 mM RU-486 1 h prior to the addition of dexamethasone (3–10 μM) 30 min prior to activation with LPS (100 μg/mL) and IFN-γ (100 U/mL). The presence of the receptor blocker showed a clear reversal of the inhibited NO (Figure 40).

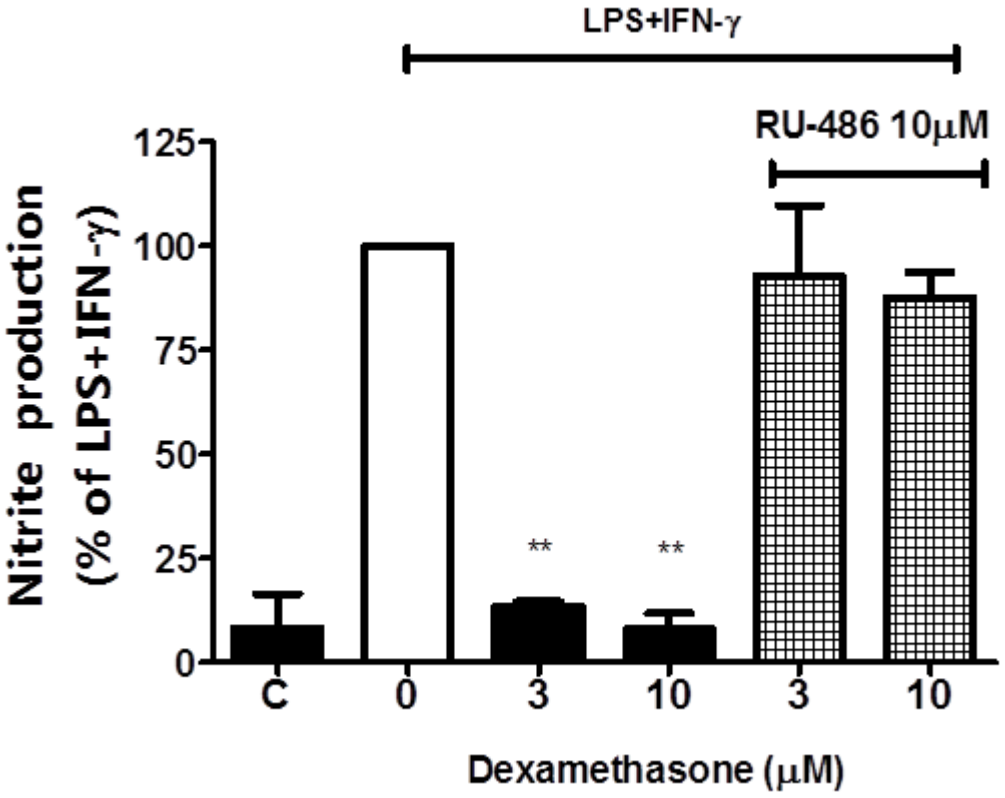

Figure 40. Effect of RU-486 on the inhibition of NO production caused by dexamethasone. Confluent monolayers of RASMCs in 24-well plates were pretreated for 1 h with RU-486 at 10 μM, followed by the addition of 3 and 10 μM of dexamethasone 30 min prior to activation with 100 μg/mL of LPS and 100 U/mL of IFN-γ for 24 h. The culture medium was analysed by Griess assay to determine total nitrite levels following the method described in section 2.6. Data are expressed as a percentage of nitrite production, with the response to LPS (100

μg/mL) plus IFN-γ (100 U/mL) taken as 100%. Data are the M ± SEM of at least three independent experiments. Statistical differences were determined by one-way ANOVA, followed by Dunnett's multiple comparisons test of the normalised data;** denotes $p < .01$ compared to activated control.

5.3.7 Effect of RU-486 on the inhibition of iNOS expression caused by dexamethasone

To determine whether effects of dexamethasone on the inhibition of iNOS expression involved an interaction with the GCR, experiments were conducted in the presence of RU-486, in which cells were pretreated with 10 μM of RU-486 1 h prior to the addition of dexamethasone 30 min prior to activation with LPS (100 μg/mL) and IFN-γ (100 U/mL). The presence of the receptor blocker indicated a clear reversal of the inhibited NO (Figure 41).

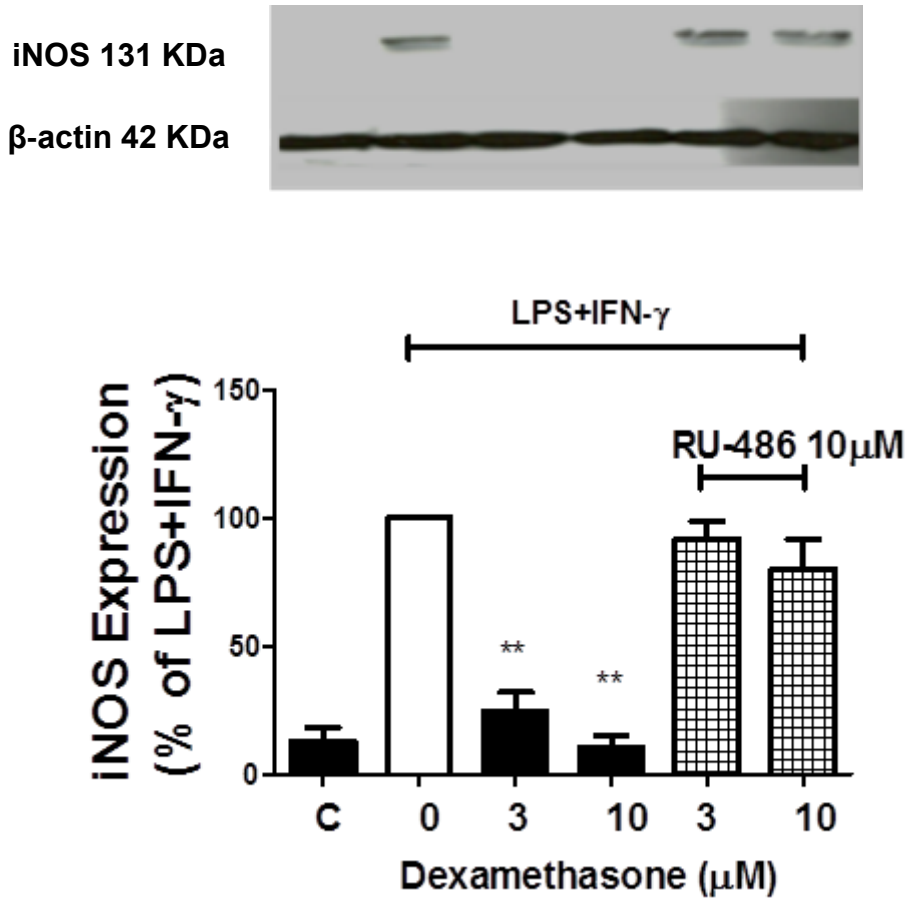

Figure 41. Effect of RU-486 on the inhibition of iNOS expression caused by dexamethasone. Confluent monolayers of RASMCs in 24-well plates were pretreated for 1 h with RU-486 at 10 μM, followed by the addition of 3 and 10 μM of dexamethasone 30 min before activation with 100 μg/mL of LPS and 100 U/mL of IFN-γ for 24 h. The expression of iNOS was determined by western blotting following the method described in section 2.9. The blot is representative of at least three independent experiments, and the bar graph depicts densitometric data expressed as a percentage of iNOS expression, with the response to LPS (100 μg/mL) plus IFN-γ (100 U/mL) taken as 100%. Data represent the M ± SEM of at least three independent experiments. Statistical differences were determined by one-way ANOVA, followed by Dunnett's multiple comparisons test of the normalised data; **denotes $p < .01$ compared to activated control.

5.3.8 Effect of RU-486 on the inhibition of NO production by hydrocortisone

To determine whether the effects of hydrocortisone on the inhibition of NO production involved an interaction with the GCR, experiments were performed with RU-486. As in the

studies with dexamethasone, cells were pretreated with 10 μM of RU-486 1 h prior to the addition of hydrocortisone (3–10 μM) 30 min prior to activation with LPS (100 μg/mL) and IFN-γ (100 U/mL). The presence of RU-486 prevented the inhibition of NO synthesis with hydrocortisone (Figure 42).

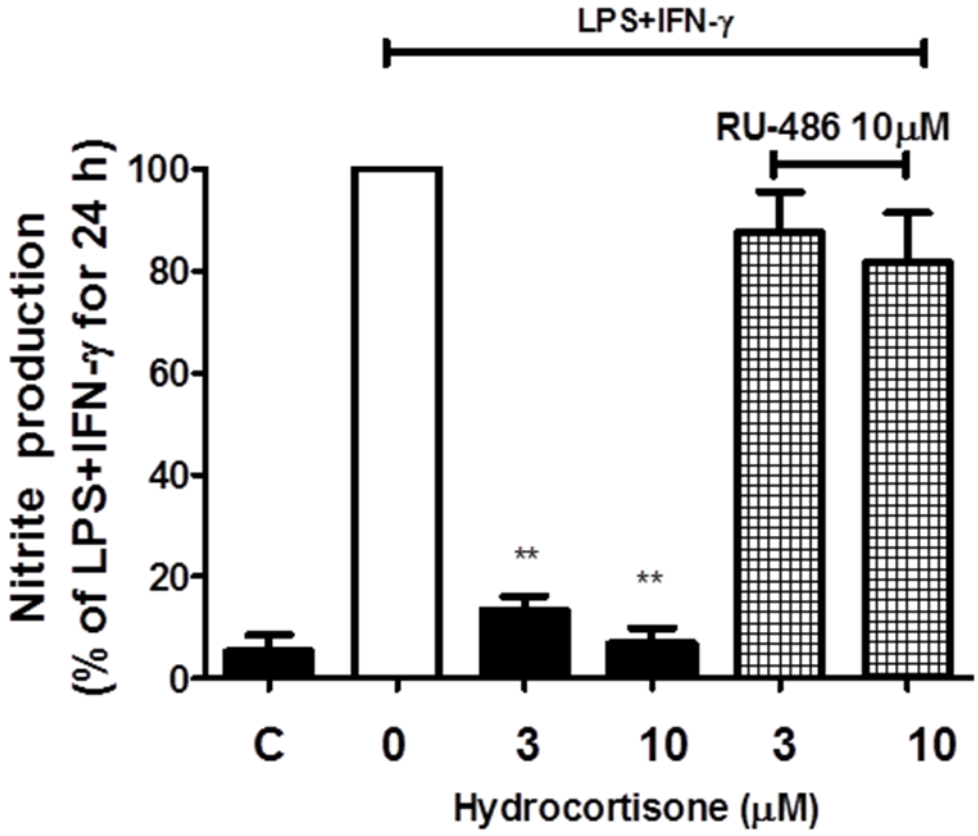

Figure 42. Effect of RU-486 on the inhibition of NO production caused by hydrocortisone. Confluent monolayers of RASMCs in 24-well plates were pretreated for 1 h with RU-486 at 10 μM, followed by the addition of 3 and 10 μM hydrocortisone 30 min prior to activation with 100 μg/mL of LPS and 100 U/mL of IFN-γ for 24 h. The culture medium was analysed by Griess assay to determine total nitrite levels following the method described in section 2.6. Data are expressed as a percentage of nitrite production, with the response to LPS (100 μg/mL) plus IFN-γ (100 U/mL) taken as 100%. Data are the M ± SEM of at least three independent experiments. Statistical differences were determined by one-way ANOVA, followed by Dunnett's multiple comparisons test of the normalised data; **denotes $p < .01$ compared to activated control.

5.3.9 Effect of RU-486 on the inhibition of iNOS expression by hydrocortisone

As with dexamethasone, experiments were performed to determine whether the hydrocortisone inhibition of iNOS expression involved an interaction with the GCR. Cells were pretreated with 10 μM of RU-486 for 1 h prior, followed by hydrocortisone (3 –10 μM) for 30 min prior to activation with LPS (100 μg/mL) and IFN-γ (100 U/mL). Consistent with its effects on nitrite production and responses to dexamethasone, RU-486 reversed inhibitions of iNOS expression caused by hydrocortisone and restored protein levels nearly back to the activated control level (Figure 43).

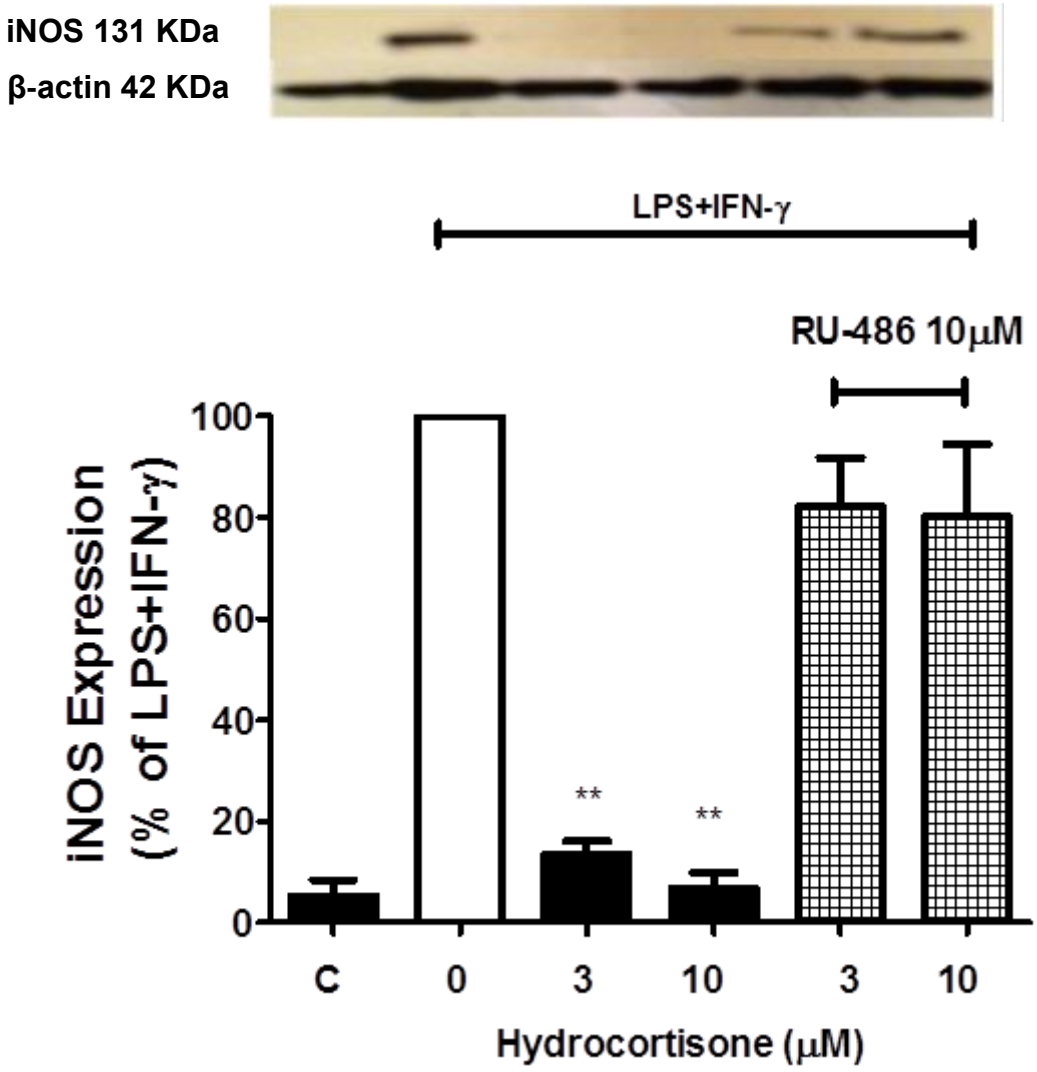

Figure 43. Effect of RU-486 on the inhibition of iNOS expression caused by hydrocortisone. Confluent monolayers of RASMCs in 24-well plates were pretreated for 1 h with RU-486 at 10 μM, followed by the addition of 3 and 10 μM of hydrocortisone 30 min prior to activation with 100 μg/mL of LPS and 100 U/mL of IFN-γ for 24 h. The expression of iNOS was determined by western blotting following the method described in section 2.9. The blot is representative of at least three independent experiments, and the bar graph depicts densitometric data expressed as a percentage of iNOS expression, with the LPS (100 μg/mL) plus IFN-γ (100 U/mL) response taken as 100%. Data represent the M ± SEM of at least three independent experiments. Statistical differences were determined by one-way ANOVA, followed by Dunnett's multiple comparisons test of the normalised data; **denotes $p < .01$ compared to activated control.

5.3.10 Effect of RU-486 on the inhibition of NO production by fluticasone

To complete the series of studies to determine whether the GCs acted via the GCR in suppressing NO synthesis, cells were pretreated in parallel experiments with 10 µM of RU-486 for 1 h, followed by treatment with fluticasone (1–3 nM) for 30 min prior to activation with LPS (100 µg/mL) and IFN-γ (100 U/mL). As in the experiments described above, the presence of the receptor blocker completely reversed the partial inhibitions in nitrite accumulation caused by fluticasone (Figure 44), thereby indicating the involvement of the GC receptor in the actions of fluticasone, as well as dexamethasone and hydrocortisone.

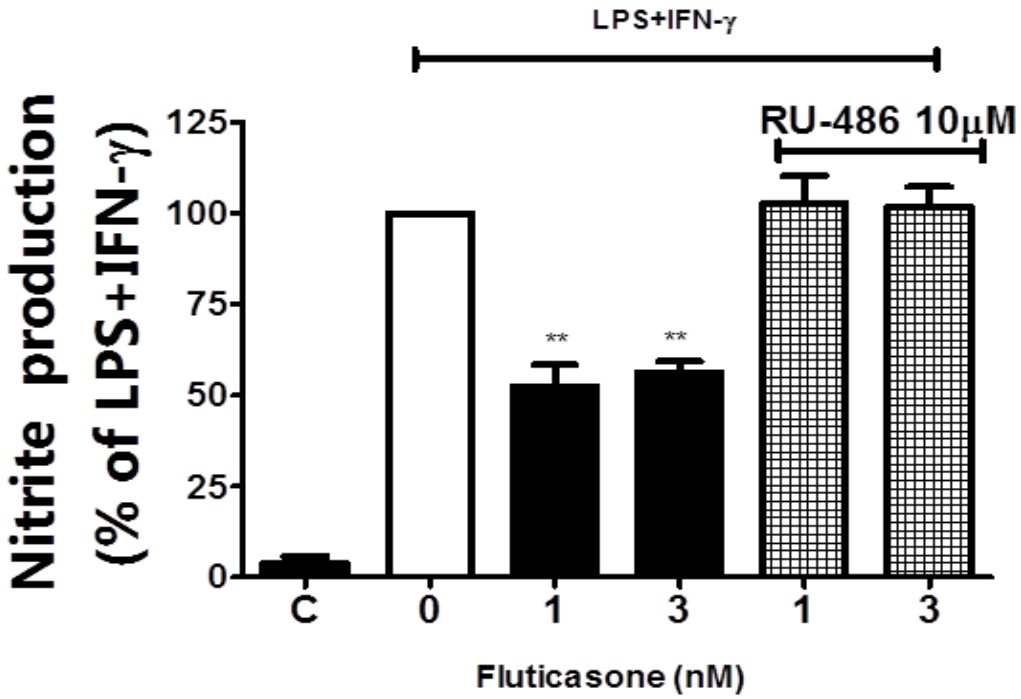

Figure 44. Effect of RU-486 on the inhibition of NO production caused by fluticasone. Confluent monolayers of RASMCs in 24-well plates were pretreated for 1 h with RU-486 at 10 µM followed by the addition of 1 and 3 nM fluticasone 30 min prior to activation with 100 µg/mL of LPS and 100 U/mL of IFN-γ for 24 h. The culture medium was analysed by Griess assay to determine total nitrite levels according to the method described in section 2.6. Data are expressed as a percentage of nitrite production, with the response to LPS (100 µg/mL) plus IFN-γ (100 U/mL) taken as 100%. Data are the M ± SEM of at least three independent experiments. Statistical differences were determined by one-way ANOVA, followed by Dunnett's multiple comparisons test of the normalised data; **denotes $p < .01$ compared to activated control.

5.3.11 Effect of RU-486 on the inhibition of iNOS expression caused by fluticasone

To determine whether the inhibition of iNOS expression by fluticasone is also mediated via the GCR, cells were pretreated with 10 μM of RU-486 1 h prior to the addition of fluticasone (1 –3 nM) 30 min prior to activation with LPS (100 μg/mL) and IFN-γ (100 U/mL). The presence of RU-486 reversed the inhibition of iNOS caused by fluticasone (Figure 45).

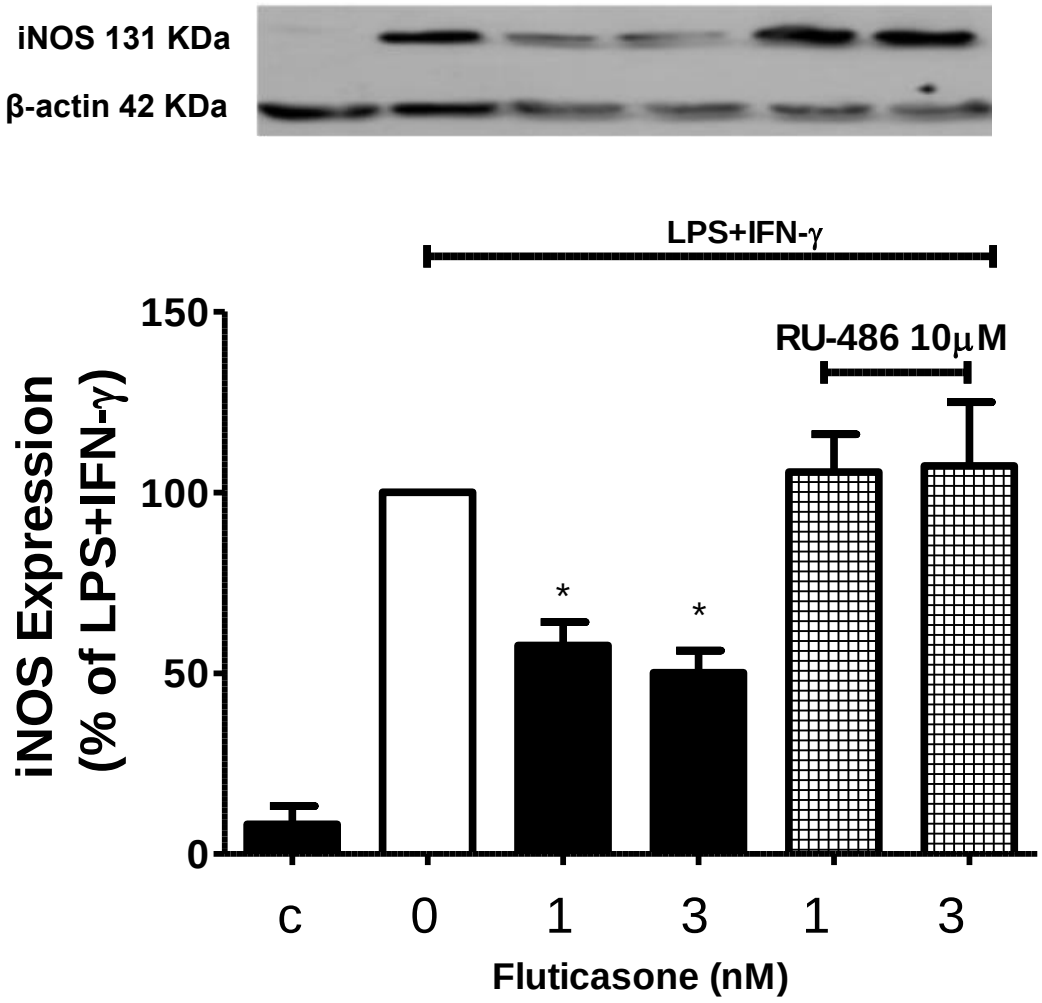

Figure 45. Effect of RU-486 on the inhibition of iNOS expression caused by fluticasone. Confluent monolayers of RASMCs in 24-well plates were pretreated for 1 h with RU-486 at 10 μM, followed by the addition of 1 and 3 nM of fluticasone 30 min prior to activation with 100 μg/mL of LPS and 100 U/mL of IFN-γ for 24 h. The expression of iNOS was determined by western blotting following the method described in section 2.9. The blot is representative of at least three independent experiments, and the bar graph depicts densitometric data expressed as a percentage of iNOS expression, with the LPS (100 μg/mL) plus IFN-γ (100 U/mL) response taken as 100%. Data represent the M ± SEM of at least three independent experiments. Statistical differences were determined by one-way ANOVA, followed by Dunnett's multiple comparisons test of the normalised data; *denotes $p < .05$ compared to activated control.

5.3.12 Effect of MR blockade on the inhibition of NO production by dexamethasone

Since dexamethasone and hydrocortisone exert effects independent of their actions on the GCR, additional studies were conducted to determine whether dexamethasone or hydrocortisone, if not both, had any additional effects, especially on the MR, that could contribute to the actions demonstrated on NO production and iNOS expression. Fluticasone was also investigated in this series of experiments to establish the selectivity of the MR antagonist eplerenone.

To investigate dexamethasone in particular, confluent monolayers of cells were pretreated with eplerenone (0.1–10.0 μM) 1 h prior to the addition of dexamethasone at 10 μM 30 min before activation with LPS and IFN-γ. Ultimately, eplerenone failed to reverse the inhibition of nitrite production caused by dexamethasone, even at concentrations of up to 10 μM (Figure 46), in marked contrast to RU-486, which completely reversed the inhibitions of NO caused by dexamethasone, thereby suggesting that the latter might not act via MR in suppressing NO synthesis.

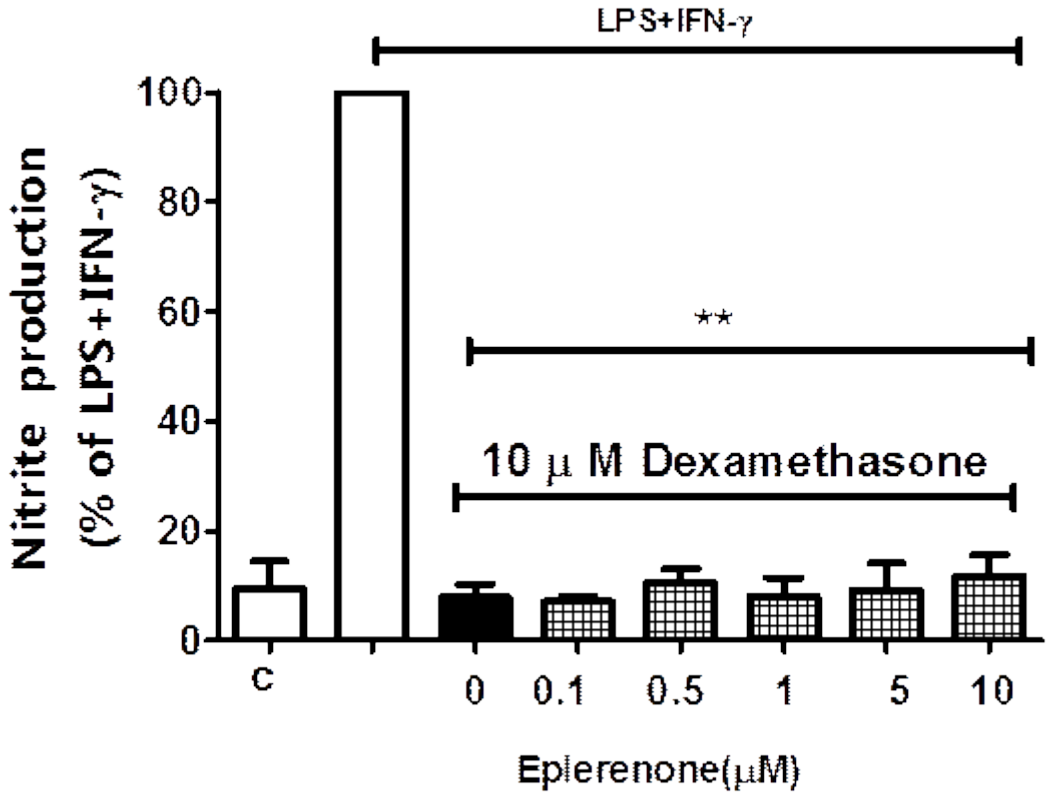

Figure 46. Effect of eplerenone on the inhibition of NO production caused by dexamethasone. Confluent monolayers of RASMCs in 24-well plates were pretreated for 1 h with eplerenone at 0.1–10.0 μM, followed by the addition of 10 μM of dexamethasone 30 min prior to activation with 100 μg/mL of LPS and 100 U/mL of IFN-γ for 24 h. The culture medium was analysed by Griess assay to determine total nitrite levels following the method described in section 2.6. Data are expressed as a percentage of nitrite production, with the response to LPS (100 μg/mL) plus IFN-γ (100 U/mL) taken as 100%. Data are the M ± SEM of at least three independent experiments. Statistical differences were determined by one-way ANOVA, followed by Dunnett's multiple comparisons test of the normalised data; ** denotes $p < .01$ compared to the activated control.

5.3.13 Effect of MR blockade on the inhibition of iNOS expression by dexamethasone

To determine whether the effects of dexamethasone on the inhibition of iNOS expression occured via an interaction with the MR, further experiments looked at changes in iNOS expression in the presence of eplerenone (0.1–10.0 μM) which was preincubated with confluent monolayers of cells 1 h prior to the addition of dexamethasone at 10 μM, for 30 min before activation with LPS and IFN-γ for 24 h. Consistent with data on nitrite accumulation, eplerenone did not alter inhibitions of iNOS expression by dexamethasone, confirming that it did not act through MR in suppressing the expression of iNOS in the smooth muscle cell model used for the studies of this thesis.

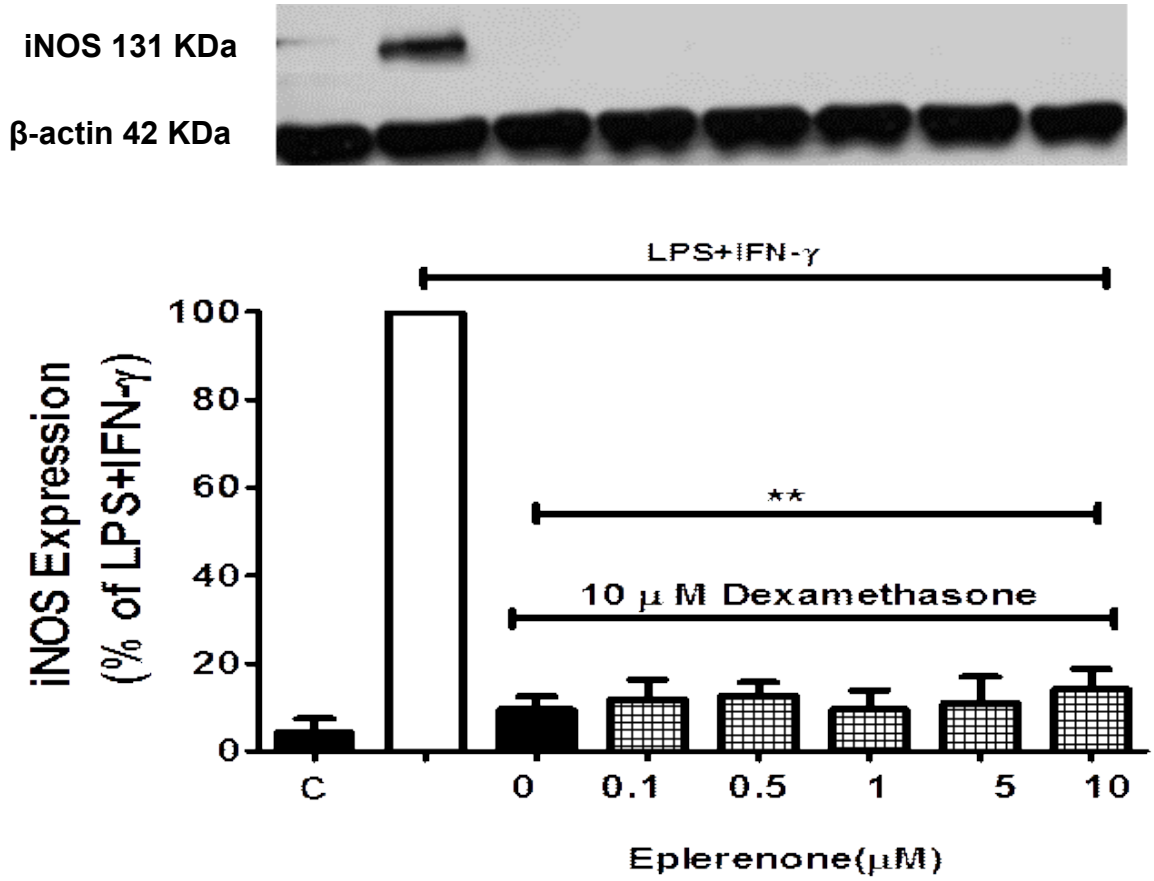

Figure 47. Effect of eplerenone on the inhibition of iNOS expression caused by dexamethasone. Confluent monolayers of RASMCs in 24-well plates were pretreated for 1 h with eplerenone at 0.1–10.0 μM, followed by addition of 10 μM of dexamethasone 30 min prior to activation with 100 μg/mL of LPS and 100 U/mL of IFN-γ for 24 h. The expression of iNOS was determined by western blotting following the method described in section 2.9. The blot is representative of at least three independent experiments, and the bar graph depicts densitometric data expressed as a percentage of iNOS expression, with the response to LPS (100 μg/mL) plus IFN-γ (100 U/mL) taken as 100%. Data represent the M ± SEM of at least three independent experiments. Statistical differences were determined by one-way ANOVA, followed by Dunnett's multiple comparisons test of the normalised data; ** denotes $p < .01$ compared to the activated control.

5.3.14 Effect of MR blockade on the inhibition of NO production by hydrocortisone

Following the studies with dexamethasone, hydrocortisone was investigated to determine whether its inhibition of NO production occured via an interaction with the MRs. As already described, eplerenone (0.1–10.0 μM) was incubated with confluent monolayers of cells for 1 h prior to the addition of hydrocortisone at 10 μM for 30 min before activation with LPS and IFN-γ for 24 h. However, no significant change in the inhibition of iNOS expression levels caused by hydrocortisone resulted (Figure 48).

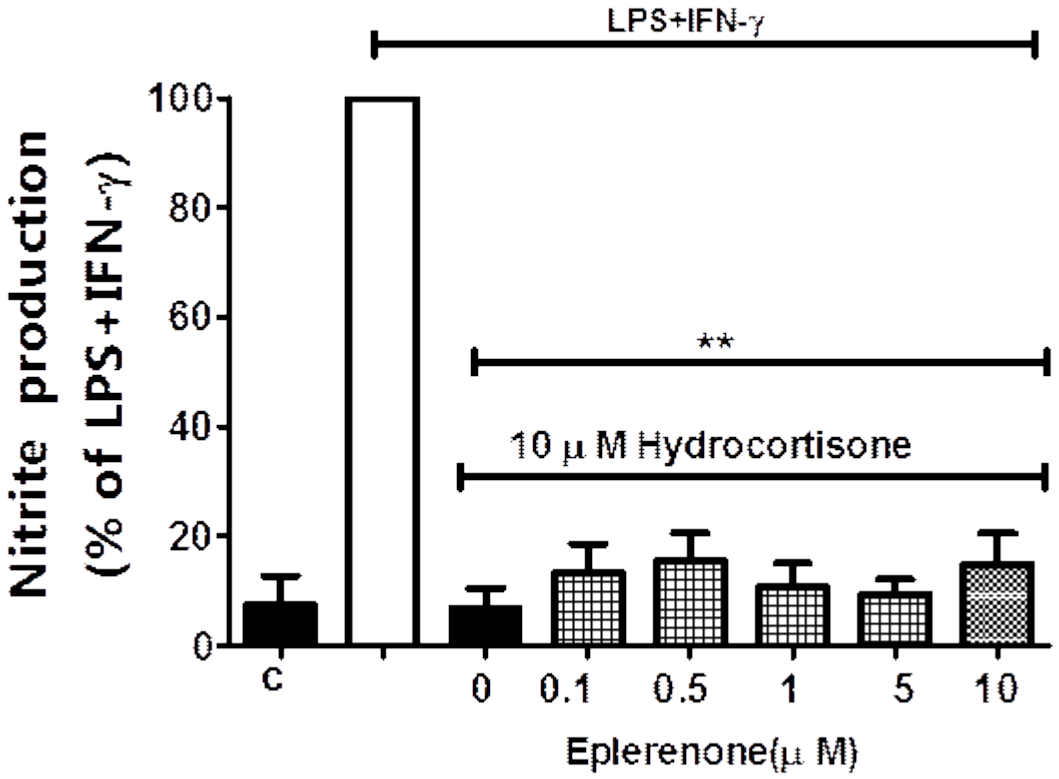

Figure 48. Effect of eplerenone on the inhibition of NO production caused by hydrocortisone. Confluent monolayers of RASMCs in 24-well plates were pretreated for 1 h with eplerenone at 0.1–10.0 μM, followed by the addition of 10 μM of hydrocortisone 30 min prior to activation with 100 μg/mL of LPS and 100 U/mL of IFN-γ for 24 h. The culture medium was analysed by Griess assay to determine total nitrite levels following the method described in section 2.6. Data are expressed as a percentage of nitrite production, with the response to LPS (100 μg/mL) plus IFN-γ (100 U/mL) taken as 100%. Data are the M ± SEM of at least three independent experiments. Statistical differences were determined by one-way ANOVA, followed by Dunnett's multiple comparisons test of the normalised data; ** denotes $p < .01$ compared to the activated control.

5.3.15 Effect of MR blockade on the inhibition of iNOS expression by hydrocortisone

Consistent with its lack of effect on the inhibition of NO production, eplerenone (0.1–10.0 μM) also failed to reverse inhibitions of iNOS expression by hydrocortisone when coincubated with confluent monolayers of cells for 1 h prior to the addition of hydrocortisone at 10 μM for 30 min before activation with LPS and IFN-γ for 24 h.

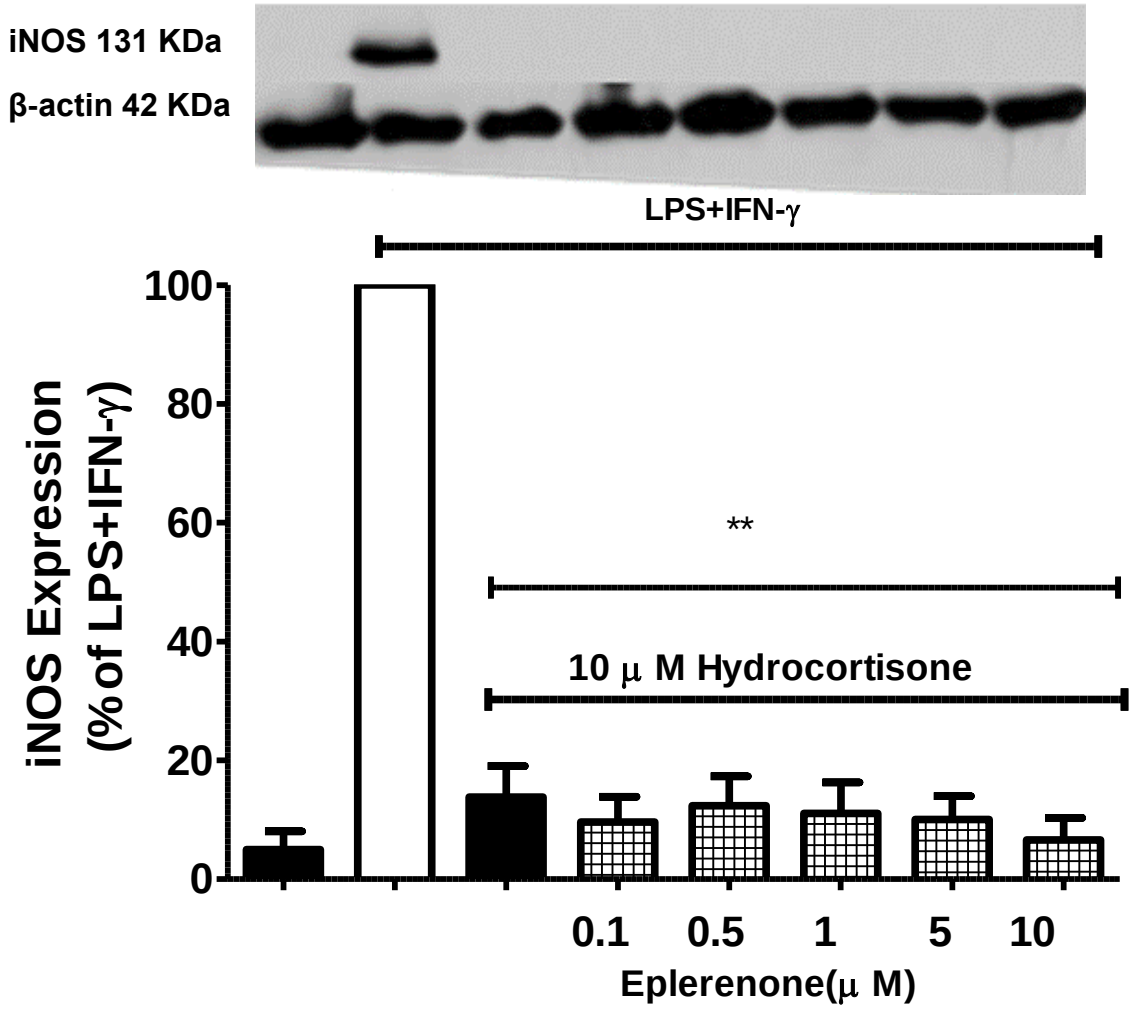

Figure 49. Effect of eplerenone on the inhibition of iNOS expression caused by hydrocortisone. Confluent monolayers of RASMCs in 24-well plates were pretreated for 1 h with eplerenone at 0.1–10.0 μM, followed by the addition of 10 μM hydrocortisone 30 min prior to activation with 100 μg/mL of LPS and 100 U/mL of IFN-γ for 24 h. The expression of iNOS was determined by western blotting following the method described in section 2.9. The blot is representative of at least three independent experiments, and the bar graph depicts densitometric data expressed as a percentage of iNOS expression, with the response to LPS (100 μg/mL) plus IFN-γ (100 U/mL) taken as 100%. Data represent the M ± SEM of at least three independent experiments. Statistical differences were determined by one-way ANOVA, followed by Dunnett's multiple comparisons test of the normalised data; ** denotes $p < .01$ compared to the activated control.

5.3.16 Effect of MR blockers on the inhibition of NO production by fluticasone

In parallel experiments, the effects of eplerenone (0.1–10.0 μM) on fluticasone-induced inhibition of NO production were investigated, despite knowledge that fluticasone does not act on MR. The purpose of this study was to determine the selectivity of eplerenone should it have any effect on the actions of dexamethasone or hydrocortisone. Ultimately, eplerenone neither altered responses to either compund nor affected the inhibition of induced nitrite accumulation caused by fluticasone (Figure 50).

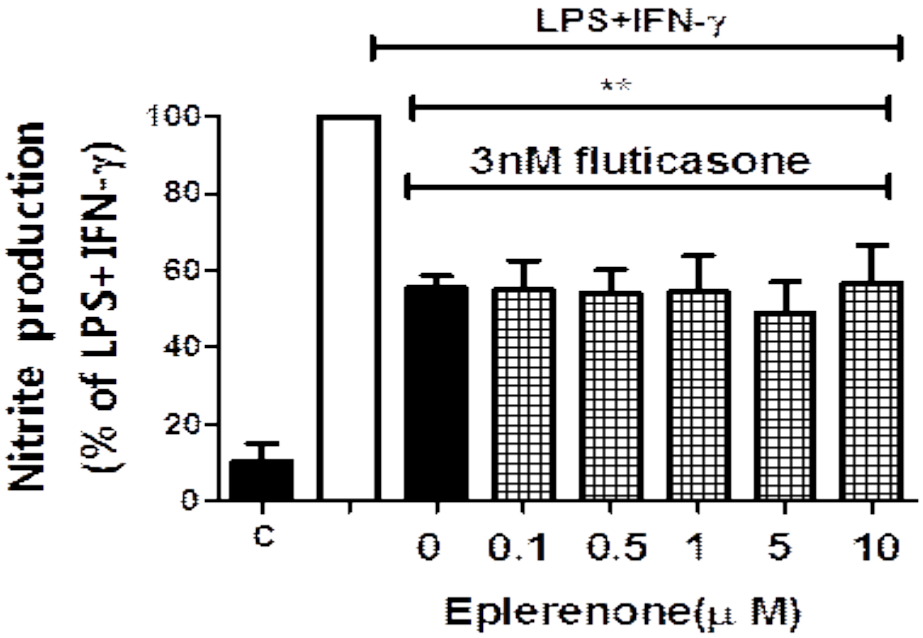

Figure 50. Effect of eplerenone on the inhibition of NO production caused by fluticasone. Confluent monolayers of RASMCs in 24-well plates were pretreated for 1 h with eplerenone at 0.1–10.0 μM, followed by the addition of 3 nM of fluticasone 30 min prior to activation with 100 μg/mL of LPS and 100 U/mL of IFN-γ for 24 h. The culture medium was analysed by Griess assay to determine total nitrite levels following the method described in section 2.6. Data are expressed as a percentage of nitrite production, with the response to LPS (100 μg/mL) plus IFN-γ (100 U/mL) taken as 100%. Data are the M ± SEM of at least three independent experiments. Statistical differences were determined by one-way ANOVA, followed by Dunnett's multiple comparisons test of the normalised data. ** denotes $p < .01$ compared to the activated control.

5.3.17 Effect of MR blockade on the inhibition of iNOS expression by fluticasone

For completeness, the potential effect of eplerenone on fluticasone inhibition of iNOS expression was investigated as well. However, as with NO production, eplerenone (0.1–10.0 μM) did not regulate the inhibitory actions of fluticasone (3 nM) on the induction of iNOS (Figure 51).

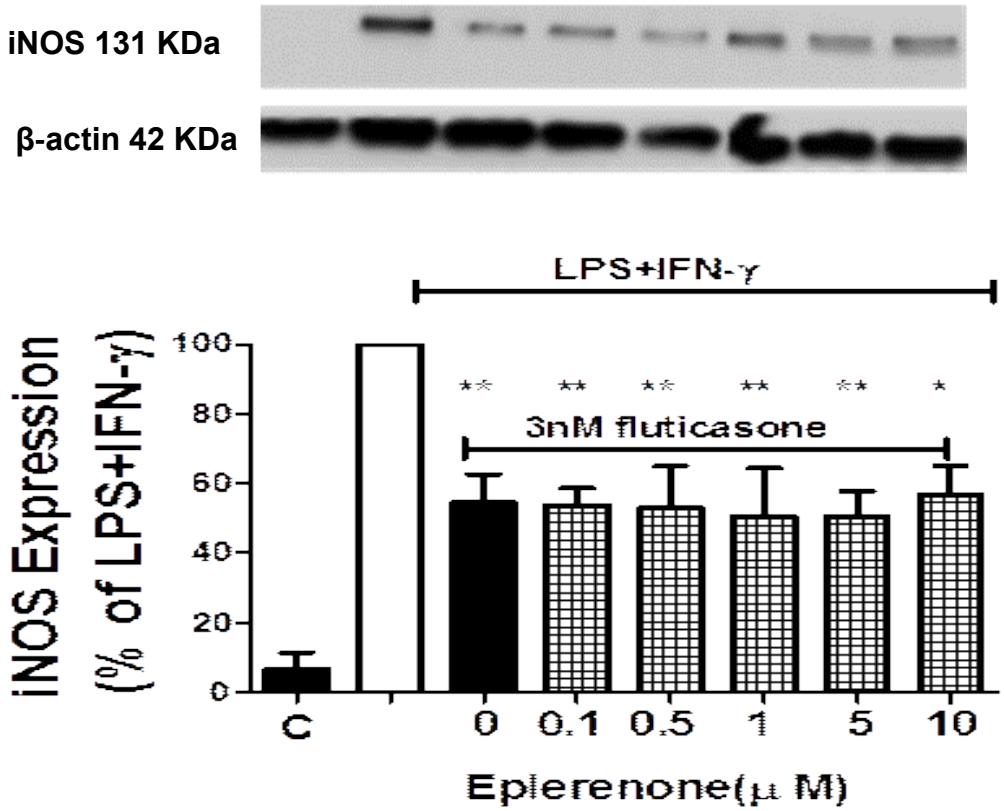

Figure 51. Effect of eplerenone on the inhibition of iNOS expression caused by fluticasone. Confluent monolayers of RASMCs in 24-well plates were pretreated for 1 h with eplerenone at 0.1–10.0 μM, followed by the addition of 3 nM of fluticasone 30 min prior to activation with 100 μg/mL of LPS and 100 U/mL of IFN-γ for 24 h. The expression of iNOS was determined by western blotting following the method described in section 2.9. The blot is representative of at least three independent experiments, and the bar graph depicts densitometric data expressed as a percentage of iNOS expression, with the response to LPS (100 μg/mL) plus IFN-γ (100 U/mL) taken as 100%. Data represent the M ± SEM of at least three independent experiments. Statistical differences were determined by one-way ANOVA, followed by Dunnett's multiple comparisons test of the normalised data; * denotes $p < .05$ and **$p < .01$, respectively, compared to the activated control.

5.4 Discussion

The aim of this chapter was to investigate whether GCRs or MRs, if not both, are involved in GCs' inhibition of iNOS expression and NO production. As an MTT assay demonstrated, the different concentrations of GCR or MR blockers studied with different GCs in both the presence and absence of LPS and IFN-γ had no cytotoxic effect. Such responses of the compounds are thus taken as a true representation of their pharmacological effects, not as a consequence of cytotoxic action.

Investigating the role of GCR in the cell system developed for this thesis involved the classical GCR antagonist RU-486, which is both a GC and progesterone receptor antagonist (Mao et al., 1992) widely used in implicating or regulating GC actions (Gagne et al., 1985; Hu et al., 2003; Jung–Testas & Baulieu, 1983; Shibata et al., 2009), in abortions, and in Cushing's syndrome (El-Refaey et al., 1995; Johanssen & Allolio, 2007). Moreover, RU-486 has been reported to suppress the effect of dexamethasone on NO production and iNOS expression in different cell types, including RASMCS (Godfrey et al., 2011), rat embryonal cortical neurons (Golde et al., 2003), and RAW 264.7 cells (Walker et al., 1997). Such action was confirmed in the studies conducted for this thesis to extend beyond dexamethasone to include hydrocortisone and fluticasone, neither of which have been investigated in RASMCs. In doing so, it was particularly important to demonstrate action on the GCR since both dexamethasone and hydrocortisone have non-GCR targets. Both compounds also abolished iNOS expression and function, whereas the more selective GCR agonist, fluticasone, only partially suppressed iNOS expression and NO production. Data showed that RU-486 prompted a complete reversal of the inhibitory actions of not only fluticasone, but also dexamethasone and hydrocortisone. Those findings confirm that all three compounds act through the GCR in regulating the LPS and IFN-γ induction of iNOS, at least in RASMCs.

Moreover, data representing dexamethasone are consistent with previous findings regarding the same type of cell (Godfrey et al., 2011).

Data generated with hydrocortisone showed that RU-486 reverse the inhibition of iNOS expression and function, as consistent with findings in N9 murine microglia (Chang & Liu, 2000). However, no data representing similar effects in RASMCs or on fluticasone are available other than the findings of this thesis, which makes its data novel. Moreover, we have also demonstrated that inhibition of NO production occurred as a consequence of the inhibition of iNOS expression which was seen over the same concentration range as those found to inhibit nitrite accumulation.

RU-486 act as a glucocorticoids antagonist with Ki = 6 nM, and Ki = 15 nM for progesterone (Eda et al., 2015). Again, these concentrations do not correlate with the concentrations used in this thesis and indeed in other publications in the literature due to the complexity of cell systems compared to test tubes.

Mineralocorticoids constitute a class of corticosteroids with a critical role in salt and water homeostasis (Edelman et al., 1963). MRs, by extension, are expressed in many cells, including vascular smooth muscle and endothelial cells (Jaisser & Farman, 2016), and their antagonists (e.g., spironolactone) are used as antihypertensives. Such antagonists, however, can cause severe adverse side effects, including menstrual disturbances and male impotence (Hughes & Cunliffe, 1988). In response, more selective mineralocorticoid blockers have been developed, including eplerenone (Pitt et al., 2003), which is used in treating congestive heart failure and hypertension (Craft, 2004). Eplerenone is more selective than spironolactone, which has progestogenic and antiandrogenic actions that pose potentially severe side effects (de Gasparo et al., 1987; Struthers et al., 2008). Their blockade of mineralocorticoids

prevents the action of its agonist, aldosterone, which raises blood pressure by increasing sodium reabsorption.

The main mineralocorticoid hormones have demonstrated an ability to inhibit iNOS expression and function in many cell types. Aldosterone, for instance, inhibits iNOS in neonatal rat cardiomyocytes, in which the effects were reversed by spironolactone (Chun et al., 2003), as well as inhibits iNOS in RASMCs, which was reversed with RU-486 but not with mineralocorticoid antagonists spironolactone and eplerenone (Godfrey et al., 2011). By contrast, aldosterone had no effect on iNOS in mouse macrophages (Harizi et al., 2008). Interestingly, other studies have found that spironolactone inhibits iNOS in RASMCs (Godfrey et al., 2011) and in rat aortic adventitia (Deng et al., 2010), a contraindication possibly explained by species differences or, if not also, the nonselectivity of spironolactone, which might interfere with different receptors or pathways, if not both.

To identify whether MRs play any role in inducing iNOS or producing NO in the cell system developed for the studies of this thesis, experiments were performed using eplerenone over a concentration range within the range used to block MRs in other studies. Interestingly, blocking MRs with eplerenone did not affect inhibited iNOS expression or NO production by GCs. Such findings confirm that MRs play no significant role in our system and that the observed inhibitory actions of dexamethasone, hydrocortisone, and fluticasone are highly likely to be mediated predominantly via the GCR. Unclear, however, is why the more selective GC, fluticasone, caused only partial inhibition, where dexamethasone and hydrocortisone virtually abolished iNOS and NO synthesis. The role of other steroids such as sex steroids could be investigated in future work. Sex steroids are hormones including Oestrogens, progesterone and androgens that play a critical role in reproductive function. Oestrogens is a female hormone which is responsible for the development and regulation of

the female reproductive system. Oestrogens is also produced at a low level in males and is responsible for physiological and pathological conditions (Lombardi et al., 2001). It acts by binding to oestrogenic receptors which when bound translocate from the cytosol into the nucleus then interact with a class of nuclear proteins which lead to activation of transcription. Progesterone is another steroid hormone which binds to progesterone receptors and plays a critical role in in reproductive function and bone metabolism (von et al., 2016). In addition, androgen is one of the important hormonal steroids which play a significant role in development of the male reproductive system and binds to androgen receptors to regulate gene expression. In addition to the regulation of sex steroids in reproductive function, sex steroids are also very important in inflammation regulation (Gilliver, 2010).

In this thesis, we focused on GCs and MRs involvement in the action of GCs in the reduction of iNOS expression and function. However, Other steroid receptors could be involved in this action, but due to time constraints, this potential involvement will have to be investigated in future.

6. Role of p38 MAPKs and Akt on Fluticasone-Induced Inhibition of iNOS expression and NO Production in RASMCs

6.1 Introduction

P38 MAPKs are protein kinases activated in response to various stimuli such as cytokines, heat shock, and stress (Cuadrado & Nebreda, 2010). Biological responses associated with p38 activation include various inflammatory diseases (Hollenbach et al., 2004; Johnson & Bailey, 2003), apoptosis (Wada & Penninger, 2004), and cell differentiation (Hu et al., 2003). More relevant to this thesis, p38 MAPK is critically involved in the expression of iNOS expression and NO production in RASMCs (Baydoun et al., 1999).

Akt, or protein kinase B, is a serine–threonine kinase that regulates a multitude of biological processes, including cell survival and apoptosis, as well as acts as part of signal transduction in response to growth factors and extracellular stimuli (Song et al., 2005). More importantly, it is involved in iNOS expression and function in RASMCs (Hattori et al., 2003).

Since data found earlier in the studies for this thesis have shown that fluticasone reduces iNOS expression and function, additional experiments were performed to determine whether those effects occur via p38 or Akt, if not both. The studies focused on those kinases due to time constraints, and it is acknowledged that other signalling pathways are possibly involved, including the p42 or p44 MAPK (Doi et al., 2000), protein kinase C (Scott–Burden et al., 1994) or c-Jun N-terminal kinase (Chan & Riches, 2001). Time constraints also limited the studies in this thesis to fluticasone, partly due to its focus on the GC component that regulates iNOS induction. At the same time, of the three compounds investigated, fluticasone is not as well characterised in relation to iNOS expression. Nevertheless, it is worth establishing whether dexamethasone or hydrocortisone directly regulate p38 or Akt, if not both, the findings regarding which could be further extended to other kinase pathways.

6.2 Material and Methods

6.2.1 Experimental conditions

6.2.1.1 Time dependent activation of phospho-p38 (P-p38) MAPK

Confluent monolayers of RASMCs were treated with LPS (100 μg/mL) and IFN-γ (100 U/mL) at different time points between 0.5 and 24 h. The expression of phospho-p38 (P-p38) was determined by western blotting following the method described in section 2.9.

6.2.1.2 Effect of different concentrations of SB203580 and LY294002 on NO production and iNOS expression

Confluent monolayers of RASMCs in 24-well plates were pretreated for 1 h with SB203580 at 0.1–10.0 μM or LY294002 at 0.1–10.0 μM prior to activation with 100 μg/mL of LPS and 100 U/mL of IFN-γ for 24 h. The culture medium was analysed using Griess assay to determine total nitrite levels following the method described in section 2.6, and the expression of iNOS was determined by western blotting following the method described in section 2.9. Changes in cell viability were examined by MTT assay following the method described in section 2.4.

6.2.1.3 Effects of fluticasone, SB203580, and LY294002 on iNOS expression, nitrite production, and P-p38 and P-Akt expression

Confluent monolayers of RASMCs were pretreated for 1 h with RU-486, SB203580, or LY294002 at 10 μM, followed by the addition of fluticasone at 3 nM for 30 min prior to activation with LPS and IFN-γ. The culture medium was analysed by Griess assay to determine total nitrite levels. The expressions of iNOS, P-p38, and P-Akt in cell lysates were determined by western blotting following the method described in section 2.9.

6.3 Results

6.3.1 Effects of SB203580 or LY294002 on the viability of RASMCs

This experiment was conducted to determine whether different concentrations of SB203580 or LY294002 with or without activation with LPS and IFN-γ exerted any cytotoxic effects on the cell model. Considered to be 100% viable, control cells were compared to cells treated with different concentrations of SB203580 and LY294002 in the presence and absence of LPS and IFN-γ.

Despite the decreased metabolism of MTT, the decrease was marginal, as concentrations of either SB203580 (Figure 52) or LY294002 (Figure 53) increased, and were not statistically significant. Additional studies were therefore performed using the concentration range examined in the studies on cytotoxicity.

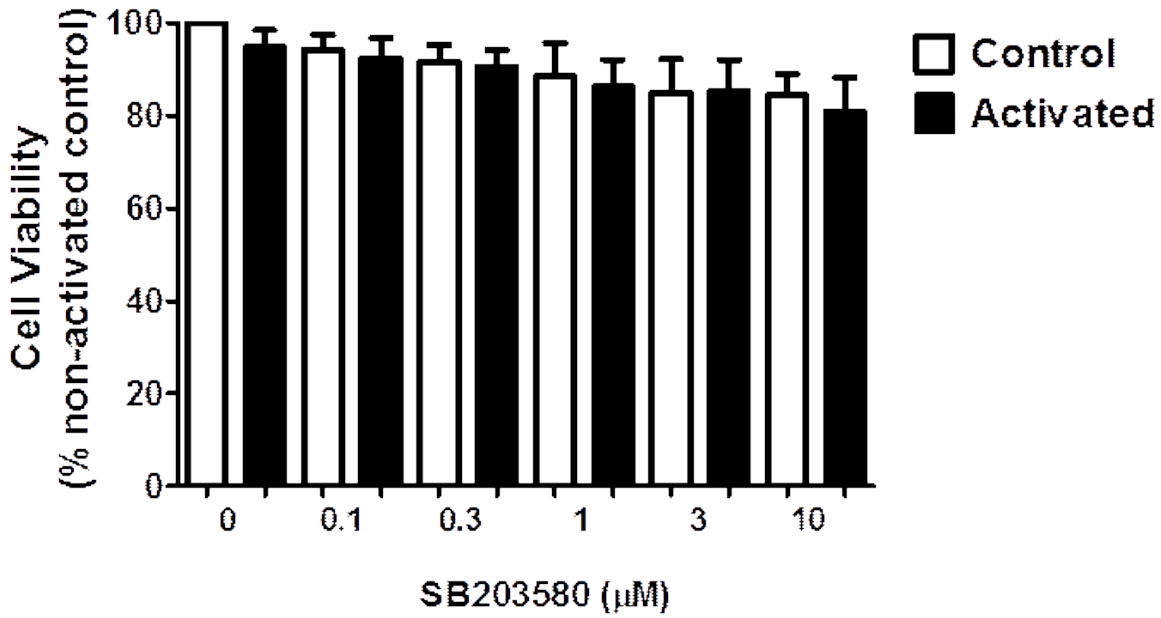

Figure 52. Effect of different concentrations of SB203580 on cell viability in RASMCs. Confluent monolayers of RASMCs in 96-well plates were pretreated with only CM, different concentrations of SB203580 (0.01–10.00 μM), or only SB203580 (0.01–10.00 μM) for 1 h prior to activation with both LPS (100 μg/mL) and IFN-γ (100 U/mL) for 24 h. The metabolism of MTT was determined colourimetrically following the method described in section 2.4. The white bars represent controls, and the black ones represent activated cells. Data are presented as the percentage of viable cells compared to the controls and represent the M ± SEM of at least three individual experiments. Statistical differences were determined by one-way ANOVA, followed by Dunnett's multiple comparisons test of the normalised data; $p > .05$ confirmed that there was no significant difference compared to the nonactivated control.

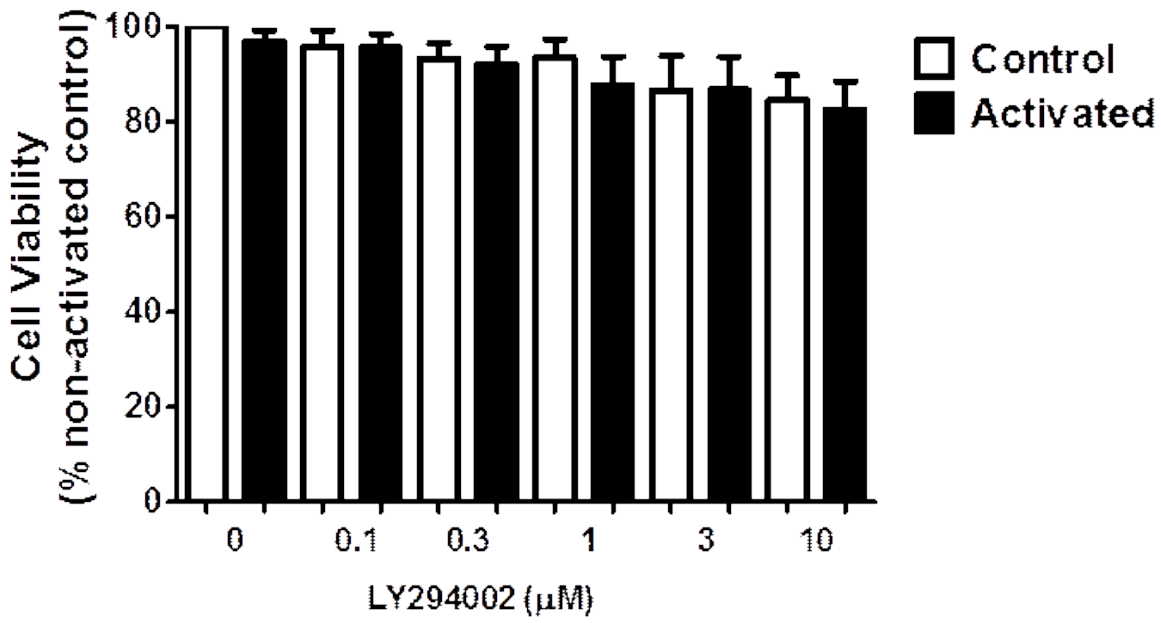

Figure 53. Effect of different concentrations of LY294002 on cell viability in RASMCs. Confluent monolayers of RASMCs in 96-well plates were pretreated with either CM alone, with different concentrations of LY294002 (0.01 to 10.00 μM) alone, or with LY294002 (0.01–10.00 μM) for 1 h prior to activation with both LPS (100 μg/mL) and IFN-γ (100 U/mL) for 24 h. The metabolism of MTT was determined colourimetrically following the method described in section 2.4. The white bars represent controls, and the black ones represent activated cells. Data are presented as the percentage of viable cells compared to the controls and represent the M ± SEM of at least three individual experiments. Statistical differences were determined by one-way ANOVA, followed by Dunnett's multiple comparisons test of the normalised data; $p > .05$ confirmed that there was no significant difference compared to the nonactivated control.

6.3.2 Effect of different concentrations of SB203580 on NO production

This experiment was conducted to investigate the effect of different concentrations of the p38 MAPK inhibitor on NO production. Confluent monolayers of cells were pretreated with different concentrations of SB203580 (0.1–10.0 μM) 1 h prior to activation with LPS and IFN-γ. Results in Figure 54 show that SB203580 decreased NO in a concentration dependent manner significant at 1–10 μM, with peak responses at 10 μM given nitrite levels that matched basal control levels.

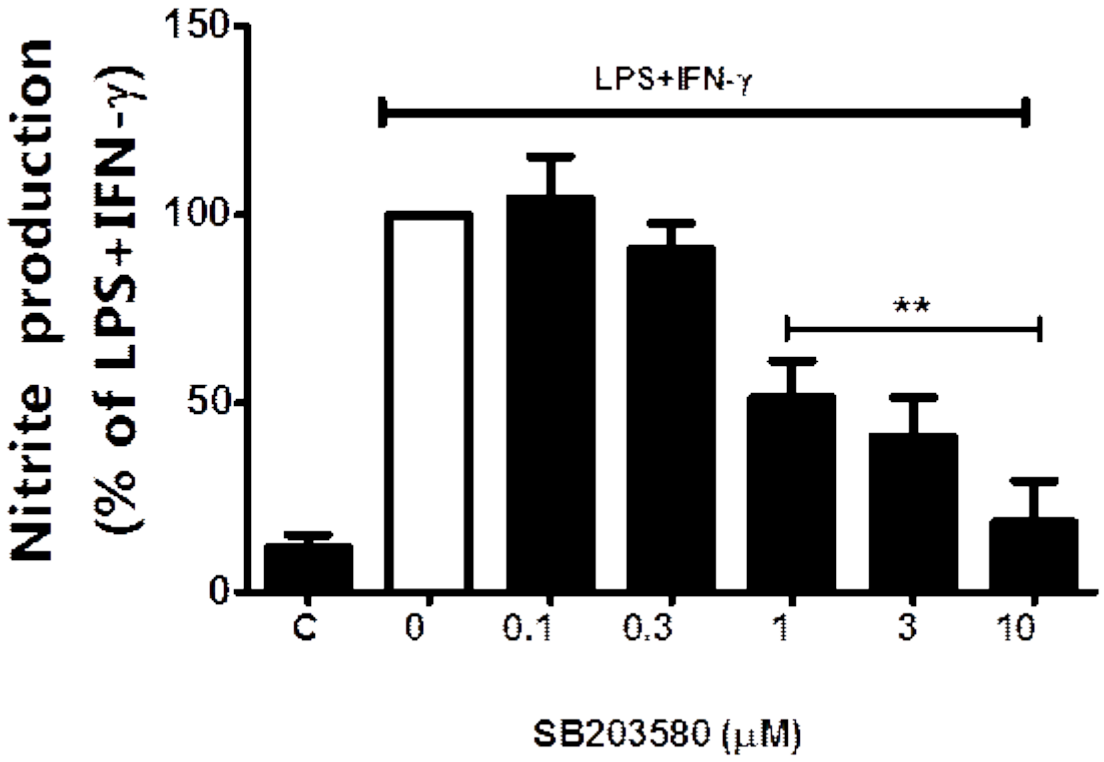

Figure 54. Effect of SB203580 on NO in RASMCs. Confluent monolayers of RASMCs in 24-well plates were pretreated with concentrations of SB203580 at 0.1–10.0 μM for 1 h prior to activation with 100 μg/mL of LPS and 100 U/mL of IFN-γ for 24 h. The culture medium was analysed by Griess assay to determine total nitrite levels following the method described in section 2.6. Data are expressed as a percentage of nitrite production, with the response to LPS (100 μg/mL) + IFN-γ (100 U/mL) taken as 100%. Data are the M ± SEM of at least three independent experiments. Statistical differences were determined by one-way ANOVA, followed by Dunnett's multiple comparisons test of normalised data; ** denotes $p < .01$ compared to the activated control.

6.3.3 Effect of different concentrations of SB203580 on iNOS expression

Following observations that SB203580 blocked nitrite production, additional experiments were performed to determine whether that effect was due to the suppression of iNOS expression. Confluent monolayers of cells were pretreated with different concentrations of SB203580 (0.1–10.0 μM) 1 h prior to activation with LPS and IFN-γ. Results in Figure 55 shows consistency with earlier changes found in NO production, in that SB203580 decreased

iNOS expression in a concentration dependent manner and to a statistically significant degree at 1–10 μM, as well as virtually abolished iNOS expression with 10 μM of the drug, which mirrors its actions on NO synthesis (Figure 54).

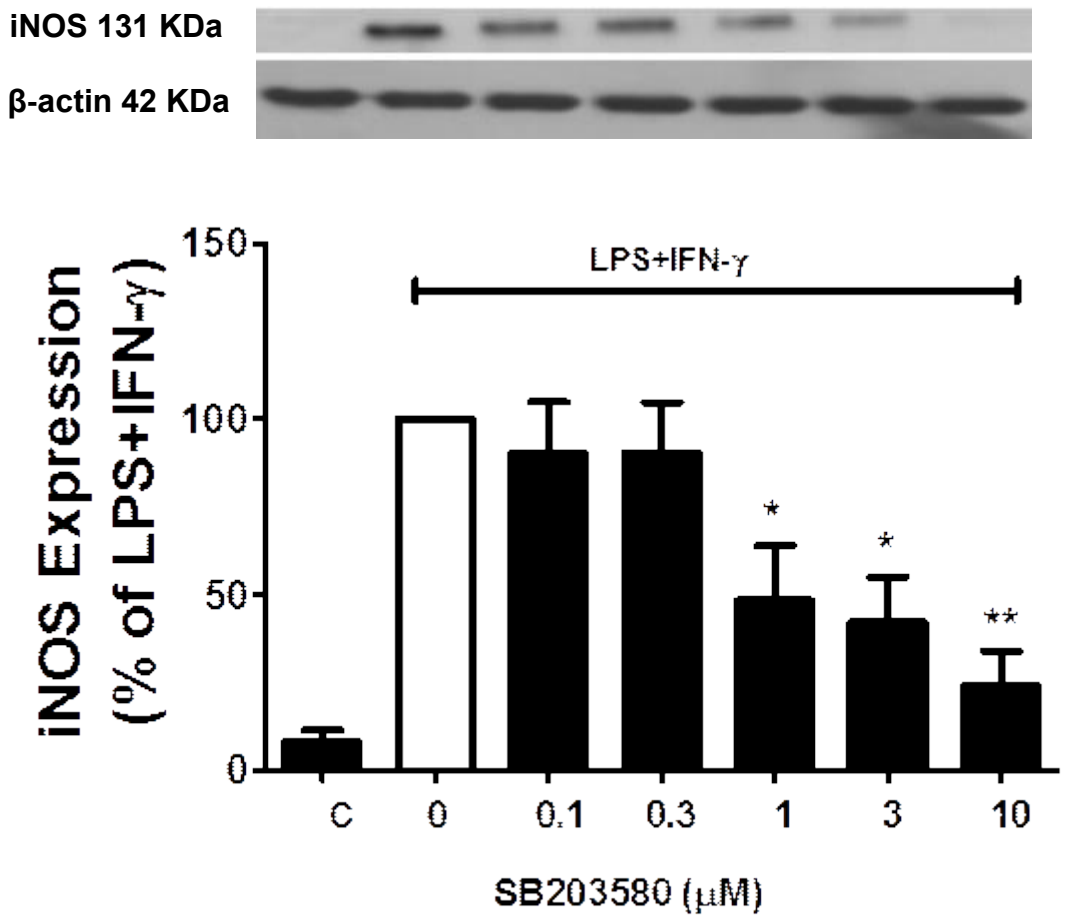

Figure 55. Effect of SB203580 on iNOS expression in RASMCs. Confluent monolayers of RASMCs in 24-well plates were pretreated with concentrations of SB203580 at 0.1–10.0 μM for 1 h prior to activation with 100 μg/mL of LPS and 100 U/mL of IFN-γ for 24 h. The expression of iNOS was determined by western blotting following the method described in section 2.9. The blot is representative of at least three independent experiments, and the bar graph depicts densitometric data expressed as a percentage of iNOS expression, with the response to LPS (100 μg/mL) plus IFN-γ (100 U/mL) taken as 100%. Data represent the M ± SEM of at least three independent experiments. Statistical differences were determined by one-way ANOVA, followed by Dunnett's multiple comparisons test of the normalised data; * denotes $p < .05$ and **$p < .01$ compared to the activated control.

6.3.4 Time dependent activation of P-p38 MAPK

That SB203580 inhibited both iNOS and NO production suggests a critical role for p38 MAPK in the induction of those processes. Experiments were therefore conducted to investigate the time dependent activation of p38 MAPK via its phosphorylation by LPS and IFN-γ. Data in Figure 56 show that the p38 MAPK was activated in a time dependent manner following exposure to LPS and IFN-γ. More importantly, the response appears to be biphasic, with levels of the phosphorylated protein increasing rapidly in the first hour, then declining by 2 h, and increasing in a time dependent fashion. In this second phase, levels of P-p38 expression at 12–24 h postactivation exceeded those in the first hour.

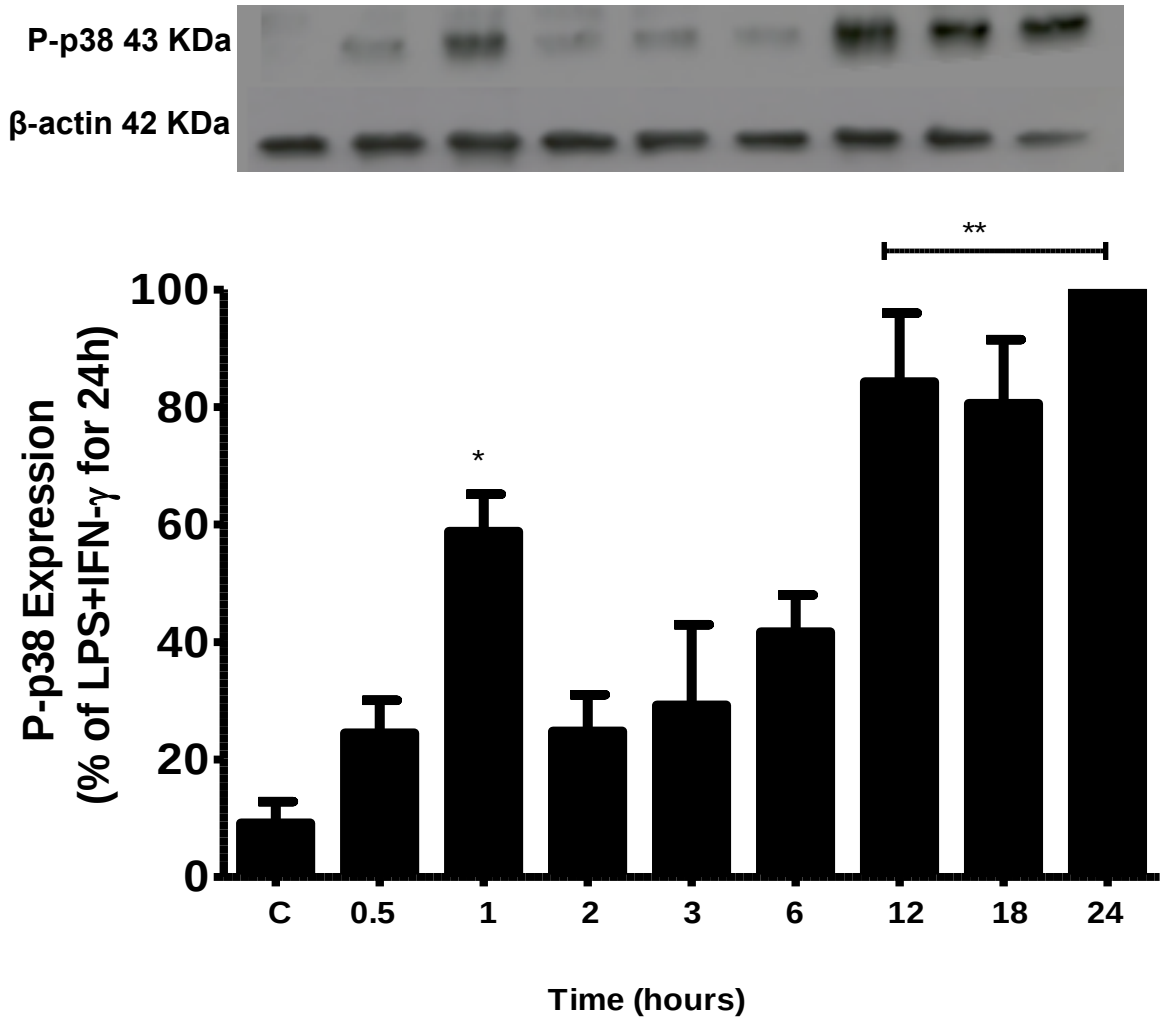

Figure 56. Time dependent activation of P-p38 MAPK. Confluent monolayers of RASMCs in 24-well plates were pretreated with 100 µg/mL of LPS and 100 U/mL of IFN-γ at different time points. The expression of P-p38 expression was determined by western blotting following the method described in section 2.9. The blot is representative of at least three independent experiments, and the bar graph depicts densitometric data expressed as a percentage of iNOS expression, with the response to LPS (100 µg/mL) plus IFN-γ (100 U/mL) for 24 h taken as 100%. Data represent the M ± SEM of at least three independent experiments. Statistical differences were determined by one-way ANOVA, followed by Dunnett's multiple comparisons test for normalised data; * denotes $p < .05$ and **$p < .01$ compared to the control.

6.3.5 Effect of different concentrations of LY294002 on NO production

Another experiment was performed to confirm whether Akt signalling is also required for the activation of iNOS expression and NO production in RASMCs. Confluent monolayers of cells were pretreated with different concentrations of LY294002 (0.1–10.0 µM) 1 h prior to activation with LPS and IFN-γ. LY294002 also decreased NO production in a concentration dependent manner, which was significant at 10 µM (Figure 57). However, LY294002 was seemingly less potent than SB203580 at lower concentrations due to less marked inhibitions.

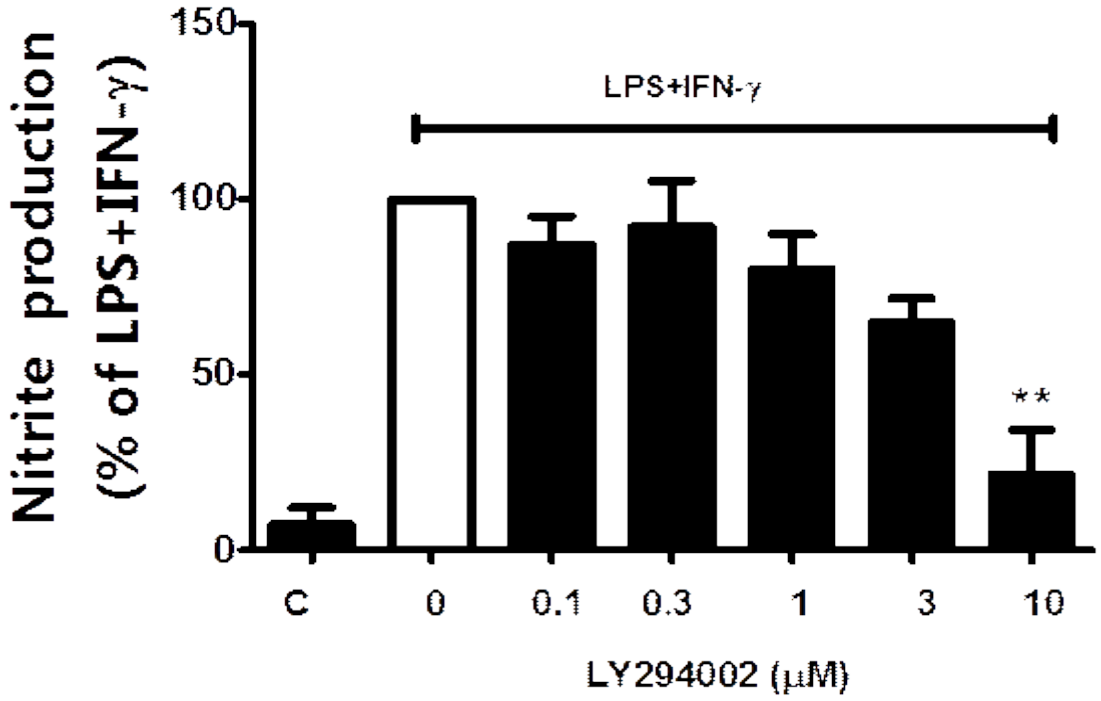

Figure 57. Effect of LY294002 on NO production in RASMCs. Confluent monolayers of RASMCs in 24-well plates were pretreated with concentrations of LY204002 at 0.1–10.0 µM for 1 h prior to activation with 100 µg/mL of LPS and 100 U/mL of IFN-γ for 24 h. The culture medium was analysed by Griess assay to determine total nitrite levels following the method described in section 2.6. Data are expressed as a percentage of nitrite production, with the response to LPS (100 µg/mL) + IFN-γ (100 U/mL) taken as 100%. Data are the M ± SEM of at least three independent experiments. Statistical differences were determined by one-way ANOVA, followed by Dunnett's multiple comparisons test of normalised data; ** denotes $p < .01$ compared to the activated control.

6.3.6 Effect of different concentrations of LY294002 on iNOS expression

Additional experiments were conducted to investigate the effect of different concentrations of the Akt inhibitor on iNOS expression. Confluent monolayers of cells were pretreated with different concentrations of LY294002 (0.1–10.0 μM) 1 h prior to the activation of cells with LPS and IFN-γ. LY294002 also decreased iNOS expression in a concentration dependent manner in a trend mirroring that observable on NO production (Figure 58).

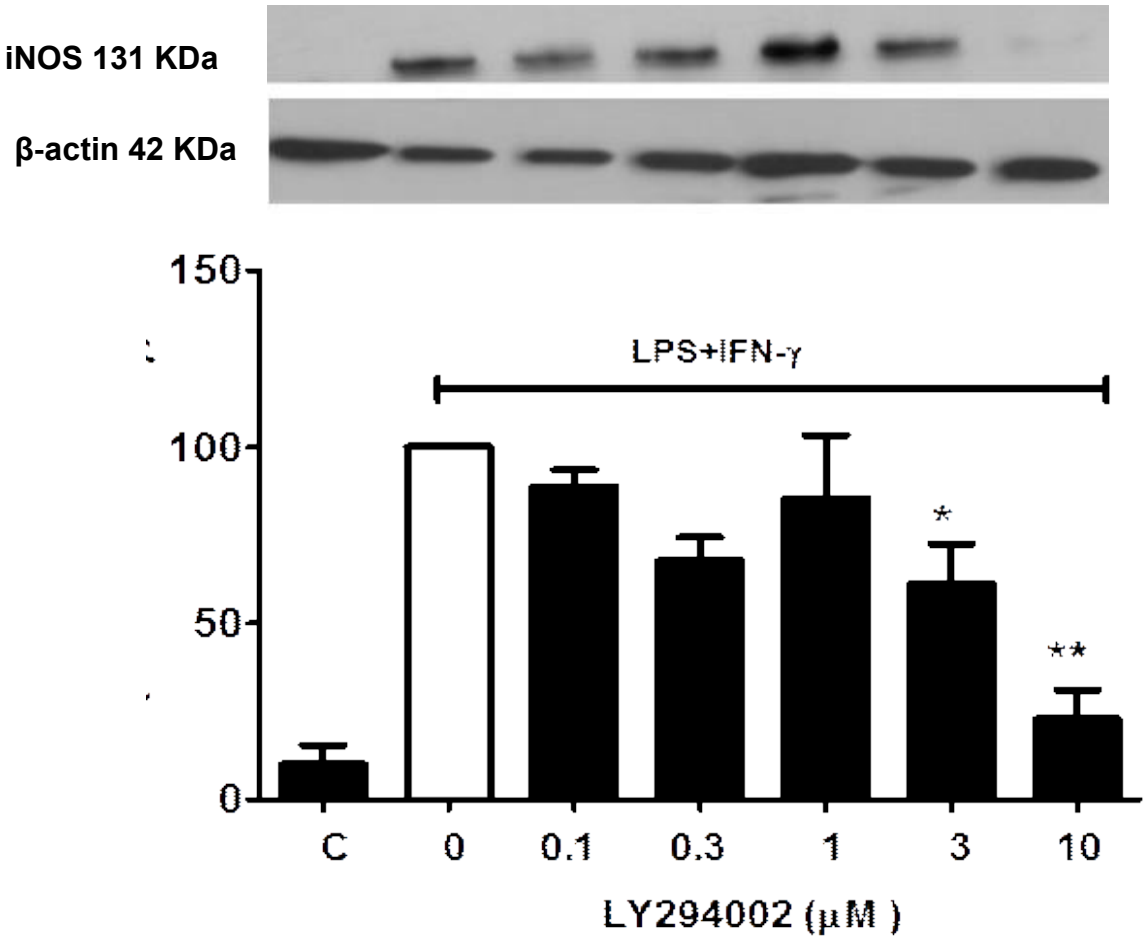

Figure 58. Effect of LY294002 on iNOS expression in RASMCs. Confluent monolayers of RASMCs in 24-well plates were pretreated with concentrations of LY204002 at 0.1–10.0 μM for 1 h prior to activation with 100 μg/mL of LPS and 100 U/mL of IFN-γ for 24 h. The expression of iNOS was determined by western blotting following the method described in section 2.9. The blot is representative of at least three independent experiments, and the bar graph depicts densitometric data expressed as a percentage of iNOS expression, with the response to LPS (100 μg/mL) plus IFN-γ (100 U/mL) taken as 100%. Data represent the M ± SEM of at least three independent experiments. Statistical differences were determined by one-way ANOVA, followed by Dunnett's multiple comparisons test of the normalised data; * denotes $p < .05$ and **$p < .01$ compared to the activated control.

6.3.7 Summary of the effects of fluticasone, SB203580, LY294002, and RU-486 on NO production

The experiments conducted to investigate the effects of p38 inhibitor, Akt inhibitor, fluticasone and RU486 on NO production are summarised in Figure 59 below for further clarification. Confluent monolayers of RASMCs were pretreated for 1 h with RU-486, SB203580, or LY294002 at 10 μM, followed by the addition of fluticasone at 3 nM. Fluticasone was added 30 min prior to the activation of LPS and IFN-γ. Data show a significant reduction of induced NO production using SB203580, LY294002, and fluticasone, but not with RU-486. The effect of fluticasone was reversed, however, with the use of RU-486 (Figure 59).

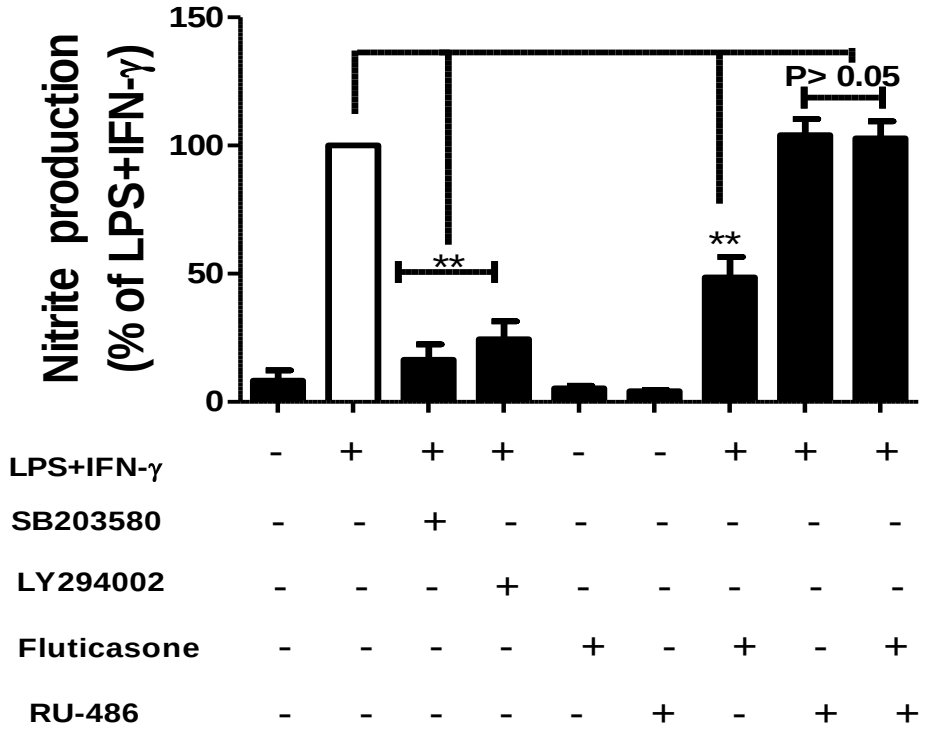

Figure 59. Effects of fluticasone, SB203580, LY294002, and RU-486 on NO production. Confluent monolayers of RASMCs were pretreated for 1 h with RU-486, SB203580, and LY294002 at 10 μM, followed by the addition of fluticasone at 3 nM 30 min prior to activation with 100 μg/mL of LPS and 100 U/mL of IFN-γ for 24 h. The culture medium was analysed by Griess assay to determine total nitrite levels following the method described in section 2.6. Data are expressed as the percentage of nitrite production, with the response to LPS (100 μg/mL) + IFN-γ (100 U/mL) taken as 100%. Data are the M ± SEM of at least three independent experiments. Statistical differences were determined using a one-way ANOVA, followed by Dunnett's multiple comparisons test. ** denote $p < .01$ compared to the activated control.

6.3.8 Summary of the effects of fluticasone, SB203580, LY294002, and RU-486 on iNOS expression

Experiments conducted to investigate the effects of the p38 inhibitor, Akt inhibitor, fluticasone, and RU-486 on iNOS expression are summarised in Figure 60. Confluent monolayers of RASMCs were pretreated for 1 h with RU-486, SB203580, or LY294002 at 10 μM, followed by the addition of fluticasone at 3 nM. Fluticasone was added 30 min prior to the activation of LPS and IFN-γ. Data show a significant reduction of iNOS expression using SB203580, LY294002, and fluticasone, but not with RU-486. The effect of fluticasone was reversed, however, with the use of RU-486 (Figure 60).

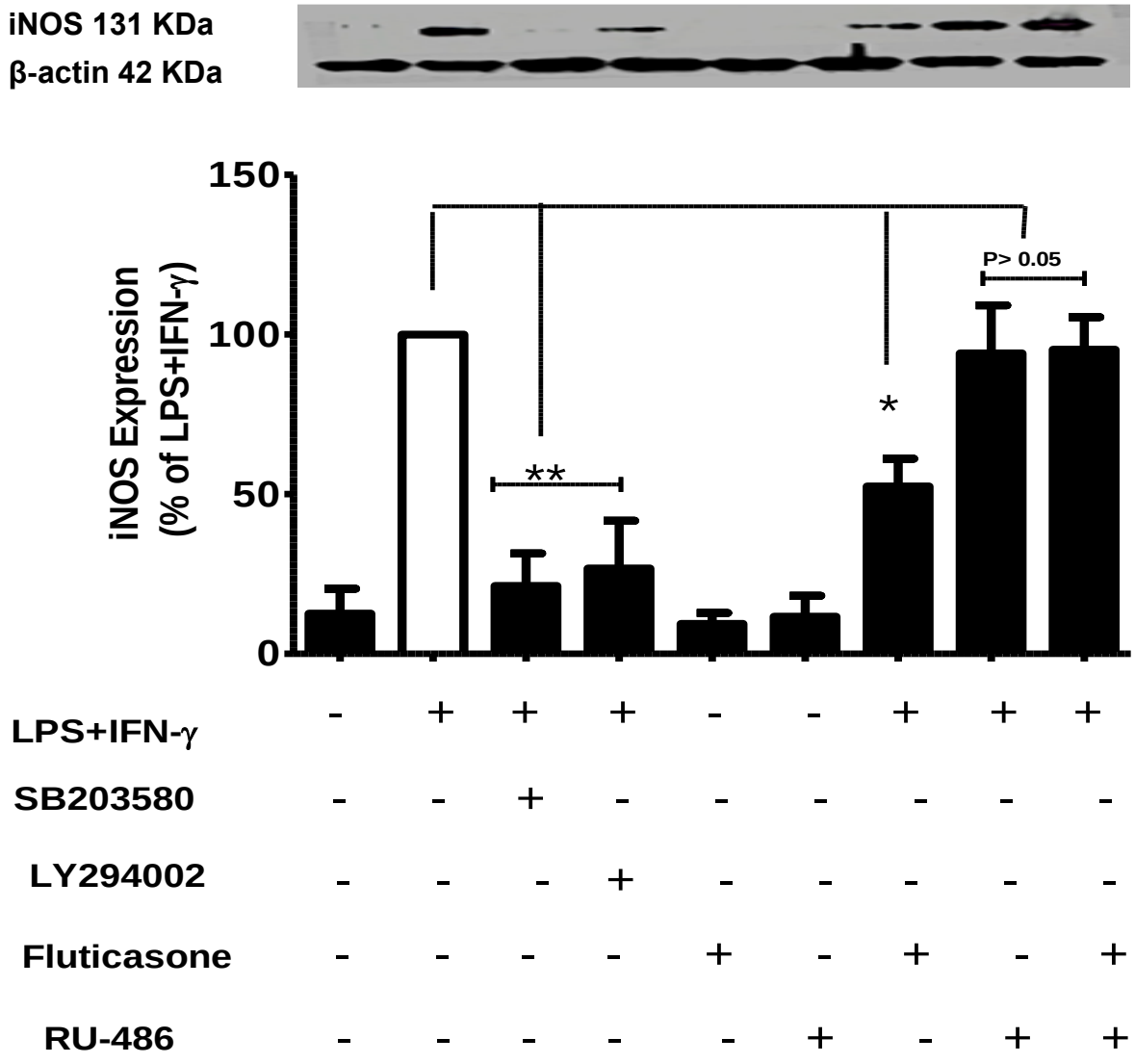

Figure 60. Effects of fluticasone, SB203580, LY294002, and RU-486 on iNOS expression. Confluent monolayers of RASMCs were pretreated for 1 h with RU-486, SB203580, and LY294002 at 10 μM, followed by the addition of fluticasone at 3 nM 30 min prior to activation with 100 μg/mL of LPS and 100 U/mL of IFN-γ for 24 h. The expression of iNOS was determined by western blotting following the method described in section 2.9. The blot is representative of at least three independent experiments, and the bar graph depicts densitometric data expressed as a percentage of iNOS expression, with the response to LPS (100 μg/mL) plus IFN-γ (100 U/mL) taken as 100%. Data represent the M ± SEM of at least three independent experiments. Statistical differences were determined by one-way ANOVA, followed by Dunnett's multiple comparisons test of the normalised data; * denotes $p < .05$ and **$p < .01$ compared to the activated control.

6.3.9 Effects of fluticasone, SB203580, LY294002, and RU-486 on P-p38 expression

The results presented above demonstrate clearly that iNOS expression and, in turn, NO production depended on p38 activation. Additional experiments were therefore performed to determine whether the inhibition of both iNOS and NO synthesis by fluticasone was mediated by the suppression of the p38 MAPK pathway by the GC. Results were expected to be of considerable interest, since no evidence currently suggests that fluticasone or any other GCs exert their effects by inhibiting intracellular MAPK signalling in RASMCs. For the experiments, confluent monolayers of RASMCs were pretreated either with only fluticasone (3 nM) or for 1 h with RU-486 (10 μM), followed by the addition of fluticasone at 3 nM for 30 min prior to the activation of LPS and IFN-γ. Cells treated with SB203580 and LY294002 at 10 μM were used for comparison. Lysates were generated 24 h postactivation and subjected to western blotting in order to detect P-p38 MAPK. Results showed significant inhibitions of the activation of p38 MAPK by SB203580, LY294002, and fluticasone. In each case, P-p38 levels were significantly lower than those in LPS- and IFN-γ-activated cells (Figure 61). More importantly, fluticasone suppressed the activation of p38 MAPK to levels also observed with SB203580 and LY294002, thereby suggesting that fluticasone is as potent in regulating p38 activation and its signalling as the two pharmacological inhibitors. Interestingly, SB203580, which is reported to inhibit the activity of p38 MAPK instead of its activation, also blocked p38 phosphorylation.

In additional studies with RU-486, results showed that RU-486 could reverse the inhibition of P-p38 by fluticasone and restore P-p38 levels to those of the activated controls (Figure 61). RU-486 alone did not alter basal or activated P-p38 expression. Altogether, and as this study demonstrates for the first time, the findings strongly suggest that fluticasone inhibits p38 activation by acting on its GCR.

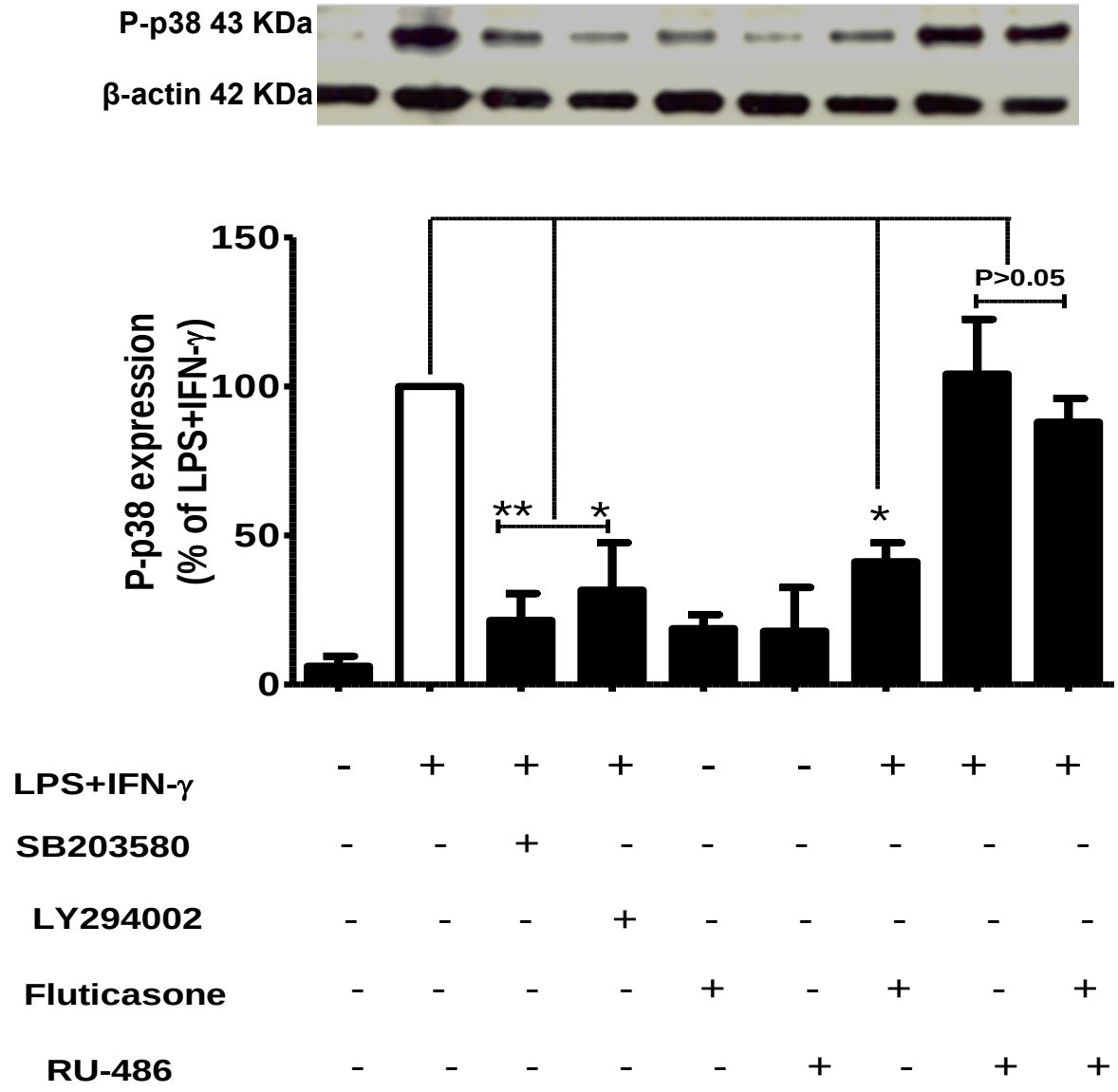

Figure 61. Effects of fluticasone, SB203580, LY294002, and RU-486 on P-p38 expression. Confluent monolayers of RASMCs were pretreated for 1 h with RU-486, SB203580, or LY294002 at 10 μM or with fluticasone at 3 nM for 30 min prior to activation with 100 μg/mL of LPS and 100 U/mL of IFN-γ for 24 h. The expression of P-p38 was determined by western blotting following the method described in section 2.9. The blot is representative of at least three independent experiments, and the bar graph depicts densitometric data expressed as a percentage of P-p38 expression, with the response to LPS (100 μg/mL) plus IFN-γ (100 U/mL) taken as 100%. Data represent the M ± SEM of at least three independent experiments. Statistical differences were determined by one-way ANOVA, followed by Dunnett's multiple comparisons test of the normalised data; * denotes $p < .05$ and ** $p < .01$ compared to the activated control.

6.3.10 Effects of fluticasone, SB203580, LY294002, and RU-486 on P-Akt

Other experiments were performed to gauge whether fluticasone also regulates P-Akt expression. Confluent monolayers of RASMCs were pretreated either with fluticasone (3 nM) alone or for 1 h with RU-486 (10 μM), followed by the addition of fluticasone at 3 nM for 30 min prior to the activation of LPS and IFN-γ. As in previous experiments, cells treated with SB203580 and LY294002 at 10 μM were used for comparison. Lysates were generated after activation and subjected to western blotting in order to detect P-Akt. Data in Figure 62 reveal that control cells had high levels of P-Akt, which suggest the unanticipated basal activation of the kinase. Activation with LPS and IFN-γ, however, nearly doubled the levels of P-Akt. More importantly, that increase was blocked as fluticasone reduced P-Akt back to control levels, in an inhibition reversed by RU-486. Levels of inhibition with fluticasone were comparable to those with SB203580 and LY294002, which again suggests that fluticasone is as effective in regulating Akt activation and signalling as SB203580 and LY294002 (Figure 62).

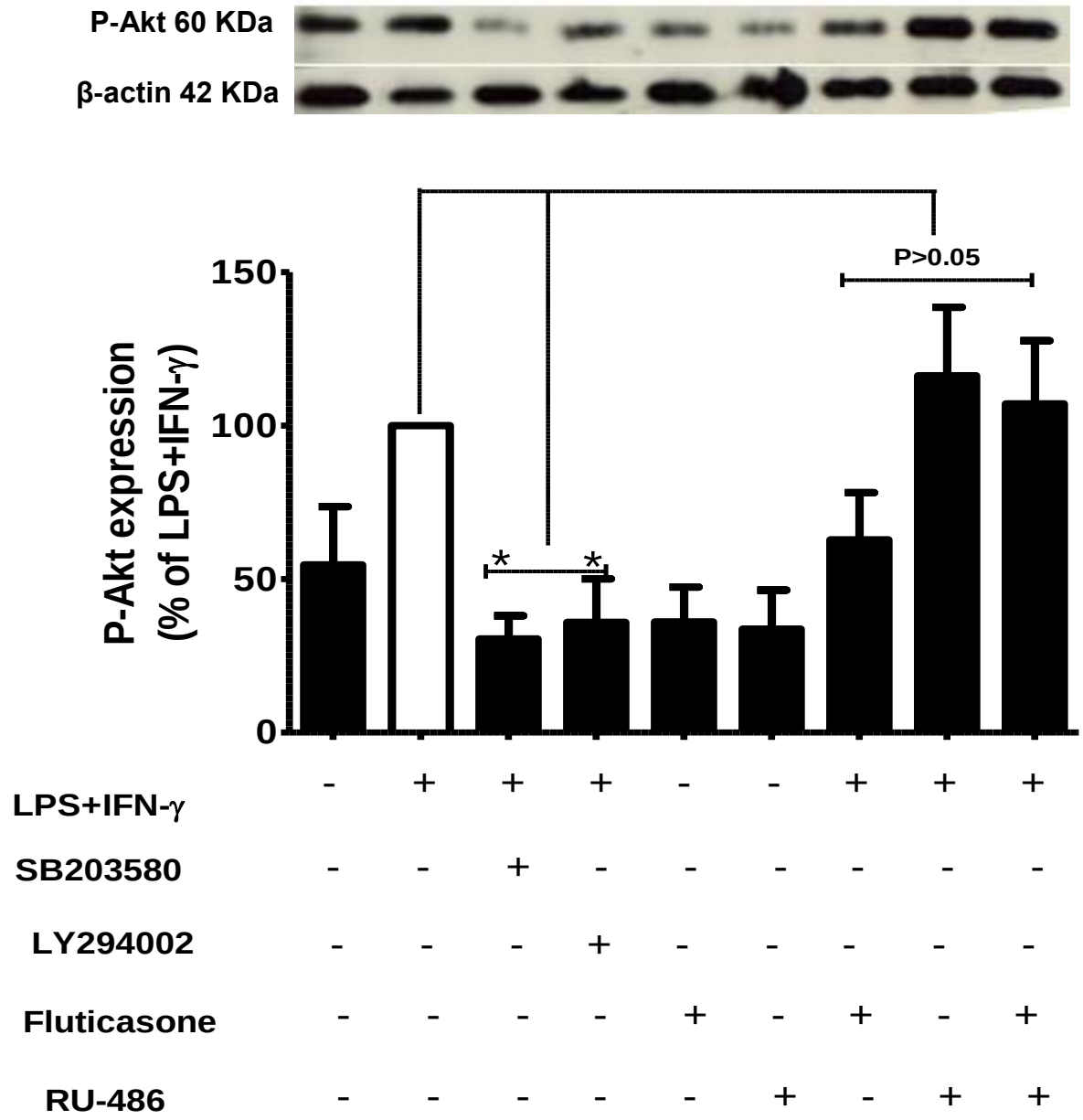

Figure 62. Effects of fluticasone, SB203580, LY294002 and RU-485 on P-Akt expression. Confluent monolayers of RASMCs were pretreated for 1 h with RU-486, SB203580, or LY294002 at 10 μM or with fluticasone at 3 nM 30 min prior to activation with 100 μg/mL of LPS and 100 U/mL of IFN-γ for 24 h. The expression of P-Akt was determined by western blotting following the method described in section 2.9. The blot is representative of at least three independent experiments, and the bar graph depicts densitometric data expressed as the percentage of P-Akt expression, with the response to LPS (100 μg/mL) plus IFN-γ (100 U/mL) taken as 100%. Data represent the M ± SEM of at least three independent experiments. Statistical differences were determined by one-way ANOVA, followed by Dunnett's multiple comparisons test of the normalised data; * denotes $p < .01$ compared to the activated control.

6.4 Discussion

The studies described in this chapter sought to determine whether fluticasone has any effect on P-p38 or P-Akt expression, if not both, since they play a critical role in regulating iNOS expression (Baydoun et al., 1999; Hattori et al., 2003). Prior to initiating the studies, the potential cytotoxic effect of the different concentrations of SB2035 and LY294002, both with and without LPS and IFN-γ, were ruled out by way of MTT assay. Results showed that both compounds were tolerated quite well and caused little or no change in the metabolism of MTT under all conditions examined.

P38 MAPK has been activated via various stimuli, including proinflammatory cytokines and LPS, which prompts the expression of P-p38. Such phosphorylation accounts for various biological effects, including the activation of transcription factors such as NF-κB (Saklatvala, 2004).

Changes in the phosphorylation of p38 MAPK were investigated to identify the time course of activation by monitoring changes in the levels of expression of the phosphorylated proteins. Interestingly, the activation of p38 MAPK in the cell system examined in the studies for this thesis appears to be biphasic, with an initial peak response after 1 h that declined at 2 h, yet increased again in a time dependent manner over 24 h, during which levels of P-p38 were greater than those in the first hour of activation. That finding suggests that the activation of p38 is in parallel with the expression of iNOS. Moreover, the initial phase of the biphasic response is consistent with the findings of other studies showing that LPS and IFN-γ activated p38 at 0.5 and 1 h postactivation, but decreased thereafter (Lamon et al., 2010; Yamakawa et al., 1999).

To confirm whether the p38 MAPK was indeed involved with the induction of iNOS and thus a potential target for fluticasone in regulating iNOS expression and function, additional experiments were performed that exploited SB203580, a potent inhibitor of the p38α and β MAPKs (Zarubin & Jiahuai, 2005). Results confirmed a role for p38, since SB203580 inhibited both iNOS expression and nitrite accumulation in a concentration dependent manner. Those observations are consistent with the findings of previous studies with the same cell type (i.e., RASMCs), in which SB203580 reduced iNOS expression and function in a concentration dependent manner (Baydoun et al., 1999). Interestingly, in the earlier study, SB203580 caused a biphasic action in which lower concentrations (0.1 μM) increased NO productions, but higher concentrations (>1 μM) inhibited it (Baydoun et al., 1999). No such enhancement occurred in the current studies, although higher concentrations reduced iNOS expression and function in a concentration dependent manner. The reason for the discrepancy remains unclear and requires further investigation. What is clear, however, is that p38 activation might be critical for inducing iNOS and that its inhibition prompts the suppression of iNOS.

Consistent with the findings reported above, p38 was activated via phosphorylation, and the levels of the phosphorylated protein increased in activated cells expressing iNOS. Intriguingly, the expression of P-p38 was significantly suppressed in the presence of SB203580, which suggests that SB203580 can act upstream to block p38 activation. That effect, however, would contradict the known pharmacological action of SB203580 as an inhibitor of p38 MAPK. Indeed, it has been reported that SB203580 competes with ATP for its binding site and inhibits the activity of p38 MAPKs, particularly the α and β isoforms (Kumar et al., 1999). In doing so, it inhibits the downstream MAPKAPK-2 and other targets of p38. The inhibition of P-p38 expression was not further investigated in the studies for this

thesis due to time constraints; however, it can be speculated that SB203580 might not be as specific for p38 as reported, since at certain concentrations (≥10 μM) it can also interact with other signalling pathways that directly regulate p38 phosphorylation. Interestingly, other reports have suggested that SB203580 can inhibit the activation of p38 by binding to the inactive form and thus reducing the active form (Frantz et al., 1998). Such action could explain the data presented in this thesis, although further clarification of it and the other proposed mechanism is necessary.

Apart from investigating the p38 MAPK pathway, the studies for this thesis also sought to determine whether Akt signalling was critical to the cell system used. Studies were therefore performed to investigate that pathway using LY294002, an inhibitor of phosphatidylinositol 3 kinase (PI3k) that causes the inhibition of Akt, which plays a critical role in iNOS expression and function. Indeed, the incubation of cells with the antagonists prior to activation with LPS and IFN-γ significantly inhibited iNOS expression and, in turn, NO production, especially at concentration of 10 μM. That result is consistent with previous findings regarding RASMCs also highlighting that LY294002 reduced iNOS expression and function in a concentration dependent manner by inhibiting the activation of NF-κB (Hattori et al., 2003).

In addition to the effects reported above, Akt phosphorylation enhanced in activated cells even though basal expression was relatively high. The reasons for the latter result remain unclear; however, since Akt is activated in response to growth factors, the pathway could have been activated basally by growth factors in the CM. In any case, basal levels enhanced following activation, as inhibited by both SB203580 and LY294002; the latter's action was expected because its inhibition of PI3 kinase also inhibits Akt activation. By contrast, SB203580 was not expected to have caused any inhibition of the pathway since it is

reportedly selective of p38 MAPK and inhibits its activity. However, as already noted, SB203580 inhibits p38 phosphorylation, and at least one report has suggested that high concentrations of SB203580 can inhibit the phosphorylation of Akt in cytokine-activated lymphocytes (Lali, et al., 2000). Similarly, cross-talk between Akt and p38 has been demonstrated in macrophages, in a process in which SB203580 inhibits the phosphorylation of Akt (McGuire et al., 2013). Accordingly, SB203580 might have other off-target effects that could explain responses observed regarding P-Akt in the present studies, which could be inhibited via other actions of the compound not yet determined. Further studies are clearly needed to address those discrepancies.

Perhaps the most novel finding of the studies reported in this chapter is that fluticasone blocked both p38 and Akt phosphorylation and that its effects were sensitive to inhibition by RU-486, which suggests an action via GCRs. This present study is the first to identify that novel mechanism of action that could explain the inhibition of iNOS expression and function by fluticasone. The finding is also consistent with that of another study, which demonstrated that fluticasone reduces both P-p38 and P-Akt in respiratory syncytial virus-infected human foetal lung fibroblasts (Seki et al., 2013). Although dexamethasone and hydrocortisone were not investigated in the current study due to time constraints, it has been reported in mast cells that dexamethasone reduces the phosphorylation of Akt via the GCR (Andrade et al., 2004). Similar actions could also be possible in our cell model.

Although the mechanism by which fluticasone inhibits the activation of p38 and Akt was not investigated in the current study, others have reported that fluticasone can induce phosphatases that, in turn, dephosphorylate p38 and Akt. The potential phosphatase is MKP-1, which fluticasone induced in airway smooth muscle cells (Manetsch et al., 2013).

Dexamethasone has also been reported to inactivate p38 MAPK via its ability to induce MKP-1 in HeLa cells (King et al., 2009; Lasa et al., 2002) and RA fibroblast-like synoviocytes (Toh et al., 2004). An important GC action is via the GC-induced leucine zipper, which studies have shown inhibits Akt (Ayroldi & Riccardi, 2009). It is also possible that the responses observed in the present studies are mediated by that action, although such a hypothesis requires further investigation.

SB203580 IC50 is 0.5 μM and the IC50 of LY294002 is 0.97 μM (Chaussade et al., 2007; Lali et al., 2000). This is however in cell free assay. As mentioned earlier the cell model is more complex and therefore requires higher concentrations compared to test tube studies using purified targets under well controlled and defined conditions. For example, LY204002 concentration used in cell lines is up to 50 μM instead of 0.5 μM in cell free assay (Semba et al., 2002).

7. Transcriptional and Post-Transcriptional Regulation of iNOS Expression by Fluticasone

7.1 Introduction

The basic principles of the central dogma is that DNA codes for RNA, which in turn codes for protein (Figure 63), in a process involving both the transcription and translation of the gene coding for the target protein leading to its synthesis and expression.

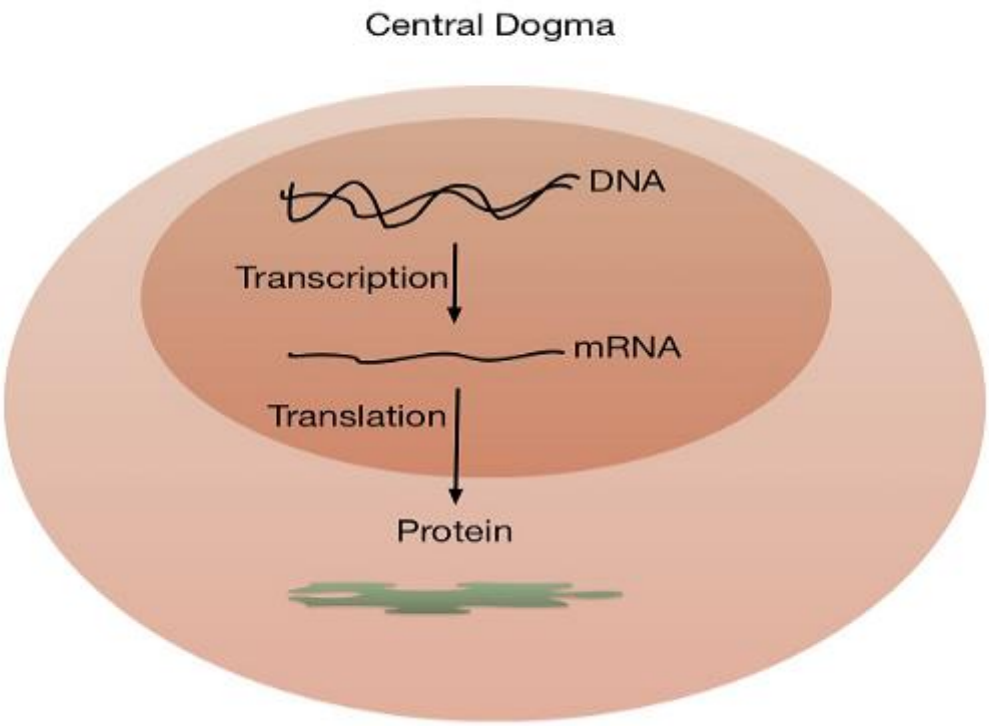

Figure 63. The central dogma

Results show that GCs reduce iNOS protein levels, and additional data generated in the studies for this thesis suggest that their actions, or at least those of fluticasone, might be mediated in part via the regulation of key intracellular signalling pathways, including that of p38 MAPK and Akt. It remains unclear, however, whether those GCs act at transcriptional, translational, or post-translational levels, if not in some combination of those means.

Previous reports have suggested that dexamethasone might reduce iNOS by suppressing NF-κB (Matsumura et al., 2001), whereas in RASMCs, the same compound enhanced iNOS

mRNA but suppressed iNOS protein expression, which implies action at the post-transcriptional level (Thakur & Baydoun, 2012).

In response, this chapter sought to investigate whether GCs regulate iNOS protein expression by action at the translational level. Studies conducted to that end focused on protein kinase R, an important translational regulator that acts via the phosphorylation of eukaryotic translation initiation factor EIF2α. The imidazolo-oxindole PKR inhibitor C16 was used to determine whether PKR regulated iNOS expression and function. Additional investigations were also performed to identify the role of fluticasone on PKR and EIF2α activation.

7.2 Material and Methods

7.2.1 Real-time quantitative reverse transcriptase polymerase chain reaction (qPCR) of iNOS's mRNA expression

Polymerase chain reaction (PCR) is a technique developed in 1983 by Kary Mullis (Mullis et al., 1986) and enables the researcher to amplify and produce multiple copies of a targeted DNA sequence. Real-time PCR has the same principle as PCR but has many advantages, including the fact that amplification can be quantified and watched with the reaction progression in 'Real Time' using florescence probes. This precise quantification of the amplified DNA allows the researchers to analyse their samples concisely.

During the PCR reaction, the reaction mix was heated to 95^{o}C, at which point the double stranded DNA "melted" into single strands. The temperature was then decreased to 60^{o}C in order to allow the primer to bind to the targeted gene. After this, the temperature was rise to 75^{o}C, which is the optimal temperature for the polymerase. At the end of this cycle, the targeted gene had amplified twice. The PCR machine repeats this cycle around 45 times, yielding a large amount of amplified targeted DNA.

The amount of the amplified DNA correlates to the fluorescence, which is measured and plotted during each cycle. The Cycle threshold (C_t) is an intersection between the amplification curve and the threshold line, which represent the amount of florescence where the amount of fluorescence exceeds the background fluorescence. A higher C_t value indicates lower amplified DNA and vice versa. All PCR reactions were performed on a Quantica real time machine (Techne. UK)

7.2.2 Isolation of RNA

Cells were grown in a T25 tissue culture flask to confluence and incubated with LPS (100 µg/mL) and IFN-γ (100 U/mL) for 24 h before being treated with 1 mL of RNA STAT-60 and repeatedly pipetted. For complete dissociation of nucleoprotein complexes, the homogenate was transferred to Eppendorf tubes and stored at room temperature for 5 min. Next, 0.2 mL of chloroform was added to each tube for every 1 mL of RNA STAT-60, and the tubes were vigorously shaken for at least 15 s. Each tube was centrifuged for 15 min at 4 °C at 13,226 xg. Layers of homogenate separated clearly into a top aqueous layer containing RNA, an intermediate white layer containing DNA and proteins, and a lower red layer containing chloroform. Each aqueous layer was transferred into a new Eppendorf tube, 0.5 mL of isopropanol was added, and the tubes were mixed and stored for 10 min at room temperature, followed by centrifugation at 13,226 xg at 4 °C for 10 min. The supernatant was removed and the precipitated RNA at the bottom of the tube washed with 1 mL of 75% ethanol per 1 mL of RNA STAT-60. Each tube was centrifuged at 4,402 xg for 5 min at 4 °C and the supernatant discarded. The RNA pallet was subsequently dried and dissolved in 36 µL of autoclaved distilled water.

7.2.3 Purification of isolated RNA

TURBO DNase was used to remove the contaminant DNA from RNA samples by adding 0.1volume of 10× TURBO DNase buffer to the previously dissolved RNA followed by the addition of 1 µL of TURBO DNase. This mixture was then properly mixed and incubated on a digital heat plate for 30 min at 37 °C. One µL of DNase inactivation reagent was added to the mixture and incubated at room temperature for 5 min with frequent mixing, followed by centrifugation at 9,469 xg for 1.5 min. The colourless supernatant contained the RNA, whereas the DNase inactivation reagent precipitated at the bottom. The colourless supernatant was transferred into another Eppendorf tube and quantified.

7.2.4 Agarose gel electrophoresis

Agarose gel electrophoresis was undertaken to determine the purity of the isolated RNA samples. After 1% of agarose was prepared in a gel running buffer, the mixture was placed in a microwave (450 W) for 1–2 min to dissolve the agarose. The mixture was allowed to cool, after which a comb was placed in the cassette, and the agarose solutions were poured into the cassette. The gel set for 30 min, after which the comb was removed and the cassette placed into the tank, which was then filled with gel running buffer.

One µL of RNA sample was mixed with 3 µL of loading buffer and 6 µL of RNase-free water. The marker was prepared by adding 2 µL of bromophenol blue and 2 µL of DNase-free water. The marker and samples were loaded into the wells and run at 100 V until the loading buffer migrated three quarters of the gel, which took approximately 90 min. The gel was transferred into a 0.5 µg/mL ethidium bromide staining solution for 15 min, destained using distilled water for 15 min, and visualised under ultraviolet light to examine the 28S and 18S ribosomal bands.

7.2.5 RNA quantification

After 200 µL of sterile distilled water in a cuvette was prepared as the blank and calibrated to zero, 10 µL of RNA samples were diluted in 190 µL of sterile distilled water. The quantity and purity of RNA concentration was measured using a UV spectrophotometer (Eppendorf Biophotometer, Germany). RNA quantity and purity was determined using a spectrophotometer by determining the ratio of absorbance at 260 nm and at 280 nm (A260/A280) in DDW. The purity of the RNA was considered of high quality if the 260/280 ratio was >1.8. It was therefore ensured that the RNA used in all qPCR studies in this thesis exceeded 1.8 and on average the 260/280 ratio determined was between 1.92 to 2.12.

7.2.6 Reverse transcription of RNA to cDNA

A high-capacity RNA-to-cDNA kit was used to convert RNA to cDNA. A total volume of 20 mL of the reaction (Table 6) was prepared using 2 µg of the total RNA isolated.

Table 6. Preparation of samples for reverse transcription (RT)

Component	+RT	-RT
2× RT buffer	10 µL	10 µL
20× Enzyme mix	1 L	-
RNA sample	Calculated volume = 2 µg	Calculated volume = 2 µg
Nuclease-free water	Up to 20 µL	Up to 20 µL
Total per reaction	20 µL	20 µL

7.2.7 Master mix preparation

The master mix was prepared by mixing SYBR Green with forward and reverse iNOS primers and the previously prepared cDNA. The iNOS primer sequence is shown in Table 7. A total of 100 µM of the primers was prepared as a stock solution in autoclaved distilled water, and 10 µM of the working solution was used in the master mix (Table 8).

Table 7. Primer sequences used in PCR analysis

gene	Forward primer	reverse primer	design
iNOS	GGAAGAGGAACAACTACTG	AAATACCGCATACCTGAAG	(Garr, 2014)

Table 8. Master mix preparation

Component	Volume (µL)
SYBR Green	10
Forward primer	1
Reverse primer	1
cDNA sample	2
Nuclease-free water	6
Total	20

7.2.8 Calculation of relative gene expression levels

The fold change of expression was calculated as:

$$\Delta Ct\ target = Ct\ control - Ct\ sample$$

$$\Delta Ct\ Reference = Ct\ control - Ct\ sample$$

The final standard deviation equalled the square root of the *SD* of target Ct_2 + *SD* of reference Ct_2.

$$\Delta\Delta Ct\ Target = \Delta Ct\ Target - \Delta Ct\ Reference$$

The fold change equalled $2^{-Ct\ target\ sample}$.

7.2.9 Housekeeping genes (HKGs) as reference genes

Housekeeping genes (HKG) are genes expressed and required for maintaining basic cellular function. In PCR, HKGs are used to normalise and validate results. Among the most commonly used HKGs is glyceraldehyde-3-phosphate dehydrogenase, although several HKGs were examined as part of the studies for this thesis in order to ensure that the most stable HKG was selected. Those examined included cyclophilin A (CYC A), tyrosine 3-

monooxygenase/tryptophan 5-monooxygenase activation protein zeta, calnexin, ubiqutin C, ribosomal protein L13A (RPL13A), β-actin, glyceraldehyde-3-phosphate dehydrogenase, and β2-microglobulin. The result from the initial screen indicated that the most stable HKGs were RPL13A, followed by CYC A (Garr, 2014). RPL13A was thus used in additional studies. Housekeeping genes were purchased from PrimerDesign (UK) and their functions are highlighted in Table 9.

Table 9. Housekeeping genes and their functions

HKG	function
β2-microglobulin (β2M)	major histocompatibility complex
cyclophilin A (CYC A)	takes part in protein-folding processes
Glyceraldehyde-3-phosphate dehydrogenase (GAPDH)	glycolysis
Tyrosine 3-monooxygenase/tryptophan 5-monooxygenase activation protein, zeta (YWHAZ)	potential role in regulating insulin sensitivity
Calnexin (CANX)	protein folding
Ribosomal protein L13A (RPL13A)	Eukaryotic translational regulation

7.2.10 Experimental conditions

7.2.10.1 Time dependent activation of iNOS mRNA expression

Confluent monolayers of RASMCs in T25 flasks were pretreated with culture medium or with LPS (100 μg/mL) and IFN-γ (100 U/mL) for time points ranging from 1 to 24 h. Levels of iNOS mRNA were determined following the method described in section 7.2.

7.2.10.2 Effect of fluticasone on iNOS mRNA expression

Confluent monolayers of RASMCs in T25 flasks were pretreated with 3 nM of fluticasone for 30 min before incubation with LPS (100 μg/mL) and FN-γ (100 U/mL) for 24 h. Levels of iNOS mRNA were determined following the method described in section 7.2.

7.2.10.3 Effect of PKR inhibitor on NO production and iNOS expression

Confluent monolayers were pretreated with C16 (30–300 nM) for 30 min prior to activation with LPS (100 μg/mL) and FN-γ (100 U/mL). The culture medium was analysed by Griess assay to determine total nitrite levels following the method described in section 2.6, and the expression of iNOS was determined by western blotting following the method described in section 2.9. The changes in cell viability were examined by MTT assay following the method described in section 2.4.

7.2.10.4 Time course induction of P-PKR or P-EIF2α

Confluent monolayers of RASMCs in a 24-well plate were incubated with LPS (100 μg/mL) and IFN-γ (100 U/mL) at different time points from 0.25 to 24 h. The expression of P-PKR and P-EIF2α were determined in cell lysates by western blotting following the method described in section 2.9.

7.2.10.5 Effect of fluticasone on P-PKR expression and P-EIF2α expression

Confluent monolayers of RASMCs in a 24-well plate were pretreated with fluticasone 30 min prior to activation with LPS (100 μg/mL) and IFN-γ (100 U/mL). In parallel studies, cells were activated with LPS and IFN-γ in the absence of fluticasone or with medium alone. The expression of P-PKR and P-EIF2α was monitored by western blotting in lysates generated at 1, 3, and 24 h after activation.

7.3 Results

7.3.1 Confirmation of quality of isolated RNA

This experiment was conducted to ensure that the RNA used in the study was pure. This quality check was conducted using agarose gel electrophoresis. Results (Figure 64) indicate that the RNA was pure and without contamination or degradation, given clear bands of 28S

and 18S ribosomal RNA fragments without evidence of degradation or smear. Such conditions were true not only for controls, but also for cells treated with fluticasone alone and together with LPS and IFN-γ.

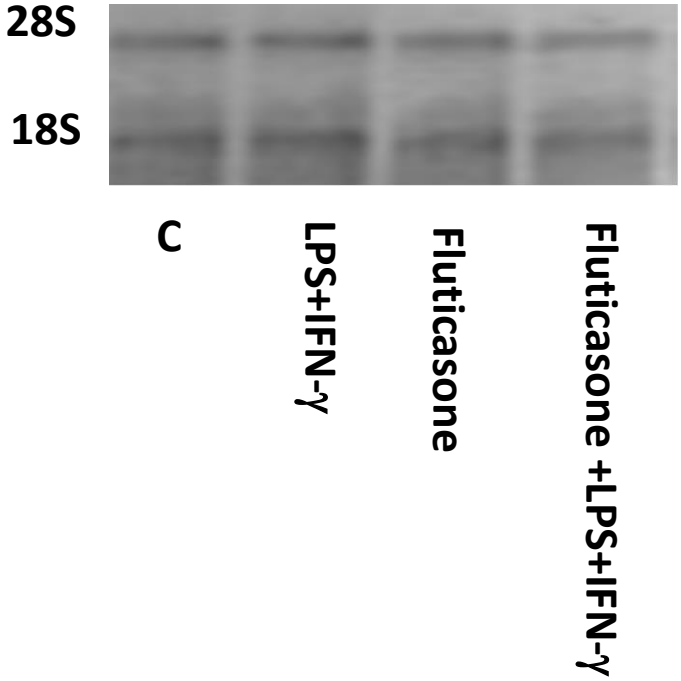

Figure 64. Agarose gel electrophoresis of RNA isolated from controls and cells treated with fluticasone in the absence and presence of LPS and IFN-γ. Total RNA samples were extracted from confluent untreated control or cells treated with 3 nM fluticasone in the absence and presence of LPS (100 μg/mL) and IFN-γ (100 U/mL). The samples were mixed with bromophenol blue (1:1) and subjected to gel electrophoresis at 5 V/cm for 45 min on 1% agarose gel. The gel was transferred into a chamber with TBE buffer containing 10 μg/mL ethidium bromide for 20 min and visualised under a transilluminator. The figure represents at least three independent experiments.

7.3.2 Time dependent activation on iNOS mRNA expression

Time dependent activation on iNOS mRNA expression was assessed to investigate the time course of expression of iNOS mRNA after cell activation with LPS and IFN-γ for 1, 3, 6, 12, and 24 h. As Figure 65 shows, iNOS mRNA increased after 6 h and peaked after 24 h of activation.

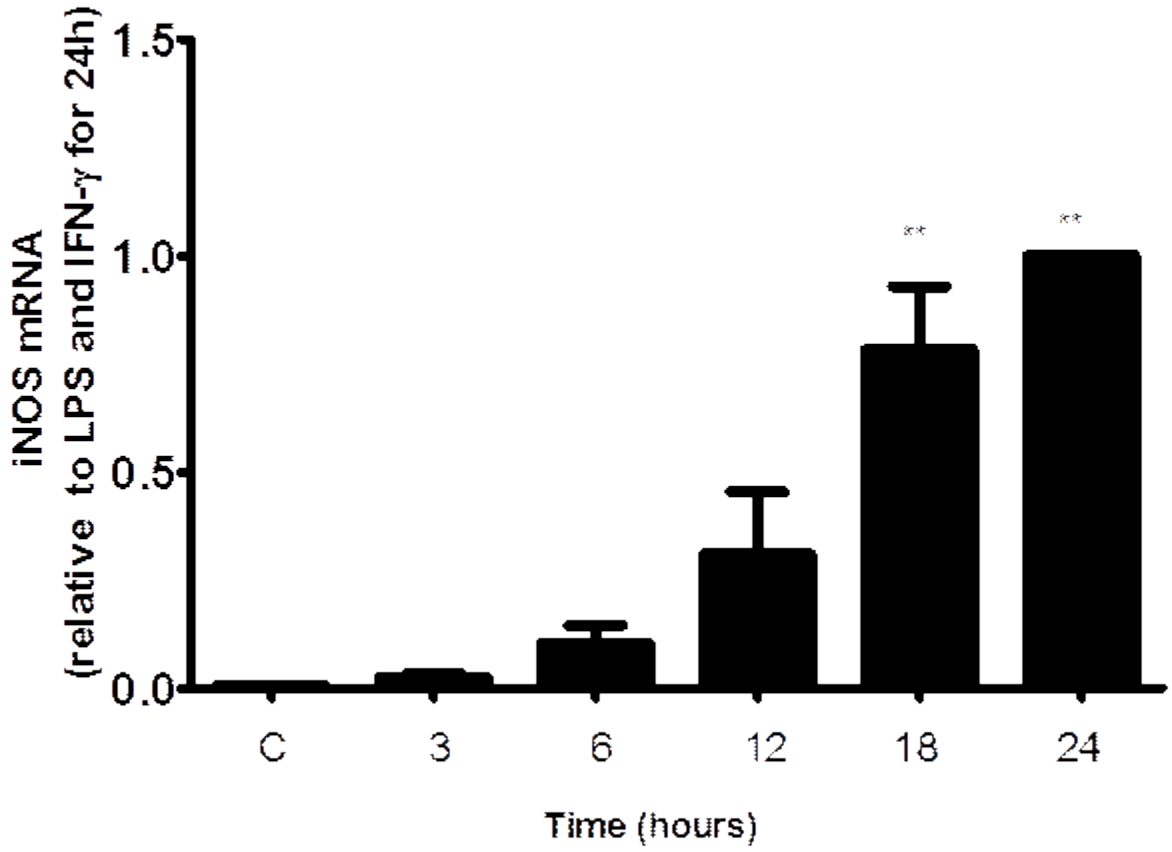

Figure 65. Time dependent of activation on iNOS mRNA in RASMCs. Confluent monolayers of RASMCs in a T25 flask were activated with LPS (100 µg/mL) and IFN-γ (100 U/mL) at different time points. Levels of iNOS mRNA were determined following the method described in section 7.2. Data are expressed as fold-based changes, with the response to LPS (100 µg/mL) and IFN-γ (100 U/mL) at 24 h taken as one fold. Data are the M ± SEM of at least three independent experiments. Statistical differences were determined by one-way ANOVA, followed by Dunnett's multiple comparisons test of the normalised data; ** denotes $p < .01$ compared to the control.

7.3.3 Effect of fluticasone on iNOS mRNA

The effect of fluticasone on iNOS mRNA in cell activation was evaluated with LPS and IFN-γ for 24 h. Data in Figure 66 show little iNOS mRNA in controls, which was significantly induced in cells activated with LPS and IFN-γ. Such findings are consistent with the fact that iNOS is not constitutively expressed in smooth muscle cells but induced following activation. More importantly, the induction of iNOS mRNA was significantly inhibited by fluticasone and reduced levels by more than 50%.

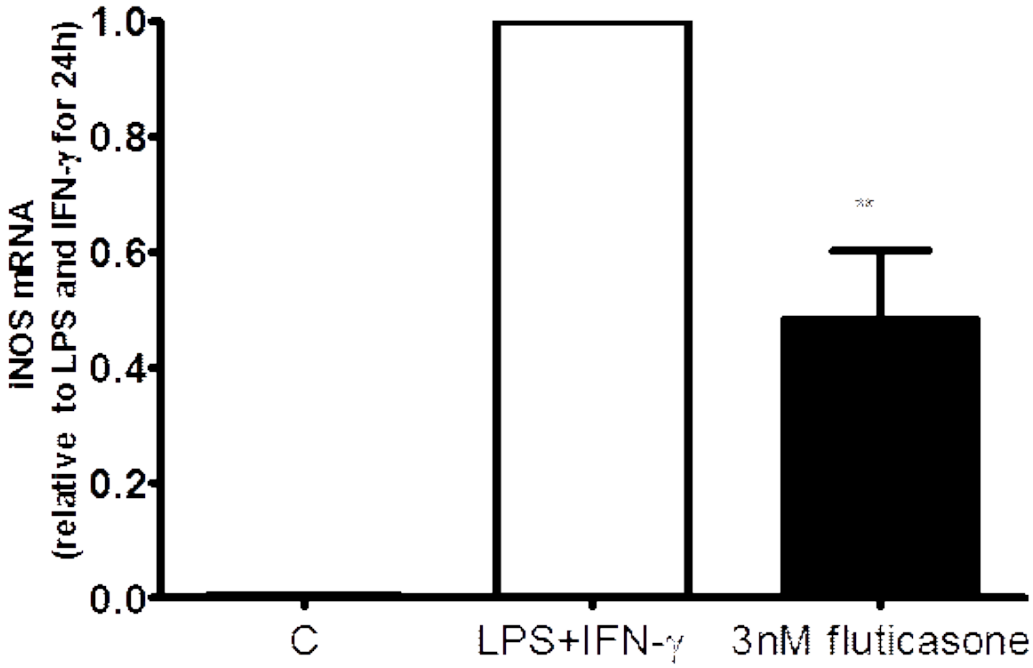

Figure 66. Effect of fluticasone on iNOS mRNA expression in RASMCs. Confluent monolayers of RASMCs in T25 flasks were pretreated with 3 nM of fluticasone for 30 min before incubation with LPS (100 μg/mL) and FN-γ (100 U/mL) for 24 h. Levels of iNOS mRNA were determined following the method described in section 7.2. Data are expressed as fold changes, with the response to LPS (100 μg/mL) plus IFN-γ (100 U/mL) for 24 h taken as one fold. Data are the M ± SEM of at least three independent experiments. Statistical differences were determined by one-way ANOVA, followed by Dunnett's multiple comparisons test of the normalised data; ** denotes $p < .01$ compared to the activated control.

7.3.4 Effect of PKR inhibitor C16 on the viability of RASMCs

Another experiment was conducted to determine whether different concentrations of C16 either with or without LPS and IFN-γ exerted any cytotoxic effects on the model by way of MTT assay following the method described in section 2.4. Confluent monolayers of RASMCs were pretreated with different concentrations of C16 (30–1,000 nM) only or with C16 30 min prior to activation with LPS and IFN-γ. Data showed that C16 was tolerated well except at the highest concentration (1 □M), which appeared to cause a statistically significant suppression of MTT metabolism by reducing it by approximately 30% (Figure 67). That concentration was therefore excluded from subsequent experiments.

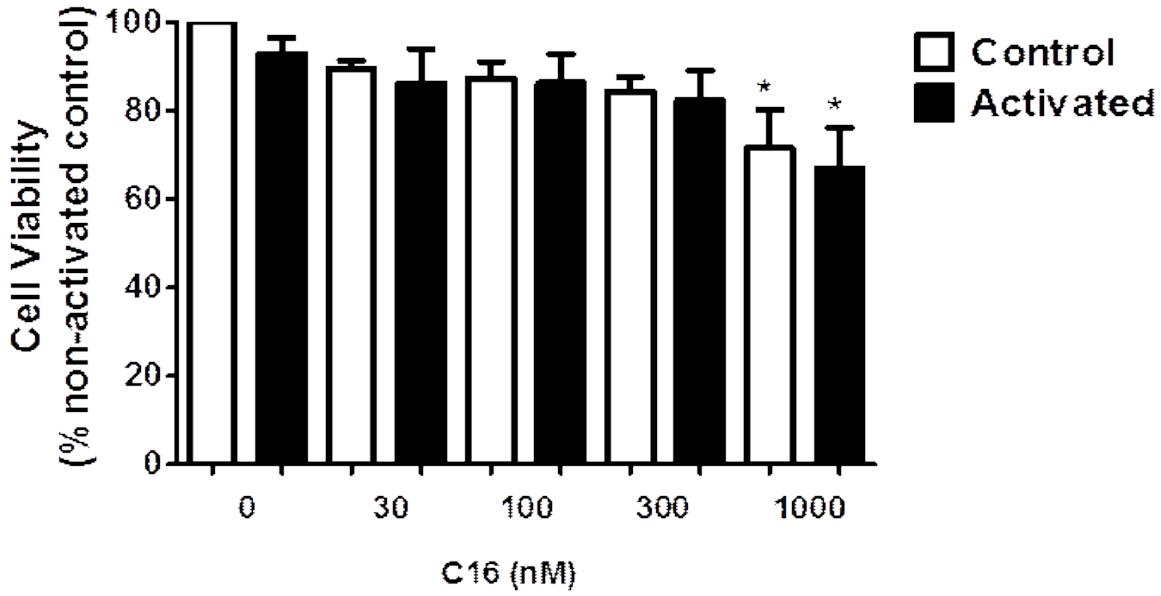

Figure 67. Effect of C16 on the viability of RASMCs. Confluent monolayers of RASMCs in 96-well plates were incubated with only CM, different concentrations of C16 (30–1,000 nM), or preincubated with C16 (30–1000 nM) for 30 min prior to activation with LPS (100 μg/mL) and IFN-γ (100 U/mL) for 24 h. The metabolism of MTT was determined colourimetrically following the method described in section 2.4. The white bars represent controls, and the black ones represent activated cells. Data are presented as the percentage of viable cells compared to the controls and represent the M ± SEM of at least three individual experiments. Statistical differences were determined by one-way ANOVA, followed by Dunnett's multiple comparisons test of the normalised data; * denotes $p < .05$ compared to the nonactivated control.

7.3.5 Effect of PKR inhibitor on NO production

Prior to investigating whether PKR is regulated in activated RASMCs and by GCs, studies were performed to determine whether PKR plays any critical role in the expression of iNOS and NO production. Cells were preincubated with increasing concentrations of C16 (30–300 nM) for 30 min prior to activation with LPS and IFN-γ. Nitrite levels were subsequently determined in the culture medium using Griess assay following the method described in section 2.6. As Figure 68 shows, C16 inhibited NO production in a concentration dependent

manner, albeit only partially with the highest concentration used (300 nM). Higher concentrations could not be used due to the cytotoxicity previously demonstrated.

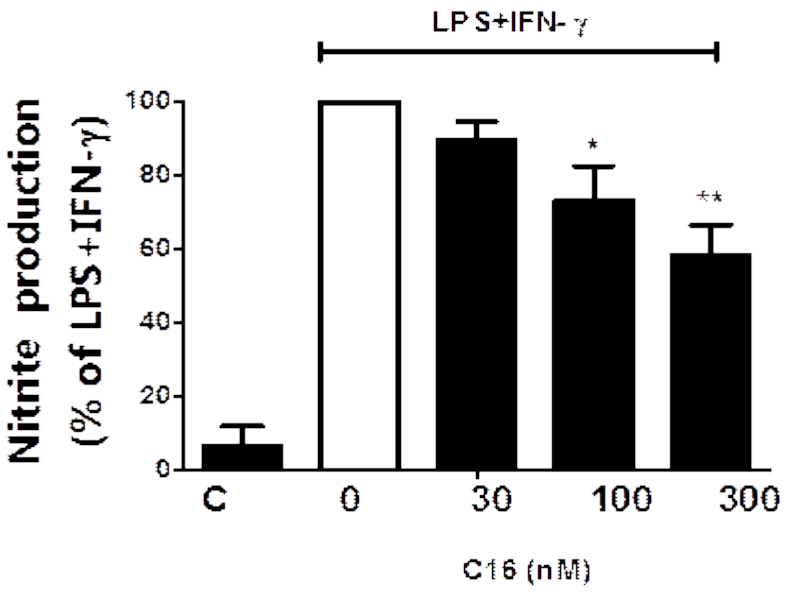

Figure 68. Concentration dependent effect of C16 on nitrite production. Confluent monolayers of RASMCs in 24-well plates were pretreated with concentrations of C16 at (30–300 nM) for 30 min before activation with 100 µg/mL of LPS and 100 U/mL of IFN-γ for 24 h. Controls were incubated with CM only. The culture medium was analysed by Griess assay to determine total nitrite levels following the method described in section 2.6. Data are expressed as a percentage of nitrite production, with the response to LPS (100 µg/mL) plus IFN-γ (100 U/mL) taken as 100%. Data are the M ± SEM of at least three independent experiments. Statistical differences were determined by one-way ANOVA, followed by Dunnett's multiple comparisons test of the normalised data; * denotes $p < .05$ and ** $p < .01$ compared to the activated control.

7.3.6 Effect of PKR inhibitor on iNOS expression

Changes in iNOS expression were also investigated using cell lysates generated under identical conditions. As data in Figure 69 show, C16 inhibited iNOS expression in a similar manner and over the same concentration range as for NO production.

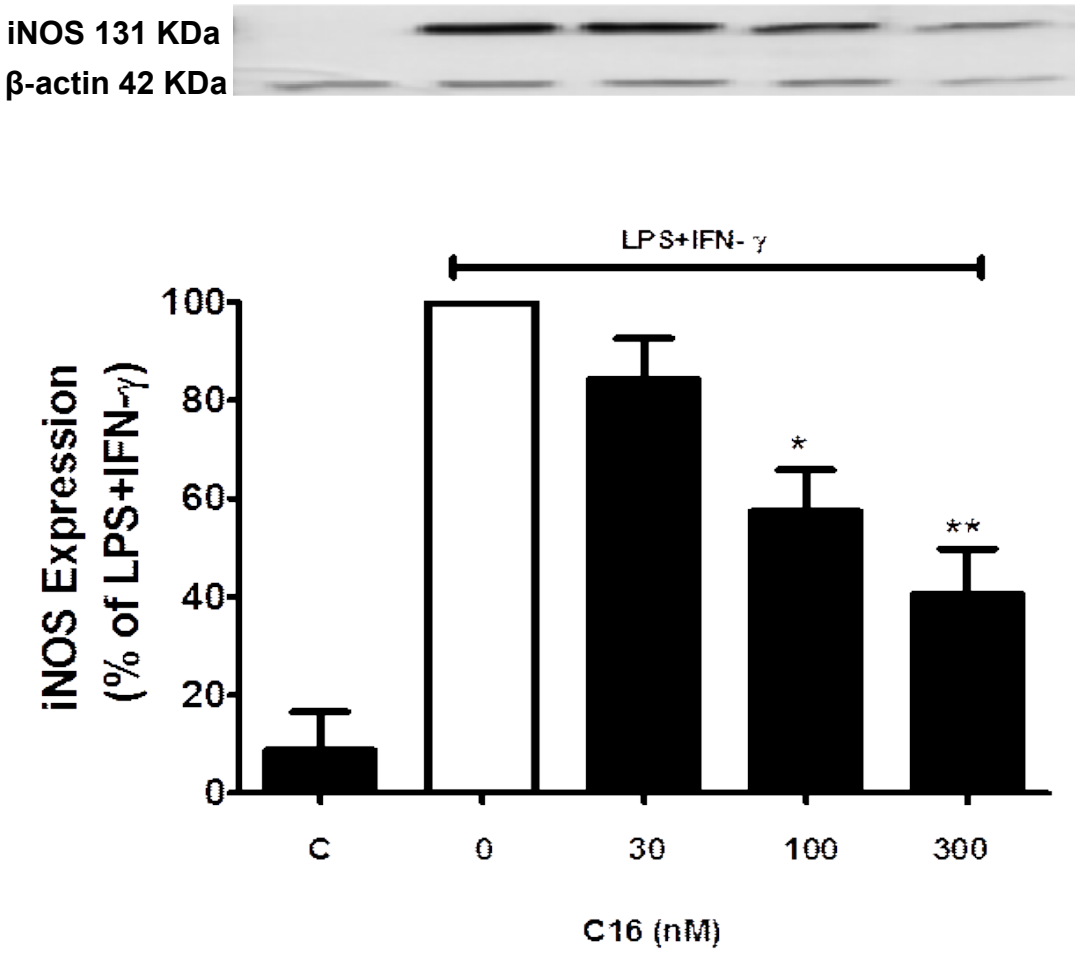

Figure 69. Concentration dependent effect of C16 on iNOS expression. Confluent monolayers of RASMCs in 24-well plates were pretreated with C16 (30–300 nM) for 30 min before activation with 100 µg/mL of LPS and 100 U/mL of IFN-γ for 24 h. The expression of iNOS was determined by western blotting following the method described in section 2.9. The blot is representative of at least three independent experiments, and the bar graph depicts densitometric data expressed as a percentage of iNOS expression, with the response to LPS (100 µg/mL) plus IFN-γ (100 U/mL) taken as 100%. Data represent the M ± SEM of at least three independent experiments. Statistical differences were determined by one-way ANOVA, followed by Dunnett's multiple comparisons test of the normalised data; * denotes $p < .05$ and ** $p < .01$ compared to the activated control.

7.3.7 Time course induction of P-PKR

Since the findings reported above suggested that PKR might be involved in inducing iNOS, additional experiments were performed to determine whether PKR is expressed in RASMCs and, more importantly, whether its phosphorylated form is altered following the activation of cells to express iNOS. Confluent monolayers of cells were incubated with LPS and IFN-γ for different time points ranging from 0.25 to 24 h. Results showed high levels of expression of P-PKR in both control and activated cells. Interestingly, no significant difference emerged between the two (Figure 70), which suggests that the kinase is perhaps already highly phosphorylated under basal conditions. Alternatively, PKR might not be responsive to LPS and IFN-γ, though that hypothesis would contradict the findings with C16 that suggest a role for PKR and thus requires additional investigation.

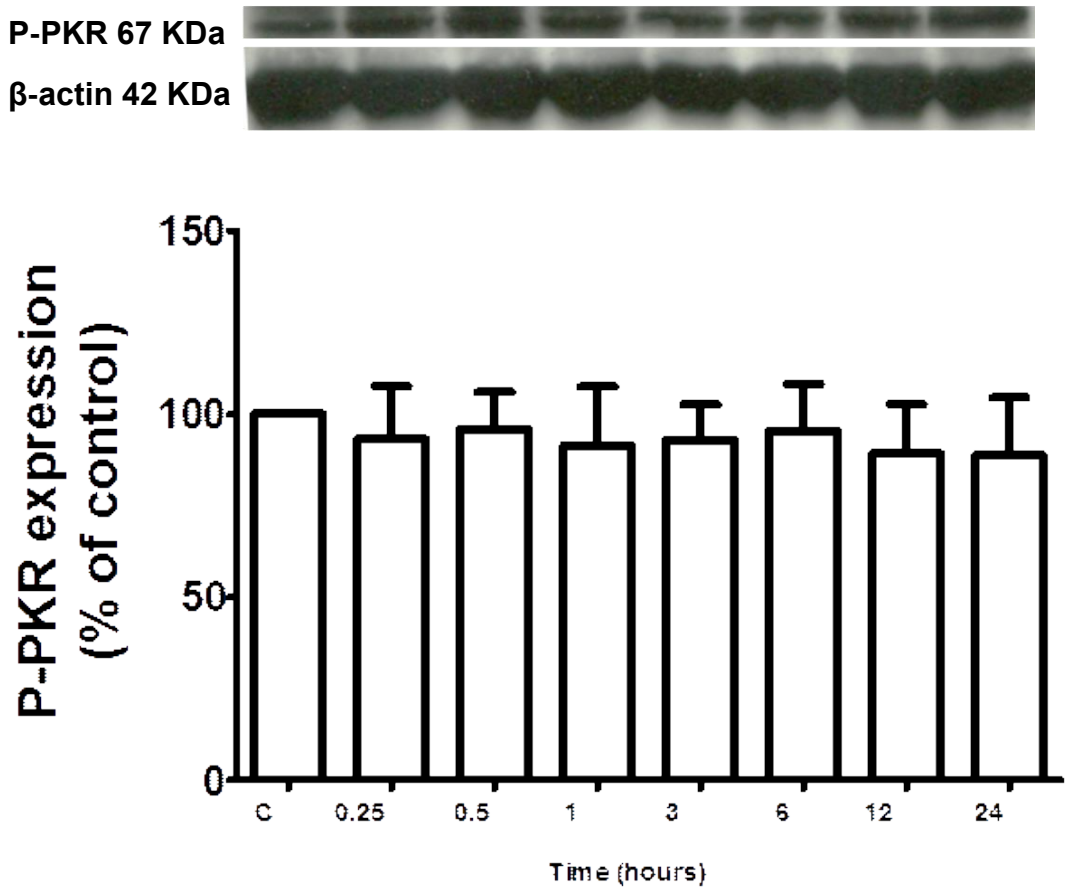

Figure 70. Time course activation of P-PKR. Confluent monolayers of RASMCs in 24-well plates were incubated with LPS (100 μg/mL) and IFN-γ (100 U/mL) at different time points ranging from 0.25 to 24 h. The expression of P-PKR was determined by western blotting following the method described in section 2.9. The blot is representative of at least three independent experiments, and the bar graph depicts densitometric data expressed as the percentage of P-PKR, with control responses taken as 100%. Data represent the M ± SEM of at least three independent experiments. Statistical differences were determined by one-way ANOVA, followed by Dunnett's multiple comparisons test.

7.3.8 Effect of fluticasone on P-PKR expression

Another experiment was conducted to investigate whether fluticasone has any effect on P-PKR expression. Confluent monolayers of RASMCs were incubated with fluticasone (3 nM) at different time points ranging from 1 to 24 h for 30 min prior to activation with LPS and

IFN-γ. Results shown in Figure 71 indicated that the expression of P-PKR was not significantly affected by fluticasone at any time point examined.

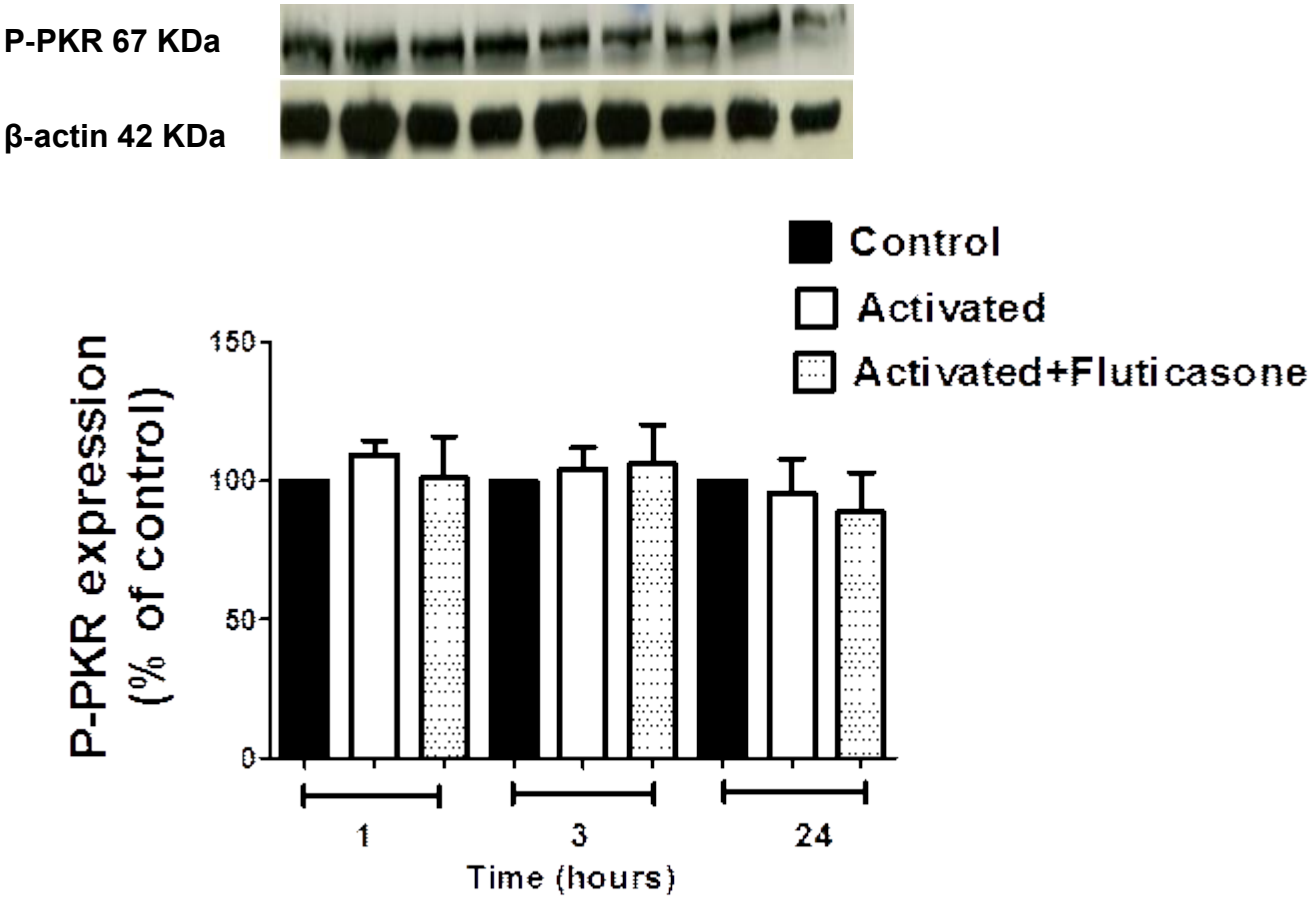

Figure 71. Effect of fluticasone on P-PKR expression at different time points. Confluent monolayers of RASMCs in 24-well plates were incubated with CM alone or activated with LPS (100 μg/mL) and IFN-γ (100 U/mL) for 1, 3, and 24 h in the absence and presence of fluticasone (3 nM), which was added 30 min prior to activation. The expression of P-PKR was determined by western blotting following the method described in section 2.9. The blot is representative of at least three independent experiments, and the bar graph depicts densitometric data expressed as the percentage of P-PKR expression, with control responses taken as 100%. Data represent the M ± SEM of at least three independent experiments. Statistical differences were determined by one-way ANOVA, followed by Dunnett's multiple comparisons test.

7.3.9 Time course induction of P-EIF2α

Another experiment was performed to determine whether RASMCs express P-EIF2α and whether the activation of cells altered its expression. Confluent monolayers of RASMCs were incubated with LPS and IFN-γ for different time points ranging from 0.25 to 24 h. Cell lysates were probed for P-EIF2α expression by western blotting. Control cells expressed significant levels of P-EIF2α, and as with PKR, the levels did not change significantly following the activation of cells with LPS and IFN-γ.

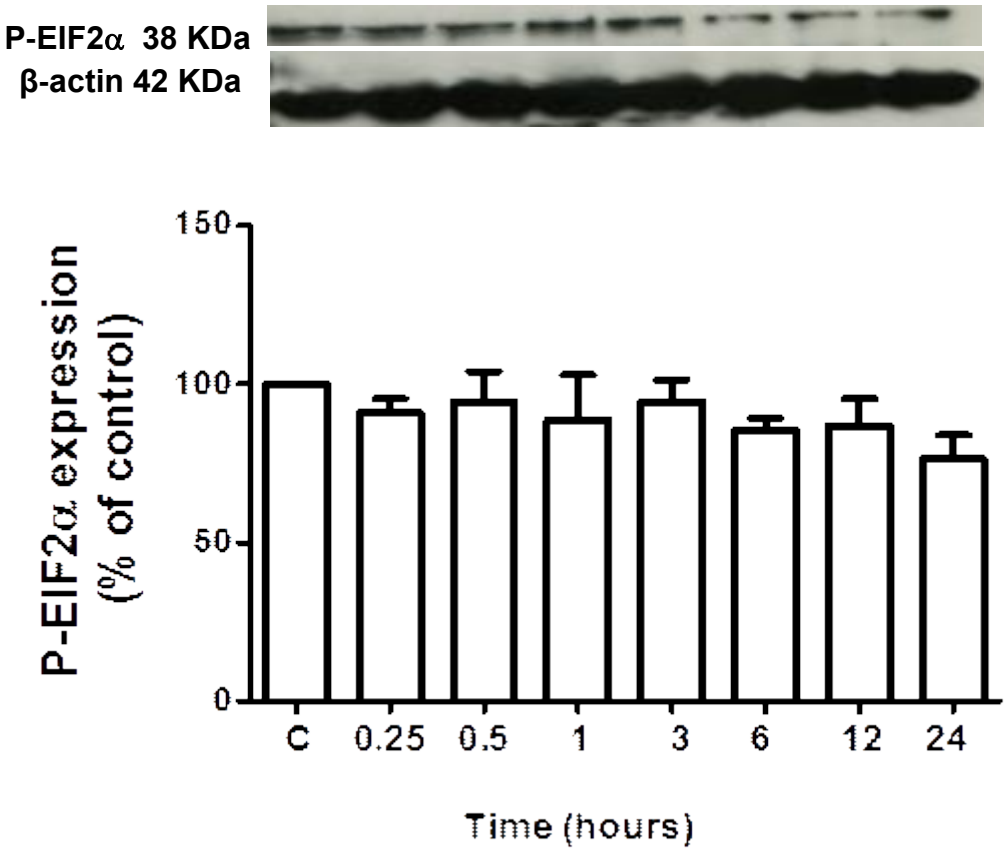

Figure 72. Time course activation of P-EIF2α. Confluent monolayers of RASMCs in 24-well plates were incubated with LPS (100 μg/mL) and IFN-γ (100 U/mL) at different time points ranging from 0.25 to 24 h. The expression of P-EIF2α was determined by western blotting following the method described in section 2.9. The blot is representative of the M ± SEM of at least three independent experiments, and the bar graph depicts densitometric data expressed as the percentage of P-EIF2α expression, with the control response taken as 100%. Statistical differences were determined by one-way ANOVA, followed by Dunnett's multiple comparisons test.

7.3.10 Effect of fluticasone on P-EIF2α expression

The effects of fluticasone on P-EIF2α were also investigated under conditions identical to those described for P-PKR. Consistent with the findings on P-PKR, P-EIF2α expression was

not significantly affected by fluticasone. Taken together, those data strongly suggest that the PKR–EIF2α signalling pathway might not be affected by LPS and IFN-γ; however, it cannot be ruled out that the pathway might already be optimally activated under basal conditions. Consequently, it remains to be investigated whether the PKR–EIF2α signalling pathway can be implicated in the induction of iNOS.

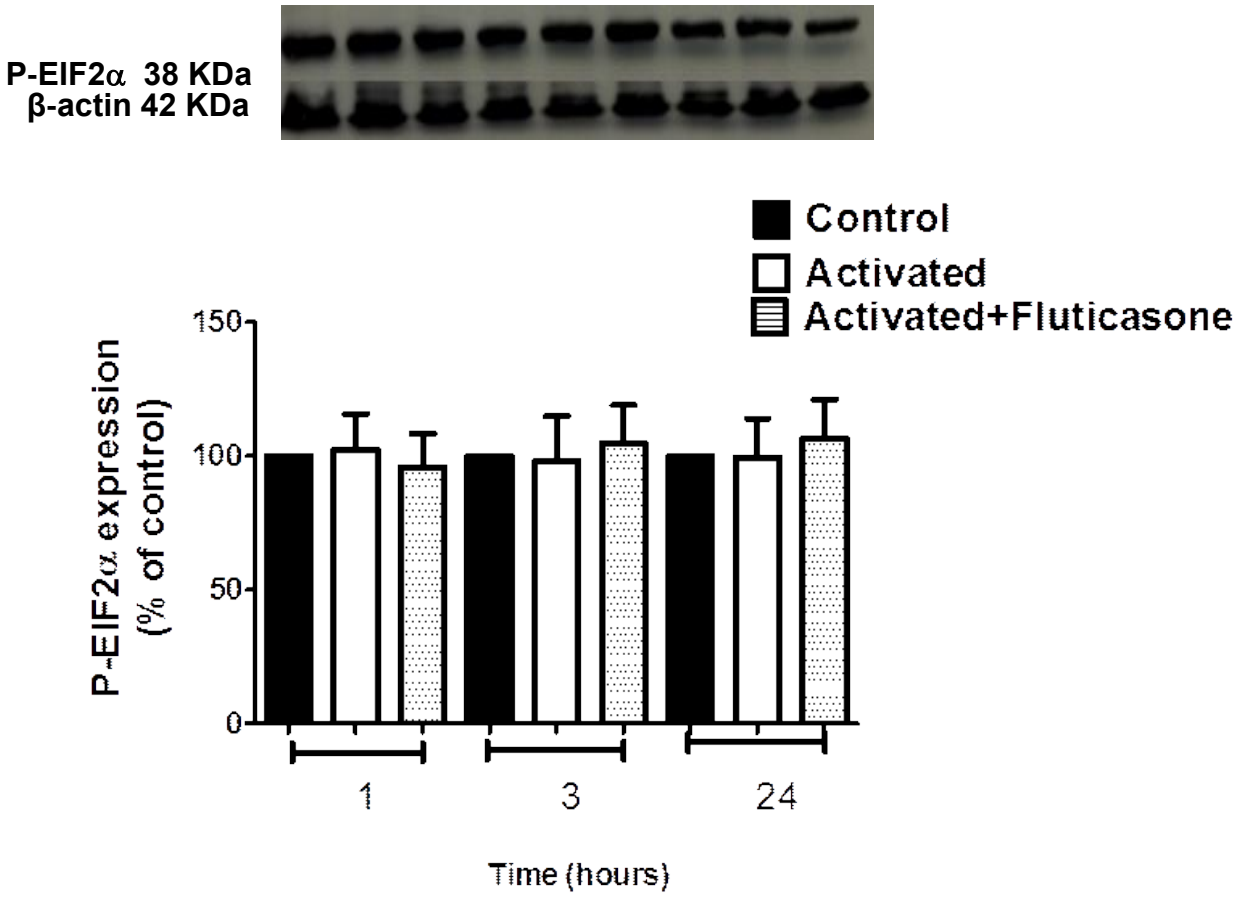

Figure 73. Effect of fluticasone on P-EIF2α expression at different time points.Confluent monolayers of RASMCs in 24-well plates were incubated with CM alone or activated with LPS (100 μg/mL) and IFN-γ (100 U/mL) for 1, 3, and 24 h in the absence and presence of fluticasone at 3 nM, which was added 30 min before activation. The expression of P-EIF2α was determined by western blotting following the method described in section 2.9. The blot is representative of the M ± SEM of at least three independent experiments, and the bar graph depicts densitometric data expressed as the percentage of P-EIF2α expression, with control responses taken as 100%. Statistical differences were determined by one-way ANOVA, followed by Dunnett's multiple comparisons test.

7.4 Discussion

This final chapter of results sought to link pretranscriptional cellular signalling events to those that might occur at the translational level, by particularly focusing on a less well-studied signalling pathway involving PKR and EIF2α. PKR appears to play a central role in mediating responses to stress signals and is reported to interact with other stress-mediated signalling pathways, including that involving p38 MAPK, which was investigated in chapter 6. EIF2α, by contrast, is required to initiate the translation stage of protein synthesis, in which the ribosome builds proteins according to information encoded on the mRNA.

The strategy to determine whether PKR–EIF2α might be the downstream pathway leading to iNOS expression first involved investigating the effects of C16 on induced NO synthesis and iNOS expression. That step was followed by establishing the expression profiles of both P-PKR and P-EIF2α, followed by studies with fluticasone to determine whether its actions are mediated by the PKR–EIF2α pathway. First, however, studies were performed to examine the time course of activation of iNOS mRNA expression using qPCR analysis. For such studies, it was important to ensure that high-quality mRNA was isolated from cells, as established by gel electrophoresis of the purified mRNA, which showed clear bands of 28s and 18s without smear, degradation, or contamination. Such an outcome provided assurance of the samples generated, which were subsequently used in PCR.

The analysis of total mRNA using specific iNOS primers revealed a detectable increase of iNOS mRNA at 6 h, which peaked at 24 h. That result is consistent with the findings of previous research (Hecker et al., 1999). Interestingly, the time course for the maximal

expression of iNOS mRNA seems to vary depending on the cell type. In smooth muscle cells, expression seems to require 24 h to peak. In macrophages stimulated with LPS, by contrast, iNOS mRNA is expressed far earlier at 2 h and plateaued at 12 h after activation (Tajima et al., 2012). Although the reason for the time difference in expression is unclear, in any case the protein produced functions equally well in the different cell systems.

In different cell types, GCs have been suggested to inhibit iNOS expression and function at the transcriptional level by interfering with transcription factor NF-κB (Katsuyama et al., 1999; Kleinert et al., 1996; Salzman et al., 1996). However, contradictory reports suggest that dexamethasone inhibits iNOS expression, functions post-transcriptionally, and actually enhances iNOS mRNA at the transcriptional level (Thakur & Baydoun, 2012). It was thus unclear whether other GCs such as fluticasone also exerted similar actions on iNOS mRNA expression. Fluticasone was thus investigated for its possible effect on iNOS mRNA expression. In contrast to data obtained with dexamethasone (Thakur & Baydoun, 2012), data for fluticasone showed decreased iNOS mRNA, which is consistent with its inhibition of iNOS expression and functions.

To demonstrate whether PKR played a role in expressing iNOS, the imidazolo-oxindole PKR inhibitor C16 was exploited. First, however, studies were performed to determine whether it caused any cytotoxicity to RASMCs, with the chief aim of examining whether different concentrations of C16 had any cytotoxic effect on RASMCs. The compound appeared to be tolerated well, though a higher concentration of 1 μM indicated a significant reduction of cell viability. Thus, that concentration was excluded from subsequent studies.

The PKR inhibitor showed a concentration dependent reduction of iNOS expression and function. Such an effect has not been investigated in RASMCs, meaning that this thesis marks the first report of such action for C16. This novel finding can be explained by the fact that PKR can activate NF-κB (Kumar et al., 1994), which has been proven critical for iNOS induction. The inhibition of PKR by C16 therefore inhibits NF-κB, which results in inhibiting iNOS expression. Other studies have reported that PKR is required for p38 MAPK activation and for the innate immune response to bacterial endotoxin (Goh et al., 2000). Accordingly, the inhibition of PKR by C16 would inhibit p38 MAPK, which could result in a blockade of NF-κB and thus iNOS expression. All of those potential mechanisms now remain to be confirmed.

Fluticasone did not show any significant effect on the phosphorylation of PKR, which suggests that the kinase might not be involved in fluticasone's effect on iNOS expression and function. Since PKR is linked to EIF2α, additional studies were performed to investigate the effect of fluticasone on its phosphorylation. As with PKR, EIF2α was also not affected by fluticasone; thus, fluticasone's effect on the inhibition of iNOS expression and function does not seem to occur via those factors. However, research of different cell types has indicated the involvement of PKR on iNOS expression via the activation of NF-κB, and p38 MAPK (Goh et al., 2000; Kumar et al., 1994; Maggi et al., 2000). Additionally, in astrocytes, arginine depletion reduces iNOS protein, but not mRNA, via the phosphorylation of EIF2α (Lee et al., 2003).

Collectively, the results of the studies indicate that C16 reduces iNOS expression and function. However, that effect does not seem to occur via the PKR–EIF2α signalling pathway, meaning that the actual mechanism involved now remains to be established.

8. General Discussion

The research described in this thesis was conducted to dissect the GC component that regulates iNOS expression and function. The research was completed in part by comparing previously used nonselective GCs (i.e., dexamethasone and hydrocortisone) with a more selective GC (i.e., fluticasone). Other studies were also performed to investigate the possible mechanisms behind the effect of GC.

The exposure of vascular smooth muscle cells to cytokines resulted in the production of inflammatory proteins such as iNOS, which subsequently resulted in the production of high amounts of NO that could be responsible for pathological effects associated with the xpression of iNOS, including the vasorelaxation and hypotension that accompanies septic shock (Kirkebøen & Strand, 1999). This proves that the use of RASMCs in our model is justifiable as the results obtained are consistent with several other reports and with our previous findings demonstrating that RASMCs readily respond to LPS and IFN-γ to induce iNOS and NO production (Baydoun et al., 1999; Knowles et al., 1990) cost-effective and producible.

As expected, iNOS was routinely induced in response to LPS and IFN-γ and caused the sustained release of NO, and both LPS and IFN-γ peaked after 24 h of activation. Table 10 summarises the induction of iNOS in different type of cells in response to various stimuli.

Table 10. Cell activation with inflammatory mediators

Inflammatory mediator	**Cell types**	**Reference**
LPS	Human macrophage cell line THP-1	Liu et al. (2010)
TNF	Dendritic cells	Serbina et al. (2003)
IL-4	Rat eosinophils	Paoliello–Paschoalato et al. (2005)
LPS	J774 macrophages	Chen et al. (1999)
IL-1β + IFN-γ	Skeletal muscle cells	Adams et al. (2002)
LPS + IFN-γ	RASMCs	Baydoun et al. (1999)
IL-1 β	RASMCs	Katsuyama et al. (1999)

The results of the studies conducted for this thesis are consistent with those of the research summarised in Table 10, especially those using LPS and IFN-γ. Although the precise mechanisms that mediate iNOS expression and NO production are complex, it has been suggested that LPS might induce iNOS mRNA, whereas IFN-γ acts to stabilise it (Weisz et al., 1994). In skeletal muscle cells, IFN-γ has been shown to augment the ability of IL-1β to induce iNOS via different mechanisms involving IFN-γ's elevation of the expression of IL-1β receptor mRNA to enhance iNOS expression (Adams et al., 2002).

Many studies have investigated the effects of GCs on iNOS expression in various cell systems, yet all have proposed a different mechanism, as summarised in Table 11.

Table 11. Inhibitory mechanisms of iNOS and NO by GCs

GC	Cell type	Mediator	Proposed mechanism	Reference(s)
Dexamethasone	RASMCs	IL-1β LPS + IFN-γ	Inhibits NF-κB	Katsuyama et al. (1999) and Matsumura et al. (2001)
Dexamethasone	RASMCs	LPS + IFN-γ	Occurs post-transcriptionally	Thakur and Baydoun (2012)
Dexamethasone	Human epithelial cells	TNF-α IL-1β IFN-γ	Inhibits NF-κB	Kleinert et al. (1996)
Dexamethasone	Mouse macrophages	LPS	Inhibits NF-κB	Jeon et al. (1998)
Dexamethasone	Mouse macrophages	LPS + IFN-γ	Decreases iNOS mRNA stability	Söderberg et al. (2007)
Dexamethasone	Rat mesangial cells	IL-1β	Decreases iNOS protein stability	Kunz et al. (1996)

The different mechanisms can be explained in part by the fact that the studies used different cell types and species.

Other data have shown that dexamethasone inhibits iNOS expression in different cell types, including mesangial cells (Kunz et al., 1996), human lung epithelial cells (Robbins et al., 1994), hepatocytes (Geller et al., 1994), cultured rat cardiocytes (Tsujino et al., 1994), human joint-derived cells such as chondrocytes, synovial fibroblasts, and osteoblasts (Grabowski et al., 1996), human airway epithelial cells (Kao et al., 2001), cultured rat astrocytes (Lavista et

al., 1999), J774 macrophages (Korhonen et al., 2002), C6 glioma cells (Shinoda et al., 2003), neonate rat brain cells (Wang et al., 2005), chromaffin cells (Pérez–Rodríguez et al., 2009), and RASMCs (Thakur & Baydoun, 2012; Wileman etal., 1995). Hydrocortisone has also been reported to inhibit iNOS expression and function in several different cell types, including rat microglial cells (Lieb et al., 2003), murine macrophages and bovine chondrocytes (Patel et al., 1999), human chondrocytes (Palmer et al., 1993), and RASMCs (Suzuki et al., 1994). Fluticasone, by contrast, has been less well characterised but has been shown to reduce human bronchial NO flux in asthmatic patients (Lehtimaki et al., 2001). No studies on fluticasone's effects on iNOS expression in smooth muscle cells have been previously conducted, however. In the studies conducted for this thesis, dexamethasone and hydrocortisone showed a complete inhibition of iNOS and NO production, as consistent with the findings of previous research. By contrast, fluticasone showed only a partial inhibition. Since fluticasone is a more selective GC, it is reasonable to conclude that the induction of iNOS is only partially regulated by GCs. Dexamethasone and hydrocortisone are not selective GCs, and the complete inhibitions reported might therefore involve other receptors, as summarised in Table 12.

Table 12. Different GCs and their action at different receptors

GC	**Receptor(s)**	**Reference(s)**
Dexamethasone	GCRs, MRs, progesterone, oestrogen, and androgen	Bigsby (1993), Inder et al. (2010), Lan et al. (1982), and Yang et al. (2001)
Hydrocortisone	MRs, androgen, and progesterone	Born et al. (1987), Karalis et al. (1996), and Sonneveld et al. (2005)
Fluticasone	Primarily GCRs	Austin et al. (2002)

To further explore the GC component of the effects of dexamethasone, hydrocortisone, and fluticasone, studies were performed using RU-486, a compound widely used as a GCR antagonist. In the studies conducted for this thesis, RU-486 reversed the inhibition of iNOS expression and NO production caused by all three GCs. That finding is consistent with the

results of several other studies that have used dexamethasone and hydrocortisone (Table 13); however, the present studies are the first to demonstrate that RU-486 also blocks the inhibitory effects of fluticasone on iNOS expression, especially in RASMCs.

Table 13. RU-486's reversal effects on the inhibition of iNOS expression and function by GCs

GC	**Cell type**	**Reference**
Dexamethasone	RASMCs	Godfrey et al. (2011)
Dexamethasone	Rat embryonal cortical neurons	Golde et al. (2003)
Dexamethasone	RAW 264.7 cells	Walker et al. (1997)
Hydrocortisone	N9 murine microglia cell line	Chang and Liu (2000)

Although RU-486 is widely used to implicate actions mediated via GCRs, it also acts as a progesterone antagonist by blocking its receptor. It is therefore likely that both dexamethasone and hydrocortisone regulate iNOS expression not only via GCRs, but potentially also via the progesterone receptor.

Additional studies were performed using eplerenone as an MR antagonist, with the aim of determining whether MRs mediated the regulation of expression of iNOS. The compound was without effect, for it failed to modify the inhibitions caused by either dexamethasone or hydrocortisone. Eplerenone can therefore be ruled out as a critical player in the cell system developed for the studies of this thesis.

Earlier studies found that p38 MAP kinase activation is associated with the induction of proinflammatory mediators (Schindler et al., 2007), as well as that the activation of p38 MAPK is associated with iNOS expression and function in RASMCs, in which SB203580 inhibits iNOS expression and function (Baydoun et al., 1999). At the same time, Akt has been shown to play a crucial role in the inflammation and activation of TLR (Troutman et al., 2012), as well as in iNOS expression and function via the activation of NF-κB (Hattori et al.,

2003). Data from the studies conducted for this thesis indicated that fluticasone reduced the activation of both p38 MAPK and Akt. Such results could explain the mechanism by which fluticasone reduced iNOS expression and function.

In human foetal lung fibroblasts, fluticasone reduced the activation in both p38 and Akt as well (Seki et al., 2013). That reduction was reversed by RU-486, which suggests that fluticasone reduced the activation of those signalling pathways via GCRs. Additionally, fluticasone and other GCs have been shown to induce MKP-1 (King et al., 2009; Lasa et al., 2002; Manetsch et al., 2013; Toh et al., 2004). Thus, the selective GC might activate a phosphatase that dephosphorylates both p38 and Akt, which could explain the actions of fluticasone in inhibiting iNOS expression reported in this thesis, the proposed pathway for which is summarised in Figure 74.The regulation of iNOS expression often involves regulating its mRNA, which could be a target for GCs. Indeed, several studies have shown that GCs regulate iNOS mRNA in several different cell systems (Table 14).

Table 14. Ability of GCs to reduce iNOS mRNA in different cell types

GC	**Cell type**	**Reference(s)**
Methylprednisolone	Rat lung	Sukumaran et al. (2012)
Dexamethasone	Rat lung cells	Yu et al. (2009)
Dexamethasone	Neonatal rat brain cells	Wang et ail. (2005)
Budesonide or prednisolon	Colonic biopsy cells from ulcerative colitis patients	Linehan et al. (2005)
Dexamethasone	RASMCs	Katsuyama et al. (1999) and Matsumura et al. (2001)
Dexamethasone	Rat alveolar macrophages	Hammermann et al. (2000)
Dexamethasone	Rat hepatocytes	De Vera et al. (1997)

Although no studies have reported similar effects for fluticasone, one has claimed that fluticasone can act on upstream signalling pathways to regulate transcriptional events. By

extension, studies were performed to determine whether that GC regulated upstream kinases (i.e., p38 and Akt) associated with iNOS induction and whether it altered iNOS mRNA expression. Results of the latter study clearly show that fluticasone inhibited iNOS mRNA expression at concentrations that blocked the enzyme protein expression. Again, the studies conducted for this thesis are the first to report that finding and confirm that fluticasone can act at the transcriptional level to suppress iNOS induction.

Other studies have shown that GCs reduced iNOS expression and function post-transcriptionally. In rat hepatocytes, dexamethasone reduced iNOS expression and function by destabilising iNOS mRNA, presumably because dexamethasone inhibited the iNOS gene antisense transcript, which is responsible for stabilising iNOS mRNA (Ozaki et al., 2010). In addition, in C6 glioma cells, dexamethasone caused an 83% inhibition of iNOS expression, but reduced iNOS mRNA by only 10%, which suggests that dexamethasone acts at the post-transcriptional level (Shinoda et al., 2003). In RASMCs, dexamethasone showed a reduction in iNOS expression and function but enhanced iNOS mRNA (Thakur & Baydoun, 2012). That outcome contradicts findings in the same cell types in Table 14. Although the reason for the discrepancy remains unclear, it could reflect differences in experimental approaches. In Matsumura et al.'s (2001) study, iNOS mRNA was detected after incubation with LPS and IFN-γ for 6 h, whereas in the present studies the activation period was 18 h. In addition, Katsuyama et al. (1999) reported that the cells were activated by IL-1β, whereas they were activated by LPS and IFN-γ in this study.

Little is known about the regulation of iNOS at the post-transcriptional level, and targets for such studies are limited. Of interest, however, is the double-stranded RNA-dependent PKR activated by IFNs and double-stranded RNA. PKR can activate NF-κB and thus iNOS expression in human astrocytes (Auch et al., 2004), which suggests it role in iNOS expression. Additionally, the activation of the kinase phosphorylates translation factor EIF2α

and, in turn, reduces protein expression. That pathway was therefore investigated, and results showed that PKR inhibitor reduced iNOS expression and function. Interestingly, the activation of cells with LPS and IFN-γ showed no difference in P-PKR and P-EIF2α expression. Fluticasone also had no effect on the expression of either protein. Such observations suggest that PKR and EIF2α might not be involved in the cell model developed for the studies of this thesis; however, that conclusion might be oversimplified, especially since data with the PKR inhibitor show that the latter blocked iNOS expression and function. Further studies are required to fully understand the role of at least PKR in similar systems and to determine whether the inhibitor does indeed regulate iNOS by blocking PKR.

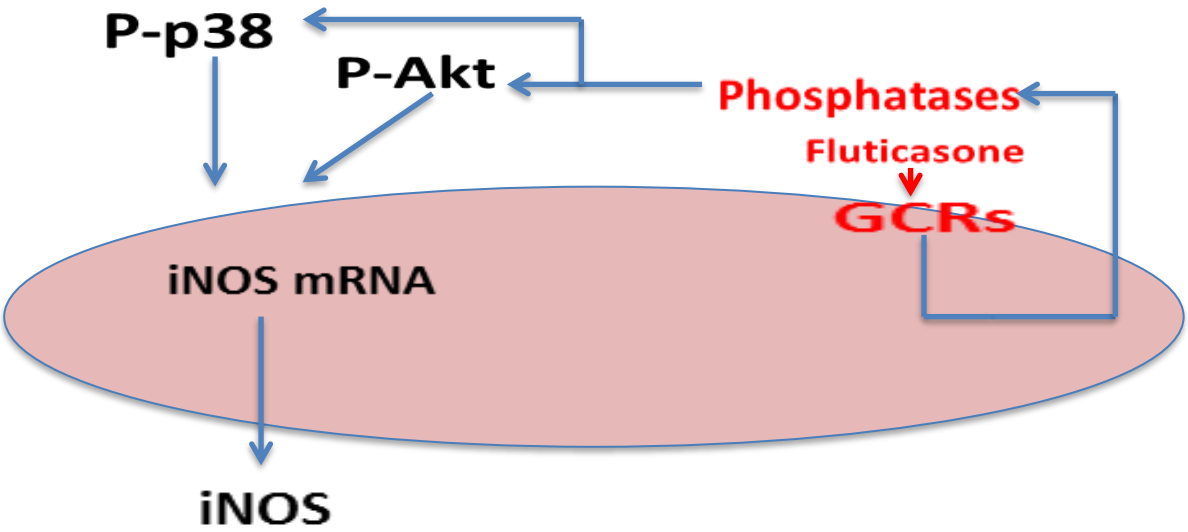

Figure 74. Suggested mechanism by which fluticasone reduces iNOS expression and function

Conclusions

The mechanisms by which GCs regulate iNOS expression and function are not fully understood. The two nonselective GCs (i.e., dexamethasone and hydrocortisone) inhibited iNOS expression and function completely, whereas the more selective GC (i.e., fluticasone) showed only partial inhibition. Consequently, other additional receptors or pathways might mediate the actions observed with the nonselective GCs. The selective GC could dephosphorylate p38 and Akt, which are critical in regulating iNOS expression and function. These novel data suggest that fluticasone reduce iNOS expression and function via p38 and Akt. That action of fluticasone seems to occur via GCRs, whereas MRs are excluded. Moreover, the induction of iNOS and NO in RASMCs seems to occur independently of EIF2α.

Future Studies

The studies conducted in this thesis have shed some light on the potential role of GCs and the underlying mechanisms through which they act to regulate the induction of iNOS, at least in RASMCs. The studies have, however, also indicated several additional objectives for future research, including

- To investigate the effect of dexamethasone and hydrocortisone on p38 and Akt, given data showing that fluticasone acts via those signalling pathways;
- To investigate the effect of GCs on transcription factor (NF-κB), since the activation of NF-kB is important for the expression of iNOS;
- To investigate the effect of fluticasone on MKP-1, since it could be activated by fluticasone and responsible for its dephosphorylation action;
- To investigate the effect of nonselective GCs on iNOS expression and function in the presence of steroid antagonists including oestrogens, progesterone, and androgens since existing data suggest that other receptors could be involved in the inhibitory action of dexamethasone and hydrocortisone on iNOS expression and function.

References

Abraham, S. M., Lawrence, T., Kleiman, A., Warden, P., Medghalchi, M., Tuckermann, J., . . . Clark, A. R. (2006). Antiinflammatory effects of dexamethasone are partly dependent on induction of dual specificity phosphatase 1. *The Journal of Experimental Medicine, 203*(8), 1883-1889. doi:jem.20060336 [pii]

Adams, V., Nehrhoff, B., Spate, U., Linke, A., Schulze, P. C., Baur, A., . . . Schuler, G. (2002). Induction of iNOS expression in skeletal muscle by IL-1beta and NFkappaB activation: An in vitro and in vivo study. *Cardiovascular Research, 54*(1), 95-104. doi:S0008636302002286 [pii]

Adcock, I. M., Nasuhara, Y., Stevens, D. A., & Barnes, P. J. (1999). Ligand-induced differentiation of glucocorticoid receptor (GR) trans-repression and transactivation: Preferential targetting of NF-κB and lack of I-κB involvement. *British Journal of Pharmacology, 127*(4), 1003-1011.

Akashi, S., Saitoh, S., Wakabayashi, Y., Kikuchi, T., Takamura, N., Nagai, Y., . . . Adachi, Y. (2003). Lipopolysaccharide interaction with cell surface toll-like receptor 4-MD-2 higher affinity than that with MD-2 or CD14. *The Journal of Experimental Medicine, 198*(7), 1035-1042.

Akira, S., Uematsu, S., & Takeuchi, O. (2006). Pathogen recognition and innate immunity. *Cell, 124*(4), 783-801.

Al-Ali, M., Eames, C., & Howarth, P. (1998). Exhaled nitric oxide; relationship to clinicophysiological markers of asthma severity. *Respiratory Medicine, 92*(7), 908-913.

Al-Harbi, N. O., Imam, F., Al-Harbi, M. M., Ansari, M. A., Zoheir, K. M., Korashy, H. M., . . . Ahmad, S. F. (2016). Dexamethasone attenuates LPS-induced acute lung injury through inhibition of NF-κB, COX-2, and pro-inflammatory mediators. *Immunological Investigations, 45*(4), 349-369.

Almawi, W. Y., & Melemedjian, O. K. (2002). Negative regulation of nuclear factor-kappaB activation and function by glucocorticoids. *Journal of Molecular Endocrinology, 28*(2), 69-78. doi:JME01061 [pii]

Anderson, T. J. (2004). Nitric oxide, atherosclerosis and the clinical relevance of endothelial dysfunction. *The role of nitric oxide in heart failure* (pp. 55-70) Springer.

Andrade, M. V., Hiragun, T., & Beaven, M. A. (2004). Dexamethasone suppresses antigen-induced activation of phosphatidylinositol 3-kinase and downstream responses in mast cells. *Journal of Immunology (Baltimore, Md.: 1950), 172*(12), 7254-7262. doi:172/12/7254 [pii]

Armour, K. E., Van'T Hof, R. J., Grabowski, P. S., Reid, D. M., & Ralston, S. H. (1999). Evidence for a pathogenic role of nitric oxide in Inflammation-Induced osteoporosis. *Journal of Bone and Mineral Research, 14*(12), 2137-2142.

Auch, C. J., Saha, R. N., Sheikh, F. G., Liu, X., Jacobs, B. L., & Pahan, K. (2004). Role of protein kinase R in double-stranded RNA-induced expression of nitric oxide synthase in human astroglia. *FEBS Letters, 563*(1-3), 223-228.

Austin, R. J., Maschera, B., Walker, A., Fairbairn, L., Meldrum, E., Farrow, S. N., & Uings, I. J. (2002). Mometasone furoate is a less specific glucocorticoid than fluticasone propionate. *The European Respiratory Journal, 20*(6), 1386-1392.

Avontuur, J. A., Nolthenius, R. P. T., van Bodegom, J. W., & Bruining, H. A. (1998). Prolonged inhibition of nitric oxide synthesis in severe septic shock: A clinical study. *Critical Care Medicine, 26*(4), 660-667.

Ayroldi, E., Cannarile, L., Migliorati, G., Nocentini, G., Delfino, D. V., & Riccardi, C. (2012). Mechanisms of the anti-inflammatory effects of glucocorticoids: Genomic and nongenomic interference with MAPK signaling pathways. *FASEB Journal : Official Publication of the Federation of American Societies for Experimental Biology, 26*(12), 4805-4820. doi:10.1096/fj.12-216382 [doi]

Ayroldi, E., & Riccardi, C. (2009). Glucocorticoid-induced leucine zipper (GILZ): A new important mediator of glucocorticoid action. *FASEB Journal : Official Publication of the Federation of American Societies for Experimental Biology, 23*(11), 3649-3658. doi:10.1096/fj.09-134684 [doi]

Baydoun, A., Wileman, S., Wheeler-jones, C., Marber, M., Mann, G., Pearson, J., & Closs, E. (1999). Transmembrane signalling mechanisms regulating expression of cationic amino acid transporters and inducible nitric oxide synthase in rat vascular smooth muscle cells. *Biochem.J, 344*, 265-272.

Baydoun, A. R., Bogle, R. G., Pearson, J. D., & Mann, G. E. (1993). Selective inhibition by dexamethasone of induction of NO synthase, but not of induction of l-arginine transport, in activated murine macrophage J774 cells. *British Journal of Pharmacology, 110*(4), 1401-1406.

Bian, K., & Murad, F. (2014). What is next in nitric oxide research? from cardiovascular system to cancer biology. *Nitric Oxide, 43*, 3-7.

Bigsby, R. M. (1993). Progesterone and dexamethasone inhibition of estrogen-induced synthesis of DNA and complement in rat uterine epithelium: Effects of antiprogesterone compounds. *The Journal of Steroid Biochemistry and Molecular Biology, 45*(4), 295-301.

Bonafini, C., Marzotto, M., Olioso, D., & Bellavite, P. (2015). Biological activity of interferon gamma and lipopolysaccharide on the nitric oxide production in C6 astroglioma cells and some unexpected effects of potentization. *International Journal of High Dilution Research, 14*(2), 23-27.

Bone, R. C. (1994). Gram-positive organisms and sepsis. *Archives of Internal Medicine, 154*(1), 26-34.

Born, J., Zwick, A., Roth, G., Fehm-Wolfsdorf, G., & Fehm, H. L. (1987). Differential effects of hydrocortisone, fluocortolone, and aldosterone on nocturnal sleep in humans. *Acta Endocrinologica, 116*(1), 129-137.

Bousquet, J., Mantzouranis, E., Cruz, A. A., Aït-Khaled, N., Baena-Cagnani, C. E., Bleecker, E. R., . . . Busse, W. W. (2010). Uniform definition of asthma severity, control, and exacerbations: Document presented for the world health organization consultation on severe asthma. *Journal of Allergy and Clinical Immunology, 126*(5), 926-938.

Bowen, R., & Haslam, R. J. (1991). Effects of nitrovasodilators on platelet cyclic nucleotide levels in rabbit blood; role for cyclic AMP in synergistic inhibition of platelet function by SIN-1 and prostaglandin E1. *Journal of Cardiovascular Pharmacology, 17*(3), 424-433.

Brunelli, L., Crow, J. P., & Beckman, J. S. (1995). The comparative toxicity of nitric oxide and peroxynitrite to escherichia coli. *Archives of Biochemistry and Biophysics, 316*(1), 327-334.

Calixto, J. B., Medeiros, R., Fernandes, E. S., Ferreira, J., Cabrini, D. A., & Campos, M. M. (2004). Kinin B1 receptors: Key G-protein-coupled receptors and their role in inflammatory and painful processes. *British Journal of Pharmacology, 143*(7), 803-818.

Campos, M. M., Leal, P. C., Yunes, R. A., & Calixto, J. B. (2006). Non-peptide antagonists for kinin B 1 receptors: New insights into their therapeutic potential for the management of inflammation and pain. *Trends in Pharmacological Sciences, 27*(12), 646-651.

Cech, T. R., Bennett, D., Jasny, B., Kelner, K. L., Miller, L. J., Szuromi, P. D., . . . Ray, L. B. (1992). The molecule of the year. *Science, 258*, 1861.

Chaussade, C., Rewcastle, G. W., Kendall, J. D., Denny, W. A., Cho, K., Gronning, L. M., . . . Shepherd, P. R. (2007). Evidence for functional redundancy of class IA PI3K isoforms in insulin signalling. *The Biochemical Journal, 404*(3), 449-458. doi:BJ20070003 [pii]

Ceneviva, G. D., Tzeng, E., Hoyt, D. G., Yee, E., Gallagher, A., Engelhardt, J. F., . . . Pitt, B. R. (1998). Nitric oxide inhibits lipopolysaccharide-induced apoptosis in pulmonary artery endothelial cells. *The American Journal of Physiology, 275*(4 Pt 1), L717-28.

Chan, E. D., & Riches, D. W. (2001). IFN-gamma + LPS induction of iNOS is modulated by ERK, JNK/SAPK, and p38(mapk) in a mouse macrophage cell line. *American Journal of Physiology.Cell Physiology, 280*(3), C441-50.

Chang, J. Y., & Liu, L. (2000). Inhibition of microglial nitric oxide production by hydrocortisone and glucocorticoid precursors. *Neurochemical Research, 25*(7), 903-908.

Chen, C., Chen, Y. H., & Lin, W. W. (1999). Involvement of p38 mitogen-activated protein kinase in lipopolysaccharide-induced iNOS and COX-2 expression in J774 macrophages. *Immunology, 97*(1), 124-129. doi:imm747 [pii]

Chun, T., Bloem, L. J., & Pratt, J. H. (2003). Aldosterone inhibits inducible nitric oxide synthase in neonatal rat cardiomyocytes. *Endocrinology, 144*(5), 1712-1717.

Cooke, M., John P, & Dzau, M., Victor J. (1997). Nitric oxide synthase: Role in the genesis of vascular disease. *Annual Review of Medicine, 48*(1), 489-509.

Coutinho, A. E., & Chapman, K. E. (2011). The anti-inflammatory and immunosuppressive effects of glucocorticoids, recent developments and mechanistic insights. *Molecular and Cellular Endocrinology, 335*(1), 2-13.

Craft, J. (2004). Eplerenone (inspra), a new aldosterone antagonist for the treatment of systemic hypertension and heart failure. *Baylor University Medical Center. Proceedings, , 17*(2) 217.

Crofford, L. J. (1997). COX-1 and COX-2 tissue expression: Implications and predictions. The Journal of Rheumatology.Supplement, 49, 15-19.

Cronauer, M., Ince, Y., Engers, R., Rinnab, L., Weidemann, W., Suschek, C., . . . Sies, H. (2007). Nitric oxide-mediated inhibition of androgen receptor activity: Possible implications for prostate cancer progression. *Oncogene, 26*(13), 1875-1884.

Cruz, M. T., Duarte, C. B., Gonçalo, M., Figueiredo, A., Carvalho, A. P., & Lopes, M. C. (2001). Granulocyte–macrophage colony-stimulating factor activates the transcription of nuclear factor kappa B and induces the expression of nitric oxide synthase in a skin dendritic cell line. *Immunology and Cell Biology, 79*(6), 590-596.

Cuadrado, A., & Nebreda, A. R. (2010). Mechanisms and functions of p38 MAPK signalling. *The Biochemical Journal, 429*(3), 403-417. doi:10.1042/BJ20100323 [doi]

Cuenda, A., & Rousseau, S. (2007). p38 MAP-kinases pathway regulation, function and role in human diseases. *Biochimica Et Biophysica Acta (BBA)-Molecular Cell Research, 1773*(8), 1358-1375.

Cuzzocrea, S., Mazzon, E., Dugo, L., Genovese, T., Di Paola, R., Ruggeri, Z., . . . Puzzolo, D. (2003). Inducible nitric oxide synthase mediates bone loss in ovariectomized mice. *Endocrinology, 144*(3), 1098-1107.

Dabo, S., & Meurs, E. F. (2012). dsRNA-dependent protein kinase PKR and its role in stress, signaling and HCV infection. *Viruses, 4*(11), 2598-2635.

de Gasparo, M., Joss, U., Ramjoue, H. P., Whitebread, S. E., Haenni, H., Schenkel, L., . . . Schmidlin, J. (1987). Three new epoxy-spirolactone derivatives: Characterization in vivo and in vitro. *The Journal of Pharmacology and Experimental Therapeutics, 240*(2), 650-656.

de Gouw, H. W., Verbruggen, M. B., Twiss, I. M., & Sterk, P. J. (1999). Effect of oral L-arginine on airway hyperresponsiveness to histamine in asthma. *Thorax, 54*(11), 1033-1035.

De Vera, M. E., Taylor, B. S., Wang, Q., Shapiro, R. A., Billiar, T. R., & Geller, D. A. (1997). Dexamethasone suppresses iNOS gene expression by upregulating I-kappa B alpha and inhibiting NF-kappa B. *The American Journal of Physiology, 273*(6 Pt 1), G1290-6.

Delgado-Roche, L., Hernandez, Y., Venturi, I., Wilkins, I., & Alvarez, D. (2016). Early atherosclerosis development in female apolipoprotein E-deficient mice is associated with an increased vascular oxidative stress. *Oxidants and Antioxidants in Medical Science, 5*(1), 15-20.

Deng, C. N., Shen, L. H., & Tang, C. S. (2010). Effect of spironolactone on L-arginine/iNOS/NO pathway of aortic adventitia in spontaneously hypertensive rats. *Zhonghua Yi Xue Za Zhi, 90*(6), 424-426.

Di Rosa, M., Radomski, M., Carnuccio, R., & Moncada, S. (1990). Glucocorticoids inhibit the induction of nitric oxide synthase in macrophages. *Biochemical and Biophysical Research Communications, 172*(3), 1246-1252.

Doi, M., Shichiri, M., Katsuyama, K., Marumo, F., & Hirata, Y. (2000). Cytokine-activated p42/p44 MAP kinase is involved in inducible nitric oxide synthase gene expression independent from NF-. KAPPA. B activation in vascular smooth muscle cells. *Hypertension Research, 23*(6), 659-667.

Doherty, G. M., Lange, J. R., Langstein, H. N., Alexander, H. R., Buresh, C. M., & Norton, J. A. (1992). Evidence for IFN-gamma as a mediator of the lethality of endotoxin and tumor necrosis factor-alpha. Journal of Immunology (Baltimore, Md.: 1950), 149(5), 1666-1670.

Decker, T., & Kovarik, P. (2000). Serine phosphorylation of STATs. *Oncogene, 19*(21)

Drexler, H., & Hornig, B. (1999). Endothelial dysfunction in human disease. *Journal of Molecular and Cellular Cardiology, 31*(1), 51-60.

Druce, L., Thorpe, C., & Wilton, A. (2008). Mineralocorticoid effects due to cortisol inactivation overload explain the beneficial use of hydrocortisone in septic shock. *Medical Hypotheses, 70*(1), 56-60.

Dubois, R. N., Abramson, S. B., Crofford, L., Gupta, R. A., Simon, L. S., Van De Putte, L. B., & Lipsky, P. E. (1998). Cyclooxygenase in biology and disease. *FASEB Journal : Official Publication of the Federation of American Societies for Experimental Biology, 12*(12), 1063-1073.

Eda, M., Kuroda, T., Kaneko, S., Aoki, Y., Yamashita, M., Okumura, C., . . . Koyama, N. (2015). Synthesis and biological evaluation of cyclopentaquinoline derivatives as nonsteroidal glucocorticoid receptor antagonists. *Journal of Medicinal Chemistry, 58*(12), 4918-4926.

Edelman, I. S., Bogoroch, R., & Porter, G. A. (1963). On the mechanism of action of aldosterone on sodium transport: The role of protein synthesis. *Proceedings of the National Academy of Sciences of the United States of America, 50*, 1169-1177.

El-Refaey, H., Rajasekar, D., Abdalla, M., Calder, L., & Templeton, A. (1995). Induction of abortion with mifepristone (RU 486) and oral or vaginal misoprostol. *New England Journal of Medicine, 332*(15), 983-987.

Epstein, F. H., & Parrillo, J. E. (1993). Pathogenetic mechanisms of septic shock. *New England Journal of Medicine, 328*(20), 1471-1477.

Evans, C. H. (1995). Nitric oxide: What role does it play in inflammation and tissue destruction? *Agents and Actions.Supplements, 47*, 107-116.

Evans, T., Carpenter, A., Silva, A., & Cohen, J. (1994). Inhibition of nitric oxide synthase in experimental gram-negative sepsis. Journal of Infectious Diseases, 169(2), 343-349.

Farrell, A. J., Blake, D. R., Palmer, R. M., & Moncada, S. (1992). Increased concentrations of nitrite in synovial fluid and serum samples suggest increased nitric oxide synthesis in rheumatic diseases. *Annals of the Rheumatic Diseases, 51*(11), 1219-1222.

Fechir, M., Linker, K., Pautz, A., Hubrich, T., Forstermann, U., Rodriguez-Pascual, F., & Kleinert, H. (2005). Tristetraprolin regulates the expression of the human inducible nitric-oxide synthase gene. *Molecular Pharmacology, 67*(6), 2148-2161. doi:mol.104.008763 [pii]

Ferrero, E., & Goyert, S. M. (1988). Nucleotide sequence of the gene encoding the monocyte differentiation antigen, CD14. *Nucleic Acids Research, 16*(9), 4173.

Forstermann, U., & Sessa, W. C. (2012). Nitric oxide synthases: Regulation and function. *European Heart Journal, 33*(7), 829-37, 837a-837d. doi:10.1093/eurheartj/ehr304 [doi]

Francis, S. H., Busch, J. L., Corbin, J. D., & Sibley, D. (2010). cGMP-dependent protein kinases and cGMP phosphodiesterases in nitric oxide and cGMP action. Pharmacological Reviews, 62(3), 525-563. doi:10.1124/pr.110.002907 [doi]

Franco, L., Talamini, G., Carra, G., & Doria, D. (1999). Expression of COX-1, COX-2, and inducible nitric oxide synthase protein in human gastric antrum with helicobacter pylori infection ☆. Prostaglandins & Other Lipid Mediators, 58(1), 9-17.

Frantz, B., Klatt, T., Pang, M., Parsons, J., Rolando, A., Williams, H., . . . O'Neill, E. A. (1998). The activation state of p38 mitogen-activated protein kinase determines the efficiency of ATP competition for pyridinylimidazole inhibitor binding. *Biochemistry, 37*(39), 13846-13853.

Funk, C. D. (2001). Prostaglandins and leukotrienes: Advances in eicosanoid biology. *Science (New York, N.Y.), 294*(5548), 1871-1875. doi:10.1126/science.294.5548.1871 [doi]

Furchgott, R. F., & Zawadzki, J. V. (1980). The obligatory role of endothelial cells in the relaxation of arterial smooth muscle by acetylcholine. *Nature, 288*(5789), 373-376.

Gabriel, S. E. (2001). The epidemiology of rheumatoid arthritis. *Rheumatic Disease Clinics of North America, 27*(2), 269-281.

Gagne, D., Pons, M., & Philibert, D. (1985). RU 38486: A potent antiglucocorticoid in vitro and in vivo. *Journal of Steroid Biochemistry, 23*(3), 247-251.

ccharide. *Journal of Biological Chemistry, 272*(2), 1226-1230.

Garr, E. D. (2014). JAK/STAT signalling in the induction of the L-arginine-nitric oxide pathway in macrophages and vascular smooth muscle cells.

Geller, D. A., & Billiar, T. R. (1998). Molecular biology of nitric oxide synthases. *Cancer and Metastasis Reviews, 17*(1), 7-23.

Geller, D. A., Freeswick, P. D., Nguyen, D., Nussler, A. K., Di Silvio, M., Shapiro, R. A., . . . Billiar, T. R. (1994). Differential induction of nitric oxide synthase in hepatocytes during endotoxemia and the acute-phase response. *Archives of Surgery, 129*(2), 165-171.

Geller, D. A., Nussler, A. K., Di Silvio, M., Lowenstein, C. J., Shapiro, R. A., Wang, S. C., . . . Billiar, T. R. (1993). Cytokines, endotoxin, and glucocorticoids regulate the expression of inducible nitric oxide synthase in hepatocytes. *Proceedings of the National Academy of Sciences of the United States of America, 90*(2), 522-526.

Ghosh, S., May, M. J., & Kopp, E. B. (1998). NF-κB and rel proteins: Evolutionarily conserved mediators of immune responses. *Annual Review of Immunology, 16*(1), 225-260.

Gilliver, S. C. (2010). Sex steroids as inflammatory regulators. The Journal of Steroid Biochemistry and Molecular Biology, 120(2), 105-115.

Ginnan, R., Guikema, B. J., Singer, H. A., & Jourd'heuil, D. (2006). PKC-delta mediates activation of ERK1/2 and induction of iNOS by IL-1beta in vascular smooth muscle cells. American Journal of Physiology.Cell Physiology, 290(6), C1583-91. doi:00390.2005 [pii]

Gioannini, T. L., Teghanemt, A., Zhang, D., Coussens, N. P., Dockstader, W., Ramaswamy, S., & Weiss, J. P. (2004). Isolation of an endotoxin-MD-2 complex that produces toll-like receptor 4-dependent cell activation at picomolar concentrations. *Proceedings of the National Academy of Sciences of the United States of America, 101*(12), 4186-4191. doi:10.1073/pnas.0306906101 [doi]

Gkaliagkousi, E., Ritter, J., & Ferro, A. (2007). Platelet-derived nitric oxide signaling and regulation. *Circulation Research, 101*(7), 654-662. doi:101/7/654 [pii]

Godfrey, V., Martin, A., Struthers, A., & Lyles, G. (2011). Effects of aldosterone and related steroids on LPS-induced increased expression of inducible NOS in rat aortic smooth muscle cells. *British Journal of Pharmacology, 164*(8), 2003-2014.

Goel, S., JHA, G., AGarwal, N., Singh, T., & Soren, B. (2014). Role of L arginine in treatment of osteoporosis. *International Journal of Orthopaedics, 1*(4)

Goh, K. C., deVeer, M. J., & Williams, B. R. (2000). The protein kinase PKR is required for p38 MAPK activation and the innate immune response to bacterial endotoxin. *The EMBO Journal, 19*(16), 4292-4297.

Golde, S., Coles, A., Lindquist, J. A., & Compston, A. (2003). Decreased iNOS synthesis mediates dexamethasone-induced protection of neurons from inflammatory injury in vitro. *European Journal of Neuroscience, 18*(9), 2527-2537.

Goldstein, A. S. (2001). Effect of seeding osteoprogenitor cells as dense clusters on cell growth and differentiation. *Tissue Engineering, 7*(6), 817-827.

Grabowski, P. S., England, A. J., Dykhuizen, R., Copland, M., Benjamin, N., Reid, D. M., & Ralston, S. H. (1996). Elevated nitric oxide production in rheumatoid arthritis: Detection using the fasting urinary nitrate: Creatinine ratio. *Arthritis & Rheumatism, 39*(4), 643-647.

Grabowski, P. S., Macpherson, H., & Ralston, S. H. (1996). Nitric oxide production in cells derived from the human joint. *British Journal of Rheumatology, 35*(3), 207-212.

Greenlund, A. C., Farrar, M. A., Viviano, B. L., & Schreiber, R. D. (1994). Ligand-induced IFN gamma receptor tyrosine phosphorylation couples the receptor to its signal transduction system (p91). *The EMBO Journal, 13*(7), 1591-1600.

Groeneweg, F. L., Karst, H., de Kloet, E. R., & Joels, M. (2011). Rapid non-genomic effects of corticosteroids and their role in the central stress response. *The Journal of Endocrinology, 209*(2), 153-167. doi:10.1530/JOE-10-0472 [doi]

Grosser, T., Fries, S., & FitzGerald, G. A. (2006). Biological basis for the cardiovascular consequences of COX-2 inhibition: Therapeutic challenges and opportunities. The Journal of Clinical Investigation, 116(1), 4-15. doi:10.1172/JCI27291 [doi]

Gustafsson, L., Leone, A., Persson, M., Wiklund, N., & Moncada, S. (1991). Endogenous nitric oxide is present in the exhaled air of rabbits, guinea pigs and humans. *Biochemical and Biophysical Research Communications, 181*(2), 852-857.

Hafezi-Moghadam, A., Simoncini, T., Yang, Z., Limbourg, F. P., Plumier, J., Rebsamen, M. C., . . . Prorock, A. J. (2002). Acute cardiovascular protective effects of corticosteroids are mediated by non-transcriptional activation of endothelial nitric oxide synthase. *Nature Medicine, 8*(5), 473-479.

Hamid, Q., Springall, D. R., Polak, J., Riveros-Moreno, V., Chanez, P., Bousquet, J., . . . Redington, A. (1993). Induction of nitric oxide synthase in asthma. *The Lancet, 342*(8886), 1510-1513.

Hammermann, R., Dreissig, M. D., Mossner, J., Fuhrmann, M., Berrino, L., Gothert, M., & Racke, K. (2000). Nuclear factor-kappaB mediates simultaneous induction of inducible nitric-oxide synthase and up-regulation of the cationic amino acid transporter CAT-2B in rat alveolar macrophages. *Molecular Pharmacology, 58*(6), 1294-1302.

Han, E. D., MacFarlane, R. C., Mulligan, A. N., Scafidi, J., & Davis, A. E.,3rd. (2002). Increased vascular permeability in C1 inhibitor-deficient mice mediated by the bradykinin type 2 receptor. *The Journal of Clinical Investigation, 109*(8), 1057-1063. doi:10.1172/JCI14211 [doi]

Hansel, T. T., Kharitonov, S. A., Donnelly, L. E., Erin, E. M., Currie, M. G., Moore, W. M., . . . Barnes, P. J. (2003). A selective inhibitor of inducible nitric oxide synthase inhibits exhaled breath nitric oxide in healthy volunteers and asthmatics. *FASEB Journal : Official Publication of the Federation of American Societies for Experimental Biology, 17*(10), 1298-1300. doi:10.1096/fj.02-0633fje [doi]

Harding, H. P., Novoa, I., Zhang, Y., Zeng, H., Wek, R., Schapira, M., & Ron, D. (2000). Regulated translation initiation controls stress-induced gene expression in mammalian cells. *Molecular Cell, 6*(5), 1099-1108.

Harizi, H., Mormède, P., & Corcuff, J. (2008). Inter-strain differences in glucocorticoid and mineralocorticoid effects on macrophage and lymphocyte functions in mice. *Journal of Neuroimmunology, 204*(1), 38-42.

Hart, C. M. (1999). Nitric oxide in adult lung disease. *CHEST Journal, 115*(5), 1407-1417.

Hattori, Y., Hattori, S., & Kasai, K. (2003). Lipopolysaccharide activates akt in vascular smooth muscle cells resulting in induction of inducible nitric oxide synthase through nuclear factor-kappa B activation. *European Journal of Pharmacology, 481*(2), 153-158.

Hattori, Y., Kasai, K., & Gross, S. S. (1999). Cationic amino acid transporter gene expression in cultured vascular smooth muscle cells and in rats. *The American Journal of Physiology, 276*(6 Pt 2), H2020-8.

Hausenloy, D. J., & Yellon, D. M. (2009). Cardioprotective growth factors. *Cardiovascular Research, 83*(2), 179-194. doi:10.1093/cvr/cvp062 [doi]

Haziot, A., Ferrero, E., Köntgen, F., Hijiya, N., Yamamoto, S., Silver, J., . . . Goyert, S. M. (1996). Resistance to endotoxin shock and reduced dissemination of gram-negative bacteria in CD14-deficient mice. *Immunity, 4*(4), 407-414.

Haziot, A., Lin, X. Y., Zhang, F., & Goyert, S. M. (1998). Cutting edge: The induction of acute phase proteins by lipopolysaccharide uses a novel pathway that is CD14-independent. *The Journal of Immunology, 160*(6), 2570-2572.

Hecker, M., Cattaruzza, M., & Wagner, A. H. (1999). Regulation of inducible nitric oxide synthase gene expression in vascular smooth muscle cells. *General Pharmacology: The Vascular System, 32*(1), 9-16.

Heim, M. H., Kerr, I. M., Stark, G. R., & Darnell Jr, J. E. (1995). Contribution of STAT SH2 groups to specific interferon signaling by the jak-STAT pathway. *Science, 267*(5202), 1347.

Hess, J., Angel, P., & Schorpp-Kistner, M. (2004). AP-1 subunits: Quarrel and harmony among siblings. *Journal of Cell Science, 117*(Pt 25), 5965-5973. doi:117/25/5965 [pii]

Hesslinger, C., Strub, A., Boer, R., Ulrich, W., Lehner, M., & Braun, C. (2009). Inhibition of inducible nitric oxide synthase in respiratory diseases. *Biochemical Society Transactions, 37*(4), 886.

Hilliquin, P., Borderie, D., Hernvann, A., Menkes, C., & Ekindjian, O. (1997). Nitric oxide as S-nitrosoproteins in rheumatoid arthritis. *Arthritis & Rheumatism, 40*(8), 1512-1517.

Hofmann, W., & Goger, D. (1976). A simple method for differentiating vascular smooth muscle cells and fibroblasts in tissue culture. *Virchows Archiv A, 370*(1), 77-83.

Hollenbach, E., Neumann, M., Vieth, M., Roessner, A., Malfertheiner, P., & Naumann, M. (2004). Inhibition of p38 MAP kinase- and RICK/NF-kappaB-signaling suppresses inflammatory bowel

disease. *FASEB Journal : Official Publication of the Federation of American Societies for Experimental Biology, 18*(13), 1550-1552. doi:10.1096/fj.04-1642fje [doi]

Hu, Q., Cho, M. S., Thiagarajan, P., Aung, F. M., Sood, A. K., & Afshar-Kharghan, V. (2017). A small amount of cyclooxygenase 2 (COX2) is constitutively expressed in platelets. Platelets, 28(1), 99-102.

Hu, Y., Chan, E., Wang, S. X., & Li, B. (2003). Activation of p38 mitogen-activated protein kinase is required for osteoblast differentiation. *Endocrinology, 144*(5), 2068-2074.

Hu, X., Li, W. P., Meng, C., & Ivashkiv, L. B. (2003). Inhibition of IFN-gamma signaling by glucocorticoids. *Journal of Immunology (Baltimore, Md.: 1950), 170*(9), 4833-4839.

Hughes, B. R., & Cunliffe, W. (1988). Tolerance of spironolactone. *British Journal of Dermatology, 118*(5), 687-691.

Ialenti, A., Moncada, S., & Rosa, M. (1993). Modulation of adjuvant arthritis by endogenous nitric oxide. *British Journal of Pharmacology, 110*(2), 701-706.

Ignarro, L. J., Buga, G. M., Wood, K. S., Byrns, R. E., & Chaudhuri, G. (1987). Endothelium-derived relaxing factor produced and released from artery and vein is nitric oxide. *Proceedings of the National Academy of Sciences of the United States of America, 84*(24), 9265-9269.

Inder, W. J., Jang, C., Obeyesekere, V. R., & Alford, F. P. (2010). Dexamethasone administration inhibits skeletal muscle expression of the androgen receptor and IGF-1–implications for steroid-induced myopathy. *Clinical Endocrinology, 73*(1), 126-132.

Jaffrey, S. R., & Snyder, S. H. (1995). Nitric oxide: A neural messenger. *Annual Review of Cell and Developmental Biology, 11*(1), 417-440.

Jaisser, F., & Farman, N. (2016). Emerging roles of the mineralocorticoid receptor in pathology: Toward new paradigms in clinical pharmacology. *Pharmacological Reviews, 68*(1), 49-75. doi:10.1124/pr.115.011106 [doi]

Janeway Jr, C. A., & Medzhitov, R. (2002). Innate immune recognition. *Annual Review of Immunology, 20*(1), 197-216.

Jeon, Y. J., Han, S. H., Lee, Y. W., Yea, S. S., & Yang, K. (1998). Inhibition of NF-κB/Rel nuclear translocation by dexamethasone: Mechanism for the inhibition of iNOS gene expression. *IUBMB Life, 45*(3), 435-441.

Jin, R. C., & Loscalzo, J. (2010). Vascular nitric oxide: Formation and function. *Journal of Blood Medicine, 2010*(1), 147-162. doi:10.2147/JBM.S7000 [doi]

Johanssen, S., & Allolio, B. (2007). Mifepristone (RU 486) in cushing's syndrome. *European Journal of Endocrinology / European Federation of Endocrine Societies, 157*(5), 561-569. doi:157/5/561 [pii]

Johnson, G. V., & Bailey, C. D. (2003). The p38 MAP kinase signaling pathway in Alzheimer's disease. *Experimental Neurology, 183*(2), 263-268.

Juliet, P. A., Hayashi, T., Daigo, S., Matsui-Hirai, H., Miyazaki, A., Fukatsu, A., . . . Ignarro, L. J. (2004). Combined effect of testosterone and apocynin on nitric oxide and superoxide production in PMA-differentiated THP-1 cells. *Biochimica Et Biophysica Acta (BBA)-Molecular Cell Research, 1693*(3), 185-191.

Jung-Testas, I., & Baulieu, E. (1983). Inhibition of glucocorticosteroid action in cultured L-929 mouse fibroblasts by RU 486, a new anti-glucocorticosteroid of high affinity for the glucocorticosteroid receptor. *Experimental Cell Research, 147*(1), 177-182.

Kadekaro, M. (2004). Nitric oxide modulation of the hypothalamo-neurohypophyseal system. *Brazilian Journal of Medical and Biological Research, 37*(4), 441-450.

Kanno, K., Hirata, Y., Imai, T., & Marumo, F. (1993). Induction of nitric oxide synthase gene by interleukin in vascular smooth muscle cells. *Hypertension, 22*(1), 34-39.

Kao, Y. J., Piedra, P. A., Larsen, G. L., & Colasurdo, G. N. (2001). Induction and regulation of nitric oxide synthase in airway epithelial cells by respiratory syncytial virus. *American Journal of Respiratory and Critical Care Medicine, 163*(2), 532-539.

Karalis, K., Goodwin, G., & Majzoub, J. A. (1996). Cortisol blockade of progesterone: A possible molecular mechanism involved in the initiation of human labor. *Obstetrical & Gynecological Survey, 51*(11), 669-671.

Karpuzoglu, E., & Ahmed, S. A. (2006). Estrogen regulation of nitric oxide and inducible nitric oxide synthase (iNOS) in immune cells: Implications for immunity, autoimmune diseases, and apoptosis. *Nitric Oxide, 15*(3), 177-186.

Kassel, O., Sancono, A., Krätzschmar, J., Kreft, B., Stassen, M., & Cato, A. C. (2001). Glucocorticoids inhibit MAP kinase via increased expression and decreased degradation of MKP-1. *The EMBO Journal, 20*(24), 7108-7116.

Katsuyama, K., Shichiri, M., Kato, H., Imai, T., Marumo, F., & Hirata, Y. (1999). Differential inhibitory actions by glucocorticoid and aspirin on cytokine-induced nitric oxide production in vascular smooth muscle cells 1. *Endocrinology, 140*(5), 2183-2190.

Kawai, T., & Akira, S. (2007). Signaling to NF-κB by toll-like receptors. *Trends in Molecular Medicine, 13*(11), 460-469.

Keränen, T., Moilanen, E., & Korhonen, R. (2017). Suppression of cytokine production by glucocorticoids is mediated by MKP-1 in human lung epithelial cells. *Inflammation Research, 66*(5), 441-449.

Khosla, S., Melton, L. J., & Riggs, B. L. (2011). The unitary model for estrogen deficiency and the pathogenesis of osteoporosis: Is a revision needed? *Journal of Bone and Mineral Research, 26*(3), 441-451.

Kimball, S. R. (1999). Eukaryotic initiation factor eIF2. *The International Journal of Biochemistry & Cell Biology, 31*(1), 25-29.

King, C. J., Tytgat, S., Delude, R. L., & Fink, M. P. (1999). Ileal mucosal oxygen consumption is decreased in endotoxemic rats but is restored toward normal by treatment with aminoguanidine. *Critical Care Medicine, 27*(11), 2518-2524.

King, E. M., Holden, N. S., Gong, W., Rider, C. F., & Newton, R. (2009). Inhibition of NF-kappaB-dependent transcription by MKP-1: Transcriptional repression by glucocorticoids occurring via p38 MAPK. *The Journal of Biological Chemistry, 284*(39), 26803-26815. doi:10.1074/jbc.M109.028381 [doi]

Kirkebøen, K., & Strand, Ø. (1999). The role of nitric oxide in sepsis–an overview. *Acta Anaesthesiologica Scandinavica, 43*(3), 275-288.

Kleinert, H., Schwarz, P. M., & Förstermann, U. (2003). Regulation of the expression of inducible nitric oxide synthase. *Biological Chemistry, 384*(10-11), 1343-1364.

Kleinert, H., Euchenhofer, C., Ihrig-Biedert, I., & Forstermann, U. (1996). Glucocorticoids inhibit the induction of nitric oxide synthase II by down-regulating cytokine-induced activity of transcription factor nuclear factor-kappa B. *Molecular Pharmacology, 49*(1), 15-21.

Knowles, R. G., & Moncada, S. (1994). Nitric oxide synthases in mammals. *The Biochemical Journal, 298 (Pt 2)*(Pt 2), 249-258.

Knowles, R., Salter, M., Brooks, S., & Moncada, S. (1990). Anti-inflammatory glucocorticoids inhibit the induction by endotoxin of nitric oxide synthase in the lung, liver and aorta of the rat. Biochemical and Biophysical Research Communications, 172(3), 1042-1048.

Kojda, G., & Kottenberg, K. (1999). Regulation of basal myocardial function by NO. *Cardiovascular Research, 41*(3), 514-523. doi:S0008-6363(98)00314-9 [pii]

Komers, R., & Anderson, S. (2003). Paradoxes of nitric oxide in the diabetic kidney. *American Journal of Physiology.Renal Physiology, 284*(6), F1121-37. doi:10.1152/ajprenal.00265.2002 [doi]

Korhonen, R., Lahti, A., Hamalainen, M., Kankaanranta, H., & Moilanen, E. (2002). Dexamethasone inhibits inducible nitric-oxide synthase expression and nitric oxide production by destabilizing mRNA in lipopolysaccharide-treated macrophages. *Molecular Pharmacology, 62*(3), 698-704.

Kuhr, F., Lowry, J., Zhang, Y., Brovkovych, V., & Skidgel, R. A. (2010). Differential regulation of inducible and endothelial nitric oxide synthase by kinin B1 and B2 receptors. *Neuropeptides, 44*(2), 145-154.

Kumar, S., Jiang, M. S., Adams, J. L., & Lee, J. C. (1999). Pyridinylimidazole compound SB 203580 inhibits the activity but not the activation of p38 mitogen-activated protein kinase. *Biochemical and Biophysical Research Communications, 263*(3), 825-831.

Kumar, A., Haque, J., Lacoste, J., Hiscott, J., & Williams, B. R. (1994). Double-stranded RNA-dependent protein kinase activates transcription factor NF-kappa B by phosphorylating I kappa B. *Proceedings of the National Academy of Sciences of the United States of America, 91*(14), 6288-6292.

Kumar, A., Yang, Y. L., Flati, V., Der, S., Kadereit, S., Deb, A., . . . Williams, B. R. (1997). Deficient cytokine signaling in mouse embryo fibroblasts with a targeted deletion in the PKR gene: Role of IRF-1 and NF-kappaB. *The EMBO Journal, 16*(2), 406-416. doi:10.1093/emboj/16.2.406 [doi]

Kunkel, S. L., Spengler, M., May, M. A., Spengler, R., Larrick, J., & Remick, D. (1988). Prostaglandin E2 regulates macrophage-derived tumor necrosis factor gene expression. *The Journal of Biological Chemistry, 263*(11), 5380-5384.

Kunz, D., Walker, G., Eberhardt, W., & Pfeilschifter, J. (1996). Molecular mechanisms of dexamethasone inhibition of nitric oxide synthase expression in interleukin 1 beta-stimulated mesangial cells: Evidence for the involvement of transcriptional and posttranscriptional regulation. *Proceedings of the National Academy of Sciences of the United States of America, 93*(1), 255-259.

Kuzkaya, N., Weissmann, N., Harrison, D. G., & Dikalov, S. (2003). Interactions of peroxynitrite, tetrahydrobiopterin, ascorbic acid, and thiols: Implications for uncoupling endothelial nitric-oxide synthase. *The Journal of Biological Chemistry, 278*(25), 22546-22554. doi:10.1074/jbc.M302227200 [doi]

Lali, F. V., Hunt, A. E., Turner, S. J., & Foxwell, B. M. (2000). The pyridinyl imidazole inhibitor SB203580 blocks phosphoinositide-dependent protein kinase activity, protein kinase B phosphorylation, and retinoblastoma hyperphosphorylation in interleukin-2-stimulated T cells independently of p38 mitogen-activated protein kinase. *Journal of Biological Chemistry, 275*(10), 7395-7402.

Lali, F. V., Hunt, A. E., Turner, S. J., & Foxwell, B. M. (2000). The pyridinyl imidazole inhibitor SB203580 blocks phosphoinositide-dependent protein kinase activity, protein kinase B phosphorylation, and retinoblastoma hyperphosphorylation in interleukin-2-stimulated T cells

independently of p38 mitogen-activated protein kinase. *Journal of Biological Chemistry, 275*(10), 7395-7402.

Lamon, B. D., & Hajjar, D. P. (2008). Inflammation at the molecular interface of atherogenesis: An anthropological journey. *The American Journal of Pathology, 173*(5), 1253-1264.

Lamon, B. D., Upmacis, R. K., Deeb, R. S., Koyuncu, H., & Hajjar, D. P. (2010). Inducible nitric oxide synthase gene deletion exaggerates MAPK-mediated cyclooxygenase-2 induction by inflammatory stimuli. *American Journal of Physiology.Heart and Circulatory Physiology, 299*(3), H613-23. doi:10.1152/ajpheart.00144.2010 [doi]

Lan, N. C., Graham, B., Bartter, F. C., & Baxter, J. D. (1982). Binding of steroids to mineralocorticoid receptors: Implications for in vivo occupancy by glucocorticoids*. *The Journal of Clinical Endocrinology & Metabolism, 54*(2), 332-342.

Lasa, M., Abraham, S. M., Boucheron, C., Saklatvala, J., & Clark, A. R. (2002). Dexamethasone causes sustained expression of mitogen-activated protein kinase (MAPK) phosphatase 1 and phosphatase-mediated inhibition of MAPK p38. *Molecular and Cellular Biology, 22*(22), 7802-7811.

Laskin, D. L., & Pendino, K. J. (1995). Macrophages and inflammatory mediators in tissue injury. *Annual Review of Pharmacology and Toxicology, 35*(1), 655-677.

Lavista Llanos, S., & Roldan, A. (1999). Effect of dexamethasone on nitric oxide (NO.) production by cultured astrocytes. *Biocell : Official Journal of the Sociedades Latinoamericanas De Microscopia Electronica ...Et.Al, 23*(1), 29-35.

Lee, J., Ryu, H., Ferrante, R. J., Morris, S. M.,Jr, & Ratan, R. R. (2003). Translational control of inducible nitric oxide synthase expression by arginine can explain the arginine paradox.

Proceedings of the National Academy of Sciences of the United States of America, 100(8), 4843-4848. doi:10.1073/pnas.0735876100 [doi]

Lehtimaki, L., Kankaanranta, H., Saarelainen, S., Turjanmaa, V., & Moilanen, E. (2001). Inhaled fluticasone decreases bronchial but not alveolar nitric oxide output in asthma. *The European Respiratory Journal, 18*(4), 635-639.

Lei, B., Mace, B., Dawson, H. N., Warner, D. S., Laskowitz, D. T., & James, M. L. (2014). Anti-inflammatory effects of progesterone in lipopolysaccharide-stimulated BV-2 microglia. *PloS One, 9*(7), e103969.

Leurs, R., Smit, M., & Timmerman, H. (1995). Molecular pharmacological aspects of histamine receptors. *Pharmacology & Therapeutics, 66*(3), 413-463.

Lewis, T. (1942). Pain macmillan. *New York, 192*

Lieb, K., Engels, S., & Fiebich, B. L. (2003). Inhibition of LPS-induced iNOS and NO synthesis in primary rat microglial cells. *Neurochemistry International, 42*(2), 131-137.

Lin, C., Tsai, C., Huang, W., Wang, C., Tseng, H., Wang, Y., . . . Cheng, Y. (2008). IFN-γ synergizes with LPS to induce nitric oxide biosynthesis through glycogen synthase kinase-3-inhibited IL-10. *Journal of Cellular Biochemistry, 105*(3), 746-755.

Lin, G., Chow, S., Lin, J., Wang, G., Lue, T. F., & Lin, C. (2004). Effect of cell passage and density on protein kinase G expression and activation in vascular smooth muscle cells. *Journal of Cellular Biochemistry, 92*(1), 104-112.

Linehan, J. D., Kolios, G., Valatas, V., Robertson, D. A., & Westwick, J. (2005). Effect of corticosteroids on nitric oxide production in inflammatory bowel disease: Are leukocytes the site of action?

American Journal of Physiology.Gastrointestinal and Liver Physiology, 288(2), G261-7. doi:10.1152/ajpgi.00336.2004 [doi]

Liu, J., Hong, S., Feng, Z., Xin, Y., Wang, Q., Fu, J., . . . Yin, Z. (2010). Regulation of lipopolysaccharide-induced inflammatory response by heat shock protein 27 in THP-1 cells. *Cellular Immunology, 264*(2), 127-134.

Lombardi, G., Zarrilli, S., Colao, A., Paesano, L., Di Somma, C., Rossi, F., & De Rosa, M. (2001). Estrogens and health in males. *Molecular and Cellular Endocrinology, 178*(1), 51-55.

Loscalzo, J. (2001). Nitric oxide insufficiency, platelet activation, and arterial thrombosis. *Circulation Research, 88*(8), 756-762.

Lu, Y., Yeh, W., & Ohashi, P. S. (2008). LPS/TLR4 signal transduction pathway. *Cytokine, 42*(2), 145-151.

MacGlashan, D. (2003). Histamine: A mediator of inflammation. *Journal of Allergy and Clinical Immunology, 112*(4), S53-S59.

MacLeod, C., & Kakuda, D. (1996). Regulation of CAT: Cationic amino acid transporter gene expression. *Amino Acids, 11*(2), 171-191.

MacMicking, J., Xie, Q., & Nathan, C. (1997). Nitric oxide and macrophage function. *Annual Review of Immunology, 15*(1), 323-350.

Madeddu, P., Emanueli, C., Gaspa, L., Salis, B., Milia, A. F., Chao, L., & Chao, J. (1999). Role of the bradykinin B 2 receptor in the maturation of blood pressure phenotype: Lesson from transgenic and knockout mice. *Immunopharmacology, 44*(1), 9-13

McKay, L. I., & Cidlowski, J. A. (1998). Cross-talk between nuclear factor-κB and the steroid hormone receptors: Mechanisms of mutual antagonism. *Molecular Endocrinology, 12*(1), 45-56.

Maggi, L. B., Heitmeier, M. R., Scheuner, D., Kaufman, R. J., Buller, R. M. L., & Corbett, J. A. (2000). Potential role of PKR in double-stranded RNA-induced macrophage activation. *The EMBO Journal, 19*(14), 3630-3638.

Manetsch, M., Rahman, M. M., Patel, B. S., Ramsay, E. E., Rumzhum, N. N., Alkhouri, H., . . . Ammit, A. J. (2013). Long-acting β 2-agonists increase fluticasone propionate-induced mitogen-activated protein kinase phosphatase 1 (MKP-1) in airway smooth muscle cells. *PloS One, 8*(3), e59635.

Mao, J., Regelson, W., & Kalimi, M. (1992). Molecular mechanism of RU 486 action: A review. *Molecular and Cellular Biochemistry, 109*(1), 1-8.

Marnett, L. J. (2009). The COXIB experience: A look in the rearview mirror. *Annual Review of Pharmacology and Toxicology, 49*, 265-290.

Matejovic, M., Krouzecky, A., Martinkova, V., Rokyta Jr, R., Kralova, H., Treska, V., . . . Novak, I. (2004). Selective inducible nitric oxide synthase inhibition during long-term hyperdynamic porcine bacteremia. *Shock, 21*(5), 458-465.

Matsumura, M., Kakishita, H., Suzuki, M., Banba, N., & Hattori, Y. (2001). Dexamethasone suppresses iNOS gene expression by inhibiting NF-κB in vascular smooth muscle cells. *Life Sciences, 69*(9), 1067-1077.

Maurer, M., Bader, M., Bas, M., Bossi, F., Cicardi, M., Cugno, M., . . . Leeb-Lundberg, F. (2011). New topics in bradykinin research. *Allergy, 66*(11), 1397-1406.

Maurice, D. H., & Haslam, R. J. (1990). Molecular basis of the synergistic inhibition of platelet function by nitrovasodilators and activators of adenylate cyclase: Inhibition of cyclic AMP breakdown by cyclic GMP. *Molecular Pharmacology, 37*(5), 671-681.

McCartney-Francis, N., Allen, J. B., Mizel, D. E., Albina, J. E., Xie, Q. W., Nathan, C. F., & Wahl, S. M. (1993). Suppression of arthritis by an inhibitor of nitric oxide synthase. *The Journal of Experimental Medicine, 178*(2), 749-754.

McGuire, V. A., Gray, A., Monk, C. E., Santos, S. G., Lee, K., Aubareda, A., . . . Arthur, J. S. (2013). Cross talk between the akt and p38alpha pathways in macrophages downstream of toll-like receptor signaling. *Molecular and Cellular Biology, 33*(21), 4152-4165. doi:10.1128/MCB.01691-12 [doi]

McMahon, S. B., Bennett, D. L., & Bevan, S. (2006). Inflammatory mediators and modulators of pain. *Wall and Melzack's Textbook of Pain, 5*, 49-72.

McManus, L. M., & Pinckard, R. N. (2000). PAF, a putative mediator of oral inflammation. *Critical Reviews in Oral Biology and Medicine : An Official Publication of the American Association of Oral Biologists, 11*(2), 240-258.

Medzhitov, R., Preston-Hurlburt, P., & Janeway, C. A. (1997). A human homologue of the drosophila toll protein signals activation of adaptive immunity. *Nature, 388*(6640), 394-397.

Mendelsohn, M. E., O'Neill, S., George, D., & Loscalzo, J. (1990). Inhibition of fibrinogen binding to human platelets by S-nitroso-N-acetylcysteine. *The Journal of Biological Chemistry, 265*(31), 19028-19034.

Messmer, U. K., & Brune, B. (1996). Nitric oxide-induced apoptosis: P53-dependent and p53-independent signalling pathways. *The Biochemical Journal, 319 (Pt 1)*(Pt 1), 299-305.

Messmer, U. K., Lapetina, E. G., & Brune, B. (1995). Nitric oxide-induced apoptosis in RAW 264.7 macrophages is antagonized by protein kinase C- and protein kinase A-activating compounds. *Molecular Pharmacology, 47*(4), 757-765.

Michelson, A. D., Benoit, S. E., Furman, M. I., Breckwoldt, W. L., Rohrer, M. J., Barnard, M. R., & Loscalzo, J. (1996). Effects of nitric oxide/EDRF on platelet surface glycoproteins. *The American Journal of Physiology, 270*(5 Pt 2), H1640-8.

Molina-Holgado, F., Grencis, R., & Rothwell, N. J. (2001). Actions of exogenous and endogenous IL-10 on glial responses to bacterial LPS/cytokines. *Glia, 33*(2), 97-106.

Moncada, S., & Higgs, E. (2006). The discovery of nitric oxide and its role in vascular biology. *British Journal of Pharmacology, 147*(S1), S193-S201.

Moro, M. A., Russel, R. J., Cellek, S., Lizasoain, I., Su, Y., Darley-Usmar, V. M., . . . Moncada, S. (1996). cGMP mediates the vascular and platelet actions of nitric oxide: Confirmation using an inhibitor of the soluble guanylyl cyclase. *Proceedings of the National Academy of Sciences of the United States of America, 93*(4), 1480-1485.

Mullis, K., Faloona, F., Scharf, S., Saiki, R., Horn, G., & Erlich, H. (1986). Specific enzymatic amplification of DNA in vitro: The polymerase chain reaction. *Cold Spring Harbor Symposia on Quantitative Biology, 51 Pt 1*, 263-273.

Muroi, M., Ohnishi, T., & Tanamoto, K. (2002). Regions of the mouse CD14 molecule required for toll-like receptor 2-and 4-mediated activation of NF-κB. *Journal of Biological Chemistry, 277*(44), 42372-42379.

Nagai, Y., Akashi, S., Nagafuku, M., Ogata, M., Iwakura, Y., Akira, S., . . . Miyake, K. (2002). Essential role of MD-2 in LPS responsiveness and TLR4 distribution. *Nature Immunology, 3*(7), 667-672.

Newton, R. (2000). Molecular mechanisms of glucocorticoid action: What is important? *Thorax, 55*(7), 603-613.

Newton, R., & Holden, N. S. (2007). Separating transrepression and transactivation: A distressing divorce for the glucocorticoid receptor? *Molecular Pharmacology, 72*(4), 799-809. doi:mol.107.038794 [pii]

Nicoletti, V. G., Caruso, A., Tendl, E. A., Privitera, A., Console, A., Calabrese, V., . . . Stella, A. M. G. (1998). Effect of nitric oxide synthase induction on the expression of mitochondrial respiratory chain enzyme subunits in mixed cortical and astroglial cell cultures. *Biochimie, 80*(10), 871-881.

Nikolaeva, S., Bachteeva, V., Fock, E., Herterich, S., Lavrova, E., Borodkina, A., . . . Parnova, R. (2012). Frog urinary bladder epithelial cells express TLR4 and respond to bacterial LPS by increase of iNOS expression and L-arginine uptake. *American Journal of Physiology.Regulatory, Integrative and Comparative Physiology, 303*(10), R1042-52. doi:10.1152/ajpregu.00045.2012 [doi]

Nin, N., Cassina, A., Boggia, J., Alfonso, E., Botti, H., Peluffo, G., . . . Rubbo, H. (2004). Septic diaphragmatic dysfunction is prevented by mn (III) porphyrin therapy and inducible nitric oxide synthase inhibition. *Intensive Care Medicine, 30*(12), 2271-2278.

Nishida, K., Doi, T., & Inoue, H. (2000). The role of nitric oxide in arthritic joints: A therapeutic target? *Modern Rheumatology, 10*(2), 63-67.

Oakley, R. H., & Cidlowski, J. A. (2013). The biology of the glucocorticoid receptor: New signaling mechanisms in health and disease. *Journal of Allergy and Clinical Immunology, 132*(5), 1033-1044.

O'Neill, L. A. (2006). How toll-like receptors signal: What we know and what we don't know. *Current Opinion in Immunology, 18*(1), 3-9.

Ozaki, T., Habara, K., Matsui, K., Kaibori, M., Kwon, A. H., Ito, S., . . . Okumura, T. (2010). Dexamethasone inhibits the induction of iNOS gene expression through destabilization of its mRNA in proinflammatory cytokine-stimulated hepatocytes. *Shock (Augusta, Ga.), 33*(1), 64-69. doi:10.1097/SHK.0b013e3181a7fd74 [doi]

Palmer, R., Hickery, M., Charles, I., Moncada, S., & Bayliss, M. (1993). Induction of nitric oxide synthase in human chondrocytes. *Biochemical and Biophysical Research Communications, 193*(1), 398-405.

Paludan, S. (1998). Interleukin-4 and intefferon-�: The quintessence of a mutual antagonistic relationship. *Scandinavian Journal of Immunology, 48*, 459-468.

Paoliello-Paschoalato, A., Oliveira, S., & Cunha, F. (2005). Interleukin 4 induces the expression of inducible nitric oxide synthase in eosinophils. *Cytokine, 30*(3), 116-124.

Parmentier, R., Ohtsu, H., Djebbara-Hannas, Z., Valatx, J. L., Watanabe, T., & Lin, J. S. (2002). Anatomical, physiological, and pharmacological characteristics of histidine decarboxylase knock-out mice: Evidence for the role of brain histamine in behavioral and sleep-wake control. *The Journal of Neuroscience : The Official Journal of the Society for Neuroscience, 22*(17), 7695-7711. doi:22/17/7695 [pii]

Parvez, T. (2004). Postmenopausal osteoporosis. *Correspondance,*

Patel, R., Attur, M., Dave, M., Kumar, S., Lee, J., Abramson, S., & Amin, A. (1999). Regulation of nitric oxide and prostaglandin E2 production by CSAIDSTM (SB203580) in murine macrophages and bovine chondrocytes stimulated with LPS. *Inflammation Research, 48*(6), 337-343.

Pérez-Rodríguez, R., Roncero, C., Oliván, A. M., González, M. P., & Oset-Gasque, M. J. (2009). Signaling mechanisms of interferon gamma induced apoptosis in chromaffin cells: Involvement of nNOS, iNOS, and NFκB. *Journal of Neurochemistry, 108*(4), 1083-1096.

Pervin, S., Singh, R., Hernandez, E., Wu, G., & Chaudhuri, G. (2007). Nitric oxide in physiologic concentrations targets the translational machinery to increase the proliferation of human breast cancer cells: Involvement of mammalian target of rapamycin/eIF4E pathway. *Cancer Research, 67*(1), 289-299. doi:67/1/289 [pii]

Petros, A., Lamb, G., Leone, A., Moncada, S., Bennett, D., & Vallance, P. (1994). Effects of a nitric oxide synthase inhibitor in humans with septic shock. *Cardiovascular Research, 28*(1), 34-39.

Pitt, B., Remme, W., Zannad, F., Neaton, J., Martinez, F., Roniker, B., . . . Gatlin, M. (2003). Eplerenone, a selective aldosterone blocker, in patients with left ventricular dysfunction after myocardial infarction. *New England Journal of Medicine, 348*(14), 1309-1321.

Poltorak, A., He, X., Smirnova, I., Liu, M. Y., Van Huffel, C., Du, X., . . . Beutler, B. (1998). Defective LPS signaling in C3H/HeJ and C57BL/10ScCr mice: Mutations in Tlr4 gene. *Science (New York, N.Y.), 282*(5396), 2085-2088.

Portela, V. M., Zamberlam, G., & Price, C. A. (2010). Cell plating density alters the ratio of estrogenic to progestagenic enzyme gene expression in cultured granulosa cells. Fertility and Sterility, 93(6), 2050-2055.

Prueitt, R. L., Boersma, B. J., Howe, T. M., Goodman, J. E., Thomas, D. D., Ying, L., . . . Lee, D. H. (2007). Inflammation and IGF-I activate the akt pathway in breast cancer. *International Journal of Cancer, 120*(4), 796-805.

Rackow, E. C., & Astiz, M. E. (1991). Pathophysiology and treatment of septic shock. *Jama, 266*(4), 548-554.

Radomski, M. W., Palmer, R. M., & Moncada, S. (1990). Glucocorticoids inhibit the expression of an inducible, but not the constitutive, nitric oxide synthase in vascular endothelial cells. *Proceedings of the National Academy of Sciences of the United States of America, 87*(24), 10043-10047.

Radomski, M. W., Zakar, T., & Salas, E. (1996). Nitric oxide in platelets. *Methods in Enzymology, 269*, 88-107. doi:S0076-6879(96)69012-0 [pii]

Raetz, C. R., & Whitfield, C. (2002). Lipopolysaccharide endotoxins. *Annual Review of Biochemistry, 71*, 635-700. doi:10.1146/annurev.biochem.71.110601.135414 [doi]

Rankin, J. A. (2004). Biological mediators of acute inflammation. *AACN Clinical Issues, 15*(1), 3-17. doi:00044067-200401000-00002 [pii]

Rao, G. H., Krishnamurthi, S., Raij, L., & White, J. G. (1990). Influence of nitric oxide on agonist-mediated calcium mobilization in platelets. *Biochemical Medicine and Metabolic Biology, 43*(3), 271-275.

Rao, M. L., Eckel, J., & Breuer, H. (1977). Factors involved in the uptake of corticosterone by rat liver cells. *Biochimica Et Biophysica Acta (BBA)-General Subjects, 500*(2), 322-332.

Redington, A. E. (2006). Modulation of nitric oxide pathways: Therapeutic potential in asthma and chronic obstructive pulmonary disease. *European Journal of Pharmacology, 533*(1), 263-276.

Reginster, J., & Burlet, N. (2006). Osteoporosis: A still increasing prevalence. *Bone, 38*(2), 4-9.

Regoli, D., & Barabe, J. (1980). Pharmacology of bradykinin and related kinins. *Pharmacological Reviews, 32*(1), 1-46.

Revollo, J. R., & Cidlowski, J. A. (2009). Mechanisms generating diversity in glucocorticoid receptor signaling. *Annals of the New York Academy of Sciences, 1179*(1), 167-178.

Roach, J. C., Glusman, G., Rowen, L., Kaur, A., Purcell, M. K., Smith, K. D., . . . Aderem, A. (2005). The evolution of vertebrate toll-like receptors. *Proceedings of the National Academy of Sciences of the United States of America, 102*(27), 9577-9582. doi:0502272102 [pii]

Robbins, R., Barnes, P., Springall, D., Warren, J., Kwon, O., Buttery, L., . . . Polak, J. (1994). Expression of inducible nitric oxide in human lung epithelial cells. *Biochemical and Biophysical Research Communications, 203*(1), 209-218.

Saklatvala, J. (2004). The p38 MAP kinase pathway as a therapeutic target in inflammatory disease. *Current Opinion in Pharmacology, 4*(4), 372-377.

Salzman, A., Denenberg, A. G., Ueta, I., O'Connor, M., Linn, S. C., & Szabo, C. (1996). Induction and activity of nitric oxide synthase in cultured human intestinal epithelial monolayers. *The American Journal of Physiology, 270*(4 Pt 1), G565-73.

Sanchez, L. A., & Veith, F. J. (1998). Diagnosis and treatment of chronic lower extremity ischemia. *Vascular Medicine (London, England), 3*(4), 291-299.

Sarkar, R., & Webb, R. C. (1998). Does nitric oxide regulate smooth muscle cell proliferation? *Journal of Vascular Research, 35*(3), 135-142.

Shimazu, R., Akashi, S., Ogata, H., Nagai, Y., Fukudome, K., Miyake, K., & Kimoto, M. (1999). MD-2, a molecule that confers lipopolysaccharide responsiveness on toll-like receptor 4. *The Journal of Experimental Medicine, 189*(11), 1777-1782.

Schindler, J. F., Monahan, J. B., & Smith, W. G. (2007). P38 pathway kinases as anti-inflammatory drug targets. *Journal of Dental Research, 86*(9), 800-811. doi:86/9/800 [pii]

Schroder, K., Hertzog, P. J., Ravasi, T., & Hume, D. A. (2004). Interferon-gamma: An overview of signals, mechanisms and functions. *Journal of Leukocyte Biology, 75*(2), 163-189. doi:10.1189/jlb.0603252 [doi]

Schromm, A. B., Lien, E., Henneke, P., Chow, J. C., Yoshimura, A., Heine, H., . . . Golenbock, D. T. (2001). Molecular genetic analysis of an endotoxin nonresponder mutant cell line: A point mutation in a conserved region of MD-2 abolishes endotoxin-induced signaling. *The Journal of Experimental Medicine, 194*(1), 79-88.

Schüle, R., Rangarajan, P., Kliewer, S., Ransone, L. J., Bolado, J., Yang, N., . . . Evans, R. M. (1990). Functional antagonism between oncoprotein c-jun and the glucocorticoid receptor. *Cell, 62*(6), 1217-1226.

Schumann, R. R., Leong, S. R., Flaggs, G. W., Gray, P. W., Wright, S. D., Mathison, J. C., . . . Ulevitch, R. J. (1990). Structure and function of lipopolysaccharide binding protein. *Science (New York, N.Y.), 249*(4975), 1429-1431.

Scicinski, J., Oronsky, B., Ning, S., Knox, S., Peehl, D., Kim, M. M., . . . Fanger, G. (2015). NO to cancer: The complex and multifaceted role of nitric oxide and the epigenetic nitric oxide donor, RRx-001. *Redox Biology, 6*, 1-8.

Scott-Burden, T., Elizondo, E., Ge, T., Boulanger, C. M., & Vanhoutte, P. M. (1994). Simultaneous activation of adenylyl cyclase and protein kinase C induces production of nitric oxide by vascular smooth muscle cells. *Molecular Pharmacology, 46*(2), 274-282.

Seki, E., Yoshizumi, M., Tanaka, R., Ryo, A., Ishioka, T., Tsukagoshi, H., . . . Goya, T. (2013). Cytokine profiles, signalling pathways and effects of fluticasone propionate in respiratory syncytial virus-infected human foetal lung fibroblasts. *Cell Biology International, 37*(4), 326-339.

Selye, H. (1942). Correlations between the chemical structure and the pharmacological actions of the steroids 1. *Endocrinology, 30*(3), 437-453.

Semba, S., Itoh, N., Ito, M., Harada, M., & Yamakawa, M. (2002). The in vitro and in vivo effects of 2-(4-morpholinyl)-8-phenyl-chromone (LY294002), a specific inhibitor of phosphatidylinositol 3'-kinase, in human colon cancer cells. *Clinical Cancer Research : An Official Journal of the American Association for Cancer Research, 8*(6), 1957-1963.

Serbina, N. V., Salazar-Mather, T. P., Biron, C. A., Kuziel, W. A., & Pamer, E. G. (2003). TNF/iNOS-producing dendritic cells mediate innate immune defense against bacterial infection. *Immunity, 19*(1), 59-70.

Shibata, M., Katsuyama, M., Onodera, T., Ehama, R., Hosoi, J., & Tagami, H. (2009). Glucocorticoids enhance toll-like receptor 2 expression in human keratinocytes stimulated with propionibacterium acnes or proinflammatory cytokines. *Journal of Investigative Dermatology, 129*(2), 375-382.

Shinoda, J., McLaughlin, K. E., Bell, H. S., Swaroop, G. R., Yamaguchi, S., Holmes, M. C., & Whittle, I. R. (2003). Molecular mechanisms underlying dexamethasone inhibition of iNOS expression and activity in C6 glioma cells. *Glia, 42*(1), 68-76.

Singh, S., & Evans, T. W. (1997). Nitric oxide, the biological mediator of the decade: Fact or fiction? *The European Respiratory Journal, 10*(3), 699-707.

Skalli, O., Ropraz, P., Trzeciak, A., Benzonana, G., Gillessen, D., & Gabbiani, G. (1986). A monoclonal antibody against alpha-smooth muscle actin: A new probe for smooth muscle differentiation. *The Journal of Cell Biology, 103*(6 Pt 2), 2787-2796.

Smolen, J. S., Aletaha, D., Koeller, M., Weisman, M. H., & Emery, P. (2007). New therapies for treatment of rheumatoid arthritis. *The Lancet, 370*(9602), 1861-1874.

Smolen, J. S., & Steiner, G. (2003). Therapeutic strategies for rheumatoid arthritis. *Nature Reviews Drug Discovery, 2*(6), 473-488.

Söderberg, M., Raffalli-Mathieu, F., & Lang, M. A. (2007). Regulation of the murine inducible nitric oxide synthase gene by dexamethasone involves a heterogeneous nuclear ribonucleoprotein I (hnRNPI) dependent pathway. *Molecular Immunology, 44*(12), 3204-3210.

Song, C. Z., Tian, X., & Gelehrter, T. D. (1999). Glucocorticoid receptor inhibits transforming growth factor-beta signaling by directly targeting the transcriptional activation function of Smad3. *Proceedings of the National Academy of Sciences of the United States of America, 96*(21), 11776-11781.

Song, G., Ouyang, G., & Bao, S. (2005). The activation of Akt/PKB signaling pathway and cell survival. *Journal of Cellular and Molecular Medicine, 9*(1), 59-71.

Sonneveld, E., Jansen, H. J., Riteco, J. A., Brouwer, A., & van der Burg, B. (2005). Development of androgen- and estrogen-responsive bioassays, members of a panel of human cell line-based highly selective steroid-responsive bioassays. *Toxicological Sciences : An Official Journal of the Society of Toxicology, 83*(1), 136-148. doi:kfi005 [pii]

SoRelle, R. (1998). Nobel prize awarded to scientists for nitric oxide discoveries. *Circulation, 98*(22), 2365-2366.

Sousa, A. R., Lane, S. J., Cidlowski, J. A., Staynov, D. Z., & Lee, T. H. (2000). Glucocorticoid resistance in asthma is associated with elevated in vivo expression of the glucocorticoid receptor β-isoform. *Journal of Allergy and Clinical Immunology, 105*(5), 943-950.

Sprung, C. L., Annane, D., Keh, D., Moreno, R., Singer, M., Freivogel, K., . . . Forst, H. (2008). Hydrocortisone therapy for patients with septic shock. New England Journal of Medicine, 358(2), 111.

Stamler, J. S., Vaughan, D. E., & Loscalzo, J. (1989). Synergistic disaggregation of platelets by tissue-type plasminogen activator, prostaglandin E1, and nitroglycerin. *Circulation Research, 65*(3), 796-804.

Stefanovic-Racic, M., Meyers, K., Meschter, C., Coffey, J., Hoffman, R., & Evans, C. (1994). N-monomethyl arginine, an inhibitor of nitric oxide synthase, suppresses the development of adjuvant arthritis in rats. *Arthritis & Rheumatism, 37*(7), 1062-1069.

Struthers, A., Krum, H., & Williams, G. H. (2008). A comparison of the Aldosterone-blocking agents eplerenone and spironolactone. *Clinical Cardiology, 31*(4), 153-158.

Subbanagounder, G., Leitinger, N., Shih, P. T., Faull, K. F., & Berliner, J. A. (1999). Evidence that phospholipid oxidation products and/or platelet-activating factor play an important role in early atherogenesis : In vitro and in vivo inhibition by WEB 2086. *Circulation Research, 85*(4), 311-318.

Sui, X., Kong, N., Ye, L., Han, W., Zhou, J., Zhang, Q., . . . Pan, H. (2014). p38 and JNK MAPK pathways control the balance of apoptosis and autophagy in response to chemotherapeutic agents. *Cancer Letters, 344*(2), 174-179.

Sukumaran, S., Lepist, E., DuBois, D. C., Almon, R. R., & Jusko, W. J. (2012). Pharmacokinetic/pharmacodynamic modeling of methylprednisolone effects on iNOS mRNA expression and nitric oxide during LPS-induced inflammation in rats. *Pharmaceutical Research, 29*(8), 2060-2069.

Sung, C., Arleth, A. J., Shikano, K., Zabko-Potapovich, B., & Berkowitz, B. A. (1989). Effect of trypsinization in cell culture on bradykinin receptors in vascular endothelial cells. *Biochemical Pharmacology, 38*(4), 696-699.

Sugiyama, T., & Wright, S. D. (2001). Soluble CD14 mediates efflux of phospholipids from cells. *Journal of Immunology (Baltimore, Md.: 1950), 166*(2), 826-831.

Suzuki, S., Takenaka, K., Kassell, N. F., & Lee, K. S. (1994). Hemoglobin augmentation of interleukin-1β-induced production of nitric oxide in smooth-muscle cells. *Journal of Neurosurgery, 81*(6), 895-901.

Tajima, T., Murata, T., Aritake, K., Urade, Y., Michishita, M., Matsuoka, T., . . . Hori, M. (2012). EP2 and EP4 receptors on muscularis resident macrophages mediate LPS-induced intestinal dysmotility via iNOS upregulation through cAMP/ERK signals. *American Journal of Physiology.Gastrointestinal and Liver Physiology, 302*(5), G524-34. doi:10.1152/ajpgi.00264.2011 [doi]

Tak, P. P., & Firestein, G. S. (2001). NF-kappaB: A key role in inflammatory diseases. *The Journal of Clinical Investigation, 107*(1), 7-11. doi:10.1172/JCI11830 [doi]

Teng, X., Zhang, H., Snead, C., & Catravas, J. D. (2002). Molecular mechanisms of iNOS induction by IL-1 beta and IFN-gamma in rat aortic smooth muscle cells. *American Journal of Physiology.Cell Physiology, 282*(1), C144-52.

Thakur, S., & Baydoun, A. R. (2012). Post-transcriptional divergence in the regulation of CAT-2A, CAT-2B and iNOS expression by dexamethasone in vascular smooth muscle cells. *Amino Acids, 43*(2), 667-676.

Thiemermann, C. (1997). Nitric oxide and septic shock. *General Pharmacology: The Vascular System, 29*(2), 159-166.

Thomas, D. D., Espey, M. G., Ridnour, L. A., Hofseth, L. J., Mancardi, D., Harris, C. C., & Wink, D. A. (2004). Hypoxic inducible factor 1alpha, extracellular signal-regulated kinase, and p53 are regulated by distinct threshold concentrations of nitric oxide. *Proceedings of the National Academy of Sciences of the United States of America, 101*(24), 8894-8899. doi:10.1073/pnas.0400453101 [doi]

Thurmond, R. L., Gelfand, E. W., & Dunford, P. J. (2008). The role of histamine H1 and H4 receptors in allergic inflammation: The search for new antihistamines. *Nature Reviews Drug Discovery, 7*(1), 41-53.

Tiligada, E., Zampeli, E., Sander, K., & Stark, H. (2009). Histamine H3 and H4 receptors as novel drug targets. *Expert Opinion on Investigational Drugs, 18*(10), 1519-1531.

Titheradge, M. A. (1999). Nitric oxide in septic shock. *Biochimica Et Biophysica Acta (BBA)-Bioenergetics, 1411*(2), 437-455.

Tobias, P. S., Soldau, K., Gegner, J. A., Mintz, D., & Ulevitch, R. J. (1995). Lipopolysaccharide binding protein-mediated complexation of lipopolysaccharide with soluble CD14. *Journal of Biological Chemistry, 270*(18), 10482-10488.

Toh, M., Yang, Y., Leech, M., Santos, L., & Morand, E. F. (2004). Expression of mitogen-activated protein kinase phosphatase 1, a negative regulator of the mitogen-activated protein kinases, in

rheumatoid arthritis: Up-regulation by interleukin-1β and glucocorticoids. *Arthritis & Rheumatism, 50*(10), 3118-3128.

Torio, C. M., & Andrews, R. M. (2013). National inpatient hospital costs: The most expensive conditions by payer, 2011.

Tracy, R. P. (2006). The five cardinal signs of inflammation: Calor, dolor, rubor, tumor ... and penuria (apologies to aulus cornelius celsus, de medicina, c. A.D. 25). *The Journals of Gerontology.Series A, Biological Sciences and Medical Sciences, 61*(10), 1051-1052. doi:61/10/1051 [pii]

Triantafilou, M., Brandenburg, K., Kusumoto, S., Fukase, K., Mackie, A., Seydel, U., & Triantafilou, K. (2004). Combinational clustering of receptors following stimulation by bacterial products determines lipopolysaccharide responses. *The Biochemical Journal, 381*(Pt 2), 527-536. doi:10.1042/BJ20040172 [doi]

Troutman, T. D., Bazan, J. F., & Pasare, C. (2012). Toll-like receptors, signaling adapters and regulation of the pro-inflammatory response by PI3K. *Cell Cycle, 11*(19), 3559-3567.

Tsirigotis, P., Chondropoulos, S., Gkirkas, K., Meletiadis, J., & Dimopoulou, I. (2016). Balanced control of both hyper and hypo-inflammatory phases as a new treatment paradigm in sepsis. *Journal of Thoracic Disease, 8*(5), E312-6. doi:10.21037/jtd.2016.03.47 [doi]

Tsujino, M., Hirata, Y., Imai, T., Kanno, K., Eguchi, S., Ito, H., & Marumo, F. (1994). Induction of nitric oxide synthase gene by interleukin-1 beta in cultured rat cardiocytes. *Circulation, 90*(1), 375-383.

Tsutsui, M., Shimokawa, H., Tanimoto, A., Yanagihara, N., & Tamura, M. (2014). Roles of nitric oxide synthases in arteriosclerotic vascular disease: Insights from murine genetic models. *J Clin Exp Cardiolog, 5*(318), 2.

Tufvesson, E., Andersson, C., Weidner, J., Erjefält, J. S., & Bjermer, L. (2017). Inducible nitric oxide synthase expression is increased in the alveolar compartment of asthmatic patients. *Allergy, 72*(4), 627-635.

Tzeng, E., Kim, Y., Pitt, B. R., Lizonova, A., Kovesdi, I., & Billiar, T. R. (1997). Adenoviral transfer of the inducible nitric oxide synthase gene blocks endothelial cell apoptosis. *Surgery, 122*(2), 255-263.

Unno, N., Wang, H., Menconi, M. J., Tytgat, S., Larkin, V., Smith, M., . . . Fink, M. P. (1997). Inhibition of inducible nitric oxide synthase ameliorates endotoxin-induced gut mucosal barrier dysfunction in rats. *Gastroenterology, 113*(4), 1246-1257.

Vandevyver, S., Dejager, L., & Libert, C. (2012). On the trail of the glucocorticoid receptor: Into the nucleus and back. *Traffic, 13*(3), 364-374.

Vodovotz, Y., Bogdan, C., Paik, J., Xie, Q. W., & Nathan, C. (1993). Mechanisms of suppression of macrophage nitric oxide release by transforming growth factor beta. *The Journal of Experimental Medicine, 178*(2), 605-613.

von Mach-Szczypiński, J., Stanosz, S., Kościuszkiewicz, J., & Safranow, K. (2016). New aspects of postmenopausal osteoporosis treatment with micronized estradiol and progesterone. *Ginekologia Polska, 87*(11), 739-744.

Wada, T., & Penninger, J. M. (2004). Mitogen-activated protein kinases in apoptosis regulation. *Oncogene, 23*(16), 2838-2849.

Walker, G., Pfeilschifter, J., & Kunz, D. (1997). Mechanisms of suppression of inducible nitric-oxide synthase (iNOS) expression in interferon (IFN)-γ-stimulated RAW 264.7 cells by dexamethasone evidence for glucocorticoid-induced degradation of inos protein by calpain as a key step in post-transcriptional regulation. *Journal of Biological Chemistry, 272*(26), 16679-16687.

Walker, G., Pfeilschifter, J., Otten, U., & Kunz, D. (2001). Proteolytic cleavage of inducible nitric oxide synthase (iNOS) by calpain I. *Biochimica Et Biophysica Acta (BBA)-General Subjects, 1568*(3), 216-224.

Wang, Y., Vodovotz, Y., Kim, P. K., Zamora, R., & Billiar, T. R. (2002). Mechanisms of hepatoprotection by nitric oxide. *Annals of the New York Academy of Sciences, 962*(1), 415-422.

Wang, H., Wu, Y. B., & Du, X. H. (2005). Effect of dexamethasone on nitric oxide synthase and caspase-3 gene expressions in endotoxemia in neonate rat brain. *Biomedical and Environmental Sciences : BES, 18*(3), 181-186.

Wang, X., Meng, X., Kuhlman, J. R., Nelin, L. D., Nicol, K. K., English, B. K., & Liu, Y. (2007). Knockout of mkp-1 enhances the host inflammatory responses to gram-positive bacteria. *Journal of Immunology (Baltimore, Md.: 1950), 178*(8), 5312-5320. doi:178/8/5312 [pii]

Webster, J. C., Jewell, C., Sar, M., & Cidlowski, J. (1994). The glucocorticoid receptor: Maybe not all steroid receptors are nuclear. *Endocrine, 2*, 967-969.

Weisz, A., Oguchi, S., Cicatiello, L., & Esumi, H. (1994). Dual mechanism for the control of inducible-type NO synthase gene expression in macrophages during activation by interferon-gamma and bacterial lipopolysaccharide. transcriptional and post-transcriptional regulation. *The Journal of Biological Chemistry, 269*(11), 8324-8333.

Wek, R. C., Jiang, H. Y., & Anthony, T. G. (2006). Coping with stress: EIF2 kinases and translational control. *Biochemical Society Transactions, 34*(Pt 1), 7-11. doi:BST20060007 [pii]

Wileman, S. M., Mann, G. E., & Baydoun, A. R. (1995). Induction of L-arginine transport and nitric oxide synthase in vascular smooth muscle cells: Synergistic actions of pro-inflammatory cytokines and bacterial lipopolysaccharide. *British Journal of Pharmacology, 116*(8), 3243-3250.

Wink, D. A., Vodovotz, Y., Laval, J., Laval, F., Dewhirst, M. W., & Mitchell, J. B. (1998). The multifaceted roles of nitric oxide in cancer. *Carcinogenesis, 19*(5), 711-721.

Wright, S. D., Ramos, R. A., Tobias, P. S., Ulevitch, R. J., & Mathison, J. C. (1990). CD14, a receptor for complexes of lipopolysaccharide (LPS) and LPS binding protein. *Science, 249*(4975), 1431-1433.

Yamakawa, T., Eguchi, S., Matsumoto, T., Yamakawa, Y., Numaguchi, K., Miyata, I., . . . Inagami, T. (1999). Intracellular signaling in rat cultured vascular smooth muscle cells: Roles of nuclear factor-κB and p38 mitogen-activated protein kinase on tumor necrosis factor-α production 1. *Endocrinology, 140*(8), 3562-3572.

Yang, J. G., Yu, C. C., & Li, P. S. (2001). Dexamethasone enhances follicle stimulating hormone-induced P450scc mRNA expression and progesterone production in pig granulosa cells. *The Chinese Journal of Physiology, 44*(3), 111-119.

Yarovaya, G. A., & Neshkova, E. A. (2015). Kallikrein-kinin system. long history and present. (to 90th anniversary of discovery of the system). *Bioorganicheskaia Khimiia, 41*(3), 275-291.

Yu, Z., Ouyang, J., & Li, Y. (2009). Dexamethasone attenuated endotoxin-induced acute lung injury through inhibiting expression of inducible nitric oxide synthase. *Clinical Hemorheology and Microcirculation, 41*(2), 117-125.

Zarubin, T., & Jiahuai, H. (2005). Activation and signaling of the p38 MAP kinase pathway. *Cell Research, 15*(1), 11-18.

Zhang, G., & Ghosh, S. (2000). Molecular mechanisms of NF-kappaB activation induced by bacterial lipopolysaccharide through toll-like receptors. *Journal of Endotoxin Research, 6*(6), 453-457.

Zidar, N., Odar, K., Glavac, D., Jerse, M., Zupanc, T., & Stajer, D. (2009). Cyclooxygenase in normal human tissues–is COX-1 really a constitutive isoform, and COX-2 an inducible isoform? *Journal of Cellular and Molecular Medicine, 13*(9b), 3753-3763.

Appendix

Table of Chemicals and Suppliers

Chemical	Supplier
Anti-SM22 alpha antibody	Abcam, UK
BCA reagents	Fisher Scientific, UK
Bromophenol blue	Sigma–Aldrich UK
BSA	Fisher Scientific, UK
Dexamethasone	Sigma–Aldrich UK
Dulbecco's modified Eagle's medium	Fisher Scientific, UK
Eplerenone	Tocris Bioscience, UK
Foetal bovine serum	Fisher Scientific, UK
Fluticasone propionate	Sigma–Aldrich, UK
Griess reagent I	Sigma–Aldrich, UK
Griess reagent II	Sigma–Aldrich, UK
Housekeeping genes	PrimerDesign, UK
Hydrocortisone	Sigma–Aldrich, UK
IFN-γ	Calbiochem, UK
iNOS antibody	BD Biosciences, UK
iNOS primers	PrimerDesign, UK
LPS	Sigma, UK
Luminol	Sigma–Aldrich, UK
LY294002	Merck Chemicals Ltd, UK
Methanol	Fisher Scientific, UK
MTT	Sigma–Aldrich UK
P-Akt antibody	Cell Signalling, UK
PBS	Invitrogen, UK
p-Coumaric acids	Sigma–Aldrich, UK

P-EIF2α	Cell Signalling, UK
Penicillin	Fisher Scientific, UK
Phosphatase inhibitor cocktail	Sigma–Aldrich UK
P-p38 MAPK antibody	Cell Signalling, UK
P-PKR	Sigma–Aldrich UK
PVDF	Fisher Scientific, UK
RNA-to-cDNA kit	Applied Biosystems, UK
RU-486	Sigma–Aldrich, UK
SB203580	Sigma–Aldrich UK
SDS	Sigma–Aldrich UK
Sodium chloride	Fisher Scientific, UK
Streptomycin	Fisher Scientific, UK
SYBR green	Applied Biosystems, UK
Transfer apparatus	Thermo Scientific, UK
Tris-HCl	Fisher Scientific, UK
Trypan blue	Fisher Scientific, UK
Trypsin	Invitrogen, UK
Tween 20	Fisher Scientific, UK
β-mercapitalethanol	Sigma–Aldrich UK